DISSERTATION

IQGAP1 IS A NOVEL EFFECTOR OF GONADOTROPIN-RELEASING HORMONE RECEPTOR SIGNALING

Submitted by

Huda A. Alqahtani

Department of Biomedical Sciences

In partial fulfillment of the requirements

For the Degree of Doctor of Philosophy

Colorado State University

Fort Collins, Colorado

Fall 2023

Doctoral Committee:

Advisor: Gregory Amberg

Colin Clay
Michael Tamkun
Jennifer DeLuca

ABSTRACT

IQGAP1 IS A NOVEL EFFECTOR OF GONADOTROPIN-RELEASING HORMONE RECEPTOR SIGNALING

Stimulation of gonadotropin-releasing hormone (GnRH) receptors on the surface of anterior pituitary gonadotrope cells is a key signaling event for the hypothalamic-pituitary-gonadal axis. One important downstream component of GnRH receptor signaling is activation of the mitogen-activated protein kinase ERK (extracellular signal-regulated kinase), which is essential for the production of the gonadotropin luteinizing hormone. Evidence suggests that GnRH receptors reside in low-density plasma membrane domains where they participate in multiprotein signaling complexes. Here we used quantitative proteomics to identify proteins associated with low-density plasma membrane domains and to measure changes in their relative abundance in these domains in response to GnRH. Using αT3-1 gonadotropes, we identified 537 proteins in detergent-free subcellular fractions containing low-density plasma membranes. SILAC (stable isotope labeling by amino acids in cell culture) in combination with mass spectrometry demonstrated that GnRH, within 10 min, altered the association of 87 proteins with this plasma membrane fraction. Ontology analysis revealed that GnRH promoted an enrichment of actin cytoskeletal and adherens junction-related proteins including the molecular scaffold IQGAP1 and the small GTPase Rac1. Subsequent investigation revealed that the association between Rac1 and IQGAP1 increased with GnRH receptor stimulation and that GnRH increased Rac1 activity. Demonstrating functional relevance, inhibiting Rac1 reduced GnRH-dependent ERK activation. Our data reveals an upstream activation of signaling and structural molecules, including Ca2+, CDC42 and Rac1, E-cadherin, N-cadherin, and β-catenin. We also identified interactions between the scaffold protein IQGAP1 and these molecules, indicating that IQGAP1 is a fundamental regulator of GnRH-dependent signaling in gonadotropes. Furthermore, our data shows that IQGAP1 has a transcriptional regulatory role in

gonadotropes treated with GnRH. In sum, these data indicate that IQGAP1 complexed with Rac1 modulates ERK activity and as such serves as an essential effector in modulating cell polarity and cell-cell contacts in gonadotropes. Altogether, our proteomics data show that acute stimulation of GnRH receptors (3 nM for 10 min) alters the PAM fraction abundance of proteins, such as IQGAP1, mechanistically linked to gonadotrope activation.

TABLE OF CONTENTS

Chapter 1: Introduction & Literature Review

The HPG axis controls reproductive endocrine function and impacts fundamental processes ranging from reproduction to development and aging. The hypothalamic neuropeptide GnRH initiates HPG axis signaling by increasing the synthesis and secretion of the gonadotropins luteinizing hormone (LH) and follicle-stimulating hormone (FSH). GnRH stimulation of LH and FSH synthesis and secretion begins with the activation of GnRH receptors on the surface of gonadotrope cells located in the anterior pituitary. Gonadotropes are a mosaic population of cells distributed non-homogeneously throughout the anterior pituitary, where they account for only 10-15% of the endocrine cells present. Given their observed spatial dispersion and small numbers, prior work suggests that efficient gonadotrope functionality requires some degree of coordination (Alim et al., 2012; Budry et al., 2011; Featherstone et al., 2016; Golan et al., 2016b; Hodson et al., 2012a; Le Tissier et al., 2017; Lyles et al., 2010; Schaeffer et al., 2011). Although intriguing, empirical evidence supporting this hypothesis and the molecular mechanisms responsible for such coordination is minimal or altogether unsubstantiated.

The decapeptide known as gonadotropin-releasing hormone, or GnRH, is a component of the hypothalamic-pituitary-gonadal axis. The fact that GnRH is a component of this system makes it essential for human reproduction. Since its discovery in 1971 from the porcine hypothalamus as one of the earliest hypothalamic-releasing hormones by a group supervised by Nobel laureate Andrew V. Schally, it has been at the center of attention of research scientists due to its central role in reproduction not only in humans but also in all vertebrates. Five decades ago (between 4-6), GnRH was extracted from porcine hypothalamic and found to be structurally identified as a decapeptide (pGlu-His-Trp-Ser-Tyr-Gly-Leu-Arg-Pro-Gly-NH2). Evidence from many mammalian species shows that this decapeptide effectively stimulates pituitary LH and FSH secretion (Schally et al., 1971a; Schally et al., 1971b). Although this peptide was originally called the 'Luteinizing Hormone-Releasing Hormone (LH-RH)', the term 'Gonadotropin Releasing Hormone' (GnRH) is now more often used to represent its stimulatory effect on the production of both luteinizing hormone (LH) and follicle-stimulating hormone (FSH) (Schally, 2000).

There are over twenty different main structures for GnRH and its receptor in different vertebrate species, indicating that the GnRH system likely originated early in vertebrate development (Millar, 2005; Okubo and Nagahama, 2008). GnRH I refers to the GnRH structure initially discovered in mammals (Millar, 2005; Miyamoto et al., 1984). Subsequently, a second vertebrate GnRH sequence, GnRHII (pGlu-His-Trp-Ser-His-Gly-Trp-Tyr-Pro-Gly-NH2), was discovered in chicken brain (Okubo and Nagahama, 2008; White et al., 1994). Fish also exhibit a third type, designated GnRH III (Millar, 2005; White et al., 1994). Since GnRH I is the only GnRH isoform with hypophysiotropic effects in mammals, I is the only isoform referred to as GnRH in the human context (Gault et al., 2003).

In 1975, Dr. Frank Zeller introduced gonadotropins to his students at Indiana University by saying, "Knowledge of these [hormones] advanced along with advances in protein chemistry." The discovery that gonadotropins had two subunits was an early success. Recent advances in protein chemistry, carbohydrate chemistry, molecular biology, genomics, and bioinformatics, among others, have led to a deeper knowledge of these crucial hormones. Though the human gonadotropins are highlighted, data from other mammalian and lower vertebrate gonadotropins may be freely utilized to build a comparative knowledge of these crucial hormones and their genetic regulation (Ward, 1991).

In 1994, two seminal research showed the crystal structures of chemically deglycosylated urine human chorionic gonadotropin (hCG) (Lapthorn et al., 1994) and deglycosylated recombinant selenomethionyl-hCG (Wu et al., 1994). One result of these studies was to give the glycoprotein hormones a more general biological setting. Glycoprotein hormones were classified as the fourth family of the cystine knot growth factor (CKGF) superfamily due to the presence of the cystine knot motif in both subunits. These families include the transforming growth factor (TGF)- superfamily, the nerve growth factor (NGF) family, and the platelet-derived growth factor (PDGF) family. The second group includes hormones like inhibin, activin, a variety of bone morphogenic proteins, and mullerian inhibitory hormone, all of which are important in reproduction. Despite the fact that the defining characteristics of the distinct families have been summarized (Hearn and Gomme, 2000).

The pituitary gonadotrophs are cells with excitability that depend on a background network of voltage- and ligand-gated and related channels for the spontaneous firing of action potentials and calcium signaling. When GnRH receptor and other calcium-mobilizing receptors are activated, calcium is released from the endoplasmic reticulum by IP3R channels, followed by fast gonadotropin secretion. After then, the action potential firing pattern changes from tonic single spiking to periodic plateau bursting, which is required for continuous calcium signaling and gonadotropin release. Stojilkovic et al. (Stojilkovic et al., 2017) provide a review of these processes and ion channels in gonadotrophs. GnRH receptor-mediated cell shape remodeling is the subject of two studies in this volume. Furthermore, Edwards et al. (Edwards et al., 2017a) provide a review summarizing the in vivo gonadotroph cell network and its plasticity. Through activation of the actin cytoskeleton, GnRH not only enhances cell motility but also triggers membrane remodeling processes such as membrane ruffles, filopodia, and lamellipodia, allowing the cell to enter the blood vessel. The researchers note that the details of how actin polymerization triggers the activation of MAP kinases remain sketchy for the most part. Nevertheless, Rahamim-Ben Navi et al. (Rahamim-Ben Navi et al., 2017) demonstrate that ERK1/2 activation is required for GnRH-induced membrane bleb production in immortalized LT2 gonadotrophs and mice primary pituitary cells. There is an accumulation of GnRH receptor, c-Src, ERK1/2, FAK, paxillin, and tubulin in the blebs, which the researchers interpret as a typical cellular response to GnRH and therefore as another example of gonadotroph cell plasticity. Also, the blebs, which are probably important in cell migration, attract members of the signalosome, which researchers have previously characterized.

The release of hormones by gonadotropes follows a circadian rhythm, which is essential for the generation of the preovulatory LH surge in women (Bliss et al., 2010; Brinkley, 1981; Clayton and Catt, 1981; Knobil, 1974). The morphological and functional plasticity of these cells have been shown before over the female reproductive cycle (Alim et al., 2012; Childs et al., 1992a; Childs et al., 1992b). In response to GnRH and perhaps steroid stimulation, gonadotropes reorganize their cellular architecture to form processes or projections that reach into capillary sinusoids. Dr. Gwen Childs first noticed that peak LH secretory events coincided with the development of processes in GnRH-stimulated gonadotropes in

1985 (Childs, 1985). Using three-dimensional models of the pituitary vasculature and endocrine cells, Osamura and colleagues in Japan were able to show a comparable effect (Itoh et al., 2000; Itoh et al., 2003). Gonadotropes have been demonstrated to exhibit substantial plasticity in response to neuroendocrine stimulation in prior live cell investigations of ex vivo pituitary slices (Alim et al., 2012; Navratil et al., 2007). Using the ex vivo approach, exposing murine pituitary slices to GnRH triggers cell processes and the spatial repositioning of GFP-labeled gonadotropes (Navratil et al., 2007). Gonadotropes are hypothesized to enhance their interaction with the pituitary microvasculature due to the stimulation-dependent plasticity they exhibit (Navratil et al., 2007). There is evidence that gonadotropes may have a tight spatial relationship with more than one blood artery via several cellular projections (Budry et al., 2011), and gonadotropes are located significantly closer to vasculature than corticotropes. Notably, it has been reported that LH secretory granules are present in the GnRH-induced cellular projections that extend toward blood arteries (Navratil et al., 2014), suggesting that this may augment the secretory influence of gonadotropes.

Gonadotropes undergo plasticity in response to gonadotropin-releasing hormone, producing short-lived cellular structures such lamellipodia, membrane ruffles, and filopodia. By assembling actin monomers into filamentous actin (Doussau and Augustine, 2000; Pollard and Cooper, 2009; Porat-Shliom et al., 2013), the actin cytoskeleton provides structural support for these membrane remodeling activities. Within 1 minute after administration, GnRH has been shown to trigger fast dynamic interaction of the actin cytoskeleton (Navratil et al., 2007). On the other hand, GnRH-induced membrane remodeling processes are attenuated when pretreated with the pharmacological disruptor of the actin cytoskeleton, jasplakinolide (Jas) (Navratil et al., 2007). The actin cytoskeleton not only has an essential part in the structural support and migration of cells but also plays a significant function in regulating the trafficking and discharge of secretory vesicles in endocrine cells. It has been demonstrated that Primary murine gonadotropes show an approximately 3.5-fold increase in LH production in response to GnRH stimulation (Navratil et al., 2014). In contrast, primary murine pituitary cells that have been pretreated with Jas respond to GnRH stimulation with a substantial decrease in LH production relative to vehicle

(Navratil et al., 2007). Therefore, GnRH-mediated plasticity is required to maintain physiological levels of LH and to place sensitive gonadotropes near the pituitary vasculature for secretory activities.

There are a number of actin-associated proteins (Pollard and Cooper, 2009), which govern the assembly and disassembly cycles of the actin cytoskeleton. Actin polymerization may be mediated by cortactin, a filamentous actin-binding protein functioning as an actin scaffolding protein (Uruno et al., 2001; Weaver et al., 2001). Through a three-amino-acid motif at its amino terminus, cortactin binds actin-related protein (Arp) 2/3 complex, a nucleating factor that promotes actin filament branching (Uruno et al., 2001). Moreover, multiple tyrosine and serine/threonine kinases recognize cortactin as an effector molecule (Ammer and Weed, 2008; Cosen-Binker and Kapus, 2006). It has previously shown that GnRH-induced plasticity in T3-1 gonadotropes depends on cortactin stimulation, and src-induced tyrosine phosphorylation of cortactin is critical for enabling interaction with Arp3 and efficient engagement of the actin cytoskeleton (Navratil et al., 2014). Cortactin is known to have a role in controlling actin polymerization, but it may also play a role in linking intracellular signaling cascades to actin assembly activities. Remarkably, GnRH-induced ERK phosphorylation was abolished when the actin cytoskeleton was disrupted with Jas. Nevertheless, the MAPK kinase 1 inhibitor PD98059 does not suppress GnRH-induced cell migration and projections. It has been suggested by a number of lines of evidence (Navratil et al., 2014; Navratil et al., 2007) that ERK activation is not necessary for actin rearrangement in T3-1 cells, but rather an intact actin cytoskeleton is necessary for ERK activation. In agreement with these findings, GnRH treatment of HEK293 cells expressing the GnRH receptor resulted in morphological changes and a rearrangement of the cytoskeleton.

Furthermore, ERK activity was greatly attenuated after cytoskeletal disruption (Davidson et al., 2004). Although research shows that PKC is operating downstream of the actin cytoskeleton, the specific method by which actin interaction affects ERK activation is yet unknown. This is supported by the observation that phorbol 12-myristate 13-acetate-mediated direct activation of PKC was insufficient to promote cytoskeletal remodeling in gonadotropes, indicating that PKC functions downstream of the actin cytoskeleton to allow ERK activation. Actin rearrangement has recently been shown to be critical for

GnRH-mediated activation of L-type calcium channels (Dang et al., 2014), the primary calcium signal that triggers the activation of ERK (Dang et al., 2014; Mulvaney et al., 1999).

Proteins like dynamin, which is both a big GTPase and a proline-rich domain-containing protein, have mechanochemical characteristics that are crucial during membrane remodeling processes and fission (Zhang and Hinshaw, 2001). A large number of dynamin's roles seem to be linked to actin cytoskeleton remodeling (Orth and McNiven, 2003), but the technique by which this occurs is yet unknown. Many F-actin-rich cellular structures are disrupted by overexpression of dominant-negative dynamin mutant proteins defective in hydrolyzing GTP (K44A) (Gray et al., 2005; Schafer et al., 2002). In agreement with these findings, the lack of GnRH-induced actin remodeling events (Benard et al., 2017) was seen in T3-1 cells after transfection with K44A. Pharmacological suppression of dynamin GTPase activity with dynasore and dyngo has also been shown to dramatically decrease ERK activation and disrupt GnRH-induced actin rearrangement (Edwards et al., 2016). Consequently, the role of dynamin GTPase activity in actin rearrangement and consequent MAPK activation has been brought to light. Furthermore, besides increasing dynamin GTPase activity, the actin-binding protein cortactin binds dynamin through the C-terminal SH3-domain (Mooren et al., 2009). Also, it is well established that dynamin and cortactin are found together in podosomes (Ochoa et al., 2000), membrane ruffles (McNiven et al., 2000), and actin comets (Orth et al., 2002). Cortactin and dynamin have been reorganized and become colocalized in positions suggestive of significant actin rearrangement in T3-1 cells after GnRH stimulation (Edwards et al., 2016). Moreover, evidence suggests that src triggers Tyr phosphorylation of dynamin (Benard et al., 2017; Bruzzaniti et al., 2005), in addition to its role in controlling Tyr phosphorylation of cortactin. Therefore, dynamin and cortactin interact to efficiently engage the actin cytoskeleton, which in turn regulates PKC activation, VGCC opening, and ERK phosphorylation, potentially modulating GnRH-induced gonadotrope plasticity (Dang et al., 2014; Edwards et al., 2016). More research is obviously needed to determine the precise role and method by which dynamin controls gonadotrope plasticity.

Studies have shown some of the signaling intermediates GnRH uses to interact with the actin cytoskeleton, but the whole set of intermediates has yet to be identified. In addition to controlling cellular morphology in vitro and in vivo, mammalian target of rapamycin (mTOR) has been shown to communicate to the actin cytoskeleton (Jacinto et al., 2004; Thomanetz et al., 2013). Two different complexes, mTORC1 and mTORC2, are formed from the serine/threonine protein kinase mTOR. Using the LβT2 gonadotrope cell line, researchers were able to determine that mTORC2 plays a critical role in controlling membrane remodeling processes (Edwards et al., 2017b). Pharmacological suppression of mTORC2 inhibited GnRH-mediated actin rearrangement and equally reduced activation of ERK and LHβ gene expression (Edwards et al., 2017b), suggesting that mTORC2 is a key mediator of these effects. The upstream signaling molecules controlling activation of mTORC2 in LβT2 cells are unclear, despite the fact that a further crucial intermediary connecting GnRH receptor signaling to actin remodeling and ERK activation has been discovered. Rac1, a Rho GTPase, has been shown to bind to and activate mTORC2 and to contribute in the kinase's plasma membrane location (Saci et al., 2011). Rho family members are another mechanism by which GnRH controls morphology and migration in Lβt2 cells (Godoy et al., 2011). Therefore, Rac1 is a probable major player in triggering mTORC2 activation and consequent actin cytoskeleton involvement in gonadotrope cells. Collectively, several signaling networks regulate GnRH-mediated actin cytoskeletal remodeling in order to maintain normal reproductive function.

The data regarding GnRH-induced gene expression in gonadotrophs is provided by many articles. The study by Janjic et al., (Janjic et al., 2017) addresses the function of GnRH in regulating transcription, as well as basal and regulated GnRH receptor gene transcription in mammalian gonadotrophs. Activation of mitogen-activated protein kinases is a key step in the GnRH-induced transcription of genes in rats and mice, and this process is dependent on the protein kinase C signaling pathway. Continuous GnRH application, in opposition to pulsatile, suppresses controlled but not basal transcription, indicating that different components of this signaling system regulate transcription. There is evidence suggesting that GnRH-GnRH receptor signaling pathways also affect the chromatin structure of target genes, in addition to regulating their expression. Melamed et al., (Melamed et al., 2018) combine data on GnRH's effect on

chromatin modifications in gonadotroph signature genes. The scientists point out that additional epigenome profiling of gonadotropin genes may have applications in both cancer biology and the development of reproductive drugs. Addressing the same issue, Ruf-Zamojski et al., (Ruf-Zamojski et al., 2018) provide an insight into the epigenetic and single-cell transcriptional pathways of LβT2 gonadotrophs in response to GnRH stimulation by combining a unique gel bead-in-emulsion drop-seq approach with genome-wide chromatin accessibility status. In addition to providing helpful datasets, the authors describe the discovery of a potential FSH beta gene enhancer with very open chromatin. Although there was considerable variation in both baseline and GnRH-induced gene expression between individual cells, the researchers found no effect of the cell cycle stage on the gene response to GnRH. From a physiological perspective, two publications provide more guidance on GnRH/GnRH receptor signaling in pituitary gonadotrophs. Two theories based on tests in which leptin receptor gene expression in gonadotrophs was manipulated are presented by Odle et al., (Odle et al., 2017) who also explore the function of leptin in reproduction. The researchers hypothesize that these cells are activated only under ideal circumstances due to the cyclical variations in pituitary GnRH receptor expression. The findings also revealed that the hypothalamic-pituitary-gonadal axis is responsible for the permissive control of the reproductive cycle through a series of arranged actions involving many interacting target cells. Terasaka et al., (Terasaka et al., 2017) contend that the information of GnRH receptor signaling in gonadotrophs has largely disregarded the role of reactive oxygen species (ROS). In fact, ROS may inhibit MAPK activation and other signaling processes caused by GnRH receptor. In addition, researchers demonstrate that the monounsaturated fatty acid oleate may trigger ROS production in the mitochondria of LβT2 cells. This study concludes that understanding ROS signaling in gonadotrophs may provide light on how stress signaling, and the reproductive axis are integrated. As compared to the activities of GnRH/GnRH receptor, the functions of GnRH2/GnRH receptor 2 remain largely unknown. This is due to the lack of expression or function of this receptor in many mammals, including the rat and the mouse, which are the most often used experimental species. Desaulniers et al., (Desaulniers et al., 2017) provide an overview of GnRHR receptor 2 expression throughout the mammalian species. They discuss its structure and

the discovered biological roles, which are varied and are not connected to pituitary gonadotroph actions. The receptors in the brain may play a role in the organization of interactions between nutritional status and sexual behavior, whilst the receptors in the gonads have been linked to the regulation of reproduction by increasing steroidogenesis. Both types of receptors may play a part in the regulation of sexual behavior.

Oscillatory alterations in electrical activity and voltage-gated calcium influx accompany the activation of protein kinase C and InsP3 by GnRH receptor in gonadotrophs. In addition to directing transcription of several genes and gonadotropin secretion, these receptors activate a variety of mitogen-activated protein kinases. Mammalian GnRH receptors have a greater resistance to desensitization and internalization than GnRH receptors found in other vertebrates and G-protein coupled receptors because they lack a C-terminal tail. This oddity prompted studies on GnRH receptor trafficking, which led to the discovery of mutations influencing human fertility. Additionally, the GnRH ligand-receptor system has emerged as a promising therapeutic target for the treatment of some malignancies, most notably prostate cancer.

Follicle-stimulating hormone (FSH; follitropin), luteinizing hormone (LH; lutropin), thyroid stimulating hormone (TSH; thyrotropin), and chorionic gonadotropins (also of interest to reproductive physiology, but whose presence has been demonstrated only in primates and equids) are all members of the glycoprotein hormone family. Although it has been known for some time that glycoprotein hormones consist of two distinct subunits, the first evidence of noncovalently connected subunits was not discovered until the work of Li and Starman (Li and Starman, 1964), who demonstrated that acid dissociation of ovine LH decreased the molecular weight by almost half. According to a study showing structural findings, researchers hypothesized that the glycoprotein hormone subunits were distinct from one another (Ward et al., 1966). It a study proposed a model of LH, it was noted that it consists of two different chains of similar molecular structures. Crystal structures discovered for hCG corroborated this finding since the part of the molecule that could be seen by x-ray crystallography was

around the same size as oLH. As a result, the stated structures for the β subunit are 65 x 25 x 20 Å while the dimensions for hCGα are 60 x 25 x 15 Å (Wu et al., 1994).

Papkoff and Samy (Papkoff and Samy, 1967), who offered a two-phase technique for separating the different subunits by countercurrent distribution, gave the next crucial piece of information on the subunit tale. Recombination of the dissociated subunits restored around 20% of the original activity, whereas the subunits retrieved had activity on the order of 7% to 8% of the original oLH. Also noteworthy was the realization that the two subunits had distinct amino acid profiles. Around the same time, DeLaLlosa and Jutisz (De la Llosa and Jutisz, 1969) discovered that the subunits of oLH may be dissociated by urea or guanidine hydrochloride with practically total loss of action. For example, in one experiment, reassociation of the component dimer restored activity to almost 98% of its pre-dissociation state.

In subsequent work, the researchers implemented a further subunit separation approach (Lamkin et al., 1970), which proved helpful in preliminary structural investigations. C- and N-terminal amino acid investigations on subunits were made possible, as well as a comparison of subunits generated using this method with the Papkoff-Samy method (Papkoff and Samy, 1967). At the same time, researchers discovered that additional glycoprotein hormones included diverse constituents as well. Two laboratories have reported results for hCG (Morgan and Canfield, 1971; Swaminathan and Bahl, 1970). The breakdown of propionic acid in studies of bTSH showed its subunit structure (Liao and Pierce, 1970), as did studies of bTSH using counter-current distribution. The TSH subunit of Liao and Pierce was shown to be essentially similar with the S-subunit of Ward (Lamkin et al., 1970) or the CI-subunit of Papkoff and Samy (Papkoff and Samy, 1967) for oLH, making this study a landmark in our knowledge of the glycoprotein hormones. Indicative of this finding was the amino acid sequence identified by Liao and Pierce around the carbohydrate moieties of oLH (WARD et al., 1969) and TSH. Most importantly, it was shown that the CI or S-subunit of LH may reunite with the TSH to generate an active version of TSH. This finding laid the foundation for the "common subunit" hypothesis for glycoprotein hormones, which has greatly aided our knowledge of their chemistry and physiology. Based on these findings, Pierce and

colleagues (with widespread agreement) suggested the design of a common subunit and hormone-specific subunits (Pierce et al., 1971). Since then, we've called these peptide hormones "glycoproteins," and nothing has changed.

1. GnRH receptor signaling pathways in Gonadotropes

1. 1. Mitogen-Activated Protein Kinase (MAPK) / Extracellular Signal-Regulated Kinase 1/2 (ERK) Signaling Pathway.

Following the activation of Gq/11 proteins by the GnRH receptor, the phospholipase Cβ (PLCβ) enzyme is then stimulated. PLCβ, then, cleaves phosphatidylinositol-4-5-bisphosphate (PIP2) into inositol trisphosphate (IP3) and diacylglycerol (DAG) (Naor, 2009). According to Tsutsumi and Webster (Tsutsumi and Webster, 2009), IP3 causes an increase in the amount of calcium that is released from the endoplasmic reticulum into the cytosol, while DAG activates protein kinase C (PKC). Ca2+ is also responsible for the activation of some PKC isoforms, including PKC, PKCI, PKCII, and PKC (Kishimoto et al., 1989). Many studies have demonstrated that GnRH produces elevated intracellular calcium levels and PKC activation, which may activate various MAPK pathways in gonadotropes. (Bliss et al., 2010; Caunt et al., 2006; Naor, 2009). According to Murphy and Blenis's research (Murphy and Blenis, 2006), MAPKs have the ability to enter into the nucleus and activate a number of transcription factors.

It has been shown that activation of the family members MAPK1/3 (extracellular signal-regulated kinase, ERK1/2), MAPK8/9 (c-Jun N-terminal kinase, JNK1/2) and MAPK14 (p38-α) is what mediates the transcription of GnRH-induced gonadotropin subunit (Ando et al., 2001; Bernard et al., 2010; Burger et al., 2004; Haisenleder et al., 2008; Kanasaki et al., 2012; Naor and Huhtaniemi, 2013). According to Pearson, Robinson, Beers Gibson et al., research (Pearson et al., 2001), the MAPK kinase (Raf1), MAPK kinases (MEK1 and MEK2), and MAPKs (ERK1 and ERK2) are the components that make up the ERK pathway. However, a study using mice with a pituitary-targeted deletion of Raf1 indicated that Raf1 might not be necessary for ERK activation in gonadotropes (Bliss et al., 2012). This was proved by the

fact that the animals still had normal reproductive function. Furthermore, it has been shown that activation of ERK1/2 may be enhanced through a route that also involves c-Src and Ras (Kanasaki et al., 2012). This pathway was discovered by Kanasaki et al. GnRH, on the other hand, activates c-Src and Rac1/Cdc42, which, in turn, activates MAP4K (Harris et al., 2002). This stimulation of JNK and P38 pathways is what ultimately leads to the activation of MAP4K. According to Naor (Naor, 2009) and Pearson et al., (Pearson et al., 2001), these compounds first activate MAPK kinases, namely MKK4/7 and MKK3/6, which then activate JNK and p38, respectively. In response to pulsatile GnRH, these MAPK cascades, particularly the ERK pathway, have been shown to be involved in the regulation of Fshb and Lhb promoter activity (Kanasaki et al., 2005).

ERK1/2 phosphorylation was shown to be more fast and maintained in perifused LT2 cells and primary gonadotropes after stimulation with low rather than high GnRH pulse frequencies (Haisenleder et al., 1998; Kanasaki et al., 2005). Furthermore, phosphorylated ERK has been shown in higher levels in nucleus after a stimulation of low GnRH pulse frequency. It has been suggested that ERK phosphorylation is necessary for the GnRH pulse frequency-dependent differential stimulation of Fshb and Lhb expression, as shown by the distinct activation/inactivation patterns of ERK in response to various GnRH pulse frequencies (Kanasaki et al., 2005).

Many prior investigations have revealed the relevance of the ERK-dependent transcription factor, early growth response-1 protein (Egr1), for Lhb production (Dorn et al., 1999; Fortin et al., 2009; Halvorson et al., 1999; Lawson et al., 2007; Lee et al., 1996; Wolfe and Call, 1999). The involvement of ERK signaling in promoting GnRH-induced Fshb expression, on the other hand, is more debatable, despite the fact that ERK phosphorylation and Fshb expression have a similar pattern. Pharmacological suppression of MEK1, which is a kinase that stimulates ERK1/2, inhibited the activation of GnRH-induced ovine, murine, rat, and human Fshb/FSHB promoter in LβT2 gonadotropes (Bernard et al., 2010; Bonfil et al., 2004; Burger et al., 2008; Coss et al., 2007; Coss et al., 2004; Kanasaki et al., 2005).

Furthermore, MEK1 inhibition inhibited GnRH-stimulated Fshb expression in perifused male rat primary pituitary cells (Haisenleder et al., 1998). It has been found that inhibition of MEK1/2 at both high

and low GnRH pulse frequencies significantly reduced the activation of Fshb and Lhb gene expression by pulsatile GnRH (Kanasaki et al., 2005; Thompson et al., 2016). These findings show that ERK1/2 may play a role in GnRH-induced Lhb and Fshb gene expression. In vivo investigations using gonadotrope-specific ERK1/2 double knock-out mice, on the other hand, revealed only a modest reduction in the expression and secretion levels of Fshb, with acute influences on Lhb expression and secretion (Bliss et al., 2009). These findings suggest that ERK1/2 is more critical for the regulation of LH than FSH in vivo, or that alternative signaling pathways that are activated in response to GnH recompense for ERK1/2 deficiency in these animals.

A putative function for MAPK phosphatases as a modulator of this differential activity is suggested by the varied ERK phosphorylation pattern that occurs in response to various frequency of GnRH pulses. According to Kanasaki et al., (Kanasaki et al., 2012) MKPs are a kind of phosphatase that are responsible for the inactivation of MAPKs via the dephosphorylation of threonine and tyrosine residues. In gonadotropes, activating ERK and JNK enhances the activity of MKP1 and MKP2 (DUSP1 and DUSP4 respectively), which subsequently inactivates ERK, JNK, and p38 (Franklin and Kraft, 1997; Kondoh and Nishida, 2007; Zhang et al., 2001a). An upregulation of MKP1 and MKP2 expression was seen upon the activation of GnRH receptor in both in vitro studies conducted on αT3-1 cells and in vivo research carried out on mice (Zhang and Roberson, 2006). In addition, research conducted in perfused LβT2 cells revealed an increase in MKP1 expression after a high stimulation of GnRH pulse frequency (Nguyen et al., 2010; Purwana et al., 2011). This regulatory pattern is unique in comparison to the activation of ERK1/2, which is more immediately triggered and more maintained when low frequency GnRH pulses are applied (Kanasaki et al., 2005). It was shown by Nguyen et al., (Nguyen et al., 2010) that activation of ERK and Lhb promoters was inhibited when MKP1 overexpressed in LβT2 gonadotropes, whereas MKP1 knockdown using the same cell type led to elevating the activation of ERK and the expression of Lhb in response to GnRH stimulation.

These data, when taken together, point to a possible function for MKPs within a negative feedback loop that regulates MAPK activity in response to varying GnRH pulse frequency. However, a

research that was conducted by Armstrong and colleagues that used live cell imaging to monitor ERK2-GFP translocation in heterologous HeLa cells provides evidence that contradicts the possibility that this may play a role. following using pharmacological and molecular genetic techniques to decrease MKP activity, the researchers revealed that there was either very tiny or no influence on the fast and temporary ERK2-GFP translocation to the nucleus following pulsatile stimulation with GnRH (Armstrong et al., 2010).

1. *2. Wnt/β-Catenin Signaling pathway*

The majority of GnRH signals are sent by protein kinase C (PKC), which then stimulates several MAPK cascades (Benard et al., 2017; Bonfil et al., 2004; Dobkin-Bekman et al., 2006; Haisenleder et al., 2008; Harris et al., 2002; Harris et al., 2003; Levi et al., 1998a; Liu et al., 2002; Mulvaney and Roberson, 2000; Reiss et al., 1997; Roberson et al., 2005; Roberson et al., 1995; Roberson et al., 1999; White et al., 1999; Xie et al., 2005). Many DNA-binding proteins that intermediate the action of GnRH on primary, secondary, and tertiary response genes are activated by these MAPK cascades. In LβT2 cells, GnRH enhances the association of β-catenin and SF1 to the endogenous Lhb promoter-regulatory region (Gardner et al., 2007; Salisbury et al., 2007), as shown earlier. This raises the intriguing possibility that crosstalk between GnRH's G-protein coupled receptor pathway and the classical WNT/β-catenin signaling pathway controls β-catenin accumulation through GnRH.

The conventional WNT/frizzled/disheveled (Fz/Dvl) route is associated with the transcriptional actions of β-catenin (Gordon and Nusse, 2006; Kikuchi et al., 2006). This pathway promotes the suppression of a multiprotein complex including AXIN, adenomatous polyposis coli, casein kinase I, and glycogen synthase kinase3β (GSK3β). While WNT signaling is essential for the activation of β-catenin, there is mounting evidence that other G-protein coupled receptor signaling pathways, such as those controlled by protein kinase C (Jope and Johnson, 2004), protein kinase A (Hino et al., 2005; Taurin et al., 2006), and phosphatidylinositol 3-kinase (PI3K) (Lilien and Balsamo, 2005), may also activate β-

catenin. Since GnRH regulates β-catenin in gonadotropes by cross talk with the conventional WNT/β-catenin signaling pathway, PKC, PKA, and PI3K should be considered as possibilities that mediate this regulation.

It has been shown that GnRH activation of the TOP flash reporter in LβT2 cells may be prevented by either pretreatment with antide, which is a competitive inhibitor of GnRH, or with a metabolic inhibitor of Gαq/11 (Gardner et al., 2007). Based on these findings, it seems that GnRH could control β-catenin through acting on the signaling pathway mediated by PKC. Another paper indicates that PKC may increase phosphorylation, and as a result, inactivation of GSK3 (Jope and Johnson, 2004), which is similar with the findings presented here. A strong correlation between GnRH-induced increases in accumulation of β-catenin and S9 phosphorylation of GSK3β has been shown in LβT2, leaving open the possibility that GnRH may signal through the PKC pathway to inhibit activity of GSK3β (Ferris and Shupnik, 2006; Mulvaney and Roberson, 2000; Mulvaney et al., 1999), whereas Gardner and colleagues (Gardner et al., 2007) were unable to observe GnRH-dependent changes in GSK3β phosphorylation in LβT2 cells. GnRH also activates a significant signaling cascade including calcium-mediated single transduction through protein kinase C (Ferris and Shupnik, 2006; Mulvaney and Roberson, 2000; Mulvaney et al., 1999). Thus, this signaling molecule may also play a part in gonadotropes, where it regulates GnRH's effects on β-catenin.

2. Transcriptional regulation of gonadotropin subunits by GnRH

GnRH controls transcription of at least 75 genes (Benard et al., 2017; Bonfil et al., 2004; Dobkin-Bekman et al., 2006; Harris et al., 2002; Harris et al., 2003; Liu et al., 2002; Mulvaney and Roberson, 2000; Reiss et al., 1997; Roberson et al., 2005; Roberson et al., 1995; Roberson et al., 1999; Ruf et al., 2003; Ruf and Sealfon, 2004; White et al., 1999; Wurmbach et al., 2001; Xie et al., 2005; Yuen et al., 2002) by sending signals across several MAPK cascades. Based on the speed with which they respond to GnRH, the genes under its control may be categorized as "primary," "secondary," and "tertiary." Four tertiary gonadotrope signature genes (Cga, Lhb, Fshb, and Gnrhr) are expressed at certain times in

response to the GnRH transcriptional signal. The immediate early gene (IEG) family (Murphy et al., 2004) includes Egr1, Jun, and Atf3. EGR1, a member of the IEG zinc-finger C2H2 subfamily, is related to JUN and activating transcription factor 3 (ATF3), all of which are related to the IEG basic leucine zipper subfamily. The IEGs are typical main response genes because of the rapid transcriptional responses to GnRH stimulation (Wurmbach et al., 2001; Yuen et al., 2002). Their accumulation, as DNA-binding proteins, transmits GnRH responsiveness to secondary and tertiary genes that have the necessary DNA response elements. As EGR1 accumulates, it promotes transcription of secondary response genes such MAPK phosphatase 2 (Mkp2), also known as dual specificity phosphatase 4 (Dusp4) (Zhang et al., 2001b), and eventually Lhb (Buggs et al., 2006; Call and Wolfe, 2002; Dorn et al., 1999; Kaiser et al., 2000; Mouillet et al., 2004; Tremblay and Drouin, 1999; Weck et al., 2000). EGR1 is also involved in the regulation of primary response genes such as Atf3 (Bottone et al., 2005; Yamaguchi et al., 2006) and has a positive autoregulatory loop with its own gene (Adamson et al., 2005; Yu et al., 2004). Thus, EGR1 gives GnRH responsiveness to a number of genes that comprise the gonadotrope's hierarchical transcriptional network, including one of the hallmark genes, Lhb.

Through activator protein 1 (AP1), GnRH also imparts hormonal responsiveness to three (Cga, Fshb, and Gnrhr) of the four tertiary genes (Coss et al., 2004; Norwitz et al., 2002; Savage et al., 2003; Strahl et al., 1998; Vasilyev et al., 2002; White et al., 1999; Xie et al., 2005). GnRH increases AP1 activity via signaling through JUN N-terminal kinase (JNK) (Bonfil et al., 2004; Ellsworth et al., 2003; Xie et al., 2005), and JUN is always present in AP1 heterodimers (Toualbi et al., 2007). In addition to creating a heterodimer with JUN and binding to tandem cAMP response sites in the human promoter (Xie et al., 2005), ATF3 also contributes GnRH responsiveness to Cga. GnRH signaling through ERK and JNK further stimulates ATF3 protein activity and mRNA expression (Xie et al., 2005). In the same way, as EGR1 creates a positive autoregulatory loop with its own gene (Angel et al., 1988), so does JUN. Not only do these genes interact with one another, but the GnRH transcriptional signal also loops back to downregulate certain MAPK cascade members (Zhang and Roberson, 2006; Zhang et al., 2001b).

Inactivation of JNK and partial inactivation of ERK are the final results of GnRH-stimulated elevations in Mkp2/Dusp4 (Zhang and Roberson, 2006).

2. 1. The Orphan Nuclear Receptor (SF1)

All four signature genes have response elements that are specific to the orphan nuclear receptor SF1 in their respective promoter regions (Savage et al., 2003). Despite the fact that the orphan nuclear receptor seems resistant to activation by the neurohormone (Dorn et al., 1999; Halvorson et al., 1998; Kaiser et al., 2000; Salisbury et al., 2007; Tremblay and Drouin, 1999), SF1 plays an essential part in the GnRH transcriptional network (Ikeda et al., 1995; Zhao et al., 2001a, b). For example, pulses of GnRH control the transcription of mammalian Lhb genes in a dynamic manner (Bédécarrats and Kaiser, 2003; Ferris and Shupnik, 2006; Haisenleder et al., 2008; Kaiser et al., 1997). However, this dynamic regulation is a tertiary response to GnRH, and it is mediated by a faster activation of Egr1 transcription and protein synthesis (Ruf et al., 2003; Ruf and Sealfon, 2004; Tremblay and Drouin, 1999; Wurmbach et al., 2001; Yuen et al., 2002). EGR1 is considered to be the key determinant of hormone-induced transcriptional fluxes of Lhb (Dorn et al., 1999; Halvorson et al., 1998; Kaiser et al., 2000; Salisbury et al., 2007; Tremblay and Drouin, 1999). This is due to the fact that levels of SF1 continue to be resistant to changes in GnRH. However, GnRH stimulation of EGR1 is insufficient to ensure that LH reaches the essential levels needed for physiological activity in transgenic mice with SF1-deficient gonadotropes (Zhao et al., 2001a, b). In these animals, GnRH activation of EGR1 is insufficient to guarantee that LH will reach the necessary levels. These mice are sterile due to a hypogonadal state, inability to express measurable quantities of Cga, Lhb, Fshb, and Gnrhr, and lack of expression of these genes (Zhao et al., 2001a, b). On the other hand, contradictory abnormalities have been observed for male EGR1-deficient mice that were produced using various targeting designs. Fertility is affected in one but not the other, even though both have lower LH levels. Lowered levels of LH and Lhb mRNA are consistent with the idea that SF1 operates permissively to make Lhb sensitive to GnRH-induced alterations in EGR1 (Lee et al., 1996; Lee et al., 1995; Topilko et al., 1998).

2. 2. β-Catenin

The transcriptional coactivator β-catenin is often found to be linked with T cell factor (TCF)/lymphoid enhancer factor (LEF)-responsive genes that are controlled by the WNT family of secreted glycoproteins (Gordon and Nusse, 2006; Kikuchi et al., 2006). When β-Catenin binds to TCF/LEF, it triggers the release of histone deacetylase and corepressors like Groucho (officially known as GPRK2), which in turn leads to the recruitment of additional coactivators and chromatin-remodeling proteins like p300/cAMP response element-binding protein binding protein and Brahma-related gene 1 . These collective interactions provide TCF/LEF with the capability to participate in transcription (Barker et al., 2001; Gordon and Nusse, 2006; Hecht et al., 2000; Kikuchi et al., 2006; Olson et al., 2006). Growing evidence suggests that β-Catenin also coactivates a number of other transcriptional proteins. These transcriptional proteins include the androgen receptor (Song et al., 2003; Yang et al., 2002), forkhead box O (Essers et al., 2005), members of the SRY HMG box family (Zorn et al., 1999), and the basic-leucine zipper proteins JUN and FOS (Toualbi et al., 2007). According to further findings, β-Catenin works as a coactivator of SF1 when it transduces WNT signals to Dax1 (formally NR0B1) and inhibin α (officially Inha) (Gummow et al., 2003; Mizusaki et al., 2003). Furthermore, β-Catenin binds to a cluster of amino acids (235-238) in the first helix of the putative ligand-binding domain of the orphan nuclear receptor containing the activation function 1 domain (Desclozeaux et al., 2002; Mizusaki et al., 2003), resulting in the coactivation of SF1. Additionally, Increases in aromatase gene expression in granulosa cells in response to FSH have been found to be mediated by β-catenin (Parakh et al., 2006). This occurs via an interaction with SF1. Taken as a whole, these studies raise the possibility that β-Catenin is a crucial coactivator for several SF1-dependent genes.

β-Catenin and SF1 have been shown to interact functionally in order for GnRH to regulate Lhb gene expression in LβT2 cells generated from gonadotropes (Salisbury et al., 2007). There were many pieces of evidence that added up to this conclusion: Overexpression of axin 1 (AXIN) or usage of a pool of short interfering RNA specific for β-Catenin decreased the GnRH-stimulated activity of an LHB

promoter reporter construct in LβT2 cells; The transactivation activity of SF1 and EGR1, as well as their functional relationship, were both enhanced by β-Catenin overexpression; in contrast, the activity of SF1 and EGR1 was suppressed by β-Catenin short interfering RNA; both β-Catenin's accumulation and the physical association with SF1 were increased by GnRH using coimmunoprecipitation assay; In a dominant-negative form, an SF1 mutant missing a β-Catenin binding site nearly totally eliminated the synergism commonly seen between SF1 and EGR1 (Dorn et al., 1999; Halvorson et al., 1998; Mouillet et al., 2004; Tremblay and Drouin, 1999); and β-Catenin, which binds SF1 and EGR1, was shown to be more colocalized with the mouse Lhb gene's endogenous promoter region after GnRH stimulation. These findings all point to -Catenin's role as a crucial coactivator of SF1, which in turn makes the Lhb gene sensitive to GnRH-induced alterations in EGR1.

It has been hypothesized that the Lhb gene is kept in a condition ready to react to GnRH through the interaction of -Catenin and SF1, with assistance from PITX1, another important DNA-binding protein (Quirk et al., 2001; Tremblay and Drouin, 1999; Tremblay et al., 1999). In this poised condition, Lhb transcription is at low levels, comparable to the quantity of light produced by a light dimmer with its controller turned on but set at a low level. GnRH functions as a rheostat, shifting transcription from a quiescent to an active state by elevating EGR1 concentrations. Since the elevation of EGR1 in response to GnRH is only temporary and is concentration-dependent during pulsatile neurohormone secretion (Haisenleder et al., 2008; Kaiser et al., 1997; Kanasaki et al., 2005; Yuen et al., 2002), the transcriptional activity of the Lhb gene must revert to the poised state when the concentration of the zinc-finger IEG declines. Cga, Fshb, and Gnrhr expression all need SF1 (Zhao et al., 2001a, b), as was previously noted.

2. 3. TCF gene family

Several genes known to be TCF target genes are influenced by GnRH, including Jun, Fra1, and Myc (Gardner et al., 2007; Kikuchi et al., 2006; Nateri et al., 2005; Wurmbach et al., 2001; Yuen et al., 2002). The nucleus accumulation of β-catenin and the activity of a synthetic TCF-dependent reporter construct (TOP flash) have been linked to increases in the mRNAs produced by these three genes after

GnRH stimulation in LβT2 cells (Gardner et al., 2007), indicating that a functional link between β-catenin and members of the TCF gene family is necessary for GnRH-regulated expression of Jun, Fra1, and Myc. If that's the case, the GnRH-TCF pathway may have secondary targets in the JUN-responsive signature genes (Cga, Fshb, and Gnrhr).

Additional investigations showing that GnRH-regulated expression of Cga, Fshb, and Gnrhr is subordinate to β-catenin- and TCF-dependent regulation of Jun transcription are necessary to definitively confirm the hierarchical arrangement of β-catenin and TCF. The fact that TCF, JUN1, and JUN2 response elements are found in the Jun promoter-regulatory region (Nateri et al., 2005) lends credence to this hypothesis. TCF/LEF sensitive genes including Jun have been found in hematological and colon cancer cells (Mann et al., 1999; Staal et al., 2004). Cooperative transcriptional activation by β-catenin, JUN, and TCF within the framework of the Jun promoter. When tested with chromatin immunoprecipitation (ChIP), all three of these proteins bind to the Jun promoter (Nateri et al., 2005). Taken together, these studies indicate that GnRH-induced alterations in β-catenin may target Jun as a main TCF/LEF gene target. The importance of investigating this option stems from the fact that many published researches on gonadotropes has concentrated on the signaling pathways that connect GnRH to the terminal phosphorylation of JUN by JNK (Levi et al., 1998a; Mulvaney and Roberson, 2000; Xie et al., 2005).

3. Communication in Gonadotropes

3. 1. Gap Junctions

Transmembrane channels known as gap junctions (GJ) enable the unrestricted movement of cytoplasmic molecules across cells. These molecules must have a molecular weight of less than 1,000 daltons. Intercellular communication by GJ is a significant source in the transfer of cytoplasmic components (including water and ions), metabolic substrates (such as carbohydrates, amino acids, and nucleotides), and second messengers (primarily calcium, IP3, and cAMP) across cells. Gap junctions are an essential method of communication in the pituitary glands of all animals that have been investigated.

For instance, it has been shown that gap junctions are responsible for the coupling of fish pituitary cells (Golan et al., 2016a; Levavi-Sivan et al., 2005). In the rat, cells exhibit a high amount of intercellular coupling via gap junctions, which is where lucifer yellow diffusion was discovered up to 300 microns distant from the site of injection (Morand et al., 1996). In addition, the movement of materials between cells took place most prominently in lactotrophs, somatotrophs, and folliculostellate cells (FS cells). A very small percentage of LH, TSH, and ACTH cells were tagged (Morand et al., 1996). Gap junctions enable the coordinated transmission of signals and the establishment of cell networks (Abraham et al., 1979; Fauquier et al., 2001; Fletcher et al., 1975; Golan et al., 2016b; Göngrich et al., 2016; Herbert, 1979; Hodson et al., 2012b; Le Tissier et al., 2017; Soji and Herbert, 1989, 1990; Wilfinger et al., 1984), and they are thus widely regarded as essential in the coupling of pituitary cells in all animals. Gap junctions play a crucial role in the synchronization of electrical activity inside cells, as shown by Guérineau and colleagues (Guérineau et al., 1998). These clusters of pituitary cells were detected by the authors using multicellular assessment of spontaneous intracellular calcium mobilization in tissue preparations; they were also shown to be spatially contiguous and rhythmically coactive. In addition to the observation that a gap-junction blocker reduces the spread of synchronization, it was found that small molecules (Lucifer yellow, 457 Da) but not large molecules (Texas Red, 3000 Da) spread between the co-active cells, leading to the conclusion that coordination between neighboring secretory cells is mediated by gap junctions.

3. 2. Folliculostellate Cells

The pituitary gland has a glial-like cell population known as the FS cell network in all major taxa of extant vertebrates (Allaerts and Vankelecom, 2005; Borst et al., 1996; Golan et al., 2016a; Nishimura et al., 2017; Wada et al., 2014). In mammals, the FS cell network accounts for around 5-10% of the anterior pituitary cell mass and has no endocrine function. In mammals (Fauquier et al., 2001; Soji et al., 1997), birds (Nishimura et al., 2017), amphibians (Gracia-Navarro et al., 1983), and fish (Golan et al., 2016a), the gland is lined by a 3D anatomical network of agranular cells that have a distinctive stellate

structure and lengthy cytoplasmic extensions. FS cells have the potential to have paracrine effects and regulate the activity of nearby hormone-secreting pituitary cells (Denef, 2008), as they produce growth factors and cytokines in response to a wide range of external and internal stimuli, including fibroblast growth factor (FGF)-2, vascular endothelial growth factor (VEGF)-A, follistatin, and interleukin (IL)-6. It has been shown that FS cells in mammals are able to produce distinct responses in a network of endocrine cells that are surrounded by their cytoplasmic processes, resulting in functional clusters (Foster and Younglai, 1991; Shirasawa et al., 1983; Shirasawa et al., 2007). It is interesting to note that it has been shown that the projections of GnRH-neurons converge not only at the blood capillaries but also close to FS cells in the pars tuberalis (Foster and Younglai, 1991; Hattori et al., 2013). In spite of this, gap junctions between the GnRH neuron terminals and FS cells, as well as a GnRH-induced calcium response in FS cells, have been observed (Hattori et al., 2013; Mabuchi et al., 2004; Shirasawa et al., 2004).

3. 3. Paracrine Communication

The term "paracrinicity" refers to the process by which cells in the same tissue may communicate with one another via the release of certain chemicals. It is possible for the substance to accomplish its objective by diffusion in the extracellular space or through the development of direct contact (juxtacrine factors). It has been shown that the pituitary contains over a hundred chemicals that are neither autocrine nor paracrine factors. They consist of neurotransmitters, growth factors, cytokines, tissue factors such as annexin-1 and follistatin, hormones, ATP, and NO, amongst other substances (Denef, 2008). The vast majority of paracrine or juxtacrine molecules act through G protein coupled receptors, with inhibitory (Gi) or excitatory (Gs) action, activating in the majority of instances voltage gated channels activity and intracellular [Ca2+], in addition to a whole host of other receptor types that are capable of affecting down-stream kinase and protein phosphorylation status (Hodson et al., 2012a). Denef provides a comprehensive analysis that outlines the paracrine interactions that take place in the pituitary gland of animals (Denef, 2008). The first evidence of a potential paracrine interaction between endocrine cells was developed from gonadotrophs and lactotrophs, where the stimulation of gonadotrophs secretion by GnRH

prompts prolactin secretion (PRL) (De Paul et al., 2000). This was the first evidence of a possible paracrine relationship between endocrine cells.

Gonadotrophs and LH secretion throughout the estrous cycle are another example of a process in which the hypothalamic control of the pituitary does not account for the change in hormone release. Differential production of LH and FSH throughout the reproductive cycle (Herbison et al., 2008) is required for follicle development and ovulation in females. The GnRH surge, the primary stimulating factor of gonadotrophs in the hypothalamus, is thought to cause the shift in the pattern of LH pulse secretion into a surge mechanism that occurs during proestrus. However, GnRH stimulation is not the actual cause of the dramatic rise in gonadotroph responsiveness and production (Herbison et al., 2008; Leong and Thorner, 1991). It has been found that during diestrus, only a tiny percentage of gonadotrophs exhibit intracellular calcium activity in response to GnRH in vitro (Leong and Thorner, 1991). At this stage of the reproductive cycle, high doses of GnRH (100 to 1,000 nM) are required to generate the whole-population response, although there is no significant rise in LH production. In contrast, the majority of gonadotrophs release a greater quantity of LH during proestrus, and even modest GnRH concentrations are enough to stimulate a full population response. In addition to GnRH receptor expression, the gonadotroph network's reconfiguration and its association with the vasculature are essential for the increase in gonadotroph responsiveness and LH secretion that occurs during proestrus (Alim et al., 2012). Ex vivo investigations, in which tissue contacts are maintained, show that the gonadotroph network is dynamic and malleable, adjusting to the demands of proestrus by increasing the number of its cells (likely by cell proliferation and trans differentiation). Gonadotrophs also boost cell motility and the number of cell protrusions produced in the direction of other gonadotrophs and the blood vessels (Alim et al., 2012; Edwards et al., 2017a). This modulation in the rhythm and manner of LH production at various times of the reproductive cycle may be attributed to the estrous cycle-related variations in cell sensitivity to GnRH. Comparative studies of the processes of gonadotrope cell plasticity in fish and mammals have been conducted at the molecular, cellular, and population levels (Childs et al., 2020; Fontaine et al., 2020). As inputs from the reproductive axis and the environment are processed

within the network, the system output is either enhanced or diminished demonstrating context-dependent canalization of plasticity in gonadotrophs. Examples include testosterone, estradiol, and GnRH, all of which have been shown to stimulate LH secretion, cell proliferation, and GnRH receptor expression at specific concentrations and rhythms, but which, when present for longer periods of time or at higher concentrations, may desensitize the network and inhibit LH production and secretion (Durán-Pastén and Fiordelisio, 2013; Fontaine et al., 2020).

A comprehensive understanding of the processes involved in the gonadotroph function as a network requires the participation of the majority of the components involved in the network's creation, but this alone is insufficient. Because the intrinsic activity of gonadotrophs is not highly coordinated and is not connected with gonadotropin secretion (Stojilkovic et al., 2017), GnRH is a factor that is responsible for triggering the network response. Furthermore, the quantity of gonadotropin secretion is affected by the hormonal equilibrium within the reproductive axis, which involves a reorganization of the network connections. This shift is related with the GnRH stimulus, but it is not an immediate consequence of the stimulation (Alim et al., 2012; Edwards et al., 2017a). This connectivity is created primarily by means of soma-soma contact and cytoplasmic extensions, both of which are associated with gap junction-mediated intercellular communication or cytosolic connection. On the other hand, if the gonadotroph network is exclusively wired via cell-cell contact, then one may anticipate that cells that are located in close proximity to one another should display a similar pattern of response and create clusters where degrees of synchronization may be at their maximum (Göngrich et al., 2016; Hodson et al., 2012b). Paracrine communication and connectivity with FS cells also play an important role in network function (Bilezikjian et al., 2003; Childs et al., 1992a; Denef, 2008), as shown by the analysis of clusters by correlation in the patterns of calcium mobilization, which reveals that cells at a distance respond to GnRH similarly while cells in contact with or surrounded by capillaries may exhibit different responses. In addition, the gonadotroph network's structural and functional connections are malleable and undergo remodeling during the estrous cycle, likely in response to physiological demand during proestrus when LH levels are elevated (Alim et al., 2012). Further research is needed to understand the wide range of

chemicals and processes that go into network development, their proportional contributions, and the extent of their plasticity.

The analysis of the proteins that were shown to be associated with intercellular communication using a non-biased quantitative proteomic screen of clonal αT3-1 gonadotropes revealed that GnRH increased the plasma membrane association of numerous actin cytoskeletal, cell polarity and adherens junction-related proteins, which included the scaffold protein IQGAP1 and the small GTPase Rac1, Ptk7 and others, suggesting a novel mechanism in which Rac1-containing IQGAP1 signaling complexes modulate GnRH-dependent ERK activation in αT3-1 gonadotropes and serve as essential effectors for signaling events leading to an enrichment of cell-cell contacts. Therefore, we addressed a hypothesis investigating PCP and cell-cell adhesion associated proteins, including IQGAP1, and characterizing it's contribution to GnRH signaling cascades leading to altered patterns of gene expression, cytoskeletal remodeling, and cell mobility which culminate in coordinated intergonadotrope communication and function.

The IQGAP protein family has been passed down through the eukaryotic evolutionary tree (Abel et al., 2015b; Brown and Sacks, 2006; Hedman et al., 2015; Johnson et al., 2009; Malarkannan et al., 2012; Osman et al., 2013; Sanchez-Laorden et al., 2013; Smith et al., 2015; Stuart and Sellers, 2013; White et al., 2012; Wu and Chen, 2014). They perform the role of scaffold proteins, which enable the development of complexes that control the dynamics of the cytoskeleton as well as the signaling that occurs inside the cell. Because of their importance to both fundamental biology and human illness, IQGAP proteins have been the subject of much research. IQGAP1, which was discovered for the first time in 1994 (Weissbach et al., 1994), is the founder member of a family that contains three paralogs in humans (IQGAP1, IQGAP2, and IQGAP3). It is also the member of this family that has been investigated the most. Mammalian IQGAP1 orthologs have a length of about 1600 amino acids and include several domains that have the ability to influence interactions between proteins, which is consistent with the function that they are thought to play as scaffold proteins. The first suggestion of a scaffolding role for

IQGAP1 was observed when it was discovered that IQGAP1 connected Ca2+/calmodulin signaling with Cdc42 signaling (Briggs and Sacks, 2003b; Ho et al., 1999b; Osman and Cerione, 1998). It has also been hypothesized that IQGAP serves as a scaffold in the Wnt pathway (Carmon et al., 2014). Interactions with components of the RAS/MAPK pathway, however, provide possibly the best-known example of IQGAP1's scaffold role. Multiple MAPK kinases, including ERK1 and ERK2, as well as MEK1 and MEK2 (which activate ERK1 and ERK2), have been reported to bind to IQGAP1. Multiple receptor tyrosine kinases including the MEK activator BRAF have been demonstrated to bind to IQGAP1, indicating that this protein serves as a center for upstream MAPK pathway components.

Years after IQGAP1's initial discovery (Weissbach et al., 1994), more than 130 interacting proteins with a wide range of roles have been uncovered. In all eukaryotes tested, from *Saccharomyces cerevisiae* to humans, IQGAP proteins have been shown to be expressed. Three isoforms of IQGAP are expressed in mammals (Brill et al., 1996; Wang et al., 2007; Weissbach et al., 1994). IQGAP1, IQGAP2, and IQGAP3 have a similar domain composition but have different activities, tissue expression, and subcellular localization. IQGAPs control a wide range of biological processes; for example, IQGAP1 has been extensively reviewed in relation to its roles in the cytoskeleton (Briggs and Sacks, 2003a; Mateer et al., 2003), cell-cell adhesion (Kaibuchi et al., 1999a), Ca2+ and small G-protein signaling (Briggs and Sacks, 2003a), protein trafficking (Osman, 2010), neoplasia (Johnson et al., 2009; White et al., 2009), and microbial pathogenesis(Kim et al., 2011). IQGAPs control several signaling pathways through protein-protein interactions mediated by their various domains. IQGAP1 serves as a scaffold and facilitates communication between binding partners in a variety of mechanisms.

In this study, we investigated the involvement of IQGAP1 in GnRH receptor signaling and transcription using αT3 and LβT2 gonadotropes. We observed the previous studies that investigate role of IQGAP1 scaffold protein in different cascades and cell functions and apply our study using GnRH to activate the GnRH receptor in gonadotropes and study IQGAP1 protein level, as well as different

elements with/out knockdown IQGAP1. The following details are to understand IQGAP1 behavior in different signaling cascades, as well as binding partners that could interprets our data.

4. The Molecular Domains Of IQGAPS

IQGAPs have a similar domain structure and share a high degree of similarity in their amino acid sequences. IQGAP1 has 62% amino acid sequence identity with IQGAP2 and 59% with IQGAP3 (Brill et al., 1996; Xie et al., 2015b). Depending on their amino acid sequence, IQGAPs may have six different functional domains. They may attach to different partners and control the temporal and spatial organization of different signal transduction complexes due to their distinct domains (Peng et al., 2021; Watanabe et al., 2015). Calmodulin homology domains (CHDs) located at the N-terminus of IQGAPs are responsible for actin binding (Palani et al., 2021). To further regulate cell division, cell migration, and the integrity of cell-cell interactions (Trenton et al., 2020), the IQGAP1 CHD interacts with actin filaments to influence the cytoskeleton modulation that facilitates actin binding and polymerization. In addition, earlier research using CHD in cultured rat hippocampus neurons has revealed that IQGAP1 actively contributes to spine head formation (Jausoro et al., 2013).

Coiled-coil (CC) domains, also known as heptad domains, are found downstream of the CHD and are characterized by a set of repeating hydrophobic and charged amino acids (Abel et al., 2015b). Because of their CC repeat sequence, IQGAP1 and IQGAP2 are able to bind to the ERM protein family (ezrin, radixin, and myosin), which cross links actin-based cytoskeletons to plasma membranes and engages in various pathways of intracellular signaling (Liu et al., 2014; Tsukita et al., 1994). Furthermore, it has been shown that the CC repeat region of all IQGAPs isoforms drives neuronal growth and spine morphogenesis through interaction with valosin-containing protein (VCP), indicating a critical function of IQGAPs in the pathogenesis of neurological disorders (Itoh et al., 2017). Two functionally conserved tryptophans (W) in the polyproline protein-protein (WW) domain mediate interactions with other proteins, including proline-rich areas. By binding to traditional MAP kinases (MAPK) via a polyproline

motif, the WW domain of IQGAP1 promotes tumor formation, growth, and invasion (Jameson et al., 2013; Roy et al., 2004).

Similar results were shown when Ras-MAPK -mediated oncogenesis and tumor invasion were specifically reduced by disrupting IQGAP1-kinase- linkages by ectopic production of WW peptide in mice. The lifespan of tumor-bearing mice is significantly increased as a result of this impact (Jameson et al., 2013). Contradictory results were published in a subsequent research (Bardwell et al., 2017), which suggested that the WW domain of IQGAP1 was not sufficient nor required for binding to MAPK, but that the IQ domain that immediately precedes the WW domain was.

There are four isoleucine-glutamine (IQ) motifs in tandem in the IQ domain. Calmodulin, a calcium-sensing protein with broad protein target specificity, interacts with this domain (56). Epidermal growth factor receptor (EGFR) is only one of several cell surface receptors known to interact with the IQ domain (Bardwell et al., 2017; Cheung et al., 2013; Jeong et al., 2007; McNulty et al., 2011b; White et al., 2011). Epidermal carcinoma development and invasion are linked to IQGAP1's IQ domain binding to EGFR and activating the MAPK signaling cascade. The addition of a peptide mimicking the IQ motif of IQGAP1 in vivo was shown to suppress the oncogenic signaling pathway and carcinogenesis (Monteleon et al., 2015).

Following the IQ domain is a GTPase activation-related structural domain (GRD), which is the basis for the naming of IQGAPs (Abel et al., 2015b). Specifically, this domain interacts with small GTPases and is significantly similar to the functional elements of Ras GTPase activating proteins (GAPs) (Gorisse et al., 2020; Mosaddeghzadeh et al., 2021; Peng et al., 2021). GRD lacks GAP activity because its crystal structure revealed that threonine substitutes for the catalytic "arginine finger" necessary for GTP hydrolysis (Kurella et al., 2009b). Instead of hydrolyzing GTP, GRD stabilizes the GTP-bound protein in its active form. Mechanistically, the interaction between the GRD domain of IQGAP2 and small GTPases is essential for the polymerization of actin filaments during cancer development (LeCour et al., 2016b; Ozdemir et al., 2018).

Finally, IQGAPs include a RasGAP C-terminal (RGCT) structural domain that binds to many proteins, including E-cadherin and β-catenin, and plays an important role in cell-cell adhesion, cell polarization, and directional migration (Fukata et al., 2002a; Kuroda et al., 1998b; Tocker et al., 2017; Watanabe et al., 2004b). Additionally, IQGAP1 primed tumor cell metastasis and invasion by enhancing extracellular matrix (ECM) degradation via binding to the exocyst subunits through RGCT domain, while removal of the exocyst binding site inhibited the acceleration of IQGAP1-induced ECM degradation (Beaty and Condeelis, 2014; Sakurai-Yageta et al., 2008). This highlights the aggressive function of cytoskeletal remodeling mediated by IQGAP1. The binding of IQGAPs with small GTPases of the Rho family members is also critically dependent on the domains proximal to GRD, as shown by the fact that mutations of the RGCT may drastically disrupt this interaction (Elliott et al., 2012b; Li et al., 2005b; Nouri et al., 2016b; Nouri et al., 2020).

5. IQGAP1 and compartmentalized signaling

Although IQGAP1 seems to be localized at the junction, it may need to rapidly relocalize at certain moments during polarization in order to promote its various functions. The elimination of IQGAP1 at the point where T lymphocytes dock with malignancy cells is one such instance. Docking and the release of lytic granules toward the cancer cell need IQGAP1 to rapidly relocate away from the centriole docking site and the actin patch during T cell activation (Stinchcombe et al., 2006). Rapid IQGAP1 (and actin) depletion initiates the formation of an asymmetric compartment with rapid vesicle movement, comparable to a cilia transition zone (Stinchcombe et al., 2006; Stinchcombe et al., 2015). Asymmetric protein expression, secretion, activation of receptors, and trafficking occur along the apical/basolateral boundary defined by tight junctions. As a result, TJs allow for the compartmentation of signals between the apical and basolateral plasma membrane domains in polarized epithelia. IQGAP1 may act as a molecular filter for asymmetrical signaling at tight junctions and the immunological synapse. Protein trafficking to the ciliary transition zone is impeded by a diffusion barrier formed by Septin (Mellman and Nelson, 2008; Rittmeyer et al., 2008b), which has been found to interact with IQGAP1 (Hu

et al., 2010). Furthermore, IQGAP1 may serve as a quality control (QC) mechanism by modulating the temporal and spatial regulation of vesicular trafficking and growth factor receptor activation, or by controlling the rate at which TJs develop or immune cells dock. Since increased IQGAP1 expression results in weaker junctional strength and altered cellular architecture, it is probable that this QC mechanism needs meticulously managed IQGAP1 levels. In support of this, it has been shown that IQGAP1 KD cells had a more columnar shape and a significant increase in cell height, likely due to greater junctional strength (Tanos et al., 2015).

6. IQGAP impacts transcription

Despite its largely cytoplasmic nature, growing evidence suggests IQGAP1 also plays a role in the nucleus. During the G1/S phase of the cell cycle, IQGAP1 interacts with a number of nuclear proteins and accumulates in the nucleus (Johnson et al., 2011). IQGAP1 has been shown to regulate transcription in many studies.

Different transcription factors, including as estrogen receptor (ERα) (Erdemir et al., 2014), nuclear factor erythroid 2 related factor 2 (Nrf2)(Kim et al., 2013), and nuclear factor of activated T-cells 1 (NFAT1) (Sharma et al., 2011), interact with and are influenced by IQGAP1. The steroid hormone receptor ERα is a dimerizing nuclear translocator that mediates transcription after binding estrogen. IQGAP1 is essential for regular ERα transcriptional activity because of its direct binding to ERα (Erdemir et al., 2014). In a manner similar to that which it exerts on β-catenin (Briggs et al., 2002a), IQGAP1 directly interacts with Nrf2 to increase its stability (Kim et al., 2013). IQGAP1 may serve as a scaffold for MAPK and Nrf2 signaling, since further research shows that it regulates Nrf2 activation through the MEK-ERK pathway (Cheung et al., 2013). Furthermore, IQGAP2 (one isoform) has been linked to transcriptional activation(Bouwmeester et al., 2004). Activation of the transcription factor nuclear factor kappa-light-chain-enhancer of activated B cells (NF-B) is triggered by the cytokine TNFα (Hoesel and Schmid, 2013). IQGAP2 is one of many proteins that were discovered by mass spectrometry to have a role in this pathway (Bouwmeester et al., 2004). Importantly, IQGAP2 knockdown reduced the NF-B

pathway activation by TNF. Although IQGAP2's function in transcription has not yet been established, IQGAP1 seems to control certain transcription factors.

IQGAP1 has an intriguing ability to inhibit transcription (Sharma et al., 2011). Calcineurin, a Ca2+/calmodulin-dependent phosphatase, dephosphorylates the transcription factor NFAT1 in response to Ca2+ stimulation, triggering its nuclear translocation and so promoting the transcription of numerous cytokines (Müller and Rao, 2010). NFAT1 is inactive and sequestered in the cytoplasm when it is phosphorylated by NFAT1 kinases such as casein kinase 1 (CK1), dual-specificity tyrosine-regulated kinase (DYRK), and glycogen synthase kinase 3β (GSK3β). Repression of NFAT1 nuclear import is also mediated by the long intergenic non-coding RNA (lincRNA) NRON (Villacé et al., 2004), which likely does so by sequestering NFAT1's nuclear transport proteins. On the other hand, it has been proposed that NRON plays a more nuanced function by forming a large RNA-protein scaffold complex in the cytoplasm with NFAT1, two IQGAP proteins (IQGAP1 and IQGAP2), calmodulin, and three NFAT1 kinases (Sharma et al., 2011). This complex, in its inactive form, confines NFAT1 to the cytoplasm and prevents calcineurin from binding to it. Calcineurin is involved in the translocation of NFAT1 into the nucleus once it has been activated by being dephosphorylated by IQGAP1 and NFAT1 kinases. This idea is supported by the observation that knockdown of NRON and IQGAP1 increases nuclear import of NFAT1, and by the observation that T cells from NRON-depleted and T cells from IQGAP1-deficient mice both produce more NFAT1-dependent cytokines (Sharma et al., 2011). These results suggest that IQGAP1 interacts with lincRNA to inhibit gene transcription.

7. IQGAP1 Binding Proteins and activated cascades

7. 1. Cytoskeletal Components

The actin cytoskeleton controls signaling and is essential for cell viability. One of IQGAP1's early established roles was regulating the cytoskeleton. Several research groups have shown that IQGAP proteins primarily serve to alter the cytoskeleton. Yeast IQGAP homologues are essential for actomyosin

ring construction and cytokinesis (Eng et al., 1998; Epp and Chant, 1997; Lippincott and Li, 1998; Machesky, 1998), and play a role in actin filament recruitment. Tentacle development is also regulated by an IQGAP1 homologue in Hydra (Venturelli et al., 2000). Colocalizing with actin in lamellipodia, IQGAP1 from mammals has been shown to promote actin polymerization in vitro (Bashour et al., 1997b; Erickson et al., 1997; Fukata et al., 1997a) and to do so in vivo (Ho et al., 1999b). This conservation provides strong evidence that cytoskeletal control was one of IQGAP1's original functions.

Important functions for IQGAP1 have been identified in the regulation of cell adhesion, microtubule networks, and the actin cytoskeleton (Briggs and Sacks, 2003b; Mateer et al., 2003; Noritake et al., 2005). Over the last several years, it has been shown that IQGAP1 binds directly or in a complex with several other cytoskeleton-related proteins. IQGAP1 has been shown to interact with F-actin directly, controlling the assembly of actin meshwork (Boyer et al., 2011; Brill et al., 1996; Brown et al., 2007; Fukata et al., 2002a; Ho et al., 1999b; Mateer et al., 2002; Weissbach et al., 1998). In addition, IQGAP1 may interact with other proteins that have roles in reorganizing the cytoskeleton (Bielak-Zmijewska et al., 2008; Fukata et al., 2002a; Mateer et al., 2004). Cdc42 and Rac1 are among those mentioned (Bashour et al., 1997b; Fukata et al., 1997a; Hart et al., 1996), as well as APC (Tirnauer, 2004), CLIP-170 (Gundersen, 2002), Clasp2 (Watanabe et al., 2009), and EB1 (Zhang et al., 2009). The atypical polarization-dependent kinase (APC) has been shown to modulate polarized cell migration (Watanabe et al., 2004b), and it may also interact directly with IQGAP1. One of the earliest indications that IQGAP1 might be involved in cytoskeleton rearrangement came from the lab of Kaibuchi (Fukata et al., 2002a). This research demonstrated that the cytoskeleton network might be reorganized by an active tripartite complex consisting of Rac1/Cdc42, IQGAP1, and CLIP-170.

7. 1. 1. Actin

IQGAP1 can regulate actin meshwork development by interacting directly with F-actin (Boyer et al., 2011; Brill et al., 1996; Brown et al., 2007; Fukata et al., 2002a; Ho et al., 1999b; Mateer et al., 2002; Weissbach et al., 1998). IQGAP1's N-terminal CH domain, in specific, interacts directly with the actin

cytoskeleton (Le Clainche et al., 2007; Watanabe et al., 2004b). The F-actin-binding domains of the spectrin, filamin, and fimbrin families are structurally similar to the CH motif of IQGAP1 and IQGAP2. Extensive biochemical studies have shown that IQGAP1 interacts with F-actin through its CH domain, which plays a crucial role in regulating actin polymerization (Mateer et al., 2002; Mateer et al., 2004). Purified IQGAP1 has been shown to bind directly to F-actin and cross-link actin filaments forming tangled, linked bundles with gel-like characteristics (Bashour et al., 1997b).

Following additional research, it was shown that IQGAP1 promotes Arp2/3-dependent actin polymerization (Neudauer et al., 1998; Takahashi et al., 2006a) via binding to N-WASP and so stimulating assembly of branched actin filaments. It has been shown that IQGAP1 caps the barbed ends of actin, hence controlling its assembly (Mataraza et al., 2007). IQGAP1 has been proven to play a substantial role in quantitative co-localization investigations, which have indicated that N-WASp is often found in close proximity to the Arp2/3 complex in lamellipodial structures (Le Clainche et al., 2007). Furthermore, co-immunoprecipitation, pull-down, and kinetic assays show that the C-terminal half of IQGAP1 activated N-WASp by interacting with its BR-CRIB domain similar to that of Cdc42, whereas the N-terminal half of IQGAP1 interferes with this activation by association with a C-terminal region of IQGAP1 via intramolecular interactions (Le Clainche et al., 2007). Consequently, IQGAP1 structural variation acts as an auto-regulatory switch that, when activated, stimulates actin assembly in an Arp2/3-dependent way by activating N-WASp. The plus-end tracking protein Clip-170 and IQGAP1 (Swiech et al., 2011) are essential for the proper development and structure of neuronal dendritic arbors. It has been found that the creation of the Clip-170/IQGAP1 complex is dependent on a direct contact between mTOR kinase and Clip-170. This complex can control actin and tubulin cytoskeletons in developing hippocampus and cerebral cortex neurons. This means IQGAP1 may serve as the center for interactions between actin and microtubule cytoskeletons (Malarkannan et al., 2012).

Cell extension is caused by the assembly and remodeling of actin filaments, which are controlled by a wide range of actin modifying systems like actin severing and actin capping proteins like the Gelsolin/Villlin superfamily (Kwiatkowski et al., 1989; Yin, 1987) and by signaling modules that use

small GTPases to control the assembly of supramolecular actin (Dimchev et al., 2017; Keely et al., 1999; Kwong et al., 2003). Short cell extensions called filopodia include tightly structured bundles of actin filaments and are regulated in their synthesis by the Rho family small GTPase cdc42 (Brown and Sacks, 2006; Kim et al., 2000). It has been shown that the multidomain protein IQGAP1 induces filopodia development by keeping cdc42 in an active state (Swart-Mataraza et al., 2002). This protein may also play a role in the production of longer cell extensions necessary for collagen phagocytosis.

Assembly and rearrangement of actin filaments by proteins that sever and cap developing filaments are essential for the synthesis of cell extensions and the degradation of collagen by fibroblasts. Flightless I (FliI) (Arora et al., 2015) is a gelsolin family member that binds and coordinates with IQGAP1 and cdc42 to control the development of cell extensions (Arora et al., 2020). It also plays a critical role in collagen degradation by phagocytosis (Arora et al., 2017). IQGAP1 has been demonstrated to influence collagen remodeling via modulating phagocytic degradation pathways, a process that may entail an interaction between IQGAP1 and FliI. Human gingival fibroblasts (HGFs) and IQGAP1+/+ and IQGAP1-/- murine embryonic fibroblasts were used to investigate IQGAP1's function in collagen phagocytosis. HGFs-induced IQGAP1 expression was accompanied by its localization to vinculin-stained cell adhesions and locations where cell extensions are started, as well as its colocalization with FliI (Nakajima et al., 2021).

7. 1. 2. Microtubules

Microtubule dynamics are controlled by IQGAP1. Interacting with CLIP-170, a protein found at the ends of microtubules, the IQGAP1/CLIP-170 complex enables the temporary capture of microtubules in the cortex (Fukata et al., 2002a). The APC pathway is another way in which IQGAP1 regulates microtubules (Watanabe et al., 2004b). It seems that IQGAP1 and APC stabilize the plus end of the microtubule by mediating the immobilization of CLIP-170 at leading edges. Another protein involved in the pathway is CLIP-associating protein 2 (CLASP2). IQGAP1 has direct binding to CLASP2 (Watanabe et al., 2009). Intriguingly, IQGAP1 can only bind microtubules in vitro when CLASP2 is present,

suggesting that IQGAP1 binds microtubules through CLASP2. Furthermore, CLASP2 dissociates from IQGAP1, EB1 (end-binding 1), and microtubules after being phosphorylated by glycogen synthase kinase 3β (GSK-3β) (Watanabe et al., 2009). Also, Ca2+ controls, through AKAP220, the binding of CLASP2 to IQGAP1 (Logue et al., 2011b). Anchoring proteins for the kinase A (AKAPs) guide the cAMP-dependent protein kinase (PKA) to its many substrates, allowing for precise regulation of cellular processes (Wong and Scott, 2004). By boosting intracellular free Ca2+ concentrations, AKAP220 binds IQGAP1 more strongly in cells (Logue et al., 2011b). AKAP220 also binds GSK-3β, causing that protein to phosphorylate CLASP2 and render it incapable of binding IQGAP1. these results suggested that in response to an increase in cAMP, PKA phosphorylates and inhibits GSK-3β function. This leads to dephosphorylation of CLASP2, which facilitates its binding to IQGAP1 and subsequent microtubule rescue (Logue et al., 2011b). Taken together, this findingsres show that IQGAP1 plays a complicated function in microtubule dynamics, with scaffold complexes of IQGAP1 being individually regulated by a number of binding partners.

7. 1. 3. Adherens Junctions

Adherent junctions are cadherin-dependent adherent structures generated between cells (Wheelock and Johnson, 2003b). The actin cytoskeleton is associated with the cadherin family of Ca2+-dependent transmembrane adhesion molecules. By binding to E-cadherin, IQGAP1 may modulate the protein's activity (Johnson et al., 2009; Noritake et al., 2005). The association of E-cadherin with the actin cytoskeleton is weakened when IQGAP1 is overexpressed (Kuroda et al., 1998b) and translocated to areas of cell-cell contact (Li et al., 1999b). Evidence shows that IQGAP1 binds to and affects the activity of other cadherins. In combination with ERK, IQGAP1 binds neuronal- (N-) cadherin, which may be critical for synaptic remodeling associated with memory formation (Schrick et al., 2007). Furthermore, in human endothelial cells, IQGAP1 colocalizes with VE-cadherin at regions of cell-cell contact, and siRNA suppression of IQGAP1 decreases both VE-cadherin localization at adherens junctions and its phosphorylation by reactive oxygen species (Yamaoka-Tojo et al., 2006). Both of these steps are required

for capillary tube development, suggesting that IQGAP1 is involved in angiogenesis. A subsequent research (Nakhaei-Nejad et al., 2010) found IQGAP1 abundance in human endothelial cell junctions, but no change was observed in VE-cadherin at junctions when IQGAP1 was knocked down.

Moreover, it has been suggested that the protein trafficking factor IQGAP1 regulates TJ formation by altering the expression and/or localization of junctional proteins. Using the model cell line MDCK (Cereijido et al., 1978), researchers investigated this possibility and discovered that silencing IQGAP1 led to a transient CDC42-dependent increase in transepithelial electrical resistance (TER) during the earliest stages of TJ formation (Tanos et al., 2015). Inverse correlation between IQGAP1-CDC42 interaction strength and TER during epithelial development suggests that IQGAP1 may inhibit CDC42 during tight junction formation. This work demonstrated that IQGAP1 knockdown (KD) increased claudin 4 localization to TJs and decreased claudin 2 expression and localization to TJs, which may explain why TER increased after IQGAP1 KD. Consequently, IQGAP1 was shown to play a crucial role in TJ formation, and a molecular relationship between IQGAP1, CDC42, and the positional control of claudins at the beginning of epithelial polarity was discovered.

7. 2. IQGAP1 MAPK/ERK Signaling Pathway

The mitogen-activated protein kinase (MAPK) pathway is a major intracellular signaling system involved in cell proliferation, differentiation, death, angiogenesis, and tumor metastasis. In eukaryotic cells, the ERK1/2, c-Jun N-terminal kinase (JNK), p38 MAPK, and ERK5 signal transduction pathways have been identified as MAPK cascades based on the MAPK layer components. At least three protein kinases-MAP3K, MAPKK, and MAPK- compose each MAPK signaling cascade and transmit signals via their sequential activation (Plotnikov et al., 2011; Wortzel and Seger, 2011). The ERK/MAPK signaling pathway is the best understood MAPK signaling pathway, and it is central to the cell signal transduction network. whereas, the JNK and p38 MAPK pathways have been linked primarily to cellular stress and apoptosis (Chang and Karin, 2001; Khokhlatchev et al., 1998; Kolch, 2005; Kyriakis and Avruch, 2001).

As a member of the mitogen-activated protein kinase (MAPK) family, extracellular signal-regulated kinase 1/2 (ERK) is involved in the transmission of extracellular signals to their intracellular destinations. Accordingly, mitogen-activated protein kinase (MAPK) cascades are key signaling components that control fundamental processes such cell proliferation, differentiation, and stress responses (Keshet and Seger, 2010; Plotnikov et al., 2011; Sabio and Davis, 2014). Ras/Raf/MAPK, MAPKK (MEK) 1/2, MAPK (ERK1/2), and MAPK (MAPKAPK) (ribosomal s6 kinases, MAP kinase-interacting serine/threonine-protein kinases, mitogen- and stress-activated protein kinases, and cytosolic phospholipase A2) are all involved in the ERK cascade (Eblen, 2018; Roskoski, 2012; Wortzel and Seger, 2011). Basic biological activities including cell proliferation and differentiation are controlled by ERK cascades, which are highly regulated cascades. These factors control the activity of bispecific phosphatases (Patterson et al., 2009; Seternes et al., 2019; Zhou et al., 2002), scaffold proteins (Chuderland and Seger, 2005; Kolch, 2005; Morrison and Davis, 2003; Shaul and Seger, 2007), the strength and duration of signals (Marshall, 1995), and the subcellular movement of cascade components (Wainstein and Seger, 2016; Yao and Seger, 2009).

The ERK pathway may be activated by a wide variety of stimuli, including growth factors, cytokines, viruses, ligands for G-protein-coupled receptors, and oncogenes. The small G proteins Ras and Raf kinase downstream kinases ERK1/2 and MEK1/2 are the primary players in the ERK/MAPK signaling cascade. Ras is the most preserved member, which is encoded by the Ha ras, Hi ras and N ras oncogenes of the ras gene family. The raf oncogene encodes for the enzyme raf kinase. MEK1 and MEK2 are unusual dual specificity kinases that may phosphorylate Tyr 204/187 and Thr 202/185 to activate ERK (Chang and Karin, 2001).

Signaling along the MAPK pathway begins when growth factors connect to their receptors and activate Ras. Activated Ras causes the recruitment of Raf kinases to the membrane, where they catalyze the phosphorylation of MEK1 and MEK2, which in turn activates ERK1 and ERK2. In the nucleus, ERK dimerises and translocates to activate gene transcription, whereas in the cytoplasm, it phosphorylates

substrates in several subcellular locations. Activation of MEK/ERK often leads to enhanced cell survival, proliferation, and differentiation (Pearson et al., 2001).

Various regulatory proteins may alter ERK signaling. Scaffold proteins are the most numerous, varied, and pervasive component. Scaffold proteins connect the components of the successive tiers that compose up the ERK signaling cascade to create a multi-enzymatic complex, allowing for fine-tuning of ERK signals with regard to amplitude, intensity, and duration, and affording signal integrity by shielding the complex from interferences. Sublocalization-specific regulation of ERK signaling activity is another way in which scaffolds contribute to spatial selectivity (Calvo et al., 2010; Dhanasekaran et al., 2007; Garbett and Bretscher, 2014; Kolch, 2005; Witzel et al., 2012).

Over a dozen protein families have been identified as true ERK scaffold proteins. IQGAP1, an extensively studied scaffold that, along with its isoforms IQGAP2 and IQGAP3, forms a defined family of high molecular weight, multidomain proteins involved in a wide variety of signaling pathways and cellular processes, including the regulation of cell migration through the regulation of the cytoskeleton (Smith et al., 2015). In response to tyrosine kinase receptors including epidermal growth factor receptor (EGFR) and insulin-like growth factor receptor (IGFR), IQGAP1 binds to BRAF, MEK1/2, and ERK1/2, consequently controlling signal flow (Hedman et al., 2015; Roy et al., 2004). Depletion of IQGAP1 or blocking its scaffold activities also protects against RAS-ERK pathway-driven neoplasia (Jameson et al., 2013), similar to what was seen with KSR1. The phosphorylation processes that take place at each stage of the ERK cascade are thought to be optimized because to the presence of scaffold proteins. Scaffolds were originally thought to be permanently bound to MEK1/2, with the idea being that stimulated ERK1/2 would be recruited into the complex, where it would be phosphorylated by resident MEK (cis-phosphorylation), and subsequently released (Kolch, 2005). Later, it was shown that ERK may also attach constitutively to scaffolds, where it would be cis-phosphorylated by scaffold-bound MEK and then join to a free, phosphorylated ERK monomer to create a dimer. Therefore, scaffold proteins would serve as sites for ERK dimerization (Casar et al., 2009a; Casar et al., 2008, 2009b; Herrero et al., 2015).

The WW domain of IQGAP1 has been theorized to be a binding site for ERK1 and ERK2 for quite some time now (Lavoie et al., 2018; Ren et al., 2007). It has been demonstrated that WW domains, which are small units that fold into a three-stranded-β -sheet structure (Crespo and León, 2000), bind to Pro-rich sequences like PPXY and PPPR, as well as phospho-Ser/Thr-Pro sequences (Brennan et al., 2011; Kortum et al., 2005; Pan et al., 2012; Ren et al., 2004; Schiefermeier et al., 2014; Vomastek et al., 2004) in proteins. Only ERK1 and ERK2 are thought to interact with IQGAP1's WW domain (Neilsen et al., 2017). However, the IQ domain is essential for BRAF and MEK1/2 binding to IQGAP1 (Feigin et al., 2014; Lavoie et al., 2018).

The processes through which scaffolds enable ERK phosphorylation remain unclear, despite the fact that our understanding of these proteins has expanded greatly over the last several years. The incorporation of phosphorylated ERK in response to stimulation has been seen in KSR mutants that lack the ability to bind MEK (Kortum et al., 2006; McKay et al., 2011). It has been discovered via research that two distinct scaffold species, KSR1 and IQGAP1, may form functional associations with each other. Thus, "trans phosphorylation" occurs when MEK coupled to IQGAP1 binds to ERK docked at KSR1. The discovery that ERK trans-phosphorylation might account for the low cytotoxic effect of KSR-directed small-molecule inhibitors is significant in this regard. The results of this work have significant consequences for our knowledge of signal transduction because they identify scaffold protein interactions as a new, higher-order level of regulation in the ERK cascade (Martín-Vega et al., 2023).

7. *3. Phosphoinositide 3-kinase (PI3K)/Akt Signaling*

Growth factors and G-protein-coupled receptors stimulate the PI3K/Akt pathway (Cantley, 2002), in addition to signaling via the MAPK cascade. Phosphatidylinositol 3-kinase (PI3K) is activated by binding to phosphorylated tyrosine residues on growth factor receptors or adaptor proteins. This leads to the production of phosphatidylinositol 3-,4,5-trisphosphate (PtdIns-3,4,5-P3) from PtdIns-4,5-bisphosphate (PtdIns-4,5-P2). PtdIns-3,4,5-P3 recruits Akt to the cell membrane, where it is

phosphorylated, by binding to its pleckstrin homology domain. As a result of being phosphorylated, Akt is more able to catalyze the phosphorylation of other proteins that regulate cell proliferation, survival, and growth.

Evidence suggests that IQGAP1 directly links to PI3K/Akt cascade. Depleting IQGAP1 prevents VEGFR2 (Yamaoka-Tojo et al., 2004) and HER2 (White et al., 2011), respectively, from activating Akt. Furthermore, IQGAP1-null mice do not show any evidence of Akt activation in mouse cardiac tissue in response to chronic pressure overload (Sbroggiò et al., 2011). The revelation that endogenous IQGAP1 co-immunoprecipitated with Akt when Akt was extracted from mouse cardiac lysates by pulldown using a fragment of GST-IQGAP1 (Sbroggiò et al., 2011), shed light on the underlying process. However, in thyroid cancer cells, knocking down IQGAP1 had no discernible impact on Akt activation (Liu et al., 2010), suggesting that the effects are selective and occur only in certain signaling pathways. Additionally, IQGAP1 binds PtdIns-3,4,5-P3 directly, despite the fact that the role of this interaction have yet to be specified (Dixon et al., 2011).

7. 4. IQGAP1 and Rho GTPases Family

Among the best described IQGAP1 binding partners are the Rho family small GTPases Cdc42 and Rac1 (Hart et al., 1996; Joyal et al., 1997b; Kuroda et al., 1996; Owen et al., 2008b). Over the last several years, researchers have found evidence of a wider variety of small GTPases interacting with IQGAP1. ADP ribosylation factor 6 (Arf6), Rac2, Rap1, and RhoC are some of these proteins. Jeong et al. (Jeong et al., 2007)(25) showed in 2007 that IQGAP1 binds Rap1 directly. Rap1, which belongs to the Ras family, is well known for its functions in cell adhesion (Awasthi et al., 2010). GTP stimulation of Rap1 increases binding to IQGAP1, much like the relationship between IQGAP1 and Rac1/Cdc42 (Hart et al., 1996; Jeong et al., 2007; Joyal et al., 1997b; Kuroda et al., 1996). Data from many laboratories suggest that IQGAP1 regulates a wide variety of cellular processes via its interactions with small G proteins, including adhesion, trafficking, and polarization.

Rho GTPases are able to perform the function of molecular switches because they are able to cycle between an inactive state (bound to GDP) and an active state (bound to GTP) (Jaiswal et al., 2013). In general, the actions of these proteins in the plasma membrane are regulated by three different classes of regulatory proteins: guanine nucleotide dissociation inhibitors (GDIs), guanine nucleotide exchange factors (GEFs), and GTPases activating proteins (GAPs) (Mosaddeghzadeh and Ahmadian, 2021). As RHO GTPases like CDC42 transition into their active GTP-bound state, they undergo conformational changes in two areas known as switch I and II (comprising amino acids or aa 29-42 and 62-68, respectively); these areas serve as a platform for the GTP dependent, high-affinity connection of structurally and functionally varied effector proteins, such as ACK, PAK1, WASP, ROCKI, DIA, and IQGAP1, via their GTPase-binding domains (GBDs) (Abdul-Manan et al., 1999; Dvorsky and Ahmadian, 2004; Dvorsky et al., 2004; Hall, 2012; Hemsath et al., 2005; LeCour et al., 2016b; Morreale et al., 2000; Mott and Owen, 2015; Mott et al., 1999; Nouri et al., 2020; Owen and Mott, 2018; Rose et al., 2005). In all eukaryotic cells, the activation of GTPase-effector signaling further stimulates an array of different pathways (Mosaddeghzadeh and Ahmadian, 2021).

Previous research examined the function of RGCT in IQGAP and suggested it as an IQGAP 'effector domain', which binds with high affinity to the switch areas of the GTP-bound, active CDC42 (Elliott et al., 2012b; Nouri et al., 2016b; Nouri et al., 2020). The IQGAP-ΔGRD (missing aa 1122-1324) may still bind to the CDC42 GppNHp, as shown by Swart-Mataraza et al., (Swart-Mataraza et al., 2002). Li et al. mapped the IQGAP1 and CDC42 binding areas and found that the switch I and surrounding areas (residues 29-55) and the insert region (residues 122-134) are essential for high affinity binding to IQGAP1 (Li et al., 1999a). Although this was previously thought to be the case, LeCour et al., determined the crystal structure of a constitutively active form of CDC42(Q61L) bound to the IQGAP2 GRD (GRD2) and hypothesized that CDC42 binds GRD2 from two distinct locations in a 4:2 stoichiometry (LeCour et al., 2016b; Ozdemir et al., 2018). There are two types of binding sites: the 'GAPex-mode binding site' (ex stands for 'extra' subdomains that include variable N- and C- terminal flanking regions) and the 'RASGAP-mode binding site', which is highly similar to the RASGAP and CDC42GAP structures

(Nassar et al., 1998; Scheffzek et al., 1997) and has a conserved core domain (GAPc). Based on their structural analysis, Ozdemir et al., (Ozdemir et al., 2018) hypothesized that when CDC42 IH binds to the GAPex-domain, GRD2 dimerizes, and the RASGAP site is altered allosterically, therefore creating a second interaction surface for CDC42 binding and resulting in a 2:1 stoichiometry between GRD2 and CDC42 (Ozdemir et al., 2018).

The C-terminal domains of IQGAP1 (C794) and IQGAP2 (C795), including the GRD, RGCT, and CT domains, bind to CDC42, and their structure and binding characteristics have been the subject of several biophysical and biochemical investigations (Elliott et al., 2012b; Fukata et al., 1999b; Gorisse et al., 2020; Grohmanova et al., 2004; Hart et al., 1996; Kurella et al., 2009b; LeCour et al., 2016b; Li et al., 1999a; McCallum et al., 1996; Owen et al., 2008b; Ozdemir et al., 2018; Swart-Mataraza et al., 2002; Zhang et al., 1998). Clearly, the three domains bind CDC42 with varying strengths (Nouri et al., 2020). Mechanical principles underlying these interactions, however, have been elusive. The designation of a 'CDC42-specific GBD' for IQGAPs is also a matter of debate. The GTPase regulatory domain (GRD) and its RASGAP-mode interaction with the CDC42 switch regions are proposed in one model (Gorisse et al., 2020; LeCour et al., 2016b; Mataraza et al., 2003b; Owen et al., 2008b; Ozdemir et al., 2018), while in the other model (RGCT) found downstream to the GRD is proposed as being essential for high-affinity GTP-dependent binding to CDC42 (Elliott et al., 2012b; Mosaddeghzadeh et al., 2021; Nouri et al., 2016b; Nouri et al., 2020; Swart-Mataraza et al., 2002). New research has shed light on the critical role of IQGAP RGCT as the genuine GBD in the GTP-dependent recognition and binding of CDC42. It is clear that the GRD is essential for structuring CDC42 and assisting its recruitment to preexisting cues, despite the fact that it is not a primary effector domain (Mosaddeghzadeh et al., 2022).

7. 4. 1. IQGAP1 is an effector that responds to Rho GTPases

Rho GTPases have been shown to be crucial in IQGAP1 self-association (Fukata et al., 1997b). The Cdc42/Rac1-IQGAP1 interaction is thought to occur via the connection of the IQGAP1-GRD domain with the switch areas of Cdc42 and Rac1, as shown by earlier investigations (Elliott et al., 2012a; Kurella

et al., 2009a; Kuroda et al., 1998a; Mataraza et al., 2003c; Owen et al., 2008a). Cdc42 coupled to GTP (Cdc42GTP) requires the GRD-dependent connection to carry out its cellular functions, and Cdc42GTP may cause the dimerization of IQGAP1, which is necessary for IQGAP1's activities. Four Cdc42-GTP molecules attach to two GRD molecules to produce the structure of Cdc42-GTP coupled to the IQGAP1-GRD domain. Two Cdc42 s bind in a manner similar to the Ras/RasGAP-binding mode, while the other two link to "extra domain" sequences from both GRDs (LeCour et al., 2016a). In contrast, Nouri et al. published kinetic and equilibrium studies that cast doubt on the GRD-dependency of the IQGAP1-Rac/Cdc42 interaction (Nouri et al., 2016a). It has been shown via this research that the IQGAP1-RGCT domain is the linking component, strongly binding the Cdc42-GTP and Rac1 switch regions. Moreover, low-affinity binding between the IQGAP1 C-terminal region and areas close to Cdc42 and Rac1 switch sites allows for further interactions. Collectively, these interactions lead to a local conformational shift that lowers the affinity with which the IQGAP1-GRD domain binds to GTP-bound Cdc42 and Rac1. Furthermore, it is possible that the increased IQGAP1 oligomerization increases its F-actin-cross-linking activity through the Cdc42GSTGTP complex (Fukata et al., 1997b). The N-terminal 763-863 region of IQGAP1 is crucial for oligomerization, which in turn raises the quantity of active Cdc42, as shown by Ren et al. (Ren et al., 2005).

7. 4. 2. IQGAP1 links Rho GTPases to the cytoskeleton

It has been suggested that IQGAP1 acts as a direct molecular connection between Rho GTPases (Rac and Cdc42) and the actin cytoskeleton. This allows it to directly bind and cross-link MF, which is necessary for the production of MF-rich lamellipodia and filopodia (Bashour et al., 1997a). One hypothesis suggests that the interaction between IQGAP1 and active GTPases might be the mechanism responsible for the attenuation of the inhibitory effects of calmodulin bound on the actin-binding activity of IQGAP1. For actin filaments rearrangement-mediated lamellipodia production in breast cancer cells treated with HGF (Takahashi and Suzuki, 2008), Rac1-dependent and kinesin heavy chain KIF5B-mediated transportation of WAVE2/IQGAP1 complex to the cell periphery via microtubules is also

necessary. On the other hand, the unanticipated promotion of lamellipodia generation and invasion of human breast cancer cells that is mediated by the dissociation of IQGAP1 and kinesin from the Rac1/CLIP-170 complex as a result of the suppression of CLIP-170 (Suzuki and Takahashi, 2008) occurs when CLIP-170 is suppressed. Wallrabe et al. (Wallrabe et al., 2015) used three-color FRET microscopy to quantitatively evaluate and discover the unique impacts that Rac1 and Cdc42 have on the interaction of N-WASP with IQGAP1.

During protrusive motility, Golub et al. highlighted the cooperative participation of IQGAP1, Rac, and Cdc42 for the capture of MT plus ends at cell edge raft rich regions via APC protein (Golub and Caroni, 2005). In other words, these three proteins work together to grab MT plus ends. In addition, it has been shown that a tripartite complex including Rac1/Cdc42-IQGAP1-CLIP-170 is involved in the process of joining MT plus ends and cortical actin meshwork during polarizing motility. This process is susceptible to disruption by the anti-tumor synthetic triterpenoid CDDO-Im (Fukata et al., 2002b; To et al., 2008). Furthermore, the joint engagement of APC and CLIP-170 in the Rac1/Cdc42/IQGAP1-involved association mechanism of the MT plus ends to cortical actin filaments for cell polarization and directional migration can also be demonstrated in a model that was suggested by Watanabe et al.. Pursuant to this concept, CLIP-170 would be responsible for collecting MTs, while APC might have a role in giving their stability. These are two events that are essential in order to produce a stable actin meshwork at the leading edges (Watanabe et al., 2004a). It is important to note that RhoC, another member of the Rho family, is also able to bind to the C-terminal region of IQGAP1 to take it on as a downstream regulator to enhance the migration of gastric cancer cells (Wu et al., 2011).

7. 4. 3. IQGAP1 mediates cell adhesion in response to Rho GTPases

IQGAP1 may interfere with the normal E-cadherin-catenin complex by separating α-catenin from β-catenin (Fukata et al., 1999a; Kuroda et al., 1998b). This is possible because IQGAP1 and α-catenin share binding sites in the β-catenin structure. It has been shown that in MDCKII cells, Rac1 linked to GTP (Rac1GTP) interferes with the interaction between IQGAP1 and β-catenin and binds to IQGAP1 to

increase its F-actin cross-linking activity. This impact promotes E-cadherin-mediated cell-cell adhesion by increasing the interaction of actin filaments with E-cadherin/β-catenin complex through α-catenin at adhesion sites (Noritake et al., 2004b). On the other hand, TPA-induced cell scattering causes cell-cell separation, which decreases Rac1GTP levels and initiates the opposite process (Fukata et al., 2001a). Cdc42 may regulate adhesion junctions through IQGAP1 in a manner analogous to Rac1 (Lui et al., 2005). Active Rac1/Cdc42 has been found to improve the association of IQGAP1 with the tyrosine phosphatase PTPmu, which inhibits IQGAP1 binding to β-catenin and stabilizes N/R-cadherin-dependent cell adhesion during neurite outgrowth (Oblander and Brady-Kalnay, 2010).

In conclusion, these data show that IQGAP1 functions as a negative regulator of E-cadherin-mediated cell-cell adhesion. Additionally, it has been demonstrated that the active Rac1/Cdc42-IQGAP1 system may control the ratio of E-cadherin/β-catenin/α-catenin complex to E-cadherin/β-catenin/IQGAP1 complex at cell-cell contact sites, which can be a predictor of the strength of E-cadherin-mediated adhesion.

Another major mechanism through which E-cadherin-mediated adhesions become dysfunctional, even in the absence of a change in E-cadherin or catenin protein production, is E-cadherin endocytosis. By inhibiting endocytosis of E-cadherin and stabilizing the E-cadherin-based Ajs, Izumi et al. found that the Rac/Cdc42/IQGAP1 system is activated by trans-interacting E-cadherin (Izumi et al., 2004). Since stable AJs are necessary for the de novo creation of bile canaliculi structures, IQGAP1 silencing would impair the capacity of HepG2 and Huh7 cells to maintain AJs (Emadali et al., 2006). This impact of IQGAP1 can also explain its participation in the preservation of bile canaliculi structures. By recruiting IQGAP1 into the Rac-bound E-cadherin/catenins complex, protein phosphatase 2A (PP2A) is thought to have a role in sustaining cell-cell adhesion in non-malignant human mammary epithelial cells. E-cadherin endocytosis is blocked when IQGAP1, in its role as a Rac effector, promotes F-actin cross-linking and the anchoring of E-cadherin/β-catenin/α-catenin in this F-actin assembly (Takahashi et al., 2006b).

7. 4. 4. IQGAP1 regulates other cell behaviors in response to Rho GTPases

IQGAP1 actin-bundling/cross-linking activity or an N-WASP-mediated mechanism have both been shown to form actin polymers under hydroxyurea-induced DNA replication stress (Johnson et al., 2013). This is due to the increased nuclear transport of actin and its co-factors IQGAP1 and Rac1. The C-terminus of IQGAP1 has been shown to interact with MISP, an actin-binding protein (Vodicska et al., 2018).

7. 4. 4. 1. Calmodulin

Interactions between IQGAP1, small GTPases, F-actin, and other proteins may be influenced by the IQGAP1/calmodulin interaction. In a concentration-dependent manner, IQGAP1 binding to Cdc42 may be disrupted by calmodulin bound to Ca2+ (CalmodulinCa2+) by direct interaction with IQGAP1 (Joyal et al., 1997a). I addition, it has been shown that calmodulin and F-actin may compete for binding to the IQGAP1-CHD domain, and that Ca2+ can boost calmodulin binding to IQGAP1 to reduce the IQGAP1/F-actin combination. When attached to calmodulin, Ca2+ suppresses IQGAP1's participation in Cdc42 GTPase activity, freeing the small GTPases to participate in other possible activities associated to cytoskeleton reassembly (Ho et al., 1999a). Remarkably, calmodulin is more dominant than E-cadherin in the conflict for binding to IQGAP1, allowing AJs to avoid negative regulation of IQGAP1(Li et al., 1999c). Although Foroutannejad et al. believe that IQGAP1 down-regulates the adhesion sites during cell retraction via contact with calmodulin (Foroutannejad et al., 2014), these results reveal a calmodulin involvement akin to Cdc42/Rac1 in regulating AJs involving E-cadherin (Carmon et al., 2017; Deplazes et al., 2009; Fukata et al., 2001b; Lui et al., 2005; Miyoshi et al., 2005; Noritake et al., 2004a). Additionally, β-catenin/IQGAP1 interaction may be blocked by calmodulin coupled to IQGAP1 beforehand. Unexpectedly, calmodulin may increase β-catenin-mediated transcriptional coactivation in the nucleus by forming a ternary complex with IQGAP1 and β-catenin. In this complex, calmodulin indirectly influences the β-catenin nuclear translocation (Briggs et al., 2002b). Furthermore, the

Ca2+/calmodulin/IQGAP1 complex may inhibit the Ras-MAPK signaling cascade by preventing B-Raf (and perhaps MEK and ERK) from binding to IQGAP1 by changing IQGAP1's tertiary conformation (Ren et al., 2008). CalmodulinCa2+ also prevents IQGAP1 from interacting to EGFR, since this binding requires the IQ domain to IQGAP1-EGFR connection (McNulty et al., 2011a).

However, Li et al., (Li and Stuenkel, 2004) demonstrated that calmodulin binding to IQGAP1 is enhanced in the absence of Ca2+ compared to the presence of Ca2+, and that Ca2+ may cause the dissociation of bound calmodulin from IQGAP1. In spite of prior observations by Bashour et al., (Bashour et al., 1997a) that the inhibitory impact of calmodulin on the IQGAP1/F-actin binding was more potent in the absence than in the presence of Ca2+, they concluded otherwise and ascribed the discrepancy to methodological differences. Subsequent research by Kholmanskikh et al., (Kholmanskikh et al., 2006) found that Ca2+ influx dissociates IQGAP1 from calmodulin, allowing it to bind and stabilize active Cdc42 or Rac1, neuronal migration protein Lis1, and + TIPs proteins for neural motility. At the same time, a rise in intracellular calcium frees IQGAP1 from calmodulin and active Rac, allowing it to bind AKAP220 and CLASP2 proteins during microtubule polymerization in relation to migration (Logue et al., 2011a).

7. 4. 4. 2. Phosphorylation

One of IQGAP1's key post-translational regulators is phosphorylation. Endogenous IQGAP1 was shown by Li et al., (Li et al., 2005a) to regulate the cytoskeleton of neuronal cells and promote neurite outgrowth after being significantly phosphorylated by PKC at the Ser1443 and Ser1441 residues in the RasGAP C-terminal domain. The serine/threonine protein kinase GLK (also known as MAP4K3) directly phosphorylates IQGAP1 at the N-terminal Ser480 residue via interacting with the IQGAP1-WW domain through its two proline-rich regions. Cdc42 activation and Cdc42-mediated cell migration are both enhanced by this phosphorylation (Chuang et al., 2019). Furthermore, Wang et al., (Wang et al., 2009) demonstrated IQGAP1's function as a phosphorylation-sensitive conformation switch in controlling the coupling of cell growth and division during cell proliferation. Ser1443 phosphorylation of IQGAP1 in

response to mitogens causes the C-terminus to unfold, maintaining IQGAP1's interaction with active Cdc42 to promote cell division and the binding of dephosphorylated IQGAP1 with mTOR to promote cell growth. This conformational flip of IQGAP1 also leads to its constructive role in protein synthesis/exocytosis by functioning in an exocyst-septin complex bound after C-terminus folding (Rittmeyer et al., 2008a). The phosphomimetic variation S1441E has a lower affinity for Cdc42 in the absence of GTP, however Elliott et al. observed that C-terminus phosphomimetic variants S1443D and S1441E/S1443D had comparable affinities for Cdc42 as wild type IQGAP1(Elliott et al., 2012a).

7. 5. IQGAP1 and N-Cadherin

Interactions that are mediated by cadherin are essential to the development and potentiation of synapses. It has been demonstrated that N-cadherin is necessary for the creation of memories as well as the control of certain of the underlying biochemical processes. N-cadherin antagonistic peptide comprising His-Ala-Val motif (HAV-N) temporarily impaired hippocampus N-cadherin dimerization and prevented the establishment of long-term contextual fear memory, but had no effect on short-term memory, retrieval, or extinction. Learning-induced phosphorylation of a specific, cytoskeletally-associated portion of hippocampus Erk-1/2 was inhibited by HAV-N, and the distribution of IQGAP1, a scaffold protein that links cadherin-mediated cell adhesion to the cytoskeleton, modified as a result. This impact was followed by a decrease in the amount of interaction between Ncadherin/IQGAP1/Erk-2 (Schrick et al., 2007).

In the mature central nervous system, classic type I cadherins include neuronal (N)-cadherin are essential for synapse formation (Junghans et al., 2005) and the development of neural circuits (Redies, 2000). The extracellular domains mediating cell-cell adhesion play a role in controlling such events in a calcium-dependent and mostly homophilic manner (Shapiro and Colman, 1998). Docking proteins to intracellular signaling pathways (Husi et al., 2000) and multiprotein complexes including β-catenin and α-catenin (Angst et al., 2001) anchor cadherins to the actin cytoskeleton (Marambaud et al., 2003; Perron

and Bixby, 1999; Widelitz, 2005), allowing the translation of cell adhesion signals into long-term cellular responses.

According to previous research, N-cadherin was shown to function in synaptic potentiation. Significant impairment of hippocampus long-term potentiation (LTP) was seen when blocking antibodies or antagonistic peptides bearing the His-Ala-Val (HAV) pattern for classic type I cadherin dimerization were used (Tang et al., 1998). Furthermore, synaptic potentiation promotes the production and recruitment of N-cadherin to newly generated synapses, as was later observed by Bozdagi et al., (Bozdagi et al., 2000) using N-cadherin-blocking antibodies in a model of late-LTP. Data from two studies (Hagler and Goda, 1998; Murase and Schuman, 1999) revealed that N-cadherin-mediated cell adhesion has a role in memory formation.

Hippocampal N-cadherin has been shown to have an important role in the development of long-term contextual fear memories. According to biochemical evidence, one of these processes involves the activation of a subset of cytoskeletal Erk-1/2 and the subsequent interaction of this subset with IQGAP1. Memory-related synaptic remodeling may depend on N-cadherin-mediated IQGAP1/Erk-1/2 signaling in the cytoskeleton (Schrick et al., 2007).

7. *6. IQGAP1 and Wnt/β-Catenin signaling Pathway*

Wnt glycoproteins are secreted and bind to transmembrane receptors, triggering intracellular signaling cascades that ultimately result in cell proliferation, migration, differentiation, and polarity (Clevers and Nusse, 2012). The canonical route, which needs -catenin, and the non-canonical pathways, which include the PCP pathway and the Wnt/Ca2+ pathway, are the two primary mechanisms involved in establishing cell polarity (Niehrs, 2012). remarkably, IQGAP1 improves Wnt signaling across canonical and non-canonical pathways alike (Briggs et al., 2002a; Carmon et al., 2014; Goto et al., 2013a; Goto et al., 2013b).

β-catenin is both an indispensable structural component in cell-cell adhesion (Heuberger and Birchmeier, 2010) and an essential signaling protein in the canonical Wnt pathway (Niehrs, 2012). The

majority of β-catenin is found at the cell-cell junctions of epithelial cells that are in a resting state. The accumulation of β-catenin in both the cytoplasm and the nucleus is inhibited by the adenomatous polyposis coli (APC) destruction complex. This complex phosphorylates β-catenin in order to recognize it for ubiquitination and subsequent degradation. Dishevelled (Dvl) is recruited when Wnt binds to Frizzled (Fzd) and the co-receptor lipoprotein receptor-related proteins 5/6 (LRP5/6). This destabilizes the APC destruction complex. Translocation of stabilized β-catenin into the nucleus allows it to engage TCF/LEF transcription factors and stimulate Wnt target genes (Niehrs, 2012).

Multiple aspects of β-catenin activity are affected by IQGAP1. Cell-cell adhesion and actin polymerization are both controlled by IQGAP1's binding to β-catenin (Briggs and Sacks, 2003b; Kuroda et al., 1998b). In addition to regulating β-catenin, IQGAP1 has been shown to have a role in canonical Wnt signaling (Briggs et al., 2002a). The overexpression of IQGAP1 in human colon cancer cells increases nuclear accumulation and transcriptional co-activation of β-catenin. Overexpression of IQGAP1 has been shown to reduce the turnover of soluble β-catenin but not total β-catenin, as the underlying mechanism was investigated. Based on these findings, IQGAP1 seems to prevent β-catenin from being degraded in the cytoplasm and boost β-catenin's nuclear import. Building on these findings, IQGAP1 has been proposed to have a role in enhancing canonical Wnt signaling by binding to components of the Wnt pathway and facilitating their nuclear translocation. IQGAP1 forms a compound with β-catenin and Dvl in Wnt-stimulated Xenopus embryos (Goto et al., 2013a; Goto et al., 2013b). Wnt target genes are transactivated and nuclear import of the IQGAP1/β-catenin/Dvl complex is promoted by importin-β5 and Ran (Goto et al., 2013a). It is unclear, however, whether this process is also at work in mammalian cells. These data show, however, that IQGAP1 may protect β-catenin from degradation and facilitate its nuclear trafficking by functioning as a scaffold for both β-catenin and Dvl.

The interaction of IQGAP1 with R-spondins (RSPOs) is another way in which canonical Wnt signaling is facilitated (Carmon et al., 2014). There is evidence that RSPOs, which are secreted growth factors, improve Wnt signaling (Niehrs, 2012). These growth factors bind to leucine-rich repeat-

containing G-protein coupled receptors (LGRs), and this interaction is required for the binding. Through its interaction with LGR4, IQGAP1 is able to regulate the RSPO1-induced phosphorylation of LRP6 and the production of Wnt/β-catenin target genes (Carmon et al., 2014). likewise, overexpress both IQGAP1 and LGR4, a complex that includes LGR4, Dvl, LRP6, and MEK1/2 co-immunoprecipitated with IQGAP1 in mammalian cells, indicating that MEK1/2 recruitment through IQGAP1 might phosphorylate and activate LRP6, which degrades the APC destruction complex and makes it possible for β-catenin to get into the nucleus.

The Wnt/Ca2+ pathway and the planar cell polarity (PCP) pathway are two examples of non-canonical Wnt pathways (Niehrs, 2012). Different Wnt receptors, co-receptors, and downstream effectors are used to modulate their response rather than β-catenin. The small GTPases Rac and Rho are activated in response to stimulation of the PCP pathway, and this leads to reorganization of the cytoskeleton for cell polarization (Carmon et al., 2014). IQGAP1 is known to be involved in the PCP pathway. To further facilitate actin polymerization and focal adhesion, Wnt and RSPO promote IQGAP1 interaction with mDia1, N-WASP, focal adhesion kinase (FAK), and paxillin (Carmon et al., 2014). It has been shown that IQGAP1 coordinates actin dynamics and focal adhesion assembly in the non-canonical PCP pathway (Briggs and Sacks, 2003b; Mateer et al., 2003), which is consistent with its well-established involvement in controlling the actin cytoskeleton.

Chapter 2: Proteomic analysis reveals cell polarity and adhesion proteins as effectors of gonadotropin-releasing hormone receptor signaling

Summary

Stimulation of gonadotropin-releasing hormone (GnRH) receptors on the surface of anterior pituitary gonadotrope cells is a key signaling event for the hypothalamic-pituitary-gonadal axis. One important downstream component of GnRH receptor signaling is activation of the mitogen-activated protein kinase ERK (extracellular signal-regulated kinase), which is essential for the production of the gonadotropin luteinizing hormone. Evidence suggests that GnRH receptors reside in low-density plasma membrane domains where they participate in multiprotein signaling complexes. Here we used quantitative proteomics to identify proteins associated with low-density plasma membrane domains and to measure changes in their relative abundance in these domains in response to GnRH. Using αT3-1 gonadotropes, we identified 537 proteins in detergent-free subcellular fractions containing low-density plasma membranes. SILAC (stable isotope labeling by amino acids in cell culture) in combination with mass spectrometry demonstrated that GnRH, within 10 min, altered the association of 87 proteins with this plasma membrane fraction. Ontology analysis revealed that GnRH promoted an enrichment of actin cytoskeletal and adherens junction-related proteins including the molecular scaffold IQGAP1 and the small GTPase Rac1. Subsequent investigation revealed that the association between Rac1 and IQGAP1 increased with GnRH receptor stimulation and that GnRH increased Rac1 activity. Demonstrating functional relevance, inhibiting Rac1 reduced GnRH-dependent ERK activation. In sum, these data indicate that IQGAP1 complexed with Rac1 modulates ERK activity and as such serves as an essential effector in modulating cell polarity and cell-cell contacts in gonadotropes. Altogether, our proteomics data show that acute stimulation of GnRH receptors (3 nM for 10 min) alters the PAM fraction

abundance of proteins, such as actin cytoskeletal-related proteins, mechanistically linked to gonadotrope activation.

Introduction

Subcellular compartmentalization and coordination of signal transduction proteins increases the efficiency and fidelity of biochemical cascades and allows ubiquitous signaling molecules, such as calcium (Ca^{2+}), to participate in multiple intracellular processes with varying degrees of specificity and independence. In this paper, we addressed molecular mechanisms contributing to the subcellular compartmentalization and coordination of signal transduction proteins associated with the gonadotropin-releasing hormone (GnRH) receptor, a central component of the vertebrate hypothalamic-pituitary-gonadal (HPG) axis.

The HPG axis controls reproductive endocrine function and impacts fundamental processes ranging from reproduction to development and aging. The hypothalamic neuropeptide GnRH initiates HPG axis signaling by increasing synthesis and secretion of the gonadotropins luteinizing hormone (LH) and follicle-stimulating hormone (FSH). GnRH stimulation of LH and FSH synthesis and secretion begins with activation of GnRH receptors on the surface of gonadotrope cells located in the anterior pituitary. In gonadotropes, GnRH receptor activation produces two distinct intracellular Ca^{2+} signals: Ca^{2+} release from the endoplasmic reticulum (ER) through inositol-1,4,5-trisphosphate (IP_3) receptors and Ca^{2+} influx through the plasma membrane via L-type Ca^{2+} channels (Grosse et al., 2000a). These two Ca^{2+} signals increase mitogen-activated protein (MAP) kinase signaling (Mulvaney and Roberson, 2000; Mulvaney et al., 1999). Specifically, Ca^{2+} release from the ER promotes c-Jun N-terminal kinase (JNK) activity, which increases in FSH expression, while Ca^{2+} influx through L-type Ca^{2+} channels promotes extracellular signal-regulated kinase (ERK) activity, which increases LH expression.

Our published data indicate that GnRH provokes discrete sites of Ca^{2+} influx through L-type Ca^{2+} channels (Ca^{2+} sparklets) in gonadotrope-derived αT3-1 cells (Dang et al., 2014). Consistent with the work of others (Mulvaney and Roberson, 2000; Mulvaney et al., 1999), we concluded that the highly-

localized L-type Ca^{2+} channel sparklet activity observed in our experiments is necessary and sufficient for ERK activation in these cells (Dang et al., 2014). Taken together, it is reasonable to hypothesize that effective GnRH receptor signaling involves subcellular compartmentalization and coordination of relevant signal transduction proteins. Indeed, evidence suggests that in gonadotropes, GnRH receptors localize to low-density, sphingolipid and cholesterol-enriched plasma membrane microdomains (Allen-Worthington et al., 2016; Bliss et al., 2007). Importantly, localization of the GnRH receptor within low-density plasma membrane microdomains appears to be necessary for assembly of functional protein complexes and downstream signaling to ERK (Bliss et al., 2007; Navratil et al., 2010).

To further investigate proteins influenced by GnRH receptor activity in an unbiased fashion, we used a SILAC (stable isotope labeling by amino acids in cell culture)-based proteomics approach to identify and quantify the relative abundance of plasma membrane-associated proteins in response to GnRH (Ong et al., 2002). Using immortalized αT3-1 gonadotropes, we detected a significant change in ~80 plasma membrane-associated proteins following GnRH exposure. Analysis of these proteins revealed that GnRH increased the plasma membrane association of numerous actin cytoskeletal, cell polarity and adherens junction-related proteins which included the scaffold protein IQGAP1 and the small GTPase Rac1, Ptk7 and others. Evidence suggests that actin cytoskeletal remodeling is critical for GnRH receptor-dependent stimulation of gonadotropes (Dang et al., 2014; Edwards et al., 2017a; Edwards et al., 2015; Navratil et al., 2014). Indeed, following GnRH receptor stimulation, gonadotropes undergo dramatic cytoskeletal and morphological rearrangements which appear to be necessary for the transcriptional changes required for upregulation of gonadotropin synthesis (Navratil et al., 2014; Navratil et al., 2007). Our findings reveal a novel GnRH signaling mechanism involving cell polarity and adhesion proteins that accumulate at cell-cell junctions in response to GnRH treatment and involve upstream activation and association of Rac1 and IQGAP1. Importantly, and indicating functional relevance, pharmacological inhibition of Rac1 reduced ERK phosphorylation and Rac1-IQGAP1 complexes at cell junctions. Taken together, we conclude that Rac1-containing IQGAP1 signaling complexes modulate GnRH-dependent

ERK activation in αT3-1 gonadotropes and serve as important effectors for signaling events leading to an enrichment of cell-cell contacts.

Results

To facilitate discovery of novel GnRH receptor signaling mechanisms in gonadotropes, we developed a quantitative proteomics approach to identify and measure the relative abundance of proteins showing dynamic interaction with the plasma membrane in response to acute stimulation of GnRH receptors. To begin, we used subcellular fractionation to enrich our proteomic samples with plasmalemmal-associated proteins potentially regulated by GnRH receptor activation. We achieved enrichment by modifying a detergent-free fractionation technique (see Experimental Procedures) originally designed to isolate cell membranes involved with interactions between the plasma membrane and intracellular organelles such as the endoplasmic reticulum and mitochondria (Koziel et al., 2009; Pichler et al., 2001; Suski et al., 2014). Membranes obtained by this technique, termed plasma membrane-associated membranes (PAM), contain proteins involved with cellular processes such as signal transduction, Ca^{2+} homeostasis, and lipid transfer (Lebiedzinska et al., 2009; Suski et al., 2014). Although characterization of the gonadotrope PAM fraction proteome was not the specific intent of this paper *per se*, for consistency we designate subcellular fractions obtained by our modified version of this technique as PAM fractions.

Subcellular fractionation of αT3-1 gonadotropes and enrichment of plasma membrane-associated proteins potentially regulated by GnRH receptor signaling

For our experiments, we used clonal αT3-1 cells, an immortalized gonadotrope cell line with proximal GnRH receptor signaling mechanisms consistent with those observed in primary gonadotropes (Dang et al., 2014; Mulvaney and Roberson, 2000; Mulvaney et al., 1999; Windle et al., 1990). As noted above, we fractionated αT3-1 cell cultures under native (i.e., detergent-free) conditions using a modified

PAM fraction isolation technique (Suski et al., 2014). Following SDS PAGE separation of proteins from each fraction, we performed western blot analyses with cell component-representing antibodies including calreticulin (ER), tubulin (cytosol), ERK1/2 (cytosol) and flotillin 1 (plasma membrane) (Fig. 2. 1A). Similar to prior reports (Koziel et al., 2009; Suski et al., 2014), our PAM fractions showed enrichment of proteins associated with the plasma membrane (flotillin) and the ER (calreticulin) with reduced amounts of proteins associated with the cytosol (tubulin and ERK1/2).

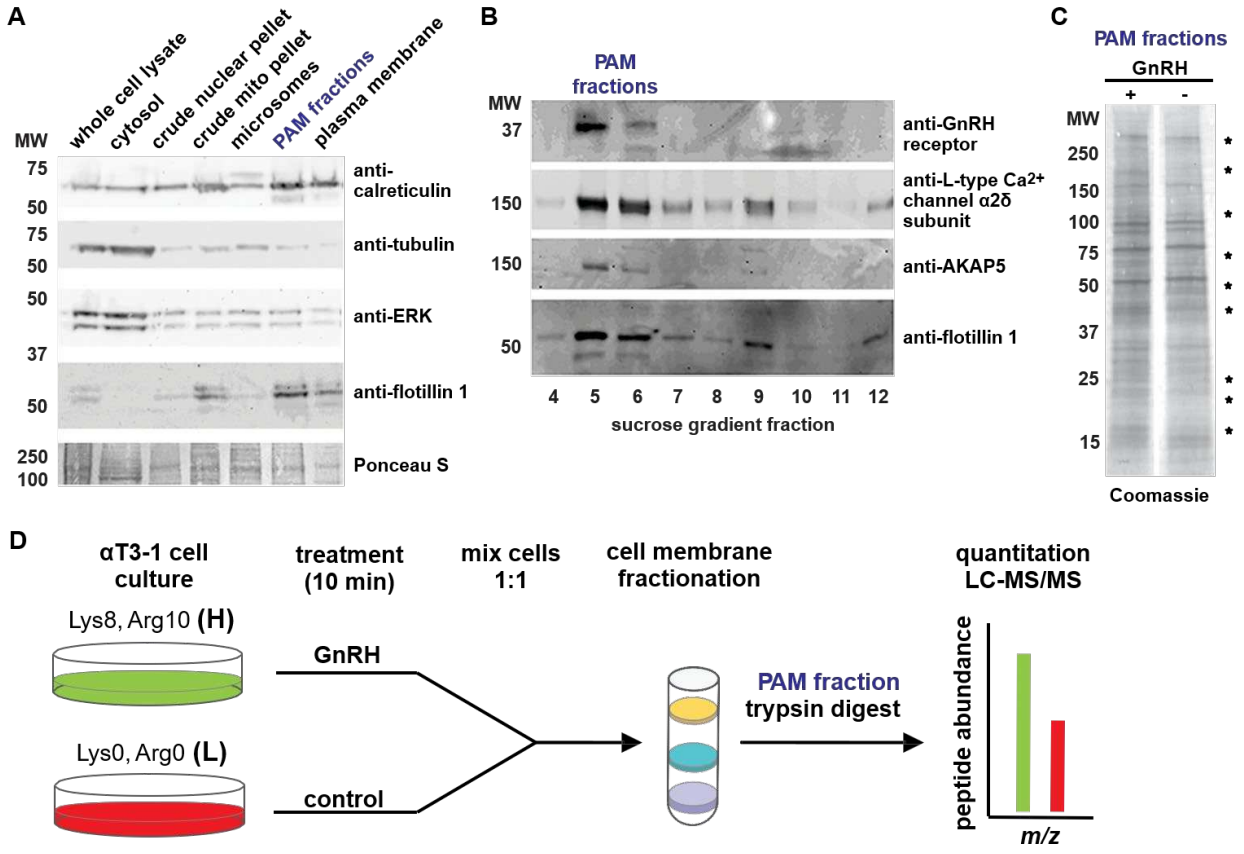

Fig. 2. 1: Subcellular fractionation of gonadotrope whole cell lysate and schematic overview of SILAC experimental approach and PAM protein identification and quantification. *A*, Representative western blots of αT3-1 cell subcellular fractions probed with antibodies raised against calreticulin (ER marker), tubulin and ERK1/2 (cytosolic markers), flotillin 1 (low-density membrane marker), and Ponceau S (total protein stain). *B*, Representative western blots of plasma membrane proteins fractionated by a sucrose gradient and probed with antibodies raised against the GnRH receptor, the L-type Ca^{2+} channel α2δ subunit, AKAP5, and flotillin 1. *C*, Coomassie stain of PAM proteins derived from αT3-1 cells treated with GnRH (10 nM for 10 min) or vehicle and resolved by SDS-PAGE. Arrows indicate protein bands differentiating the two treatment conditions. *D*, αT3-1 gonadotropes were grown in media supplemented with either 'light' lysine/arginine (Lys0, Arg0) (control group) or 'heavy' lysine ($^{13}C_6$ $^{15}N_2$)/ arginine ($^{13}C_6$ $^{15}N_4$) (Lys8, Arg10) (test group) treated with 3 nM GnRH for 10 min. Whole cell lysates from each treatment group were mixed

1:1 prior to subcellular fractionation. PAM proteins (sucrose gradient fractions 5 and 6) were precipitated, trypsin-digested and resulting peptides were identified by liquid chromatography/tandem mass spectrometry (LC-MS/MS). The relative fold-change for hormone treatment was calculated as a ratio of the number of peptides containing 'heavy' isotopes (treated) over 'light' isotopes (untreated). *Szerlong, Heather*

To further analyze αT3-1 cell PAM fractions, we separated PAM-containing crude plasma membranes by high-speed centrifugation through a sucrose gradient to produce resolvable low- to high-density plasma membrane fractions. In addition to flotillin 1, western blot analysis revealed that several GnRH receptor-associated proteins segregate into low-density PAM fractions (Fig. 2. 1B). Included are the GnRH receptor itself, L-type Ca^{2+} channel α2δ subunits, and the scaffold protein AKAP5 (which interacts with L-type Ca^{2+} channels (Fu et al., 2011; Marshall et al., 2011; Oliveria et al., 2007)). As a general indicator of possible GnRH receptor-dependent effects on low-density PAM fraction proteins, we compared the overall protein content of PAM fractions obtained from control cells to that of cells exposed to GnRH (3nM for 10 min). To do so, we separated the total protein in PAM fractions from each condition by SDS-PAGE, stained with Coomassie blue, and made a side-by-side visual comparison to highlight differences in protein band composition (Fig. 2. 1C). As expected, the protein banding patterns from control and GnRH-treated αT3-1 cells were largely comparable. However, we detected at least ten positions with clear differences between control and GnRH treatment (denoted by asterisks in Fig. 2. 1C). Collectively, we conclude that our subcellular fractionation approach sufficiently enriches our samples with low-density plasma membrane-associated proteins potentially involved with GnRH receptor signaling. Further, these observations indicate that αT3-1 cell low-density PAM fractions are sufficiently stable under our native fractionation conditions to detect potential changes in protein composition in response to GnRH receptor activation.

SILAC-based proteomic and gene ontology analysis of αT3-1 cell low-density PAM fraction proteins

We used a SILAC-based quantitative liquid chromatography/tandem mass spectrometry (LC-MS/MS) approach to investigate changes in the protein composition of αT3-1 cell low-density PAM fractions in response to GnRH receptor activation (Fig. 2. 1D). Briefly, in four independent replicates, we

grew equal amounts of αT3-1 cells in "heavy" (Lys8, Arg10) and in "light" (Lys0, Arg0) SILAC media. Upon reaching ≈ 80% confluence, we treated the "heavy" cells with GnRH (3 nM) while the "light" cells served as an untreated control. After a 10 min treatment incubation, we harvested cells from each group, combined them in equal amounts, homogenized the combined sample in hypotonic buffer, and isolated the low-density PAM fractions as described above. To prepare the resulting samples for LC-MS/MS analysis, we precipitated the total protein present in the low-density PAM fractions with trichloroacetic acid, resuspended in 6M urea, and digested with trypsin.

Using Xcalibur™ software, we generated MS/MS spectra compound lists from our four biological replicates and used them to search against the mouse UniProt protein database concatenated to a reverse database generated by Mascot and Sorcerer-SEQUEST® software. For each sample, search results were imported and pooled using Scaffold software probabilistic protein identification algorithms. We set peptide and protein probability thresholds of 95% and 99%, respectively, and required a minimum of two unique peptides for each positive protein identification. Using this stringent approach, and only considering proteins identified in at least two out of the four replicates, we identified a total of 537 unique proteins (Table S1). Unsurprisingly, and consistent with our western blot analyses (Fig. 2. 1), cellular component-based gene ontology analysis showed that nearly one-third of the proteins identified in αT3-1 gonadotrope low-density PAM fractions were classified as plasma membrane-associated proteins (Fig. 2. 2A, top). Other cellular components with high representation included proteins associated with the nucleus, ER, mitochondria, cytosol, and cytoskeleton. A complimentary biological process-based gene ontology analysis revealed the presence of proteins related to development, protein metabolism, transport, nucleic acid metabolism, signal transduction, and cell motility (Fig. 2. 2A, bottom).

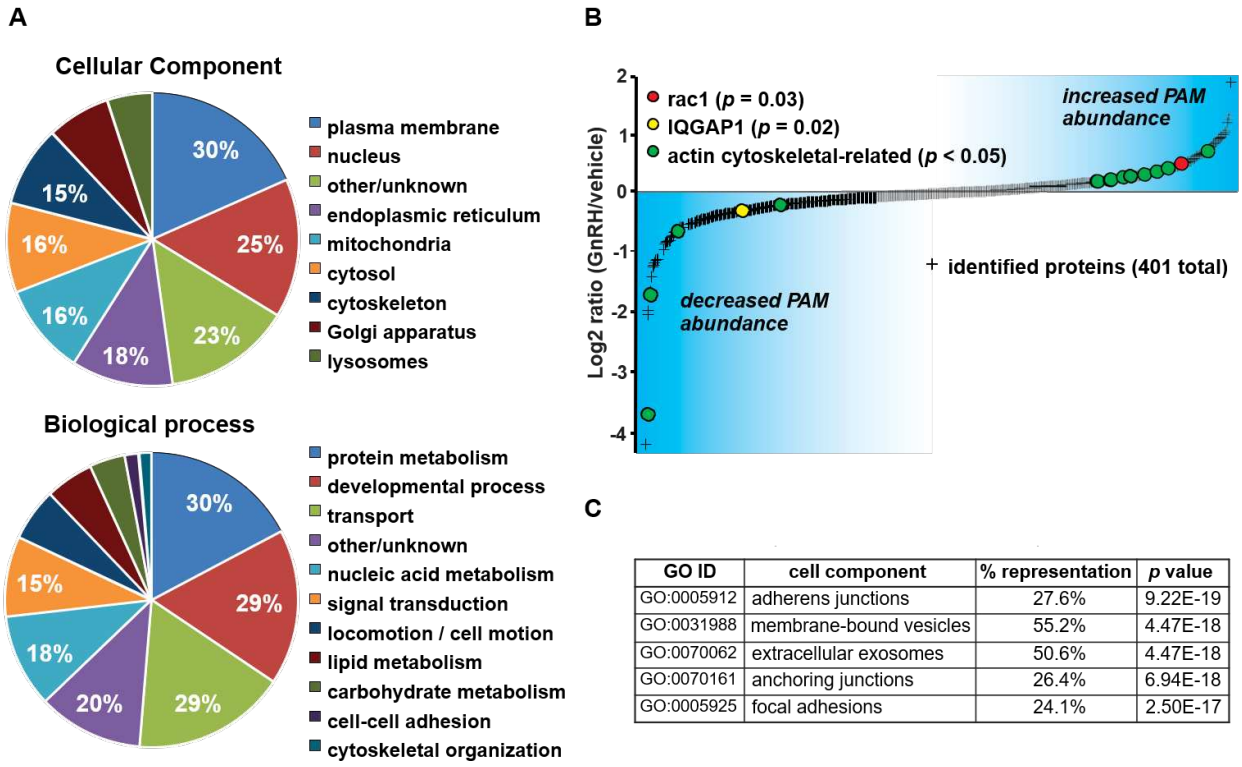

C

GO ID	cell component	% representation	*p* value
GO:0005912	adherens junctions	27.6%	9.22E-19
GO:0031988	membrane-bound vesicles	55.2%	4.47E-18
GO:0070062	extracellular exosomes	50.6%	4.47E-18
GO:0070161	anchoring junctions	26.4%	6.94E-18
GO:0005925	focal adhesions	24.1%	2.50E-17

Fig. 2. 2: Proteomic profile gonadotrope plasma membrane proteins and quantitative analysis after hormone stimulus. A, Gene ontology distribution charts of PAM proteins identified by LC-MS/MS based on cellular component (top) or biological function (bottom) for proteins identified (537 total proteins) with high significance and reproducibility in at least 2 out of 4 replicates. Pie charts indicate the percentage of proteins assigned to the indicated category using Scaffold software. Proteins assigned to multiple cellular localizations or biological functions will be counted more than once accordingly. B, Scatterplot showing normalized LOG2-transformed fold change ratios of the number of peptides derived from GnRH-treated over control proteins. Values include 401 proteins present in 3 out of 4 biological replicates with ≥ two unique peptide assignments per protein. C, Table showing GO cell component and enrichment of PAM proteins significantly affected by acute GnRH stimulus. Highly enriched GO terms are shown with corresponding % protein representation (87 proteins total) for each GO ID and p-value calculated using STRING version 10.0. *Szerlong, Heather*

Quantitative profile and gene ontology analysis of αT3-1 cell low-density PAM fraction protein abundances altered by GnRH receptor activation

To identify potential proteins regulated by GnRH receptor signaling, we performed a quantitative comparative analysis of the proteins contained in low-density PAM fractions isolated from control and GnRH-treated αT3-1 cells. For this analysis, we calculated the relative abundance of 401 proteins which were present in three out of four of our biological replicates. We averaged the log2-transformed ratio of the "heavy" (GnRH-treated) to "light" (control) peptides and plotted the fold change for each assigned protein (Fig. 2. 2B). Consistent with our Coomassie staining of PAM fraction proteins (Fig. 2. 1C), acute

GnRH exposure (3 nM for 10 min) did not alter the composition of the majority of proteins identified in αT3-1 cell low-density PAM fractions (Table S2). Infact, only 4% of the group resulted in 2-fold (or higher) change in relative abundance compared to control. However, 22% (or 87 out of 401 proteins; 41 up; 46 down) were significantly affected (p-value < 0.05) albeit at a lower magnitude (1.15-fold change and greater) and were included as GnRH-responsive protein candidates. (Fig. 2. 2B and Table S 2).

To examine the composition of low-density PAM fraction proteins influenced by GnRH receptor signaling, we pooled the proteins identified as GnRH-responsive and performed a cellular component-based gene ontology analysis using STRING bioinformatics (Fig. 2. 2C) (Huang da et al., 2009). This analysis revealed enriched GnRH-responsiveness of several cell component protein groups including membrane-bound vesicles, exosomes, and focal adhesions (Fig. 2. 2C). Interestingly, our analysis identified adherens junction-associated proteins as the GnRH-responsive cell component group with the highest level of significance (p = 9.22E-19). Adherens junctions, which are protein complexes involved with the formation of cell-cell contact sites, interact with actin cytoskeletal-related proteins and require dynamic remodeling of the actin cytoskeleton to form cell-cell junctions (Hartsock and Nelson, 2008; Yap et al., 2015; Yonemura, 2017). Consistent with the proposed importance of actin cytoskeletal remodeling to gonadotrope activation, we found that the association of 13 actin cytoskeletal-related proteins with low-density PAM fractions changed in response to GnRH receptor stimulation (Fig. 2. 2B and Table 1).

Cell polarity and adheren junction proteins accumulate at cell-cell junctions in response to GnRH

Based on our proteomics results and the identification of proteins affected by GnRH treatment, we next examined the localization of cell adhesion and polarity proteins, IQGAP1 and Ptk7, respectively, and their relationship to a known cell-cell adhesion and transcription co-activator, beta-catenin, in alpha T3-1 gonadotropes. Indirect immunofluorescence combined with confocal microscopy was used to compare IQGAP, Ptk7 and beta-catenin in control and GnRH-

treated cell cultures. Consistent with previously published data, beta-catenin accumumlated at the plasma membrane at cell-cell junctions within 60 min after GnRH treatment compared to control cells (Fig. 2. 2.5A & B). A similar pattern of redistribution was also observed with Ptk7 and IQGAP1 within the same time frame and partially co-localized with beta-catenin at cell-cell junctions. Of note, a fraction of beta-catenin and ptk7 co-localize in the nucleus albeit with a high degree of heterogeneity within the culture. Furthermore, cells sequentially stained with both anti-IQGAP1 and anti-Ptk7 antibodies reveal partial colocalization of these proteins at cell-cell juntions after GnRH treatment compared to control (Fig. 2. 2.5C). Together, our ICC analysis futher supports our hypothesis that IQGAP1 and PTK7 represent novel regulatory proteins downstream of the GnRH recepotor and further cooroborate our SILAC and LC-MS/MS analysis and identification of GnRH-responsive proteins dynamically regulated at the cell membrane.

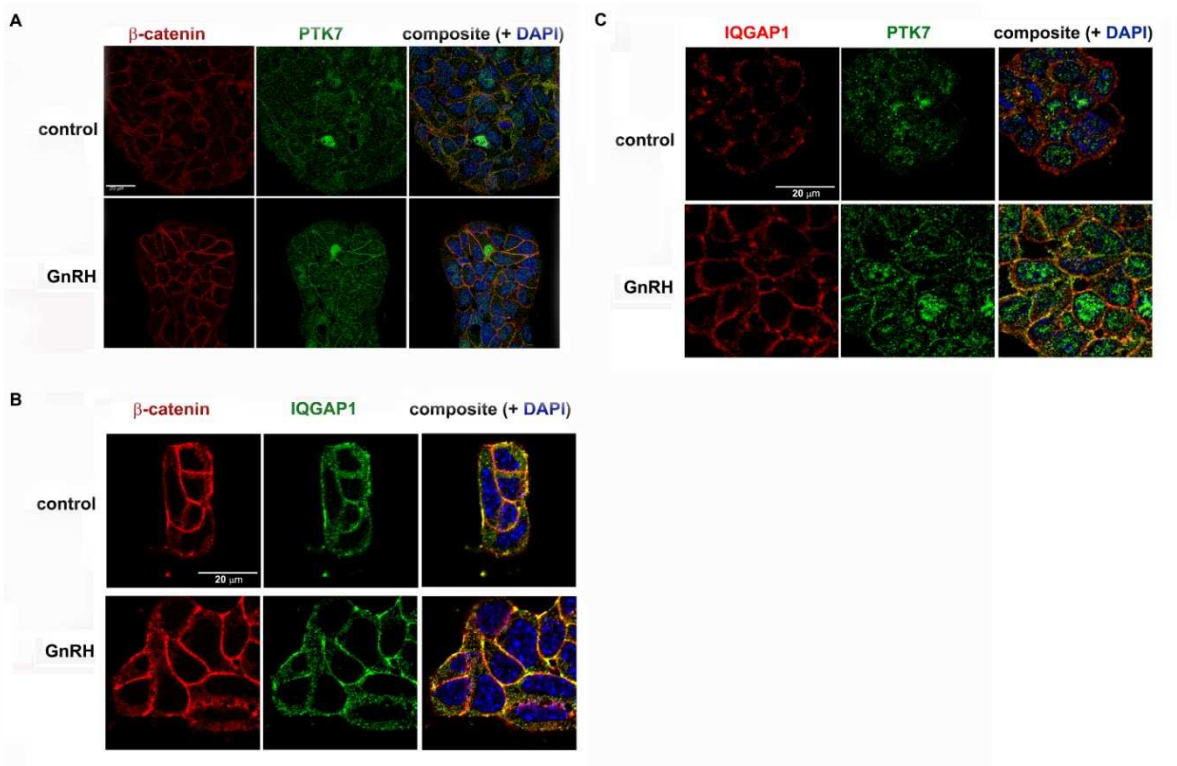

Fig. 2. 2.5: Cell polarity and cell-cell adhesion protein accumulate at cell-cell junctions in response to GnRH treatment. *A.* Representative confocal images of αT3-1 cells cultured in glass-bottom microwell dishes for 24 hr and incubated with either GnRH (20 nM) or water (control) for 60 min. Dishes were fixed with 4% paraformaldehyde and permeabilized with 0.1% Triton. Dishes were then sequentially stained first with anti-PTK7 antibody(1.5ug/ml) for 24hr followed by Alexa Fluor 488-conjugated secondary

antibody (2ug/ml), and then with anti-β-Catenin antibody (1ug/ml) for 24 hr followed by Alexa Fluor 568-conjugated secondary antibody (2ug/ml). *B.* Representative confocal images of αT3-1 cells cultured in glass-bottom microwell dishes for 24 hr and incubated with either GnRH (10 nM) or water (control) for 20 min, fixed with 4% paraformaldehyde and permeabilized with 0.1% Triton. Dishes were sequentially stained first with anti-IQGAP1 antibody (1ug/ml) followed by Alexa Fluor 488-conjugated secondary antibody (2ug/ml), and then stained with anti-β-Catenin antibody (1ug/ml) followed by Alexa Fluor 568-conjugated secondary antibody (2ug/ml) *C.* Representative confocal images of aT3-1 cells cultured in glass-bottom microwell dishes for 24 hr and incubated with either GnRH (20 nM) or water (control) for 20 min., fixed with 4% paraformaldehyde and permeabilized with 0.1% Triton. Dishes were sequentially stained first with anti-PTK7 antibody (1.5ug/ml) followed by Alexa Fluor 488-conjugated secondary antibody (2ug/ml), and then stained with anti-IQGAP1 antibody (1ug/ml) followed by Alexa Fluor 568-conjugated secondary antibody (2ug/ml). All cells were counterstained with DAPI to label nuclei and imaged under either a 40x (A) 63X (B, C) oil objective of a Zeiss LSM 800 confocal microscope. The yellow staining indicates colocalization of indicated proteins. *Szerlong, Heather*

GnRH receptor signaling promotes interaction between the small GTPase Rac1 and the scaffold protein IQGAP1

To validate our proteomic observations we narrowed our focus to the actin cytoskeleton-related proteins Rac1, a small GTPase, and IQGAP1, a multimodular scaffold protein. Evidence suggests that Rac1 and IQGAP1 participate in several actin cytoskeletal-related processes such as cell motility and formation of cell-cell junctions (Dumontier et al., 2000; Filić et al., 2012; Noritake et al., 2004b; Ruiz-Velasco et al., 2002; Watanabe et al., 2015; White et al., 2012). Our quantitative analyses revealed that GnRH increased the relative abundance of Rac1 in low-density PAM fractions 1.40-fold ($p = 0.029$) while the relative abundance of IQGAP1 decreased 0.81-fold ($p = 0.017$). To investigate potential molecular events associated with these findings, we visualized the effect of GnRH (100 nM for 10 min) on the subcellular localization of transiently expressed EGFP-Rac1 and endogenous IQGAP1 in αT3-1 cells by fluorescence confocal microscopy. Similar to stimulation of M_3 muscarinic acetylcholine receptors in CHO-M3 cells (Ruiz-Velasco et al., 2002), we found that GnRH receptor activation promoted accumulation of EGFP-Rac1 and IQGAP1 at αT3-1 cell-cell junctions (Fig. 2. 3A). Parallel experiments using an anti-Rac1 monoclonal antibody to visualize endogenous Rac1 produced comparable results (data not shown).

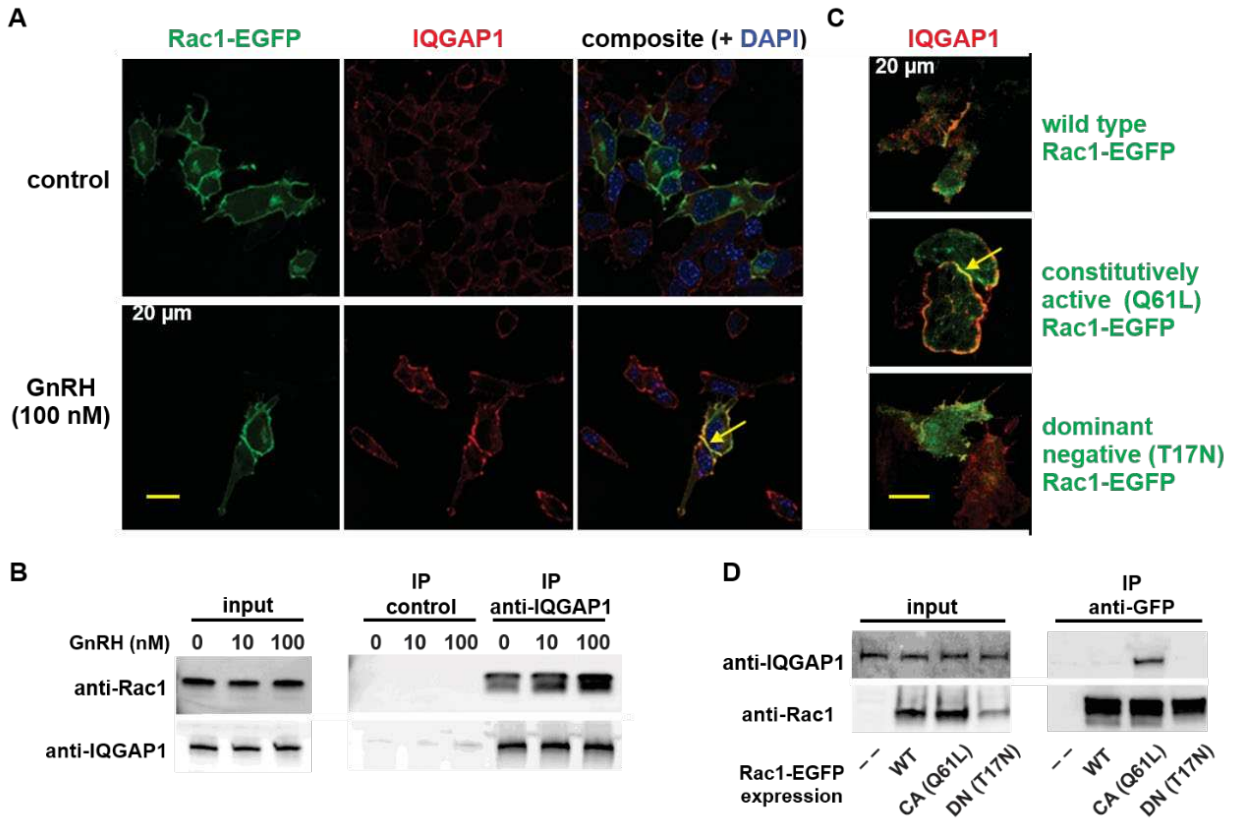

Fig. 2. 3: GnRH increases the association between Rac1 and IQGAP1 in αT3-1 cells. A, Representative confocal images showing exogenous EGFP fluorescence (green) and endogenous IQGAP1 immunofluorescence (red) in αT3-1 cells expressing wild-type Rac1-EGFP incubated with or without GnRH (100 nM for 10 min); yellow signal indicates apparent colocalization at a cell-cell contact site (arrow). B, Representative western blots of whole lysates (input) immunoprecipated with either an antibody (IP anti-IQGAP1) or serum (IP control) and probed with either anti-IQGAP1 (loading control) anti-Rac1 antibody as indicated. Cells were treated with increasing GnRH concentration (nM) for 10 min at 37C. C, Representative confocal images showing EGFP fluorescence (green) and IQGAP1 immunofluorescence (red) in αT3-1 cells expressing wild-type (*top*), constitutively active (Q61L; *middle*), and dominant negative (T17N; *bottom*) Rac1-EGFP; yellow signal indicates apparent colocalization at a cell-cell contact site (arrow) (*n* = X replicates). D, Representative western blots of whole αT3-1 cell lysates transfected with indicated Rac1-EGFP or 'empty' EGFP plasmids, immunoprecipitated with anti-GFP antibody and probed with either anti-IQGAP1 or anti-Rac1 antibody as indicated. Rac1-EGFP expression vectors include wild-type (WT), constitutively active (CA), and dominant negative (DN). *Szerlong, Heather*

Rac1 binds directly to the IQGAP1 GTPase activating protein-related domain (GRD) (Jacquemet and Humphries, 2013; Kuroda et al., 1996; Nouri et al., 2016b). To provide evidence of a physical association between Rac1 and IQGAP1 in gonadotropes, we performed co-immunoprecipitation (co-IP) experiments on αT3-1 cell lysates. Western blot analysis of αT3-1 cell protein complexes eluted from protein G-coated sepharose beads preincubated with IQGAP1 antibodies revealed a clear presence of Rac1 (Fig. 2. 3B). Although we could detect Rac1 association with IQGAP1 under basal conditions (i.e.,

in the absence of GnRH), we consistently found that GnRH exposure enhanced the association of Rac1 with IQGAP1 (Fig. 2. 3B).

To corroborate our Rac1 activity and binding experiments, we examined the effects of heterologously expressed wild-type, constitutively active (Q61L), and dominant negative (T17N) Rac1-EGFP (Subauste et al., 2000) on IQGAP1 in αT3-1 cells. We found that, in contrast to wild-type and dominant negative Rac1-EGFP, constitutively active Rac1-EGFP colocalized with endogenous IQGAP1 at cell-cell junctions in the absence of GnRH stimulation (Fig. 2. 3C). To confirm, we performed co-IP experiments with whole cell lysates derived from αT3-1 cells expressing each Rac1-EGFP and EGFP control constructs pre-incubated with anti-EGFP beads. Compared to control, IQGAP1 specifically bound to constitutively active, but not wild type or dominant negative Rac1-EGFP in the absence of GnRH (Fig. 2. 3D). Note that our co-IP experiments targeting endogenous Rac1 and IQGAP1 showed a fractional association between these proteins in the absence of GnRH (or 0 nM GnRH) (Fig. 2. 3B). We suggest that the apparent lack of IQGAP1 co-IP with wild-type Rac1-EGFP likely results from either interference from endogenous Rac1 expression or an artificially inflated abundance of exogenous Rac1-EGFP. Regardless, and consistent with previous work (Jacquemet and Humphries, 2013; Owen et al., 2008b; Ruiz-Velasco et al., 2002), our fluorescence imaging and biochemical data indicate that IQGAP1 preferencially associated with activated Rac1 in αT3-1 cells.

GnRH receptor activation promotes Rac1-dependent ERK phosphorylation

Previous work mechanistically links Rac1 with GnRH receptor-dependent stimulation of JNK MAP kinase signaling in gonadotropes (Levi et al., 1998b). However, the importance of Rac1 (and IQGAP1) to ERK-dependent MAP kinase signaling in gonadotropes is unknown. Accordingly, we investigated the kinetic and epistatic relationships between Rac1 activity and ERK phosphorylation in gonadotropes exposed to GnRH. Using a PAK-1 PBD pull-down assay that binds active Rac1-GTP with high specificity and stability (Benard et al., 1999), we found that GnRH induced a gradual increase in Rac1-GTP levels which were evident within two minutes of exposure (Fig. 2. 4A & B). Concurrently, we

found that phosphorylated ERK1/2 accumulated in the same samples and plateaued at two minutes of GnRH exposure. To establish a functional role for Rac1 in GnRH-dependent ERK phosphorylation, we compared the relative levels of phosphorylated ERK in αT3-1cells treated with GnRH (10 nM for 10 min) in the presence or absence of Rac1 inhibition. Indicating a requisite role for Rac1, our western blot analysis showed that preincubation of αT3-1 cells with a selective (Ferri et al., 2013) Rac1 inhibitor V (50 μM for 1 hour) abolished GnRH receptor-dependent ERK1/2 phosphorylation (Fig. 2. 4C & D).

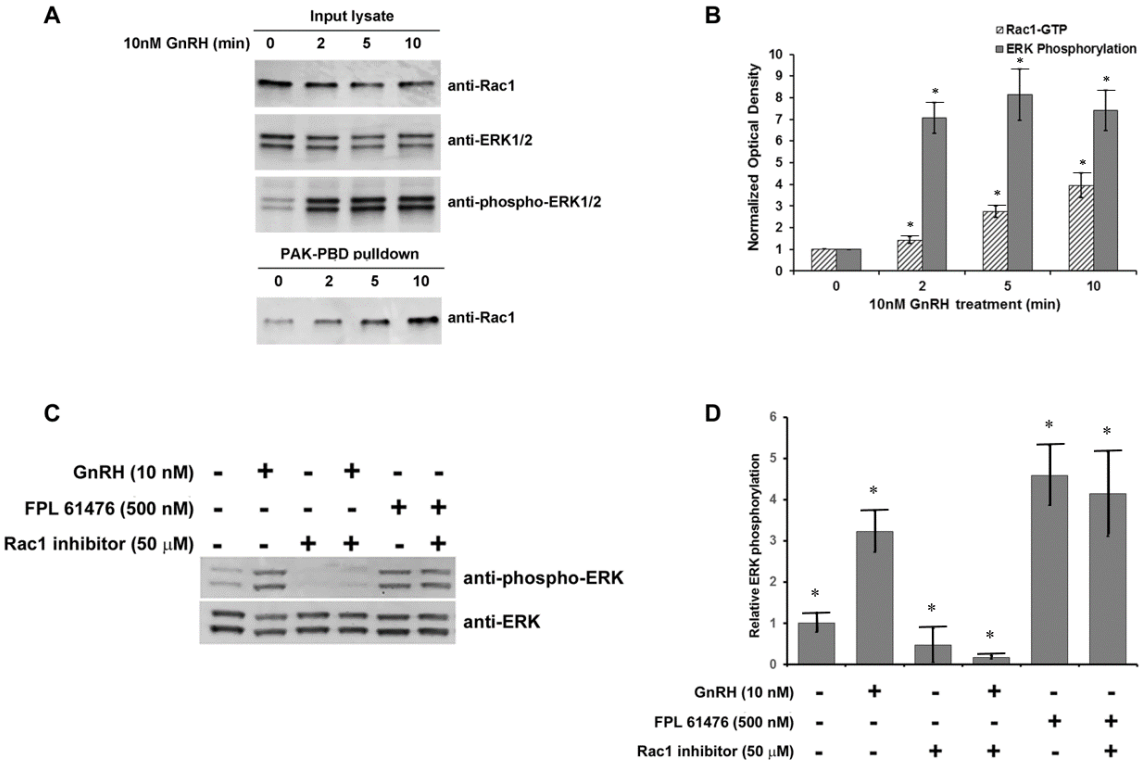

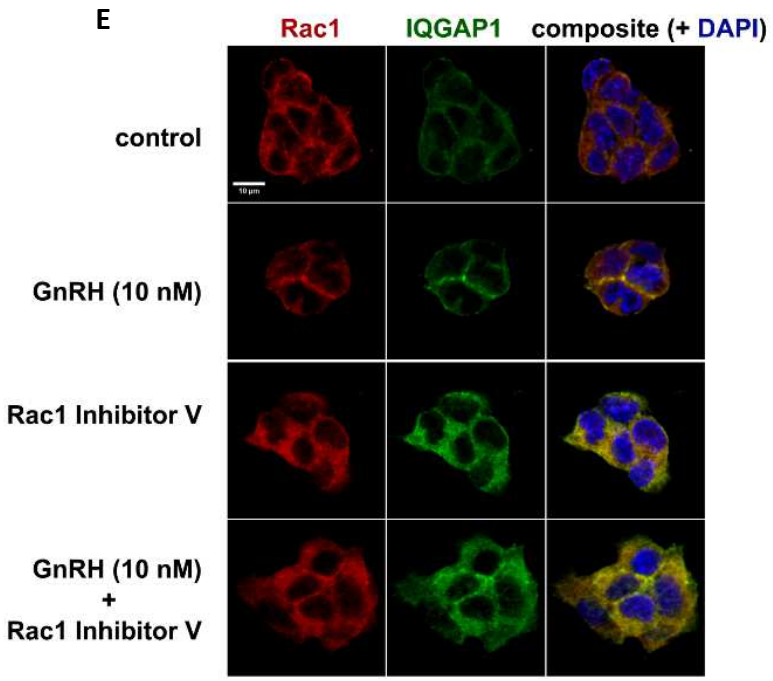

Fig. 2. 4: GnRH receptor signaling promotes Rac1-dependent ERK phosphorylation in αT3-1 cells. A, Representative western blots showing ERK phosphorylation and Rac1 activation (Rac1-GTP) in αT3-1 cells treated with GnRH (10 nM) for 2, 5, and 10 min. Whole cell lysates (*top*) were used as the input for Rac1-GTP pulldown experiments. PAK-PBD eluates containing Rac1-GTP and whole cell lysates were probed with antibodies raised against Rac1, total ERK1/2, and phosphorylated ERK1/2 as indicated. B, Quantitation of western blots (Fig. 2. 4A) with increasing GnRH treatment. The Bar graph shows the average ratio of Rac1-GTP to total Rac1 or phospho-ERK to total ERK and normalized to control (set at 1.0). Error bars indicate the SEM for 3 replicates. C, Representative western blots of whole cell lysates derived from αT3-1 cells treated with GnRH (10 nM), the L-type Ca^{2+} channel agonist FPL61476 (500 nM), or Rac1 inhibitor V (50 μM) as indicated and probed with anti-ERK and anti-phospho-ERK antibodies. D, Bar graph illustrating average band intensity ratio of p-ERK to total ERK and normalized to the control (set at1.0). Error bars indicate the SEM for 3 replicates. # and *, greater than 0 min; **, greater than 0 and 2 min; ***, greater than 0, 2, and 5 min. E, Representative confocal images showing endogenous IQGAP1 immunofluorescence (green) and endogenous Rac1 immunofluorescence (red) in αT3-1 with or without GnRH (10 nM for 10 min). Cells were pretreated (1 hour) with DMSO (control) or Rac1 inhibitor V (50 μM) followed by a 15 min treatment of either vehicle (water) or GnRH (10nM). Cells were fixed in 4% PFA and doubly stained with anti-Rac1 antibody (red) and anti-IQGAP1 (green) antibody followed by Alexa Fluor 568-conjugated goat anti-mouse and Alexa Fluor 488-conjugated goat anti-rabbit antibodies. All cells were counterstained with DAPI to label nuclei and imaged under a 63X oil objective of a Zeiss LSM 800 confocal microscope. The yellow staining indicates the colocalization of Rac1 and IQGAP1. Images show that Rac1 activation is required for GnRH-dependent IQGAP1 accumulation at cell-cell junctions. *Szerlong, Heather*

To further characterize the influence of Rac1 on GnRH receptor signaling, we tested the effects of Rac1 inhibition on L-type Ca^{2+} channel-mediated ERK phosphorylation. Evidence suggests that localized Ca^{2+} influx through L-type Ca^{2+} channels is necessary for GnRH-dependent ERK activation in gonadotropes (Dang et al., 2014; Mulvaney and Roberson, 2000; Mulvaney et al., 1999). Accordingly, we found that direct pharmacological activation of αT3-1 cell L-type Ca^{2+} channels with FPL 61476 (10 μM

for 10 min) increased ERK1/2 phosphorylation to the same extent as GnRH (Fig. 2. 4C & D). However, in contrast to GnRH-dependent ERK phosphorylation, Rac1 inhibition did not reduce ERK1/2 phosphorylation following L-type Ca^{2+} channel activation. From these data, we conclude that Rac1 functions either upstream or independently from L-type Ca^{2+} channel-mediated ERK phosphorylation. Our observation that Rac1 inhibition did not attenuate ERK phosphorylation following FPL 61476 exposure also suggests that the Rac1 inhibitor used in our experiments (Rac1 inhibitor V, Calbiochem) does not interfere with ERK activation in a general non-specific manner.

To further delineate the epistatic relationship between Rac1 and IQGAP1, confocal microscopy and indirect immunofluorescence was used to study αT3-1cells treated with Rac1 inhibitor. Prior to GnRH stimulus, cells treated with the Rac1 inhibitor show a significant dispersion of endogenously expressed Rac1 in the cytosol. Significantly, the GnRH-dependent Rac1 localization to cell-cell junctions was absent in cells pre-treated with Rac1 inhibitor prior to GnRH (compare Rac1 inhibitor V vs GnRH (10 nM) + Rac1 inhibitor V). Likewise, IQGAP1 displayed a similar distribution pattern as Rac1 under control and test conditions. IQGAP1 was highly dispersed throughout the cytoplasm in the presence of Rac1 inhibitor and failed to accumulate at cell-cell junctions in response to GnRH (Fig. 2. 4E). Cells that were not treated with Rac1 inhibitor resulted in GnRH-dependent colocalization of IQGAP1 and Rac1 at cell-cell junctions compared to control (Fig. 2. 3) and was not recruited to cell-cell junctions when first treated with the Rac1 inhibitor (compare GnRH (10nm) vs GnRH (10 nM) + Rac1 Inhibitor V).

Discussion

In the current study, we discovered substantial enrichment of proteins related with intercellular communication in clonal T3-1 gonadotropes utilizing a non-biased quantitative proteomic screen to identify proteins altered by GnRH receptor activation. The relative abundance of plasma membrane-associated proteins in response to GnRH was identified and quantified using a SILAC (stable isotope labeling by amino acids in cell culture)-based proteomics technique (Ong et al., 2002) . We found a substantial shift in 80 plasma membrane-associated proteins after GnRH treatment in immortalized T3-1 gonadotropes. In line

with earlier research, GnRH enhanced the plasma membrane association of several actin cytoskeletal, cell polarity, and adherens junction-related proteins, such as the scaffold protein IQGAP1 and the small GTPase Rac1, Ptk7 and others, utilizing a non-biased quantitative proteomic screen of clonal T3-1 gonadotropes. Our findings point to a unique mechanism in which Rac1-containing IQGAP1 signaling complexes influence GnRH-dependent ERK activation in T3-1 gonadotropes and serve as critical effectors for signaling events that lead to cell-cell contact enrichment. In support of this, we show that pharmacological suppression of Rac1 diminished ERK phosphorylation and Rac1-IQGAP1 complexes at cell junctions, indicating that this has functional significance. Overall, we conclude that Rac1-containing IQGAP1 signaling complexes influence GnRH-dependent ERK activation in T3-1 gonadotropes and serve as essential effectors for signaling events resulting in cell-cell interactions enrichment.

Cell-cell junctions are essential in establishing extracellular communication between neighboring cells and intracellular communication with various cytoskeletal elements that together create incorporated, structural continuance across the tissues. Previous work shows that many elements are known to be linked to adherens and tight junctions. Junctional adhesion proteins bind through their cytoplasmic tail to cytoskeletal and signaling proteins, allowing the adhesion proteins' anchoring to actin microfilaments and transfer intracellular signals inside the cell (Bazzoni et al., 1999; Braga, 2002; Matter and Balda, 2003; Wheelock and Johnson, 2003a). The association with actin is essential for the stabilization of the junctions and the dynamic regulation. In addition, the interaction of junctional adhesion proteins with the actin cytoskeleton might be relevant in the maintenance of cell shape and polarity (Dudek and Garcia, 2001; Lampugnani et al., 2002; Sheldon et al., 1993; Stevens et al., 2000). Interestingly, releasing some intracellular junctional proteins from junctions leads to translocating to the nucleus and modifying transcription (Ben-Ze'ev and Geiger, 1998; Bienz and Clevers, 2000; Matter and Balda, 2003). Moreover, some junctional proteins may act as scaffolds, such as IQGAP1, which binds several effector proteins and mediates their mutual interaction.

Many cell types, such as lymphocytes, osteocytes, pancreatic β cells, and endocrine cells of the anterior pituitary (e.g., gonadotropes), are characterized by functional homotypic interactions where intercellular contact and communication are not distinguished or defining characteristics (Edwards et al., 2017a; Göngrich et al., 2016; Harwood and Batista, 2008; Kelly et al., 2011; Kim et al., 2014; Le Tissier et al., 2017; Momiji et al., 2019; Stoddart et al., 2001). In studies using slices of anterior pituitary revealed that GnRH exposure prompted connexin 36 (Cx36) gap junction-dependent coordination within loosely clustered gonadotropes (intercellular distances < 250 μm) (Göngrich et al., 2016). Moreover, a study employing female Cx36-null mice showed dysfunction in the HPG axis, including decreased LH secretion, impaired ovulation, and small litter size. However, molecular mechanisms and functional outcomes associated with multicellular gonadotrope interactions are mostly hypothetical. Despite these interesting observations, the molecular mechanisms underlying intercellular communication between gonadotropes (without electrical coupling through gap junctions) are unclear.

In gonadotropes, GnRH receptor activation produces two distinct intracellular Ca2+ signals: Ca2+ release from the endoplasmic reticulum (ER) through inositol-1,4,5-trisphosphate (IP3) receptors and Ca2+ influx through the plasma membrane via L-type Ca2+ channels (Grosse et al., 2000a). These two Ca2+ signals increase mitogen-activated protein (MAP) kinase signaling (Mulvaney and Roberson, 2000; Mulvaney et al., 1999). Specifically, Ca2+ release from the ER promotes c-Jun N-terminal kinase (JNK) activity, which increases in FSH expression, while Ca2+ influx through L-type Ca2+ channels promotes extracellular signal-regulated kinase (ERK) activity, which increases LH expression. Previous published work from our group has highlighted that GnRH induced discrete sites of Ca2+ influx through L-type Ca2+ channels (Ca2+ sparklets) in gonadotrope-derived αT3-1 cells. Consistent with the work of others (Mulvaney and Roberson, 2000; Mulvaney et al., 1999), in these cells, we concluded that the highly localized L-type Ca2+ channel sparklet activity observed in our assays is both essential and sufficient for ERK activation (Dang et al., 2014). As a result, it's plausible to assume that successful GnRH receptor signaling requires subcellular compartmentalization and coordination of signal transduction proteins. Indeed, data reveals that GnRH receptors in gonadotropes are localized in low-density, sphingolipid- and

cholesterol-rich plasma membrane microdomains. (Allen-Worthington et al., 2016; Bliss et al., 2007). Importantly, GnRH receptor positioning inside low-density plasma membrane microdomains appears to be required for the formation of functional protein complexes and downstream signaling to ERK (Bliss et al., 2007; Navratil et al., 2010). Previous research indicates that actin cytoskeletal remodeling is essential for GnRH receptor-dependent activation of gonadotrope (Dang et al., 2014; Edwards et al., 2017a; Edwards et al., 2015; Navratil et al., 2014). In the presence of GnRH, gonadotropes promptly (within 60 seconds) promote actin polymerization to generate membrane ruffles, lamellipodia, and filopodia, according to previous research from our lab and others (Childs, 1985; Navratil et al., 2007). GnRH has recently been discovered to cause actin remodeling by activating cortactin, which enhances its connection with the actin-related protein (Arp) 2/3 complex, causing actin branching and remodeling (Navratil et al., 2014). Cortactin not only localizes to regions of dynamic actin-containing structures, but it also directly binds to dynamin in these locations via its C-terminal SH3-domain (McNiven et al., 2000; Ochoa et al., 2000; Orth et al., 2002). Significantly, and in line with our theory, gonadotropes undergo substantial cytoskeletal and morphological alterations in response to GnRH receptor activation, which appear to be essential for the transcriptional modifications required for upregulation of gonadotropin synthesis (Navratil et al., 2014; Navratil et al., 2007). In this process, many Actin cytoskeletal, cell polarity, and adherens junction-related proteins are recruited to intercellular junctions for the aim of establishing and increasing functional connection between gonadotropes.

IQGAP1 is a new component of the GnRH/GnRH receptor pathway with potential to enhance biological stratification and therapeutic targeting of GnRH receptor-targeted cancers. Beyond gonadotropes, other studies have shown the important role of IQGAP1 in regulating cellular processes, including cytoskeletal rearrangements in cell migration and cell adhesion (Brandt and Grosse, 2007; Machesky, 1998; Noritake et al., 2005). IQGAP1 is localized at the plasma membrane at cell-cell adhesion and associated with small Rho GTPases Rac1 or Cdc42 to regulate the adherens junction complex through the interaction with β-catenin. Importantly, IQGAP1 has been shown to associate directly to Rac1 and Cdc42 through the GTPase activating protein-related domain (GRD), making it functions as a downstream

effector (Hart et al., 1996; Kuroda et al., 1996). IQGAP1 is recognized to have a vital role in cytoskeleton regulation and actin remodeling (Briggs and Sacks, 2003b). Evidence suggests that Rac1 and IQGAP1 participate in several actin cytoskeletal-related processes such as cell motility and formation of cell-cell junctions (Dumontier et al., 2000; Filić et al., 2012; Noritake et al., 2004b; Ruiz-Velasco et al., 2002; Watanabe et al., 2015; White et al., 2012). Likewise, IQGAP1 has been shown to interacts with Cdc42 directly, causing an inhibition to the intrinsic GTPase activity of Cdc42 in vitro, which leads to the stabilization of Cdc42 in the GTP-bound state (Hart et al., 1996; Ho et al., 1999b; Swart-Mataraza et al., 2002; Zhang et al., 1997). Moreover, in a study using mammalian cells, IQGAP1 overexpression highly increases the pool of active Cdc42, leading then to induce filopodia formation (Swart-Mataraza et al., 2002), while IQGAP1 knockdown using RNA interference significantly reduces GTP-bound Cdc42 (Mataraza et al., 2003b).

IQGAP1 also associates directly with E-cadherin and affects its function (Noritake et al., 2005). Notably, the mediators of cell-cell adhesion E- and N-cadherin requires the interaction and association of IQGAP1/Cdc42/Rac1/α-catenin/β-catenin complexes (Fukata et al., 2001a; Kaibuchi et al., 1999b; Kuroda et al., 1999). Overexpression of IQGAP1 (Kuroda et al., 1998b) and its translocation to sites of cell-cell contact (Li et al., 1999b) reduce the interaction between E-cadherin and the actin cytoskeleton, leading to weakening cell-cell attachment. Furthermore, in human endothelial cells, IQGAP1 co-localizes with VE-cadherin at sites of cell-cell contact, and knockdown of IQGAP1 using siRNA inhibits the localization of VE-cadherin at adherens junctions, as well as its phosphorylation through reactive oxygen species (Yamaoka-Tojo et al., 2006). Overall, these studies indicate that IQGAP1 functions as a modulator of receptor signaling through taking inputs from heterogeneous receptors and regulating signal outputs that control reactive oxygen species production, MAPK cascades, and β-catenin-mediated transcription (Brown and Sacks, 2006).

To better understand the actions of IQGAP1 activity in response to GnRH-R activation, we used an approach that is based on examining the localization of cell adhesion and polarity proteins, IQGAP1 and Ptk7, respectively, and their relationship to a known cell-cell adhesion and transcription co-activator, β-

catenin, in αT3-1 gonadotropes. Indirect immunofluorescence combined with confocal microscopy was used to compare IQGAP, Ptk7, and β-catenin in control and GnRH-treated cell cultures. Consistent with previously published data, β-catenin accumulated at the plasma membrane at cell-cell junctions within 60 min after GnRH treatment compared to control cells. Interestingly, a similar pattern of redistribution was also observed with Ptk7 and IQGAP1 within the same time frame and partially colocalized with β-catenin at cell-cell junctions. A fraction of β-catenin and ptk7 colocalize in the nucleus, albeit with a high degree of heterogeneity within the culture. Furthermore, cells sequentially stained with both anti-IQGAP1 and anti-Ptk7 antibodies reveal partial co-localization of these proteins at cell-cell junctions after GnRH treatment compared to control. Moreover, our data showed an upstream activation and association of Rac1 and IQGAP1 in response to GnRH treatment. In support of this, we show that pharmacological inhibition of Rac1 reduced ERK phosphorylation and Rac1-IQGAP1 complexes at cell junctions, revealing that Rac1-containing IQGAP1 signaling complexes control GnRH-dependent ERK activation in αT3-1 gonadotropes and act as essential effectors for signaling processes leading to cell-cell contact enrichment.

MAPK cascades stimulate numerous DNA-binding proteins mediating the impact of GnRH on the primary, secondary, and tertiary response genes. In LβT2 cells, GnRH increases the nuclear accumulation of β-catenin (Gardner et al., 2007; Salisbury et al., 2007), leading to the growing binding of β-catenin and SF1 to the endogenous Lhb promoter-regulatory region (Salisbury et al., 2007), suggesting further crosstalk between signaling mediators of the Wnt/β-catenin pathway and those activated by GnRH. Many studies using a heterologous HEK293 model cell line and LβT2 gonadotrope cell line showed that the activation of GnRH receptor by GnRH could target mediators of the Wnt/β-catenin signaling pathway (Gardner et al., 2007; Gardner and Pawson, 2009; Salisbury et al., 2007, 2009; Salisbury et al., 2008). IQGAP1 has been reported as a scaffold MEK/ERK cascade binding directly to MEK1/2 and ERK1/2, leading to modulate their activation (Roy et al., 2004, 2005). Furthermore, a study demonstrated that IQGAP1 could form a primary signal in the periphery of the nucleus to transiently maintain Erk1/2 phosphorylation (Awasthi et al., 2010), providing strong evidence that activation of the Erk1/2 pathway can be regulated and compartmentalized by IQGAP1. Moreover, it has been reported that IQGAP1 acts as β-catenin-mediated

gene transcriptions regulator (Briggs et al., 2002a; Fukata et al., 1999b; Wang et al., 2008). The direct interaction of IQGAP1 with APC (Aoki and Taketo, 2007; Watanabe et al., 2004b) or protein phosphatase 2A (PP2A) (Suzuki et al., 2005), as well as the indirect interaction of GSK-3β (Watanabe et al., 2009), indicates that IQGAP1 has a role in Wnt signaling. Primarily, IQGAP1 was shown to bind to the C-terminus of Disheveled (DVL) (Goto et al., 2013b) via a region between the IQ domains and the GRD of IQGAP1, while β-catenin binds directly to the RGCT domain (Fukata et al., 1999b), which emphasize the role of IQGAP1 in the activation and degradation of β-catenin. In addition, PTK7 has also been shown to function in the regulation of non-canonical Wnt PCP signaling and the interaction with mediators of the canonical Wnt pathway, including Wnt ligands LRP6 receptor and β-catenin (Bin-Nun et al., 2014; Peradziryi et al., 2012; Puppo et al., 2011).

Our data shows an upstream activation and association of Rac1 and IQGAP1 in response to GnRH treatment. Indicating functional relevance, pharmacological inhibition of Rac1 reduced ERK phosphorylation and Rac1-IQGAP1 complexes at cell junctions. This demonstrates that Rac1-containing IQGAP1 signaling complexes modulate GnRH-dependent ERK activation in αT3-1 gonadotropes and serve as essential effectors for signaling events leading to an enrichment of cell-cell contacts. Moreover, our data showed a nuclear accumulation of PTK7 and β-catenin within 60 minutes of GnRH exposure by measuring the fluorescence changes of the antibodies using confocal laser microscopy. This led us to suggest additional crosstalk between some intracellular junctional proteins releasing, Interestingly, from junctions to translocating to the nucleus and modifying transcription in agreement with earlier research (Ben-Ze'ev and Geiger, 1998; Bienz and Clevers, 2000; Matter and Balda, 2003).

The signal transduction events triggered by the gonadotropin releasing hormone receptor (GnRHR) have been the subject of extensive research for many decades (Naor, 2009), resulting in a substantial body of information about the structure and kinetics of gonadotropin releasing hormone (GnRH)-induced signaling networks as significant advancements in our understanding of GnRHR signaling in several experimental systems. However, GnRH-induced signaling networks remain a challenge in the field of reproductive biology. In vivo, the differentiated gonadotrope responses to the GnRH signal in a complex

and dynamic endocrine environment. Evidence indicates that anterior pituitary cells, including gonadotropes, can participate in multicellular networks in their natural environment (Alim et al., 2012; Budry et al., 2011; Featherstone et al., 2016; Golan et al., 2016b; Hodson et al., 2012a; Le Tissier et al., 2017; Lyles et al., 2010; Schaeffer et al., 2011).

Mechanistic insights on how IQGAP1 and PTK7 function as molecular coordinators in cytoskeletal rearrangement, pathways activation, and β-catenin-mediated gene transcription are fundamental in understanding the GnRH essential signaling process. More specifically, understanding the IQGAP1 signaling events' transient temporal and spatial organization in the GnRH signaling network will provide novel insights that will aid in the development of new cellular paradigms. In addition, the nuclear accumulation of PTK7 and β-catenin and the involvement of IQGAP1 in the regulation of gene expression in gonadotropes seem to be essential in the GnRH signaling network. Therefore, further research into the precise organization role of PTK7 and IQGAP1 scaffold proteins in the GnRH signaling network and the recruitment of various signaling molecules is required. The amount of research on the function of IQGAP1 is limited, and more investigation is necessary. Since IQGAP proteins play a role in tumorigenesis (White et al., 2009), pharmacologically targeting components of IQGAP1-mediated signaling complexes could contribute to novel tumor therapies. Overall, the study illustrates the molecular mechanisms by which IQGAP1 and PTK7 regulate cellular physiology could contribute to a deeper understanding of the GnRH signaling network's regulation and, potentially, paradigm-shifting insights.

Understanding the signal transduction events triggered by the activation of gonadotropin releasing hormone receptor will improve our fundamental understanding of gonadotrope biology by directly addressing the patent knowledge gap regarding intergonadotrope-related phenomena. We expect that our observations and more investigations will reveal novel molecular targets potentially useful for experimental and clinical manipulation of gonadotrope function. After all, our results may have ramifications in various biomedical fields, including embryology and oncology, as our planer cell polarity and adherens junction-related proteins of interest influence intercellular communication during fetal development and

tumorigenesis (Gärtner et al., 2014; Golubkov and Strongin, 2014; Lei et al., 2019; Mattes and Scholpp, 2018; Shin et al., 2015).

Methodology

Antibodies

The following antibodies were used in this study: rabbit polyclonal anti-GFP (Torrey Pines Biolabs, Inc., Houston, TX), rabbit polyclonal anti-N-cadherin H-63 rabbit polyclonal anti-IQGAP1 H109, mouse monoclonal anti-IQGAP1 C-9, goat polyclonal anti-AKAP 150 N-19, rabbit polyclonal anti-ERK K-23, mouse monoclonal anti-p-ERK E-4 (Santa Cruz Biotechnology, Inc); mouse monoclonal anti-Rac1(Cytoskeleton, Inc.); rabbit polyclonal anti-GnRHR, mouse monoclonal anti-tubulin alpha, anti-PTK7 (Proteintech Group), mouse monoclonal anti-Rac1 (BD Biosciences); mouse monoclonal anti-calcium channel L type DHPR alpha 2 subunit antibody 20A (abcam); rabbit polyclonal anti-calreticulin (Novus Biologicals), mouse monoclonal anti-flotillin (a generous gift from M. Tamun**).** As secondary antibodies for immunofluorescence experiments, goat anti-mouse and goat anti-rabbit Alexa Fluor 488 and Alexa Fluor 568 (Invitrogen) were used. HRP-conjugated goat anti-rabbit, goat anti-mouse and donkey anti-goat IgGs (Santa Cruz Biotechnology) were used as secondary antibodies in western blot experiments. Immunoprecipitation experiments used recombinant Protein G-Sepharose 4B conjugate (Life Technologies).

Cell culture and transfection

Clonal αT3-1 mouse gonadotrope cells (Windle et al., 1990), a generous gift from Dr. Pamela Mellon (University of California, San Diego), were cultured in high-glucose DMEM (GE Healthcare Life Sciences) with L-glutamine supplemented with FBS (10%). Cells were maintained at 37°C in 5% CO_2 humidified air.

Cell transfection was performed by electroporation followed by 48 hours of culture for all subsequent experiments as indicated. For SILAC experiments, DMEM lacking arginine and lysine were supplemented with either "light" lysine/arginine containing unlabeled (Lys0, Arg0) (*light;* L-lysine and L-arginine (Sigma)) or "heavy" lysine ($^{13}C_6$ $^{15}N_2$) / arginine ($^{13}C_6$ $^{15}N_4$) (Lys8, Arg10) (*heavy*; L-Lysine 13C6, 99%; 15N2, 99% (CNLM-291-H) L-Arginine 13C6, 99%; 15N4, 99% (CNLM-539-H)) amino acids. After a minimum of 9 passages, cells grown in "heavy" media were treated with GnRH (3 nM) while cells cultured in "light" media remained untreated. After incubation for 10 min at 37°C in 5% CO_2, we harvested each group of cultures and mixed them in equivalent amounts based on total protein content prior to subcellular fractionation and isolation of the PAM fraction.

Subcellular fractionation

To fractionate αT3-1 cells in the absence of detergents, we modified a protocol originally developed for isolation of PAM (plasma membrane-associated membrane) fraction proteins from rat liver (Suski et al., 2014). This protocol yielded ≈ 70 µg of PAM fraction protein from αT3-1 cells grown in nine 15 cm dishes to 80% confluency. Briefly, cells were washed with PBS, pelleted and homogenized by 25 strokes using a 'tight' glass pestle. The homogenate was then processed through a series of differential centrifugation steps as described to yield the mitochrondrial, cytosolic, nuclear, et fractions. The crude PM was then further purified on a discontinuous sucrose gradient comprising sucrose at 38% (4 mL), 43% (4 mL) and 53% (3 mL)) and. After centrifugation for 2.5 hr at 95,000 x g and 4C, 0.5 mL fractions were recovered, precipitated in 6% TCA, resuspended in RIPA buffer, and total protein was quantified and stored at -80 C.

A total of four independent biological replicates were prepared using this protocol. For our proteomics experiments, ≈ 10-30 µg protein from each replicate was separately loaded and marginally resolved by SDS-PAGE. A single band for each biological replicate was excised and digested with trypsin before LC-MS/MS analysis.

In-solution trypsin digestion and liquid chromatography/tandem mass spectrometry (LC-MS/MS) data acquisition

Following quantification of PAM fraction proteins by microplate BCA protein assay (ThermoFisher, Pierce, Rockford, IL), 100 ug protein was processed for in-solution trypsin digestion as previously described (Schauer et al., 2013). Briefly, PAM fraction proteins were precipitated in the presence of 4 volumes of 100% acetone (at -20^{o}C) and resolubilized in 8M urea with 0.2% ProteaseMAX^{tm} surfactant trypsin enhancer (Promega, Madison, WI). Samples were reduced and alkylated with 5mM dithiothreitol and 5mM iodoacetamide. Trypsin was added at an enzyme to substrate ratio of 1:50 and incubated at 37^{o}C for 12-16 hours. Trypsin was deactivated with the addition of 5% trifluoroacetic acid and desalted using C18 OMIX tips (Agilent Technologies, Santa Clara, CA) using manufacturer's instructions. Peptide eluate was dried in a vacuum evaporator and resuspended in 3% acetonitrile/0.1% formic acid at a concentration of at a concentration of ≈ 1 μg/μL.

LC-MS/MS quantitative data analysis

Tandem mass spectra were extracted, charge state deconvoluted and deisotoped by ProteoWizard MSConvert (version 3.0). Spectra from all raw data files were searched against a reverse-concatenated Uniprot-*mus musculus* proteome database (downloaded November, 2015), using MaxQuant (Max Planck Institute of Biochemistry, Martinsried, Germany; version 1.5.0.0) and assuming the digestion enzyme trypsin and allowing up to two missed cleavages. MaxQuant was searched with a fragment ion mass tolerance of 0.50 Da and a parent ion tolerance of 7 ppm. Lys8 of lysine, Arg10 of arginine, oxidation (M) of methionine and carbamidomethyl (C) of cysteine were specified in MaxQuant as variable modifications. Default settings for false-discovery rates, posterior envelope probability (PEP) and minimum peptide length were specified. Further processing of the search results was performed in Scaffold Q+S (Proteome Software v.4.5.1) (Keller et al., 2002; Searle et al., 2008). Peptide identification thresholds were set at 90% probability, achieving a peptide FDR of 0.01% based on hits to the reverse database (Käll et al., 2008).

Protein identifications were accepted if they could be established at greater than 99.0% probability (0.4% FDR) and contained at least 2 identified peptides. Protein probabilities were assigned by the Protein Prophet algorithm (Nesvizhskii et al., 2003). Proteins that contained similar peptides and could not be differentiated based on MS/MS analysis alone were grouped to satisfy the principles of parsimony. Scaffold Q+ (version Scaffold_4.4.6, Proteome Software Inc., Portland, OR) was used to quantitate protein expression for proteins reproducibly identified in 3 out of the 4 biological replicates. Individual quantitative samples were normalized within each acquisition run. Intensities for each peptide identification were normalized within the assigned protein. The reference channels were normalized to produce a 1:1-fold change. All normalization calculations were performed using medians to multiplicatively normalize data. Differentially expressed proteins were determined using Mann Whitney Test analysis (p-value < 0.05). Log_2 Fold Change was used as the quantitative value and differences accepted only when ratios of at least two different peptides per protein were measured. The identified proteins, protein ratios and p-values are summarized in supplemental Table S1. String (version 10.0) or Scaffold (version 4.4.6) was used as indicated for gene ontology analysis for the indicated protein groups.

Immunoprecipitation and Rac1 activity assay

For our immunoprecipitation experiments, αT3-1 cell cultures were grown to ~80% confluence and immersed in cold IP lysis buffer (50 mM Tris 7.5, 10 mM MgCl2, 0.5M NaCl, 2% NP40, protease inhibitor cocktail (Calbiochem)). Lysates were clarified by centrifugation at (10,000 rcf for 1 min at 4C). Soluble protein lysates (1-4 mg) were diluted 1:2 in cold PBS and (500-750 ug total protein) incubated with Protein G-Sepharose 4B conjugate (Life Technologies) pre-bound to *5 uL* of primary antibody for 1 h at 4ºC. The immobilized antigen-antibody complexes were washed 3 times in IP Wash Buffer (25 mM Tris 7.5, 5 mM MgCl2, 0.25M NaCl, 1% NP40, protease inhibitor cocktail (Calbiochem)) and eluted in sample buffer prior to subsequent SDS-PAGE and western blot analysis. To measure Rac1 activity, we analyzed 2.5-

5.0 mg of αT3-1 cell lysate using the Rac1 Activation Assay Biochem Kit™ (Cytoskeleton, Inc.) according to the manufacturer's instructions.

SDS-PAGE and immunoblotting

Immunoblotting was performed with the indicated primary antibody diluted 1:1,000 overnight at 4°C. Visualization of proteins was achieved by addition of horseradish peroxidase (HRP)-conjugated secondary antibodies diluted 1:4000 in blocking buffer (3% non-fat dried milk in PBS) and blots were imaged using the enhanced chemiluminescence (ECL) method. Images were aquired using the UVP EpiChemi 3 Darkroom system and ImageQuant software for band densitometry analysis.

Immunofluorescence microscopy

αT3-1 cells were transfered to glass-bottom culture dishes (MatTek; Ashland, MA) coated with Corning® Matrigel® matrix (Corning; Tewksbury, MA) diluted 1:250 in DMEM and grown for 24 hr at 37°C in 5% CO_2 humidified air. Cells were fixed in paraformaldehyde diluted to 4% in PBS for 15 min, washed with PBS, and permeabilized with PBS containing 0.5% Triton X-100 (TX100) for 3 min. Dishes were then blocked with 10% donkey serum and 0.05% TX100 prior to incubation with the indicated primary antibody (diluted 1:250) overnight at 4°C. Proteins were then visualized by staining with either Alexa Fluor 488 or Alexa Fluor 568-conjugated secondary antibody (Invitrogen, dilution 1:1000) and counterstained with DAPI (0.2 ug/mL) as indicated. Images were acquired on either a Zeiss LSM800 confocal laser-scanning microscope (Carl Zeiss; Oberkochen, Germany) or a Tirf microscope with this or that as indicated and analyzed with ImageJ (National Institutes of Health).

Chapter 3: IQGAP1 and PTK7: Novel effectors of GnRH receptor signaling in Gonadotropes

Summary

Following GnRH receptor stimulation, gonadotropes undergo dramatic cytoskeletal and morphological rearrangements which appear to be necessary for the transcriptional changes required for upregulation of gonadotropin synthesis. Based on our proteomics results and the identification of proteins affected by GnRH treatment using a SILAC (stable isotope labeling by amino acids in cell culture)-based proteomics approach to identify and quantify the relative abundance of plasma membrane-associated proteins in response to GnRH, we detected a significant change in ~80 plasma membrane-associated proteins following GnRH exposure using immortalized αT3-1 gonadotropes. Analysis of these proteins revealed that GnRH increased the plasma membrane association of numerous actin cytoskeletal, cell polarity and adherens junction-related proteins which included the scaffold protein IQGAP1 and the small GTPase Rac1, Ptk7, β-catenin and others. In this study, we further examine the localization of cell adhesion and polarity proteins, IQGAP1 and Ptk7, respectively, and their relationship to a known cell-cell adhesion and transcription co-activator, β-catenin, in αT3-1 gonadotropes. Indirect immunofluorescence combined with confocal microscopy was used to compare IQGAP, Ptk7 and β-catenin in control and GnRH-treated cell cultures. Consistent with previously published data, β-catenin accumumlated at the plasma membrane at cell-cell junctions within 30 min after GnRH treatment compared to control cells. A similar pattern of redistribution was also observed with Ptk7 and IQGAP1 within the same time frame and partially co-localized with β-catenin at cell-cell junctions. We observe a fraction of ptk7 co-localize in the nucleus albeit with a high degree of heterogeneity within the culture. Furthermore, cells sequentially stained with both anti-IQGAP1 and anti-Ptk7 antibodies reveal partial colocalization of these proteins at cell-cell juntions after GnRH treatment compared to control. Additionally, the inhibition of IQGAP1 using siRNA suggests a regulatory role of IQGAP1 in the activation of ERK, as well as the Wnt/β-catenin signaling pathways in gonadotropes. Together, our analysis futher supports our hypothesis

that IQGAP1 and PTK7 represent novel regulatory proteins downstream of the GnRH recepotor and further cooroborate our SILAC and LC- MS/MS analysis and identification of GnRH-responsive proteins dynamically regulated at the cell membrane.

Introduction

In gonadotropes, GnRH receptor activation produces two distinct intracellular Ca2+ signals: Ca2+ release from the endoplasmic reticulum (ER) through inositol-1,4,5-trisphosphate (IP3) receptors and Ca2+ influx through the plasma membrane via L-type Ca2+ channels (Grosse et al., 2000b). These two Ca2+ signals increase mitogen-activated protein (MAP) kinase signaling (Mulvaney and Roberson, 2000; Mulvaney et al., 1999). Specifically, Ca2+ release from the ER promotes c-Jun N-terminal kinase (JNK) activity, which increases in FSH expression, while Ca2+ influx through L-type Ca2+ channels promotes extracellular signal-regulated kinase (ERK) activity, which increases LH expression. Our published data indicate that GnRH provokes discrete sites of Ca2+ influx through L-type Ca2+ channels (Ca2+ sparklets) in gonadotrope-derived αT3-1 cells. Consistent with the work of others (Mulvaney and Roberson, 2000; Mulvaney et al., 1999), we concluded that the highly-localized L-type Ca2+ channel sparklet activity observed in our experiments is necessary and sufficient for ERK activation in these cells (Dang et al., 2014). Therefore, it is reasonable to hypothesize that effective GnRH receptor signaling involves subcellular compartmentalization and coordination of relevant signal transduction proteins. Indeed, evidence suggests that GnRH receptors localize to low-density, sphingolipid, and cholesterol-enriched plasma membrane microdomains in gonadotropes (Allen-Worthington et al., 2016; Bliss et al., 2007). Importantly, localization of the GnRH receptor within low-density plasma membrane microdomains appears necessary to assemble functional protein complexes and downstream signaling to ERK (Bliss et al., 2007; Navratil et al., 2010).

Signal transduction systems are the biochemical foundations that enable cells to mount individual and appropriate biological responses to various extracellular and intracellular stimuli. Admittedly, signaling pathway dysregulation that leads to multiple diseases, such as cancer, immunological disease,

neurodegenerative disorders, and selective modulation of signaling pathways, is a research and clinical therapeutic area of considerable interest (Borders et al., 2008; McCubrey et al., 2010; Wu and Mohan, 2009). The signal transduction events triggered by GnRH receptor have been the subject of extensive research for many decades (Naor, 2009), resulting in a substantial body of information about the structure and kinetics of GnRH-induced signaling networks as significant advancements in our understanding of GnRH receptor signaling in several experimental systems. However, GnRH-induced signaling networks remain a challenge in the field of reproductive biology. In vivo, the differentiated gonadotrope responses to the GnRH signal in a complex and dynamic endocrine environment. Evidence indicates that anterior pituitary cells, including gonadotropes, can participate in multicellular networks in their natural environment (Alim et al., 2012; Budry et al., 2011; Featherstone et al., 2016; Golan et al., 2016b; Hodson et al., 2012a; Le Tissier et al., 2017; Lyles et al., 2010; Schaeffer et al., 2011). Moreover, GnRH receptors are thought to be localized to low-density, sphingolipid, and cholesterol-enriched plasma membrane microdomains where they participate in multiprotein signaling complexes in gonadotropes (Allen-Worthington et al., 2016; Bliss et al., 2007). However, molecular mechanisms and functional outcomes associated with multicellular gonadotrope interactions are mostly hypothetical.

Using a non-biased quantitative proteomic screen of clonal αT3-1 gonadotropes, we observed robust enrichment of proteins associated with intercellular communication to investigate proteins influenced by GnRH receptor activity. A SILAC (stable isotope labeling by amino acids in cell culture)-based proteomics approach was used to identify and quantify the relative abundance of plasma membrane-associated proteins in response to GnRH (Ong et al., 2002). Using immortalized αT3-1 gonadotropes, we detected a significant change in ~80 plasma membrane-associated proteins following GnRH exposure. Analysis of these proteins revealed that GnRH increased the plasma membrane association of numerous actin cytoskeletal, cell polarity and adherens junction-related proteins, which included the scaffold protein IQGAP1 and the small GTPase Rac1, Ptk7 and others, indicating that actin

cytoskeletal remodeling is essential for GnRH receptor-dependent stimulation of gonadotropes (Dang et al., 2014; Edwards et al., 2017a; Edwards et al., 2016; Navratil et al., 2014).

GnRH-responsive proteins that captured our interest include the inactive (kinase-dead) receptor protein tyrosine kinase PTK7 (Lhoumeau et al., 2011) and the multimodal scaffold protein IQGAP1 (Noritake et al., 2005). These, and other proteins identified, such as β-catenin, cdc42, and Rac1, are involved with planer cell polarity (PCP) signaling and cell-cell adhesion (Berger et al., 2017; Bonello and Peifer, 2019; Devenport, 2014; Smith et al., 2015). Importantly, organized intercellular communication and asymmetric subcellular distribution of signaling molecules are two prominent features of PCP signaling.

IQ motif containing GTPase activating protein 1, also known as IQGAP1, is a very conservative scaffold protein having a molecular weight of 190 kDa. The coding gene for IQGAP1 is located on human chromosome 15. IQGAP1 is involved in a number of different physiological processes, including cytoskeletal rearrangement, cell adhesion, and cell polarization. Additionally, it is responsible for the regulation of the mitogen-activated protein kinase (MAPK) pathway as well as the β-catenin-mediated signal transduction of transcription (Abel et al., 2015b; Johnson et al., 2009; White et al., 2009).

This protein has five main domains by which it links to other proteins: a calponin-homology domain (CHD, 44-159 aa), a poly-proline protein-protein domain (WW, 681-710 aa), a domain containing four IQ-motif (IQ, 745-864 aa), a Ras GAP-related domain (GRD, 1004-1237 aa), and a Ras GAP C-terminal domain (RGCT 1276-1657 aa) (Brown and Sacks, 2006). Binding domains regulate IQGAP1's interactions with more than a hundred different proteins (Abel et al., 2015a; Brown and Sacks, 2006; Mataraza et al., 2003a; Noritake et al., 2005; Smith et al., 2015; Tanos et al., 2018; White et al., 2012), allowing the protein to play a part in processes as diverse as the cytoskeletal structure, cell-cell adhesion, cell motility, transcription, and signal transduction via its multitude of binding partners (Hart et al., 1996; Hedman et al., 2015). Actin, calmodulin, members of the Rho GTPase family (such as Rac1 and Cdc42), β-catenin, components of the phosphoinositide 3-kinase (PI3K) /AKT pathway, and adenomatous

polyposis coli (Hedman et al., 2015; Weissbach et al., 1994) are just some of the signaling and structural proteins that IQGAP1 interacts with due to its multiple domains. IQGAP1 has been studied for years as an oncogene that promotes cancer due to its role as a scaffolding protein for numerous important oncogenic pathways (Johnson et al., 2009; White et al., 2009).

Protein tyrosine kinase 7 is a catalytically inactive receptor tyrosine kinase involved with several cellular processes, including adhesions and polarity. Sequential proteolysis governs PTK7 activity by generating protein fragments with distinct biological functions (Berger et al., 2017; Lichtig et al., 2019; Na et al., 2012; Peradziryi et al., 2012). It comprises a transmembrane region and an extracellular region with seven immunoglobulin-like loops. The PTK7 protein and the Wnt signaling pathway have been linked in a large number of research papers. The protein tyrosine kinase 7 (PTK7) is involved in the regulation of cell-fate specification and morphogenesis during earlier vertebrate and invertebrate development, and impairment of its function in vertebrates results in neural tube defects/NTDs (Andreeva et al., 2014; Bin-Nun et al., 2014; Hayes et al., 2013; Lee et al., 2012; Lu et al., 2004; Paudyal et al., 2010; Peradziryi et al., 2011; Podleschny et al., 2015; Puppo et al., 2011; Wehner et al., 2011; Williams et al., 2014; Yen et al., 2009), including in humans (Wang et al., 2015). PTK7/Otk has been identified as a new Wnt co-receptor that contributes specificity to Wnt ligand responses (Peradziryi et al., 2011). Wnt signaling pathways have been preserved throughout evolution (Clevers, 2006; Logan and Nusse, 2004; MacDonald et al., 2009; Montcouquiol et al., 2006; Petersen and Reddien, 2009) and are essential for normal embryonic development and adult tissue homeostasis.

These results provide a molecular model that may be employed to investigate the spatial and temporal dynamics of gonadotrope signaling in more detail. Multiple proteins work together in the fascinating molecular structures IQGAP1 and PTK7 to control GnRH receptor signaling and gonadotropin gene transcription.

These features encouraged us to develop the following general hypothesis for this study: GnRH-responsive planer cell polarity and adherens junction-related proteins such as PTK7 and IQGAP1

contribute to intergonadotrope communication and interactions resulting in the signaling pathway that leads to the gonadotropes productions. The primary objective of this application is to investigate the molecular role of PTK7 and IQGAP1 in mediating the GnRH signaling network in gonadotropes. This study improves our fundamental understanding of gonadotrope biology by directly addressing the patent knowledge gap regarding intergonadotrope-related phenomena. Our observations reveal novel molecular targets potentially useful for experimental and clinical manipulation of gonadotrope function. After all, our results may have ramifications in various biomedical fields, including embryology and oncology, as our planer cell polarity and adherens junction-related proteins of interest influence intercellular communication during fetal development and tumorigenesis (Gärtner et al., 2014; Golubkov and Strongin, 2014; Lei et al., 2019; Mattes and Scholpp, 2018; Shin et al., 2015).

Results

Based on our proteomics results and the identification of proteins affected by GnRH treatment using a SILAC (stable isotope labeling by amino acids in cell culture)-based proteomics approach to identify and quantify the relative abundance of plasma membrane-associated proteins in response to GnRH (Ong et al., 2002), we detected a significant change in ~80 plasma membrane-associated proteins following GnRH exposure using immortalized αT3-1 gonadotropes. Analysis of these proteins revealed that GnRH increased the plasma membrane association of numerous actin cytoskeletal, cell polarity and adherens junction-related proteins which included the scaffold protein IQGAP1 and the small GTPase Rac1, Ptk7 and others. Indeed, following GnRH receptor stimulation, gonadotropes undergo dramatic cytoskeletal and morphological rearrangements which appear to be necessary for the transcriptional changes required for upregulation of gonadotropin synthesis (Navratil et al., 2014; Navratil et al., 2007). To further examine the localization of cell adhesion and polarity proteins, IQGAP1 and Ptk7, respectively, and their relationship to a known cell-cell adhesion and transcription co-activator, β-catenin, in αT3-1 gonadotropes. Indirect immunofluorescence combined with confocal microscopy was used to compare IQGAP, Ptk7 and β-catenin in control and GnRH-treated cell cultures. Consistent with

previously published data, β-catenin accumumlated at the plasma membrane at cell-cell junctions within 30 min after GnRH treatment compared to control cells. A similar pattern of redistribution was also observed with Ptk7 and IQGAP1 within the same time frame and partially co-localized with β-catenin at cell-cell junctions. Of note, a fraction of ptk7 co-localize in the nucleus albeit with a high degree of heterogeneity within the culture. Furthermore, cells sequentially stained with both anti-IQGAP1 and anti-Ptk7 antibodies reveal partial colocalization of these proteins at cell-cell juntions after GnRH treatment compared to control. Together, our ICC analysis futher supports our hypothesis that IQGAP1 and PTK7 represent novel regulatory proteins downstream of the GnRH recepotor and further cooroborate our SILAC and LC- MS/MS analysis and identification of GnRH-responsive proteins dynamically regulated at the cell membrane.

Successful GnRH receptor activation following GnRH application in αT3-1 gonadotropes

ERK1/2 phosphorylation was shown to be faster and more maintained in perfused LβT2 cells and primary gonadotropes after stimulation with low rather than high GnRH pulse frequencies (Haisenleder et al., 1998; Kanasaki et al., 2005). Furthermore, nuclear phosphorylated ERK has been shown in greater levels after low GnRH pulse frequency stimulation. Different ERK activation/inactivation patterns in response to different GnRH pulse frequencies suggest that ERK phosphorylation is required for GnRH pulse frequency-dependent differential stimulation of Fshb and Lhb expression (Kanasaki et al., 2005).

To validate the activation of GnRH receptor in αT3-1 gonadotropes, we evaluated the ERK1/2 phosphorylation as a marker for the activation. Using the western blot, we analyzed the whole cell lysate derived from αT3-1 gonadotropes cultures treated with 10 UM GnRH for different time points (0 min, 10 min, 30 min, 90 min, 6 hrs., 24 hrs.). Data showed the ERK phosphorylation peaked significantly after 10 minutes of exposure to GnRH as the quantification data presented (Fig. 2. 1). Data indicated that ERK phosphorylation occurs fast in response to GnRH in αT3-1 gonadotropes and validates the activation of GnRH receptor.

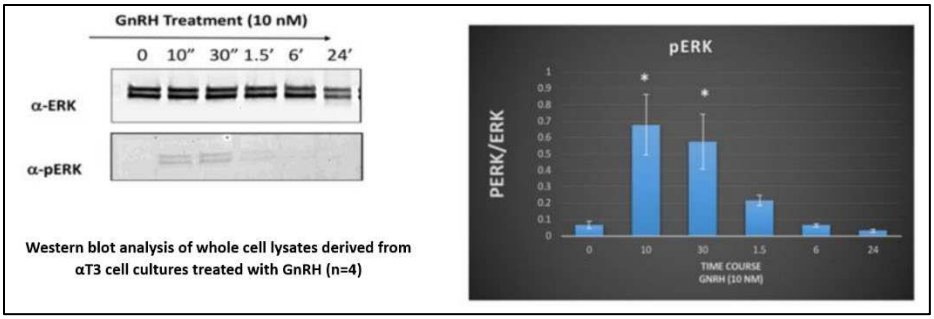

Fig. 3. 1: GnRH-dependent ERK phosphorylation: Western blot of whole cell extracts showing accumulation of p-ERK after GnRH (10 nM) in αT3 cells

GnRH receptor activation promotes intra- and extracellular PTK7 signaling, as well as the accumulation at cell-cell junctions and nucleus

Protein tyrosine kinase 7 is a catalytically inactive receptor tyrosine kinase involved with several cellular processes including adhesion and polarity. Sequential proteolysis governs PTK7 activity by generating protein fragments with distinct biological functions. To illustrate, full-length PTK7 negatively regulates ERK signaling and interacts with and sequesters β catenin. Following sequential cleavage by matrix metalloproteinase-14 (MMP-14; also, MT1-MMP) and ADAM family proteinases, soluble N-terminal ectodomain fragments inhibit the activity of full-length PTK7. Subsequent cleavage by γ secretase produces soluble intracellular C-terminal domain fragments, one of which translocates from the cytosol to the nucleus (Berger et al., 2017; Lichtig et al., 2019; Na et al., 2012; Peradziryi et al., 2012).

To validate our proteomic observations, we used the indirect immunofluorescence combined with confocal microscopy to visualize the localization and accumulation of PTK7 in αT3-1 gonadotropes in response to GnRH. We additionally used the Western blot to investigate the Sequential proteolysis governs PTK7 activity and nuclear localization of PTK7 C-terminal fragments after treating αT3-1 gonadotropes with GnRH, in parallel of using GM6001 (10 μM), which is matrix metalloproteinase inhibitor.

Our data indicate that GnRH receptor activation promotes subcellular redistribution of PTK7 accompanied by a high level at cell-cell contacts using immunofluorescence in αT3-1 gonadotropes. It

also promotes proteolysis and subcellular redistribution of PTK7. Specifically, GnRH evokes a dramatic increase in nuclear PTK7-like immunofluorescence (Fig. 3. 2A, and 3. 3) and promotes the shedding of N-terminal ectodomains and generation of intracellular C-terminal fragments which localize to the nucleus (Figs. 3. 2B & C). Importantly, matrix metalloproteinase inhibition with GM6001 (10 μM) abolishes GnRH-dependent proteolysis of PTK7 (Fig. 3. 2C).

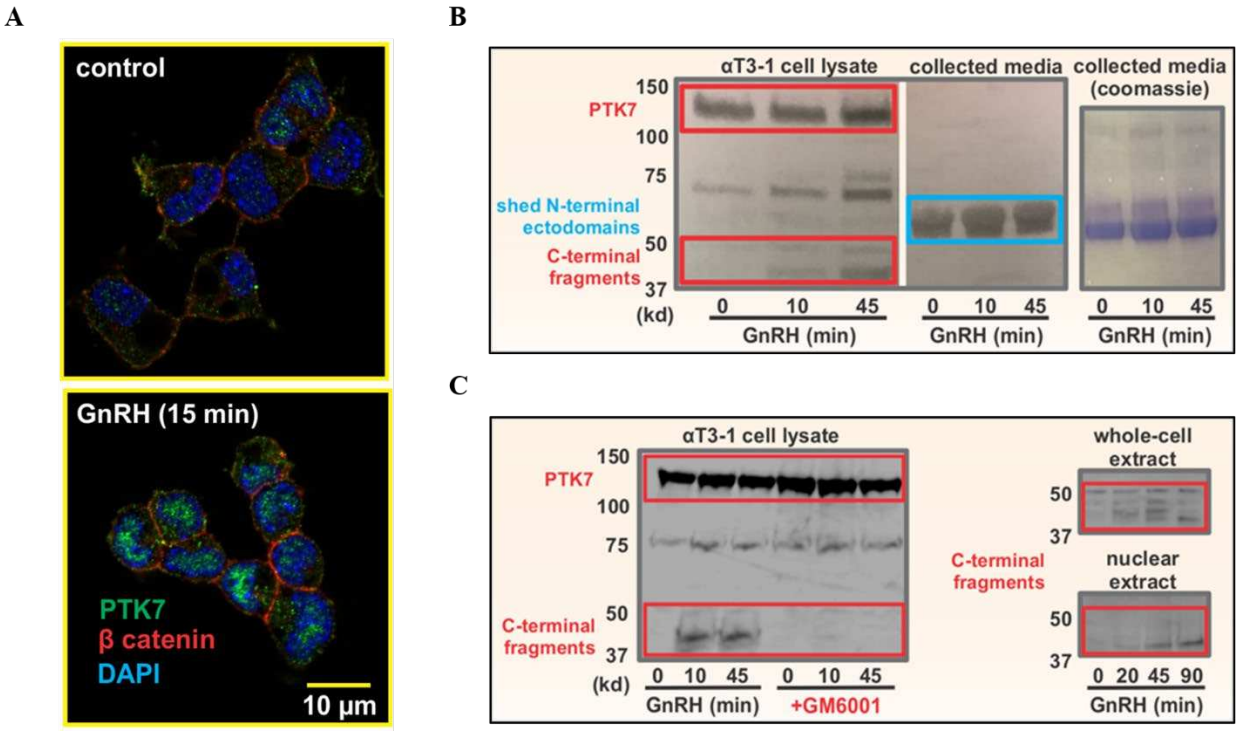

Fig. 3. 2: GnRH-dependent redistribution and proteolysis of PTK7 in αT3-1 gonadotropes. A, Representative confocal images of αT3-1 cells cultured in glass-bottom microwell dishes for 24 hr and incubated with either GnRH (20 nM) or water (control) for 15 min. Dishes were fixed with 4% paraformaldehyde and permeabilized with 0.1% Triton. Dishes were then sequentially stained first with anti-PTK7 antibody(1.5ug/ml) for 24hr followed by Alexa Fluor 488-conjugated secondary antibody (2ug/ml), and then with anti-β-Catenin antibody (1ug/ml) for 24 hr followed by Alexa Fluor 568-conjugated secondary antibody (2ug/ml). All cells were counterstained with DAPI to label nuclei and imaged under either a 63X oil objective of a Zeiss LSM 800 confocal microscope. The green staining inside the cells indicates the PTK7 accumulation inside the nuclei. B, Using αT3-1 cells, GnRH-dependent PTK7 proteolysis yields intracellular and extracellular products in response to GnRH. C, GnRH promotes MMP-dependent PTK7 proteolysis and nuclear localization of C-terminal fragments in αT3-1 gonadotropes. GM6001 is matrix metalloproteinase inhibitor.

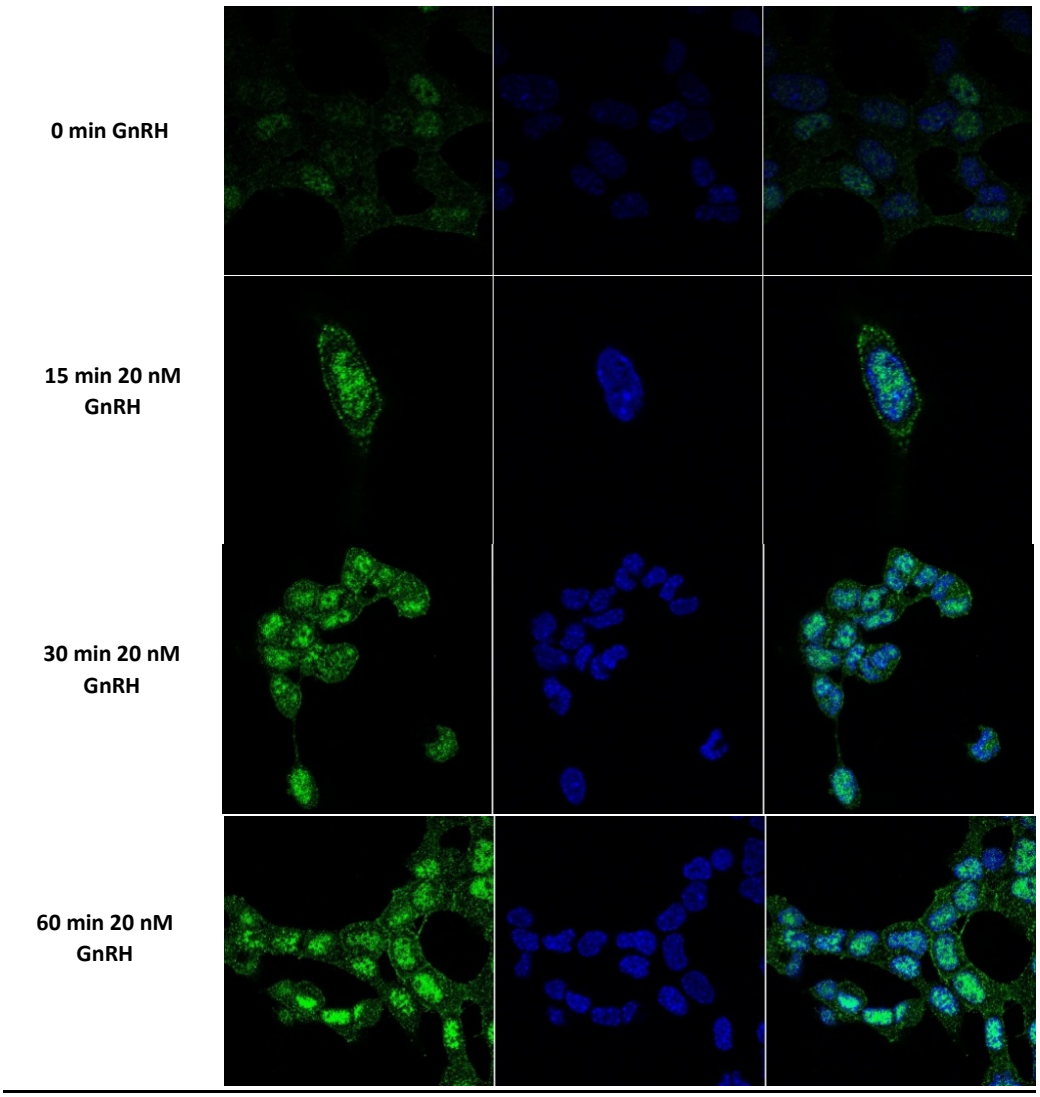

Fig. 3. 3: Representative confocal images of αT3-1 cells cultured in glass-bottom microwell dishes for 24 hr and incubated with either GnRH (10 nM) or water (control) for 10 min, fixed with 4% paraformaldehyde and permeabilized with 0.1% Triton. Dishes were sequentially stained first with anti-PTK7 antibody (1ug/ml) followed by Alexa Fluor 488-conjugated secondary antibody (2ug/ml). All cells were counterstained with DAPI to label nuclei and imaged under a 63x oil objective of a Zeiss LSM 800 confocal microscope.

IQGAP1 is expressed in mouse neurons

We started our experiments asking the question if IQGAP1 is expressed in the neurons. Therefore, we first examine the IQGAP1 expression in neurons. We used brains extracted from control mice that has no treatment to check the normal IQGAP1 expression in neurons in the normal state. All brains were washed twice, then incubated in 1x PBS for 15 minutes. Following 1x PBS washing and

incubation, brains were incubated in 4% paraformaldehyde for 24 hrs. in 4° C. The next day, all brains were processed and sliced to form Histology slides. Using the LabSat system, which runs an automatic immunocytochemistry, formalin-fixed paraffin-embedded samples of normal brain tissue were stained with anti-IQGAP1 antibody (1ug/ml) followed by Alexa Fluor 488-conjugated secondary antibody (2ug/ml) and DAPI after performing an Antigen retrieval step using 1x 6 PH Antigen retrieval buffer for 15 min. Slides then were covered with the slipcover and incubate for 24 hours allowing them to dry. Next day, Stained slides were imaged with a Vectra Polaris Automated Quantitative Pathology Imaging System. Multispectral images were analyzed with inForm® software in Dr. Mercedes lab at the microbiology department. Data showed IQGAP1 expressed in the brain tissue, and the zoom in images showed how the IQGAP1 is expressed in the cytoplasm of neurons (Fig. 3. 4).

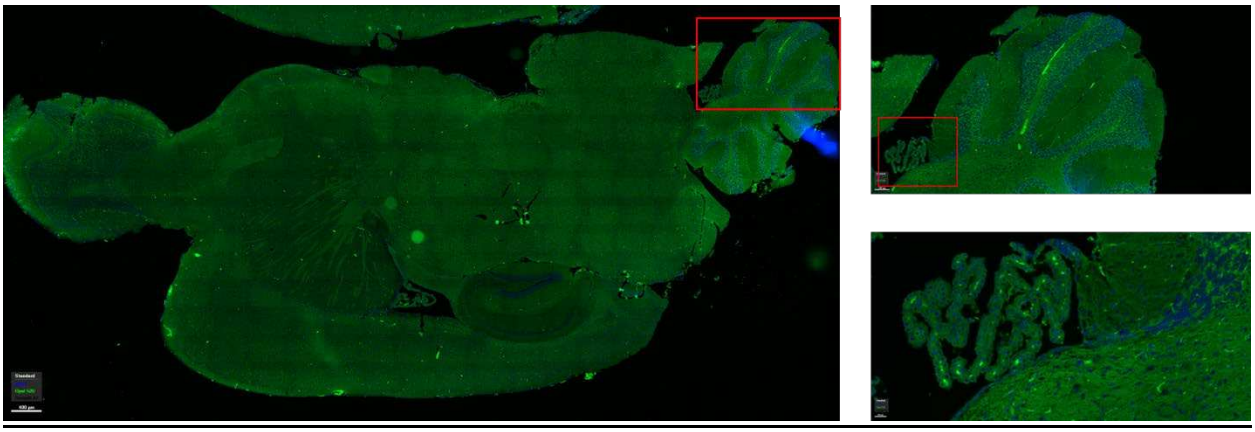

Fig. 3. 4: Left, 2-color whole slide scan of mouse brain tissue stained with anti-IQGAP1 antibody (1ug/ml) followed by Alexa Fluor 488-conjugated secondary antibody (2ug/ml) and DAPI, acquired on the Vectra Polaris with 0.25 um resolution. Right, zoomed-in image of a small field within the whole slide scan. Data shows the IQGAP1 expression in the brain tissue. Brains were extracted and processed into histology slides, which then were stained using the LabSat system to apply an indirect automatic immunocytochemistry.

Successful IQGAP1 knockdown using pre-designed silencer small interfering RNA (siRNA)

To examine the involvement of IQGAP1 in the GnRH activation pathway, and the effect of minimizing the IQGAP1 activity in response to GnRH receptor activation, we transfected αT3 and LβT2 gonadotropes using IQGAP1 pre-designed silencer siRNA. Evaluating the IQGAP1 knockdown was

accomplished using Flow Cytometry, to quantify the fluorescent intensity in αT3 gonadotropes, and the RT-PCR, to measure the IQGAP1 expression in both αT3 and LβT2 gonadotropes. Parallel experiments were applied to using GAPDH pre-designed silencer siRNA, as a positive control, as well as the negative control for the knockdown validation (Fig. 3. 5C). The data showed that we achieved more that 50% knockdown in both the fluorescence intensity using IQGAP1 conjugated antibody with AF 488 in αT3 gonadotropes (Fig. 3. 5A), as well as the IQGAP1 expression in both αT3 and LβT2 gonadotropes (Fig. 3. 5B). This allows us to assess IQGAP1's role as an effector mediating and controlling the activity of numerous binding protein partners and potential cascades activated in response to GnRH receptor activation in gonadotropes, rather than just as a novel protein with a single function in the GnRH pathway.

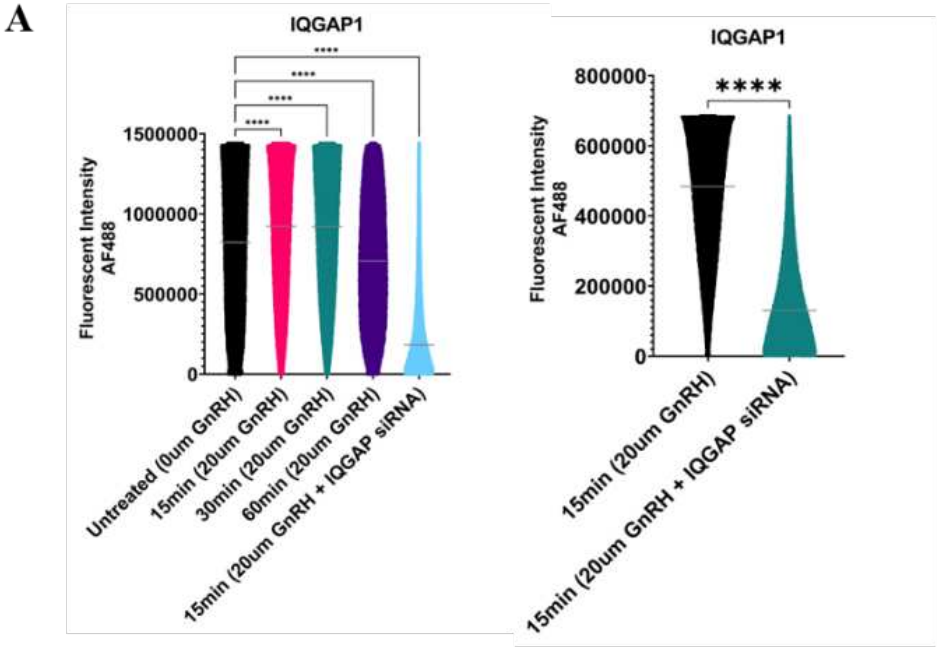

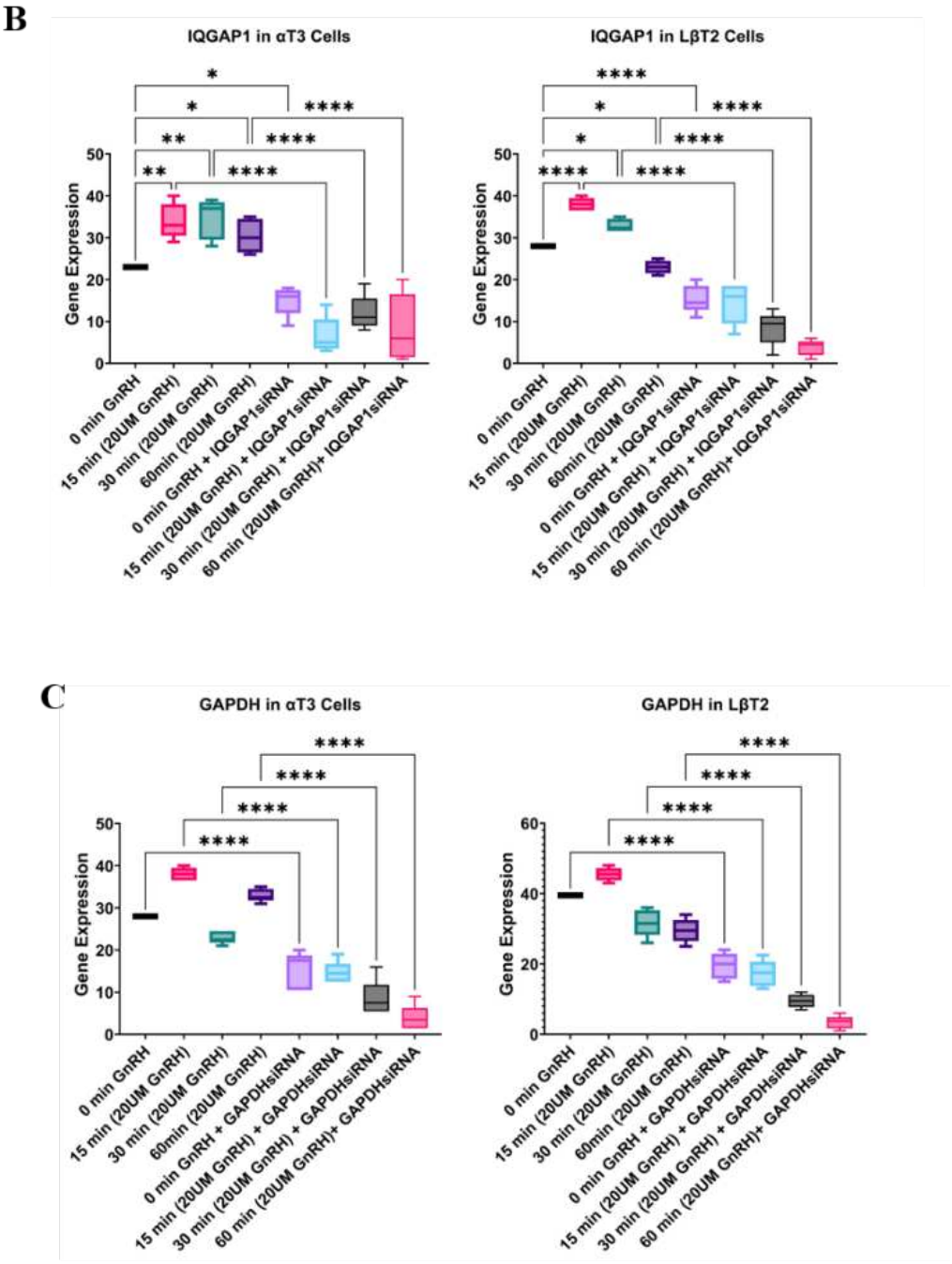

Fig. 3. 5: The validation of IQGAP1 knockdown (less than 50%) in transfected gonadotropes using IQGAP1 pre-designed silencer siRNA. A, Flow cytometry analysis using FloJo software showing the potential fluorescent intensity in control and transfected αT3 gonadotropes treated with 20 UM GnRH for different time points and stained with Anti-IQGAP1 antibody conjugated to Alexa Fluor 488. B. & C, RT-PCR analysis showing the level of gene expression of IQGAP1 and GAPDH, respectively in control and transfected αT3 and LβT2 gonadotropes treated with GnRH for different time points.

IQGAP1 increases and localizes at cell-cell junctions following GnRH receptor activation

Cell-cell junctions are essential in establishing extracellular communication between neighboring cells and intracellular communication with various cytoskeletal elements that together create incorporated, structural continuance across the tissues. Many elements are known to be linked to adherens and tight junctions. Junctional adhesion proteins bind through their cytoplasmic tail to cytoskeletal and signaling proteins, allowing the adhesion proteins' anchoring to actin microfilaments and transfer intracellular signals inside the cell (Bazzoni et al., 1999; Braga, 2002; Matter and Balda, 2003; Wheelock and Johnson, 2003a). The association with actin is essential for the stabilization of the junctions and the dynamic regulation. In addition, the interaction of junctional adhesion proteins with the actin cytoskeleton might be relevant in the maintenance of cell shape and polarity [60-63]. Interestingly, releasing some intracellular junctional proteins from junctions leads to translocating to the nucleus and modifying transcription (Ben-Ze'ev and Geiger, 1998; Bienz and Clevers, 2000; Matter and Balda, 2003). Moreover, some junctional proteins may act as scaffolds, such as IQGAP1, which binds several effector proteins and mediates their mutual interaction. It has been reported that IQGAP1 has an essential role in regulating cellular processes, including cytoskeletal rearrangements in cell migration and cell adhesion (Brandt and Grosse, 2007; Machesky, 1998; Noritake et al., 2005).

For the purpose of exploring the localization of cell adhesion and polarity proteins, IQGAP1 and Ptk7, as well as their relationship to a known cell-cell adhesion and transcription co-activator, β-catenin, indirect immunofluorescence combined with confocal microscopy was used to compare IQGAP, Ptk7, and β-catenin in control and GnRH-treated T3-1 gonadotropes cultures. β-catenin accumulated at the plasma membrane at cell-cell junctions within 60 minutes of GnRH administration, which was consistent with previously reported results. Within the same time period, a similar pattern of redistribution was seen for Ptk7 and IQGAP1, which partly colocalized with β-catenin at cell-cell junctions. A portion of ptk7 colocalize in the nucleus, but with a considerable degree of variability within the culture (Fig. 3. 6).

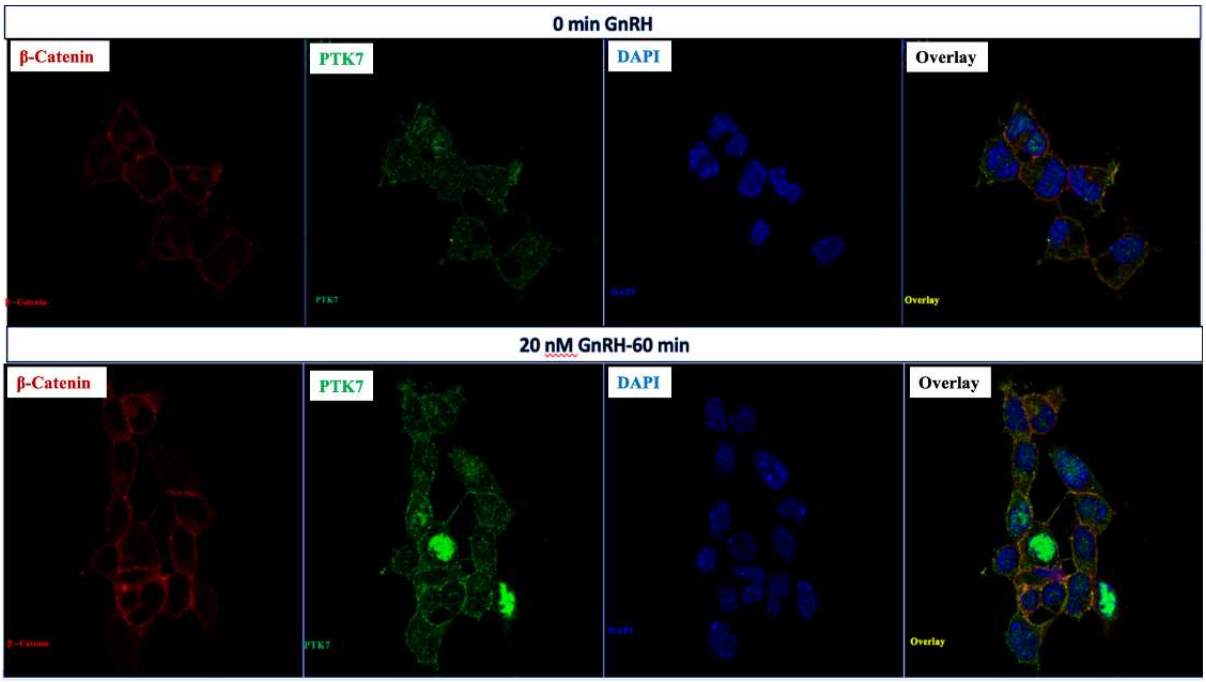

Fig. 3. 6: Representative confocal images of αT3-1 cells cultured in glass-bottom microwell dishes for 24 hr and incubated with either GnRH (10 nM) or water (control) for 10 min, fixed with 4% paraformaldehyde and permeabilized with 0.1% Triton. Dishes were sequentially stained first with anti-PTK7 antibody (1ug/ml) followed by Alexa Fluor 488-conjugated secondary antibody (2ug/ml), and then stained with anti-β-Catenin antibody (1ug/ml) followed by Alexa Fluor 568-conjugated secondary antibody (2ug/ml). All cells were counterstained with DAPI to label nuclei and imaged under a 63x oil objective of a Zeiss LSM 800 confocal microscope. The yellow staining indicates colocalization of indicated proteins.

Furthermore, cells stained with both anti-IQGAP1 and anti-Ptk7 antibodies sequentially exhibit partial co-localization of both proteins at cell-cell junctions following GnRH treatment compared to control (Fig. 3. 7A).

To quantify the fluorescent intensity of IQGAP1 in αT3-1 gonadotropes, we used Flow Cytometry that measures the signal in one single cell. We ran 250,000 events (cells) in triplicate for each sample using 96 well plate. Cells viability were measured using Ghost dye 510, and all dead cells were excluded, and the signal was measured in only live cells. Consistent with our observations using immunofluorescence, our flow cytometry results indicate an increase in the fluorescence intensity of IQGAP1-Alexa Fluor 488 conjugated antibody upon the activation of GnRH receptor (Fig. 3. 7B). Signals showed the highest level of IQGAP1 fluorescence intensity after 15 min of treating αT3-1 gonadotropes with 20 UM GnRH. Moreover, to evaluate the IQGAP1 expression in αT3-1 and LβT2

gonadotropes in response to GnRH receptor activation in different time points, we performed RT-PCR using IQGAP1 designed primer. Delta CT was measured and normalized to the house keeping gen, b-actin. The data showed that IQGAP1 expression increases after 15 min of GnRH treatment in both type of Gonadotropes (Fig. 3. 7C & D), indicating that IQGAP1 play a regulatory role mediating cell-cell junction following GnRH receptor activation.

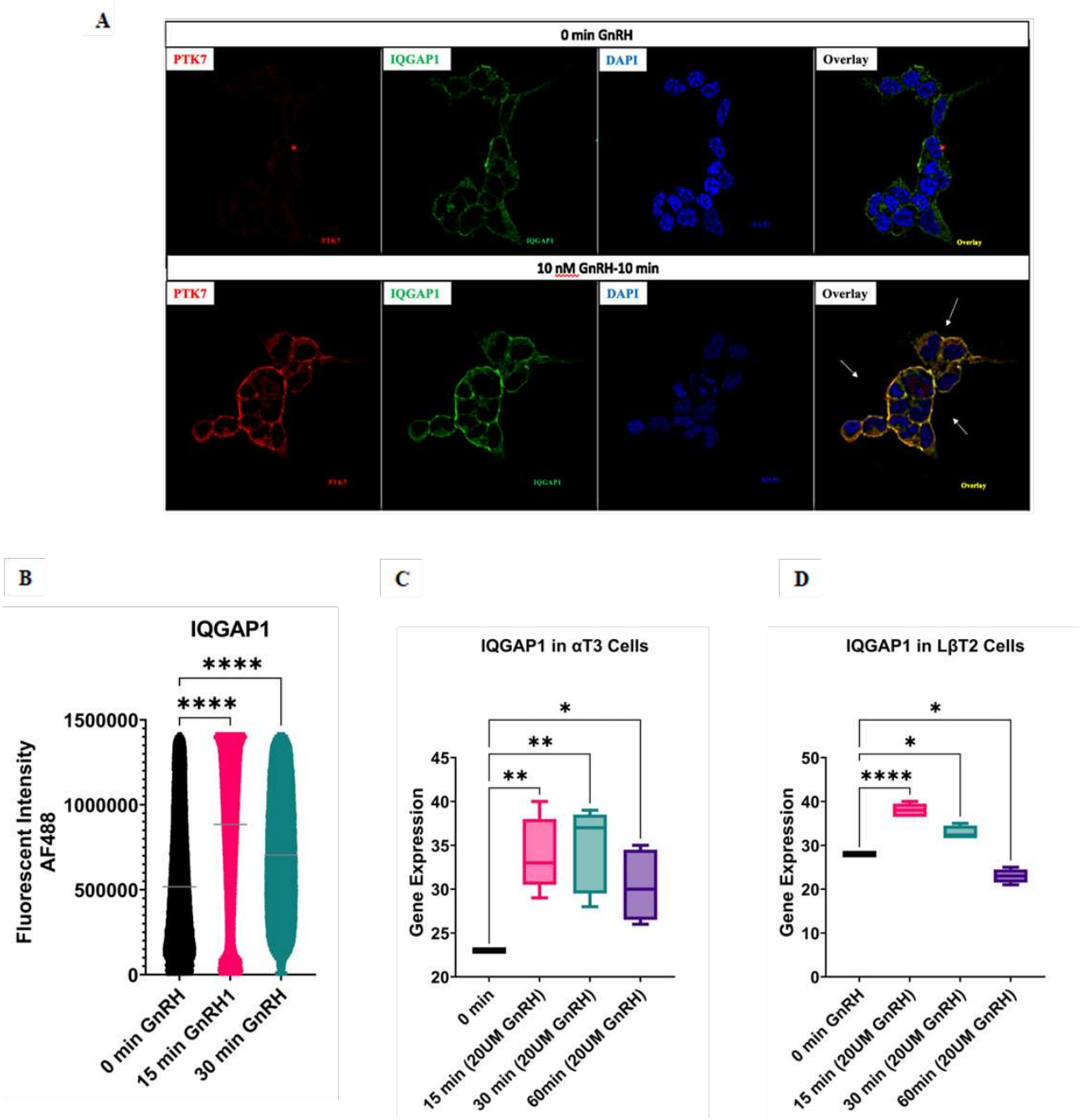

Fig. 3. 7: A, Representative confocal images of αT3-1 cells cultured in glass-bottom microwell dishes for 24 hrs. and incubated with either GnRH (10 nM) or water (control) for 10 min, fixed with 4% paraformaldehyde and permeabilized with 0.1% Triton. Dishes were sequentially stained first with anti-IQGAP1 antibody (1ug/ml) followed by Alexa Fluor 488-conjugated secondary antibody (2ug/ml), and then stained with anti-PTK7 antibody (1ug/ml) followed by Alexa Fluor 568-conjugated secondary antibody (2ug/ml). All cells were counterstained with DAPI to label nuclei and imaged under a 40x oil objective of a Zeiss LSM 800 confocal microscope. The yellow staining indicates colocalization of indicated proteins. B, The florescent intensity level of anti-IQGAP1 antibody (1ug/ml) with Alexa Fluor 488-conjugated Fluorescence in αT3-1 cells treated with 20 UM GnRH for different tie points (0, 15, 30 , 60 minutes), and prepared for the signal quantification through the Cytec Aurora Flow Cytometry system and analyzed by FloJo software. Data shows a significant increase in the florescent intensity in response to GnRH. C & D. RT-PCR data shows the IQGAP1 expression level in αT3-1 and LβT2 gonadotropes, respectively, treated with 20 UM GnRH for different time points (0, 15, 30, 60 minutes). The level of the expression varies between the gonadotrope cell lines when treated with GnRH; however, data shows a significant increase in the IQGAP1 expression level following the GnRH receptor activation in both gonadotropes cell lines.

IQGAP1 contributes to GnRH receptor-dependent signaling cascades involved with gonadotropin production

It has been reported that IQGAP1 is a scaffold MEK/ERK cascade binding directly to MEK1/2 and ERK1/2, leading to modulate their activation (Roy et al., 2004, 2005). Furthermore, a study demonstrated that IQGAP1 could form a primary signal in the periphery of the nucleus to transiently maintain Erk1/2 phosphorylation (Awasthi et al., 2010), providing strong evidence that activation of the Erk1/2 pathway can be regulated and compartmentalized by IQGAP1. Thus, it is important to understand the regulatory roles of IQGAP1 in targeting ERK1/2 pathway activation in response to GnRH, which regulates the function of gonadotropes.

Our data (Chapter 1) showed an upstream activation and association of Rac1 and IQGAP1 in response to GnRH treatment. Indicating functional relevance, pharmacological inhibition of Rac1 reduced ERK phosphorylation and Rac1-IQGAP1 complexes at cell junctions. Furthermore, we observed that IQGAP1 is mediating ERK1/2 activation in αT3-1 gonadotropes. Using IQGAP1 pre-designed silencer siRNA we observe a change in the activation level of ERK pathway (Fig. 3. 8), demonstrating that Rac1-containing IQGAP1 signaling complexes modulate GnRH-dependent ERK activation in αT3-1 gonadotropes and serve as essential effectors for signaling events leading to an enrichment of cell-cell contacts.

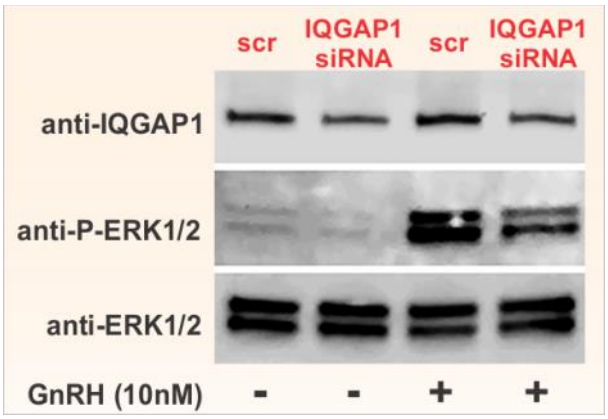

Fig. 3. 8: Whole cell lysate shows that IQGAP1 knockdown decreases GnRH-dependent ERK phosphorylation in αT3-1 gonadotropes after 10 minutes of 10 nM GnRH treatment.

In LβT2 cells, GnRH increases the nuclear accumulation of β-catenin (Gardner et al., 2007; Salisbury et al., 2007), leading to the growing binding of β-catenin and SF1 to the endogenous Lhb promoter-regulatory region (Salisbury et al., 2007), suggesting further crosstalk between signaling mediators of the Wnt/β-catenin pathway and those activated by GnRH. Many studies using a heterologous HEK293 model cell line and LβT2 gonadotrope cell line showed that the activation of GnRH receptor by GnRH could target mediators of the Wnt/β-catenin signaling pathway (Gardner et al., 2007; Gardner and Pawson, 2009; Salisbury et al., 2007, 2009; Salisbury et al., 2008).

It has been reported that IQGAP1 acts as β-catenin-mediated gene transcriptions regulator (Briggs et al., 2002a; Fukata et al., 1999b; Wang et al., 2008). The direct interaction of IQGAP1 with APC (Aoki and Taketo, 2007; Watanabe et al., 2004b) or protein phosphatase 2A (PP2A) (Suzuki et al., 2005), as well as the indirect interaction of GSK-3β (Watanabe et al., 2009), indicates that IQGAP1 has a role in Wnt signaling. Primarily, IQGAP1 was shown to bind to the C-terminus of Disheveled (DVL) (Goto et al., 2013b) via a region between the IQ domains and the GRD of IQGAP1, while β-catenin binds directly to the RGCT domain (Fukata et al., 1999b), which emphasize the role of IQGAP1 in the activation and degradation of β-catenin. Thus, it is important to understand the regulatory roles of IQGAP1 in targeting Wnt signaling mediators in response to GnRH, which regulates the function of gonadotropes. Thus, we hypothesize that the Wnt/β-catenin signaling pathway is activated in response to

GnRH, and IQGAP1 might modulate this activation. Consequently, parallel experiments assessing the activation of Wnt signaling target genes by measuring the expression level of these genes in control and knockdown of IQGAP1 conditions using treated and untreated αT3-1 gonadotropes was applied for further evaluation.

Our findings show that the level of GSK-3β fluorescence changed in response to 20 nM GnRH when visualizing with confocal microscopy (data not shown), suggesting the role of Wnt signaling mediators in GnRH signaling network in αT3-1 gonadotropes. Moreover, we observed a significant change in the signal accumulation and gene expression level of Wnt/β-catenin signaling pathway target genes using indirect immunocytochemistry combined with confocal microscopy, as well as the RT-PCR approaches in control and transfected αT3-1 gonadotropes with IQGAP1 pre-designed silencer siRAN, and treated with 20 UM GnRH. These Wnt/β-catenin signaling pathway target genes include TCF, C-Jun, and Myc that are known to be activated upon the activation of Wnt/β-catenin signaling pathway (Frame and Cohen, 2001; Grimes and Jope, 2001). We observed an increase in the signal in αT3-1 gonadotropes treated with 20 UM GnRH and stained with Anti-TCF antibody and Anti-C-June antibody followed by Alexa Fluor 488 secondary antibody, then, visualized by confocal microscopy (Fig. 2. 9A & B).

A

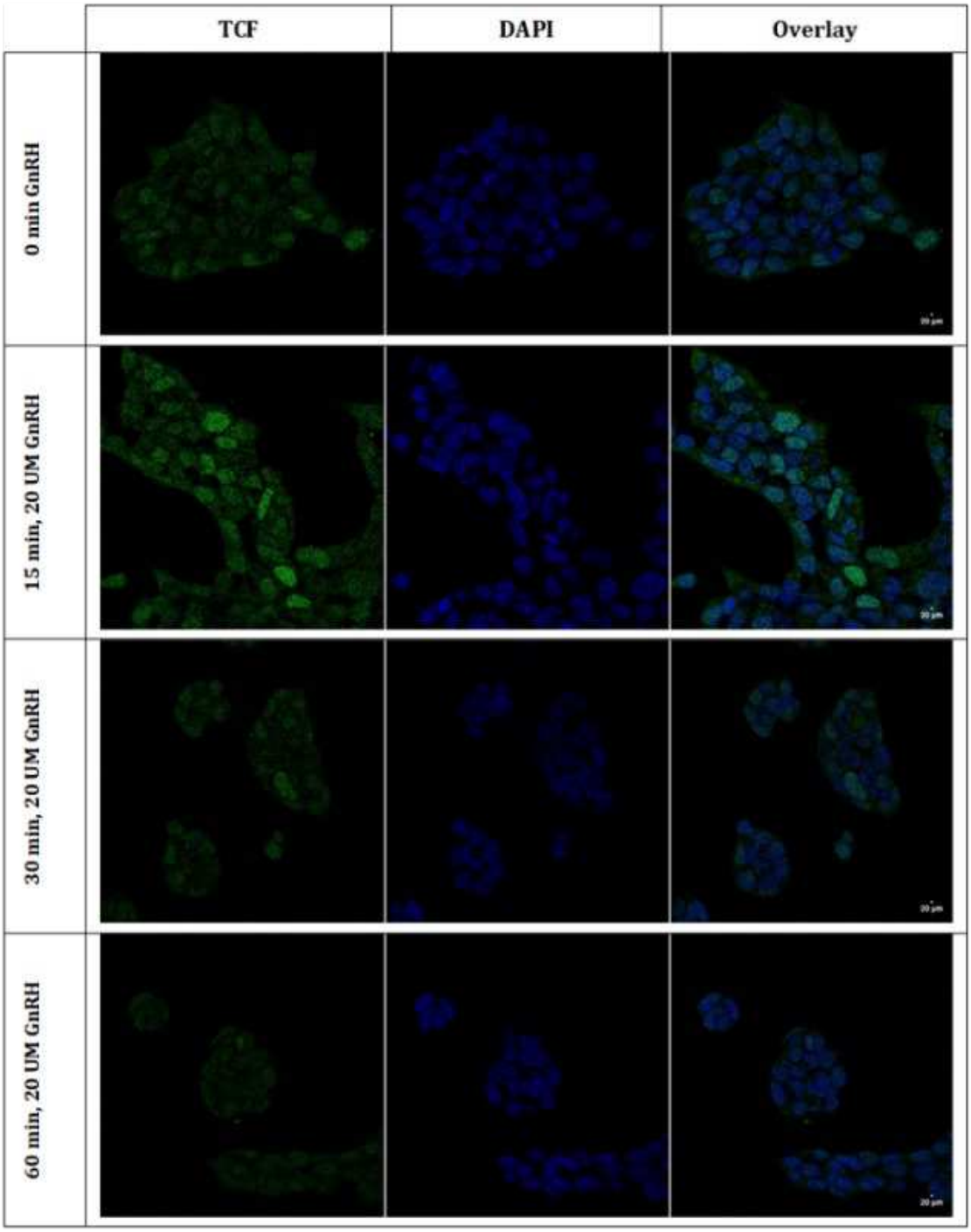
TCF
DAPI
Overlay
0 min GnRH
15 min, 20 UM GnRH
30 min, 20 UM GnRH
60 min, 20 UM GnRH

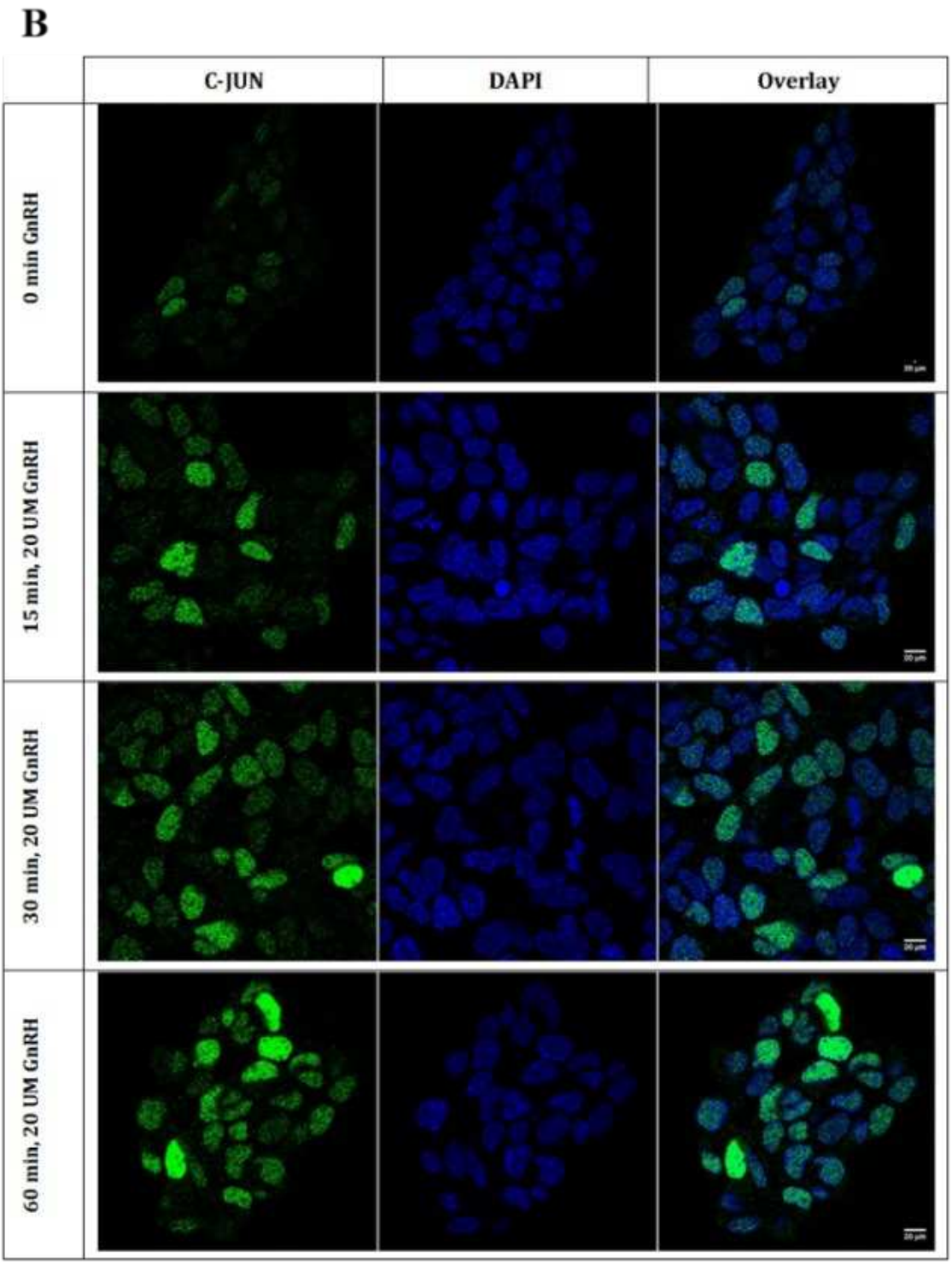

Fig. 3. 9: Representative confocal images of αT3-1 cells cultured in glass-bottom microwell dishes for 24 hrs., then, incubated with either GnRH (10 nM) or water (control) for different time points (0 min, 15 min, 30 min, 60 min), fixed with 4% paraformaldehyde and permeabilized with 0.1% Triton. Dishes were sequentially stained with: A, Anti-TCF antibody (1ug/ml) followed by Alexa Fluor 488-conjugated secondary antibody (2ug/ml), B, Anti-C-June antibody (1ug/ml) followed by Alexa Fluor 488-conjugated secondary antibody (2ug/ml). All cells were counterstained with DAPI to label nuclei and imaged under a 63x oil objective of a Zeiss LSM 800 confocal microscope.

Moreover, using in αT3-1 gonadotropes treated with 20 UM GnRH, our RT-PCR analysis shows a significant increase in the expression level of TCF and C-Jun genes (Fig. 3. 10A & B), whereas Myc gene shows a significant decrease in the expression level after 15 min of GnRH treatment (Fig. 3. 10C). Together, our ICC and RT-PCR data indicate the activation of Wnt/β-catenin signaling pathway in response to the activation of GnRH receptor.

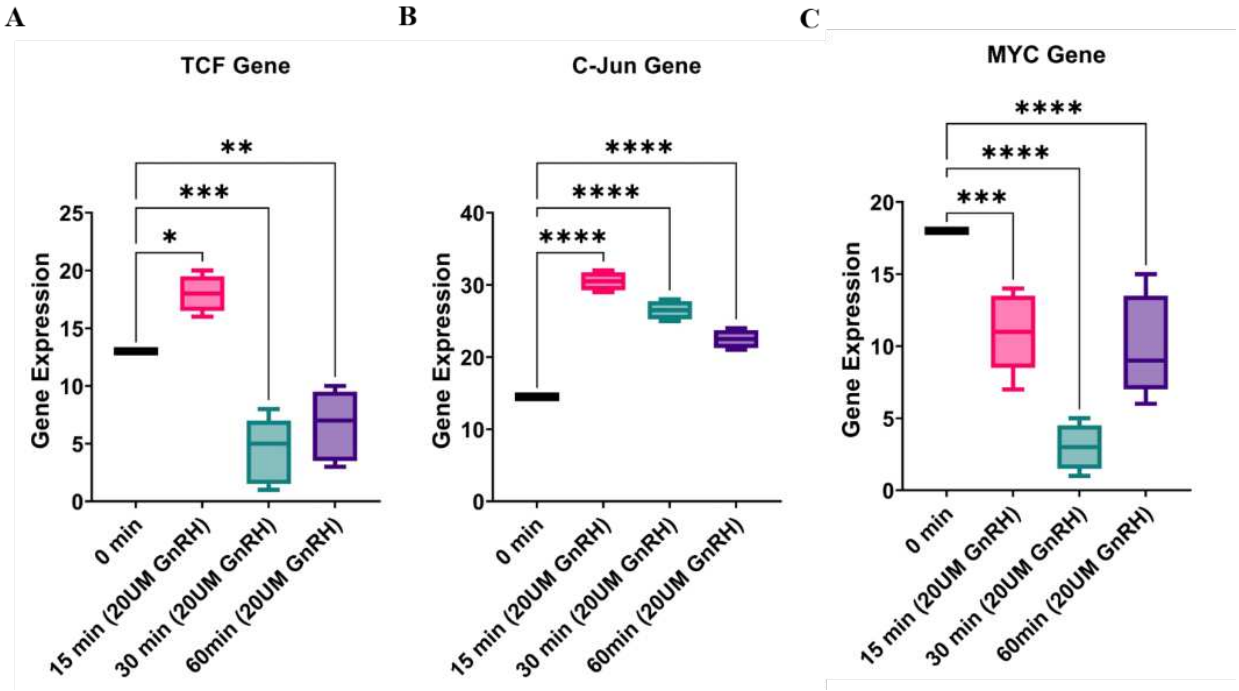

Fig. 3. 10: RT-PCR analysis showing the level of gene expression of Wnt/β-catenin signaling pathway target genes in αT3-1 gonadotropes treated with GnRH for different time points. These include **A,** TCF, **B,** C-Jun, and **C,** Myc genes that show a significant change in the expression level in response to GnRH.

To further understand the role that IQGAP1 might play to regulate the activation of Wnt/β-catenin signaling pathway, we transfected αT3-1 gonadotropes with IQGAP1 pre-designed silencer siRNA, and treated with 20 UM GnRH in different time points (0, 15, 30, 60 minutes). Then, we extracted the RNA to perform RT-PCR using TCF, C-Jun, and Myc primers. Consequently, we observed a significant increase in the expression level of TCF and Myc genes in response to GnRH (Fig. 3. 11A & C), while C-Jun gene shows a significant decrease in response to GnRH comparing to the control (Fig. 3.

11B), suggesting a transcriptional regulatory role of IQGAP1 in the Wnt/β-catenin signaling pathway target genes.

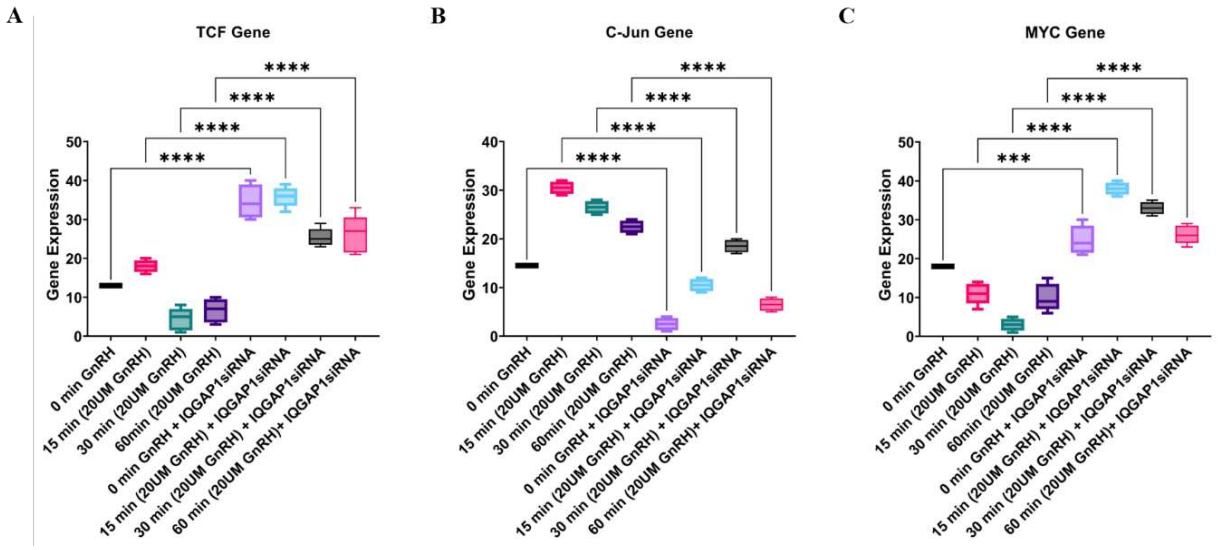

Fig. 3. 11: RT-PCR analysis showing the level of gene expression of Wnt/β-catenin signaling pathway target genes in control and transfected αT3-1 gonadotropes using IQGAP1 pre-designed silencer siRNA and treated with GnRH for different time points. These include: A, TCF, B, C-Jun, and C, Myc genes that show a significant change in the expression level in response to GnRH.

Discussion

Many cell types, such as lymphocytes, osteocytes, pancreatic β cells, and endocrine cells of the anterior pituitary (e.g., gonadotropes), are characterized by functional homotypic interactions where intercellular contact and communication are not distinguished or defining characteristics (Edwards et al., 2017a; Göngrich et al., 2016; Harwood and Batista, 2008; Kelly et al., 2011; Kim et al., 2014; Le Tissier et al., 2017; Momiji et al., 2019; Stoddart et al., 2001). In studies using slices of anterior pituitary revealed that GnRH exposure prompted connexin 36 (Cx36) gap junction-dependent coordination within loosely clustered gonadotropes (intercellular distances < 250 μm) (Göngrich et al., 2016). Moreover, a study employing female Cx36-null mice showed dysfunction in the HPG axis, including decreased LH secretion, impaired ovulation, and small litter size. Despite these interesting observations, the molecular mechanisms underlying intercellular communication between gonadotropes (without electrical coupling through gap junctions) are unclear. In our data, the proteomic screen of αT3-1 gonadotrope revealed

GnRH-responsive PCP and cell-cell adhesion associated proteins as potential candidates involved with communication between gonadotropes.

PCP signaling involves asymmetric subcellular distributions of signaling proteins leading to organized intercellular communication (Davey and Moens, 2017; Devenport, 2014; Lawrence and Casal, 2018; Mattes and Scholpp, 2018). PCP signaling mechanisms conceptually fulfill many of the mechanical requirements for functional communication between gonadotropes and cell-cell adhesion. Thus, in this study, we investigated the role of PTK7 and IQGAP1 in GnRH-dependent transcellular gonadotrope communication. We also include an examination of β-catenin, a multifunctional PCP protein associated with cell junctions that interacts with PTK7 and IQGAP1, as well as other different cascades (Golubkov and Strongin, 2014; Goto et al., 2013a; Hu et al., 2019; Lichtig et al., 2019; Smith et al., 2015).

The study concludes that stimulation of GnRH receptors in gonadotropes stimulates both intracellular and extracellular PTK7 signaling. The increase of PTK7 in T3-1 gonadotropes in response to GnRH, as shown by indirect immunofluorescence paired with confocal imaging, is accompanied by a high level at cell-cell contacts. In addition, it stimulates PTK7 proteolysis and translocation to other cellular compartments. The nuclear localization of PTK7-like immunofluorescence is dramatically enhanced in response to GnRH (Fig. 3. 2A), and this is accompanied by the release of N-terminal ectodomains and the production of intracellular C-terminal fragments that localize to the nucleus (Figs. 3. 2B & C). Importantly, blocking matrix metalloproteinases with GM6001 (10 M) prevents PTK7 from being degraded in response to GnRH (Fig. 3. 2C).

Besides, the analysis that comparing IQGAP, Ptk7, and β-catenin in control and GnRH-treated T3-1 gonadotropes cultures allowed us to better understand the role of these proteins in cell-cell adhesion and transcription. Within 60 minutes of GnRH treatment, β-catenin accumulated at the plasma membrane at cell-cell junctions, correlating with prior reports. Ptk7 and IQGAP1, which partially colocalized with β-catenin at cell-cell junctions, had a similar redistribution pattern throughout the same time period. There is some colocalization of ptk7 with the nucleus, although the amount varies widely from culture to culture

(Fig. 3. 5). Consistent with our immunofluorescence findings, we found that activation of the GnRH receptor increased the fluorescence intensity of the IQGAP1-Alexa Fluor 488 conjugated antibodies in flow cytometry (Fig. 3. 6B). After dosing T3-1 gonadotropes with 20 UM GnRH for 15 minutes, the strongest IQGAP1 fluorescence signals were seen. Moreover, IQGAP1 expression shows a significant upregulation after 15 minutes of GnRH treatment in both αT3-1 and LβT2 gonadotropes (Fig. 3. 6C & D).

Furthermore, we investigated the contribution to GnRH receptor-dependent signaling cascades involved with gonadotropin production. According to our findings in Chapter 1, GnRH treatment causes an upstream activation of Rac1 and IQGAP1. Pharmacological suppression of Rac1 decreased ERK phosphorylation and Rac1-IQGAP1 complexes at cell junctions, suggesting functional importance. Additionally, we found that IQGAP1 is responsible for activating ERK1/2 in T3-1 gonadotropes. Here, we show that Rac1-containing IQGAP1 signaling complexes modulate GnRH-dependent ERK activation in T3-1 gonadotropes and serve as essential effectors for signaling events leading to an enrichment of cell-cell contacts by using a pre-designed silencer siRNA for IQGAP1 (Fig. 3. 7). In addition, our confocal microscopy data demonstrates a dose-dependent increase in GSK-3 fluorescence in response to 20 nM GnRH, and other evidence hints to a function for Wnt signaling mediators in the GnRH signaling network in T3-1 gonadotropes. Furthermore, we found that in both control and transfected T3-1 gonadotropes with IQGAP1 pre-designed silencer siRAN and treated with 20 UM GnRH, there was a significant change in the signal accumulation of Wnt/β-catenin signaling pathway target proteins including TCF, C-Jun, and Myc (Frame and Cohen, 2001; Grimes and Jope, 2001). Confocal microscopy revealed an augmented signal in T3-1 gonadotropes treated with 20 UM GnRH, stained with Anti-TCF antibody and Anti-C-June antibody, and then detected with Alexa Fluor 488 secondary antibody (Fig. 3. 8A & B). Most of these signals are shown at the nuclei. However, the inhibition in IQGAP1 leads to a reduction in the TCF signal accumulation, whereas, C-June reveals more signal intensity in response to GnRH treatment. The expression levels of the TCF and C-Jun genes are shown to rise significantly by our RT-PCR analysis (Fig. 3. 9A & B), whereas the expression levels of the Myc gene are shown to drop

significantly after 15 min of GnRH treatment (Fig. 3. 9C). Nonetheless, we found that the expression levels of TCF and Myc genes were significantly upregulated in response to GnRH when IQGAP1 was knocked down (Fig. 3. 10A & C), while the expression of the C-Jun gene was significantly downregulated in response to GnRH when compared to the control (Fig. 3. 10B), suggesting a transcriptional regulatory role of IQGAP1 in the genes targeted by the Wnt/β-catenin signaling pathway.

Adhesions and cellular polarity are only two of the many functions of protein tyrosine kinase 7, a catalytically inactive receptor tyrosine kinase. PTK7 activity is regulated by sequential proteolysis, which produces protein fragments with diverse biological functions. Full-length PTK7 negatively regulates ERK signaling and interacts with and sequesters β-catenin. Following sequential cleavage by matrix metalloproteinase-14 (MMP-14; also, MT1-MMP) and ADAM family proteinases, soluble N-terminal ectodomain fragments inhibit the activity of full-length PTK7. Subsequent cleavage by γ secretase produces soluble intracellular C-terminal domain fragments, one of which translocate from the cytosol to the nucleus (Berger et al., 2017; Lichtig et al., 2019; Na et al., 2012; Peradziryi et al., 2012). Our findings suggest that GnRH promotes the activation of Ptk7 by activating the proteolysis that leads to the generation of intracellular C-terminal fragments that localize to the nucleus, suggesting a transcriptional regulatory role of Ptk7 in gonadotropes in response to GnRH. Moreover, the accumulation of Ptk7 at cell-cell contacts suggests another regulatory role in gonadotrope mediating the adhesions and cellular polarity in response to GnRH.

IQGAP1 on the other hand orchestrates many signaling pathways, including those that regulate cell-cell adhesion and actin filament rearrangement (Bañón-Rodríguez et al., 2014; Brown and Sacks, 2006). It has been reported that IQGAP1 inhibits cadherin-catenin-mediated cell-cell adhesion (Kuroda et al., 1998b), and IQGAP1 expression is drastically upregulated in the endothelial cell layers after vascular damage, during angiogenesis, or in chronic inflammatory disorders (Urao et al., 2010). It has also been shown that IQGAP1 functions as a scaffold for MAPK signaling. IQGAP1 modulates MAPK activity in response to EGF by binding directly to B-Raf, MEK1/2, and ERK1/2 (McNulty et al., 2011b; Ren et al.,

2007; Roy et al., 2004, 2005). In order for EGF to properly activate EGFR, IQGAP1 must form a constitutive association with EGFR. Furthermore, IQGAP1 intracellular concentration modulation suppresses EGF-dependent ERK and MEK activation. EGF produces weak tyrosine phosphorylation of EGFR in IQGAP1-deficient cells, but this phosphorylation is greatly increased by reconstitution of IQGAP1-deficient cells with wild-type IQGAP1 (McNulty et al., 2011b).

Evidence that IQGAP1 may control and compartmentalize Erk1/2 pathway activity comes from a research showing that it can create a primary signal in the nucleus's periphery to transiently sustain Erk1/2 phosphorylation (Awasthi et al., 2010). According to our findings in Chapter 1, GnRH treatment causes an upstream activation of Rac1 and IQGAP1. Reduced ERK phosphorylation and Rac1-IQGAP1 complexes at cell junctions in response to pharmacological suppression of Rac1 suggest its functional importance. Additionally, we found that IQGAP1 mediates ERK1/2 activation in T3-1 gonadotropes. By inhibiting IQGAP1 expression with a pre-designed silencing siRNA, we found that ERK pathway activation was altered (Fig. 3.7), proving that Rac1-containing IQGAP1 signaling complexes modulate GnRH-dependent ERK activation in T3-1 gonadotropes and act as crucial effectors in the signaling cascade that results in an increase in cell-cell contacts.

A significant fraction of active ERK in gonadotropes translocates to the nucleus rapidly. Numerous studies using various cell types indicate to the significance of ERK signaling in GnRH-induced transcriptional responses (Duan et al., 2002; Fowkes et al., 2002; Liu et al., 2002; Maudsley et al., 2007; Mulvaney and Roberson, 2000; Xie et al., 2008; Xie et al., 2005), suggesting the association between ERK signaling and the expression of the full complement of genes (GnRHR, FSHβ, LHβ, αGSU) that involve the genetic signature of the gonadotrope. Moreover, in LβT2 cells, it has been demonstrated that GnRH stimulates the nuclear localization of β-catenin modulating the activity of TOPflash, which is an artificial T-cell factor (TCF)/lymphoid enhancer factor (LEF)-dependent luciferase reporter. These changes were accompanied by increases in Jun, Fra1, and Myc-specific GnRH-dependent mRNAs (Gardner et al., 2007). Further interaction between signaling mediators of the Wnt/β-catenin pathway and

those activated by GnRH is suggested by the fact that GnRH enhances nucleus accumulation of β-catenin in LβT2 cells (Gardner et al., 2007; Salisbury et al., 2007), resulting in increased binding of β-catenin and SF1 to the endogenous Lhb promoter-regulatory (Salisbury et al., 2007). GnRH receptor activation by GnRH may target mediators of the Wnt/β-catenin signaling pathway, as shown by several studies using a heterologous HEK293 model cell line and LT2 gonadotrope cell line (Gardner et al., 2007; Gardner and Pawson, 2009; Salisbury et al., 2007, 2009).

There is evidence that IQGAP1 regulates gene transcription through β-catenin (Briggs et al., 2002a; Fukata et al., 1999b; Wang et al., 2008). Direct interactions between IQGAP1 and APC (Aoki and Taketo, 2007; Watanabe et al., 2004b) or protein phosphatase 2A (PP2A) (Suzuki et al., 2005) and indirect interactions between IQGAP1 and GSK-3 (Watanabe et al., 2009) point to a function for IQGAP1 in Wnt signaling. Since β-catenin binds directly to the RGCT domain (Fukata et al., 1999b), it is clear that IQGAP1 plays a significant role in the activation and degradation of β-catenin, and it has been established that IQGAP1 binds to the C-terminus of Disheveled (DVL) (Goto et al., 2013b) through a region between the IQ domains and the GRD of IQGAP1. Our RT-PCR and ICC results suggest that GnRH receptor activation triggers the Wnt/β-catenin signaling pathway. Confocal imaging revealed a shift in GSK-3β fluorescence in response to 20 nM GnRH (data not shown), supporting the hypothesis that Wnt signaling mediators play a key role in the GnRH signaling network in T3-1 gonadotropes. We also used indirect immunocytochemistry in conjunction with confocal microscopy and RT-PCR to compare the signal accumulation and gene expression between control and transfected T3-1 gonadotropes with pre-designed silencer siRNA to inhibit IQGAP1 and were then treated with 20 UM l GnRH. Genes like as TCF, C-Jun, and Myc are known to be activated in response to Wnt/β-catenin signaling pathway activation (Frame & Cohen 2001, Grimes & Jope 2001). After treating T3-1 gonadotropes with 20 UM GnRH and staining them with Anti-TCF antibody and Anti-C-June antibody followed by Alexa Fluor 488 secondary antibody, we could see a rise in signal when we viewed the cells using confocal microscopy (Fig. 3. 8A & B). After IQGAP1 inhibition, this signal changes revealing more reduction using Anti-TCF

antibody, whereas Anti-C-June antibody shows higher level of accumulation in αT3 gonadotropes treated with GnRH. The expression levels of the TCF and C-Jun genes are shown to rise significantly by our RT-PCR study (Fig. 3. 9A & B), whereas the expression levels of the Myc gene are shown to drop significantly after 15 min of GnRH treatment (Fig. 3. 9C). However, expression of TCF and Myc genes in transfected αT3-1 cells were found to be significantly upregulated in response to GnRH (Fig. 2. 10A & C), while expression of the C-Jun gene was significantly downregulated in response to GnRH compared to the control (Fig. 2. 10B), indicating a transcriptional regulatory role of IQGAP1 in the target genes of the Wnt/β-catenin signaling pathway.

Cell-cell junctions are essential in establishing extracellular communication between neighboring cells and intracellular communication with various cytoskeletal elements that together create incorporated, structural continuance across the tissues. Many elements are known to be linked to adherens and tight junctions. Junctional adhesion proteins bind through their cytoplasmic tail to cytoskeletal and signaling proteins, allowing the adhesion proteins' anchoring to actin microfilaments and transfer intracellular signals inside the cell (Bazzoni et al., 1999; Braga, 2002; Matter and Balda, 2003; Wheelock and Johnson, 2003a). The association with actin is essential for the stabilization of the junctions and the dynamic regulation. In addition, the interaction of junctional adhesion proteins with the actin cytoskeleton might be relevant in the maintenance of cell shape and polarity (Dudek and Garcia, 2001; Lampugnani et al., 2002; Sheldon et al., 1993; Stevens et al., 2000). Interestingly, releasing some intracellular junctional proteins from junctions leads to translocating to the nucleus and modifying transcription (Ben-Ze'ev and Geiger, 1998; Bienz and Clevers, 2000; Matter and Balda, 2003). Among these junctional proteins are PTK7 and IQGAP1 that acts as scaffolds, which binds several effector proteins and mediates their mutual interaction.

By coordinating the location and timing of signaling components, IQGAP1 helps fine-tune cellular signaling pathways. Multiple methods, including tethering, organelle localization, feedback signal coordination, and component sequestration, allow this protein to modulate signaling pathways.

Quantifying protein-protein interactions is essential for understanding how scaffolds organize proteins; these interactions have traditionally been characterized by biochemical methods like Western blots using recombinant proteins and whole-cell lysates and visualized by imaging methods like immunofluorescence. Also, the level of the fluorescent intensity of markers binding to proteins using Flow cytometry provides a quantitative study of the activity of proteins beside evaluating the gene expression level using RT-PCR. These methods may provide inferences about contacts, but definitive proof of physical association and the spatial and temporal dynamics of interactions. Since IQGAP1 is a big scaffold protein, it often forms protein complexes with a wide variety of other proteins, making it challenging to describe transient protein-protein interactions.

IQGAP1 plays a critical role in fine-tuning cellular signaling pathways by spatially and temporally organizing signaling components. This protein regulates signaling pathways through a variety of mechanisms, including tethering, localizing to a specific organelle, coordinating positive and negative feedback signals, and sequestering various components. Understanding how scaffolds organize proteins requires quantification of protein-protein interactions, which have been historically characterized by biochemical techniques such as Western blots using both recombinant proteins and whole-cell lysates and have been visualized using imaging techniques such as immunofluorescence. While these techniques are able to suggest interactions, verification of physical association, as well as their spatial and temporal dynamics, needs to be carried out in live cells, especially in the case of scaffold protein interactions. IQGAP1 is a scaffold protein that is typically large and tend to complex with many different proteins, making it difficult to characterize limited and temporary protein-protein interactions.

Methodology

Our general approach is to combine cutting-edge imaging with supportive biochemical and molecular measures. Our integrated functional and structural approach is designed to generate a comprehensive study involving multiple independent experimental methods to investigate the molecular

role of cell polarity and adherens junction-related proteins in mediating the intergonadotrope communication and function.

Cell Cultures

The αT3-1 and LβT2 murine gonadotrope derived cell lines, derived by the Mellon laboratory, have been used extensively in many studies investigating GnRH-activated signal transduction pathways and gonadotrope function. These cell lines were generated via targeted expression of SV40 large T antigen in developing pituitary cells (Bazzoni et al., 1999; Benard et al., 1999; Ferri et al., 2013). Both lines express the GnRHR and the αGSU. Moreover, the LβT2 cell line expresses the β subunits of LH and FSH (Braga, 2002), reflecting a more distinct phenotype of gonadotropes. All data presented were obtained using clonal αT3-1 cells (Bazzoni et al., 1999). αT3-1 cells are applicable models as they permit transfection (e.g., expressing fluorescently-tagged GnRH receptors). However, we recognize the limitations inherent to the use of this immortalized cell line. To circumvent these limitations, some experiments were performed using LβT2 murine gonadotrope-derived cell line expresses the β subunits of LH and FSH to study the response of the tertiary genes to GnRH stimulation, including Lhb, and Fshb (Wang et al., 2008).

Western Blot Analysis/ERK Activation Assay

standard immunoblotting techniques were used to assess ERK activation. These data were analyzed using ANOVA with Newman-Keuls multiple comparison post-test. This approach was used to confirm the activation of the GnRH receptor that leads to phosphorylation. Note that ERK ½ phosphorylation occurs within 5-15 mins after stimulation by GnRH.

Cell imaging and Immunofluorescence microscopy

Target cells were transferred to glass-bottom culture dishes (MatTek; Ashland, MA) coated with Corning® Matrigel® matrix (Corning; Tewksbury, MA) diluted 1:250 in DMEM and grown for 24 hr at 37 °C in 5% CO2 humidified air. Cells were fixed in paraformaldehyde diluted to 4% in PBS for 15 min, washed with PBS, and permeabilized with PBS containing 0.5% Triton X-100 (TX100) for 3 min. Dishes were then blocked with 10% donkey serum and 0.05% TX100 before incubation with the indicated primary antibody (diluted 1:250) overnight at 4° C (Table 3. 1). Proteins were then visualized by staining with either Alexa Fluor 488 or Alexa Fluor 568-conjugated secondary antibody (Invitrogen, dilution 1:1000) and counterstained with DAPI (0.2 ug/mL) as indicated. Images were acquired on either a Zeiss LSM800 confocal laser-scanning microscope (Carl Zeiss; Oberkochen, Germany) or a TIRF microscope with this or that as indicated and analyzed with ImageJ. Images were background-subtracted in ImageJ software (National Institutes of Health). Using confocal laser-scanning microscope, the parameter adjustment was performed at one time before the imaging session. The pinhole size was adjusted alternatively to have the same channel's optical thickness for all samples. The laser intensity for all samples was adjusted to be 1% for measuring 405 nm, and 2% for measuring 561 nm. The detector gain was adjusted to be maximum of 800. The settings for each experiment were uniform, and we used fresh fixed samples that were scanned once in each experiment. The imaging of control, treated, and nontreated cells were performed at one time using the same parameters setting.

Table 3. 1: Primary and Secondary Antibodies used in Immunocytochemistry for target proteins using αT3 gonadotropes.

Antibody	Species	Dilution	Company (Cat#)
IQGAP1 (C-9)	Mouse Monoclonal	1:250	Santa Cruz, Cat# SC-376021
IQGAP1 (H-109)	Rabbit Polyclonal	1:250	Santa Cruz, Cat# SC-59987
B-Catenin (3-5)	Mouse Monoclonal	1:250	Santa Cruz, Cat# SC-7963
Cdc42 (B-8)	Mouse Monoclonal	1:250	Santa Cruz, Cat# SC-8401
E-Cadherin (3-10)	Mouse Monoclonal	1:250	Santa Cruz, Cat# SC-8426
N-Cadherin (H-63)	Rabbit Polyclonal	1:250	Santa Cruz, Cat# SC-59987
Erk1 (K-23)	Mouse Monoclonal	1:250	Santa Cruz, Cat# SC-94
P-Erk (E-4)	Mouse Monoclonal	1:250	Santa Cruz, Cat# SC-7383

APC (F-3)	Mouse Monoclonal	1:250	Santa Cruz, Cat# SC-59987
Alexa Fluor 488 Goat Anti-Mouse IgG (H+L) Secondary Antibody	Goat	1:1000	Invitrogen, Thermo Fisher, Cat# A11029
Alexa Fluor 568 Goat Anti-Mouse IgG (H+L) Secondary Antibody	Goat	1:1000	Invitrogen, Thermo Fisher, Cat# A11004
Alexa Fluor 488 Goat Anti-Rabbit IgG (H+L) Secondary Antibody	Goat	1:1000	Invitrogen, Thermo Fisher, Cat# A11034
Alexa Fluor 568 Goat Anti-Rabbit IgG (H+L) Secondary Antibody	Goat	1:1000	Invitrogen, Thermo Fisher, Cat# A11036
Anti-Mouse IgG(H+L), Secondary Antibody, HRP Conjugate	Mouse	1:5000	Invitrogen, Cat# A28177
Anti-Rabbit IgG(H+L), Secondary Antibody, HRP Conjugate	Rabbit	1:5000	Invitrogen, Cat# A27036

Transfection and Knockdown Assay

αT3 gonadotropes were maintained at 37°C/5% CO2 in Hyclone Medium (DMEM) supplemented with 10% fetal bovine serum (ATCC), L-Glutamine (2 mM L-alanyl-L-glutamine), and 1% penicillin/streptomycin. Once cells reached confluence, they were exposed to 0.25% trypsin-EDTA (Gibco) and re-plated at lower density. Cells were maintained for no more than 17 passages beyond their original plating. After 2 hours, the cells were transfected using 1:500 Lipofectamine RNAiMAX Transfection reagent (Cat#13778150, Invitrogen), 1:100 Opti-MEM (Gibco), and multiple IQGAP1 pre-designed siRNA silencer to accomplish an effective knockdown (Table 3. 2). Likewise, GAPDH pre-designed siRNA silencer, as a positive control, and a negative control following the manufacturer's instructions (Wheelock and Johnson, 2003a). Cells were incubated overnight and reached confluence. Following transfection, serum starving medium was added to the cells before treated with 20 μM GnRH for different time points (0 min, 15 min, 30 min, 60 min). Cells were fixed in paraformaldehyde diluted to

4% in PBS for 15 min, washed with PBS, and permeabilized with PBS containing 0.5% Triton X-100 (TX100) for 3 min. Dishes were then blocked with 10% donkey serum following the preparation to perform immunofluorescence as mentioned above. Cells then were imaged using the confocal microscopy.

Table 3. 2: Sequences of multiple pre-designed silencers select siRNA used to knockdown IQGAP1 that is the main target, and GAPDH, which is a positive control.

Gene	siRNA Type & ID	Organism	Sense Sequence (5'->3')	Antisense	Concentration
IQGAP1	Pre-designed Silencer® Select, s78120	Mouse	GCACUCCCAUAAA GACGAATT	UUCGUCUUUAU GGGAGUGCAG	10µM
IQGAP1	Pre-designed Silencer® Select, s78119	Mouse	GCUCCGUCCUGGA UAAUGATT	UCAUUAUCCAG GACGGAGCCA	10µM
GAPDH	Pre-designed Silencer® Select, s234321	Mouse	-	-	10µM

Quantitative real-time polymerase chain reaction (qRT-PCR)

αT3 gonadotropes were plated in 100 mml culture dish, then; separated into multiple 60 mml culture dish that reached 2 x 106 cells/dish at confluency. For serum starving, cells were washed twice with 1X PBS; then, 3 ml of Free serum media Hyclone DMEM/High glucose with L-glutamine, sodium pyruvate (cytiva, Cat# SH30022.01) were added to the cells and incubated in 5% CO2 at a 37 °C incubator for 3 hours. After the incubation, a group of cells were treated with 20 µM of GnRH for different time points (0 min, 15 min, 30 min, and 60 min). Additional group of cells were transfected with 10 µM SiRNA; then, incubated in 5% CO2 at a 37 °C incubator for 24-48 hours. Which then treated with 20 µM of GnRH for 0 min, 15 min, 30 min, and 60 min. Cells were then washed twice with cold 1X PBS. Total RNA from cells was isolated using the RNeasy Mini Kit (Qiagen) according to the manufacturer's instructions. The reverse transcription reaction was performed using the ABI7500 system (Applied Biosystems, Foster City, CA, USA) following the manufacturer's instructions. The one-step QuantiFast

SYBR Green RT-PCR Kit (Qiagen) was used in combination with primers (Table 3. 3) from the QuantiTect Primer Assay (Qiagen). The incorporation of SYBR Green into the PCR products was monitored in real-time after each PCR cycle, resulting in calculating the threshold cycle or Ct value that defines the PCR cycle number at which exponential growth of PCR products begins. PCR cycle conditions were as follows: 10 minutes at 50°C, 5 minutes at 95°C, 35 to 40 cycles of 10 seconds at 95°C and 30 seconds at 60°C. Each PCR procedure included a negative control reaction without a template. To exclude residual DNA contamination of the RNA samples, RT-PCR was also performed without reverse transcriptase. Reactions were performed in 96 well format in triplicate with 25 ng total RNA per well in a Light Cycler 480 (Roche). The β-actin housekeeping gene was used as a reference for the relative quantification of the gene of interest.

Table 3. 3: RT-PCR primer sequences of target genes, reference numbers, and exon location. Primers are indicated as forward (F) or reverse (R).

Gene	Primer	Reference Sequence No.	Exon Location	Sequence
Cdh2	Primer F	NM_007664	13-14	5'-CCATCATCGCTATCCTTCTGTG-3'
	Primer R			5'-TCTTT ATCCCGCCGTTTCATC-3'
Cdc42	Primer F	NM_009861	3-4	5'-ACAGTT ATGATTGGTGGAGAGC-3'
	Primer R			5'-GTGGATAACTTAGCGGTCGTAG-3'
Cdh1	Primer F	NM_009864	3-4	5'-GAGCTGTCT ACCAAAGTGACG-3'
	Primer R			5'-AGTCTCGTTTCTGTCTTCTGAG-3'
Fshb	Primer F	NM_008045	2-3	5'-GCCGTTTCTGCATAAGCATC-3'
	Primer R			5'-TCTCGT ATACCAGCTCCTTGA-3'
C-Jun	Primer F	NM_010591	1-1	5'-GCATGGACCT AACATTCGATCT-3'
	Primer R			5'-GAGCACTACAGAAGCAATCTACA-3'
Lhb	Primer F	NM_008497	2-3	5'-GAATGAGTTCTGCCCAGTCTG-3'
	Primer R			5'-CGGACAGATGCGAAGCG-3'

Myc	Primer F	NM-010849	2-3	5'-TTCTCTCCTTCCTCGGACTC-3'
	Primer R			5'-CTTCCTCATCTTCTTGCTCTTCT-3'
Tcf7	Primer F	NM_009331	2-3	5'-CTTCAATCTGCTCATGCCCTA-3'
	Primer R			5'-TGTTCGT AGAGTGGAGAAAGC-3'
Rac1	Primer F	NM_009007	2-3	5'-GCTCATCAGTTACACGACCA-3'
	Primer R			5'-TCCATCT ACCAT AACATTGGCA-3'
IQGAP1	Primer F	NM_016721	3-4	5'-GCCACTGAATCACATTATCCGT-3'
	Primer R			5'-GGAGTCTACCTTGCCAAGC-3'
β-Actin	Primer F	NM_007393(1)	2-3	5'-ACTGCTCTGGCTCCTAGCAC-3'
	Primer R			5'-CCACCGATCCACACAGAGTA-3'
Atf3	Primer F	NM_007498	2-3	5'-TGTCTTCTCCTTTTTCTTGTTTCG-3'
	Primer R			5'-AGATGTCAGTCACCAAGTCTG-3'
EGR1	Primer F	NM_007913(1)	1-2	5'-GAGCGAACAACCCTATGAGC-3'
	Primer R			5'-AGCGGCCAGTATAGGTGATG-3'
GAPDH	Primer F	NM_008084.2	2-3	5'-CCTCGTCCCGTAGACAAAATG-3'
	Primer R			5'-TGAGGTCAATGAAGGGGTCGT-3'
Cga	Primer F	NM_009889	1-2	5'-AGCATGACCAGAATGACAGC-3'
	Primer R			5'-CCTCAGATCGACAATCACCTG-3'

Flow Cytometry

αT3 gonadotropes were plated in 100 mml culture dishes, then; separated into multiple 60 mml culture dish that reached 2 x 106 cells/dish at confluency. For serum starving, cells were washed twice with 1X PBS; then, 3 ml of Free serum media Hyclone DMEM/High glucose with L-glutamine, sodium pyruvate (cytiva, Cat# SH30022.01) were added to the cells and incubated in 5% CO2 at a 37 °C incubator for 3 hours. After the incubation, a group of cells were treated with 20 μM of GnRH for different time points (0 min GnRH, 15 min, 30 min, and 60 min). Additional group of cells were transfected with 10 μM SiRNA; then, incubated in 5% CO2 at a 37 °C incubator for 24-48 hours. Which then treated with 20 μM of GnRH for 15 min. Cells were then washed twice with cold 1X PBS. Then, 0.5

ml of Trypsin 0.05% with 0.53 mM EDTA, 1X (Corning, Cat#25-052-CI) were added to the cells; then, incubated for 1 min in 5% CO2 at a 37 °C incubator. Cells were collected in 15 ml conical tube; then centrifuge at 380 G-force for 2 min at 4°C. The pellet of cells were washed twice with 1X PBS with 4 mM EDTA (Teknova, Cat#100216-522). Following single-cell suspension of αT3 gonadotropes in 1X PBS with 4 mM EDTA, cells were incubated with a 1:5,000 dilution of Ghost Dye™ Violet 510 (CYTEK, Cat# SKU 13-0870-T100) for 30 minutes in the dark at 4°C. Cells then were washed with FACS Staining buffer twice. Following a wash with FACS staining buffer, cells were incubated with 200 µL 4% Fixation buffer of 1x Permeabilization/Fixation buffer (R&D Systems, Cat# FC009) for 15 min at room temperature. Cells were subsequently washed with 200 µL of 1x permeabilization buffer (Invitrogen, Carlsbad, CA). After that, cells were incubated with a 1:200 dilution of FC Receptor Blocker (Innovex biosciences, Cat# NB309-30) for 20 min at room temperature before being incubated for 30 minutes at 4 °C with a 1:200 dilution of fluorescently labeled (conjugated) antibody cocktail (Table 3. 4). Following a wash with FACS staining buffer, cells were washed with FACS and 4 mM Dithiothreitol (DTT) buffer (Invitrogen, Cat# B0009). Cells were then suspended in 300 µl of FACS Staining buffer. After preparing the cells, 250,000 events were collected in triplicate per sample on a Cytek Aurora Flow Cytometer (Cytek, Fremont, CA) and analyzed with FlowJo version 10.5.2 software and the cyto-feature engineering pipeline. Cell populations were identified by unsupervised feature engineering of cells by phenotype and confirmed via traditional gating methods.

Table 3. 4: Antibodies conjugated to Alexa Fluor fluorescent used to measure the intensity of the fluorescent in αT3 gonadotropes using a Cytek Aurora Flow Cytometer.

Fluorophore	Marker	Species	Dilution	Company, (Cat#)
Alexa Fluor 488	IQGAP1 (C-9)	Mouse Monoclonal	1:200	Santa Cruz, Cat# SC-376021AF488
Alexa Fluor 594	B-Catenin (E-5)	Mouse Monoclonal	1:200	Santa Cruz, Cat# SC-7963AF594
Alexa Fluor 594	Rac1, 2, 3 (G-2)	Mouse Monoclonal	1:200	Santa Cruz, Cat# SC-514583AF594
Alexa Fluor 647	Cdc42 (B-8)	Mouse Monoclonal	1:200	Santa Cruz, Cat# SC-8401AF647

Alexa Fluor 647	E-Cadherin (G-10)	Mouse Monoclonal	1:200	Santa Cruz, Cat# SC-8426AF594
Alexa Fluor 790	N-Cadherin (13A9)	Mouse Monoclonal	1:200	Santa Cruz, Cat# SC-59987AF594

Measurement of Ca2+ Activation

We subcultured αT3-1 cells in 35 mml Petri dishes and transfected with 10 μM IQGAP1 pre-designed silencer siRNA or an empty vector. After that, cells were incubated with 5 μM of Fluo-3, AM (Cat#F14218) for 25 min at 37° C. Cell were washed with fresh media to remove any dye that is not specifically associated with the cell surface. Cells, then, were incubated for a further 30 minutes to allow complete de-esterification of intracellular AM esters. Following, cells, were treated with different concentration of GnRH (0, 20, 50, 100 UM) for 15-20 min, and incubated in live cell imaging solution (Invitrogen, Cat# A14291DJ), and prepared for imaging using confocal microscopy. we measured the [Ca2+]i response at excitation wavelengths of 340 and 380 nm and an emission wavelength of 510 nm. Images were processed using imageJ software. We also measured the GnRH-dependent GCaMP calcium transients using GCaMP6s-CAAX, which is Plasma membrane targeted GCaMP6s that is calcium sensor, in live αT3-1 cells subcultured in 35 mml Petri dishes. Imaging cell surface was performed using TIRF microscopy. Holding ROI location constant, intensity was measured for ROI 1&2 for each frame for ~60 frames or ~16 seconds. Following GnRH treatment for 10 min, cells were imaged, and intensity was also measured for ROI 1&2 for each frame for ~60 frames or ~16 seconds.

F-Actin Tracker Assay

αT3 gonadotropes were maintained at 37°C/5% CO2 in Hyclone Medium (DMEM) supplemented with 10% fetal bovine serum (ATCC), L-Glutamine (2 mM L-alanyl-L-glutamine), and 1% penicillin/streptomycin. Once cells reached confluence, they were exposed to 0.25% trypsin-EDTA (Gibco) and re-plated at lower density. Cells were maintained for no more than 17 passages beyond their

original plating. After 2 hours, the cells were transfected using 1:500 Lipofectamine RNAiMAX Transfection reagent (Cat#13778150, Invitrogen), 1:100 Opti-MEM (Gibco), and multiple IQGAP1 pre-designed siRNA silencer to accomplish an effective knockdown. Cells were incubated overnight and reached confluence. Following transfection, serum starving medium was added to the cells before treated with 20 μM GnRH for different time points (0 min, 15 min, 30 min, 60 min). Cells were fixed in paraformaldehyde diluted to 4% in PBS for 15 min, washed with PBS, and permeabilized with PBS containing 0.5% Triton X-100 (TX100) for 3 min. Dishes were then blocked with 10% donkey serum following the incubation with 1X of CellMask™ Green Actin Tracking Stain for 15 min. Cells then were washed many times with 1X PBS before imaging using the confocal microscopy at excitation wavelengths of 503 nm and an emission wavelength of 512 nm. We also used TIRF images of control and transfected αT3-1 cells with GFP-UtrCH, which can track the level of F-actin in αT3-1 gonadotropes, in response to GnRHR activation. Cells were subcultured in 35 mml petri dishes and maintained for 2 hr. following with transfection; then, incubated in 5% CO2 at 37°C for 24 hrs. until they reach the target confluency. Cells were treated with 20 nM GnRH or water to evaluate the actin filament interaction in αT3-1 gonadotropes following the activation of GnRH. After that, cells were treated with nicardipine to investigate the role L-type calcium ion channel mediating the actin filaments interaction. we assessed the actin filament interaction when we treated αT3-1 gonadotropes with Nicardipine that shows high affinity for the dihydropyridine binding site (pKi = 9.7) and inhibits the L-type calcium ion channel as demonstrated by its ability to decrease the calcium ion-dependent action potential dose-dependently in ventricular papillary muscle (pIC50 = 7.15).

Quantification and Statistical Analysis

Statistical Analysis Data sets were compared using an unpaired Kruskal-Wallis one-way ANOVA with post hoc tests performed with Bonferroni correction, and p values of less than 0.05 were considered significant. Prism was used to perform statistical tests as well as to obtain descriptive statistics. Compiled data are shown as the mean ± SEM, or as histograms.

Chapter 4: IQGAP1 Mediates the GnRH Receptor Signaling and Gene Expression in Gonadotropes

Summary

IQ domain GTPase-activating scaffolding protein 1 (IQGAP1) is a scaffolding protein that participates in several cellular functions, including cytoskeletal regulation, cell adhesion, gene transcription and cell polarization. IQGAP1 coordinates the direction and impact of multiple signaling pathways by scaffolding its various binding partners, such as, including Ca2+/calmodulin signaling, Erk1/2 signaling, Wnt/ β-catenin signaling, cytoskeletal architecture, CDC42 and Rac1 signaling, E-cadherin-mediated cell–cell adhesion and β-catenin-mediated transcription. Several protein partners have been identified and described to interact with IQGAP1 in many cell types; however, the molecular relevance of many of these interactions has yet to be defined in gonadotropes. Recent study has highlighted the central regulatory functions played by the IQGAP1 scaffold in gonadotropes in response to GnRH. We use fluorescence imaging and correlation methods, including Flow cytometry and RT-PCR that allow for real-time live-cell changes in IQGAP1 localization and complex formation during signaling in gonadotropes in response to GnRH. Our data reveals an upstream activation of signaling and structural molecules, including Ca2+, CDC42 and Rac1, E-cadherin, N-cadherin, and β-catenin. we also identified interactions between the scaffold protein IQGAP1 and these molecules, indicating that IQGAP1 is a fundamental regulator of GnRH-dependent signaling in gonadotropes. Furthermore, our data shows that IQGAP1 has a transcriptional regulatory role in gonadotropes treated with GnRH. Collectively, our findings thus futher supports our hypothesis that IQGAP1 represents a novel regulatory proteins downstream of the GnRH recepotor, and further corroborate our SILAC and LC- MS/MS analysis and identification of GnRH responsive proteins dynamically regulated at the cell membrane.

Introduction

The anterior pituitary is the primary target of GnRH, which is synthesized in the hypothalamus and released into the hypophyseal portal circulation. By binding to the G protein-coupled receptor, GnRH receptor, on the surface of gonadotrope cells in the pituitary gland, it triggers a cascade of events that ultimately results in the increased production of gonadotropins (Kaiser et al., 1998). In response, LH and FSH are secreted into the bloodstream, where they go to the gonads to control processes including folliculogenesis, ovulation, spermatogenesis, and steroidogenesis (Burger et al., 2004).

Subcellular compartmentalization and coordination of signal transduction proteins increase the efficiency and fidelity of biochemical cascades and allows ubiquitous signaling molecules, such as calcium (Ca2+), to participate in multiple intracellular processes with varying degrees of specificity and independence. Evidence suggests that actin cytoskeletal remodeling is critical for GnRH receptor-dependent stimulation of gonadotropes (Dang et al., 2014; Edwards et al., 2017a; Edwards et al., 2016; Navratil et al., 2014). Notably, following GnRH receptor stimulation, gonadotropes undergo dramatic cytoskeletal and morphological rearrangements, which appear necessary for the transcriptional changes required for upregulation of gonadotropin synthesis (Navratil et al., 2014; Navratil et al., 2007). This process is mediated by the recruitment of numerous actin cytoskeletal, cell polarity, and adherens junction-related proteins to intercellular junctions for the purpose of establishing and augmenting functional connectivity between gonadotropes.

The activation of GnRH seems to trigger a dynamic assembly of microdomains inside the plasma membrane, indicating that the cytoskeleton plays a role in mediating their aggregation. Consistent with this, many of the molecules involved in controlling the actin cytoskeleton have been observed to connect with specific membrane domains (Chichili and Rodgers, 2009; Viola and Gupta, 2007). Primary cultures of mouse pituitary cells show microdomain localization of GnRHR and downstream signaling intermediates such as c-raf kinase, ERK, calmodulin, and Gaq (Navratil et al., 2003). It has been suggested that the assembly of several discrete GnRHR-containing membrane microdomains is facilitated

by GnRH (agonist) driven receptor self-association in gonadotropes, allowing for the transduction of a GnRH signal that activates ERK functionally and ultimately results in LH generation. This emphasize that GnRH-induced ERK activation is essential for LHb expression and ovulation (Cornea et al., 2001; Horvat et al., 2001). In gonadotropes, the cytoskeleton remodeling following the activation of GnRH plays an essential part in regulating the LH release (Adams and Nett, 1979; Navratil et al., 2014). It has been shown that primary mouse gonadotrope cells are unable to secrete LH when GnRH-induced actin remodeling processes are disrupted (Navratil et al., 2014). The cytoskeleton is crucial because inhibiting actin remodeling efficiently prevents not just GnRH signaling to ERK but also more acute signaling processes such as the activation of L-type calcium channels in the plasma membrane (Bliss et al., 2007; Meiri, 2004). Thus, Microdomains operate as hubs for ligand-mediated communication between the plasma membrane and the actin cytoskeleton in order to govern nucleation (Meiri, 2004).

Collectively, microdomains act as a spatial platform that enables specific regulation of a multi-protein scaffold that mediates the initiation of ERK activation in response to GnRH. Therefore, in this chapter we designed our experiments to study the different microdomains that allow the cytoskeletal remodeling following the activation of GnRH Receptor, considering our proteomics results and the identification of proteins affected by GnRH treatment using a SILAC-based proteomics approach that identify and quantify the relative abundance of plasma membrane-associated proteins in response to GnRH, we detected a significant change in ~80 plasma membrane-associated proteins following GnRH exposure using immortalized αT3-1 gonadotropes. Our findings that are presented in chapter two reveal the activation of the scaffold protein IQGAP1 and how this protein localizes at cell-cell adhesion, as well as mediates the activation of other signaling pathways following the activation of GnRH receptor. It is reasonable to hypothesize that IQGAP1 may modulate complexes of proteins that allow the activation of signaling pathways in gonadotropes in response to GnRH. Moreover, IQGAP1 might have a transcriptional regulatory role that influence the expression and production level in gonadotropes.

Results

Analysis of our proteomics results and the identification of proteins affected by GnRH treatment using a SILAC (stable isotope labeling by amino acids in cell culture)-based proteomics approach revealed that GnRH increased the plasma membrane association of numerous actin cytoskeletal, cell polarity and adherens junction-related proteins which included the scaffold protein IQGAP1 and the small GTPase Rac1, Ptk7 and others. Indeed, following GnRH receptor stimulation, gonadotropes undergo dramatic cytoskeletal and morphological rearrangements which appear to be necessary for the transcriptional changes required for upregulation of gonadotropin synthesis (Featherstone et al., 2016; Lyles et al., 2010) .

The further examination of the localization of cell adhesion and polarity proteins, IQGAP1 revealed redistribution at the plasma membrane at cell-cell junctions within 10 min after GnRH treatment compared to control αT3-1 gonadotropes using Indirect immunofluorescence combined with confocal microscopy. Moreover, the level of the fluorescent intensity showed a signficant increse in response to GnRHR activation using Flow Cytometry approach to αT3-1 gonadotropes treated with 10 UM GnRH and stained with Anti-IQGAP1 antibody conjugated with Alexa Fluor 488 fluorescence. In addition, the IQGAP1 expression revealed a significant increase in both αT3-1 and LβT2 gonadotrope cell lines after 15 min of GnRH treatment.

To understand the role of IQGAP1 in GnRH signaling pathway in gonadotropes as an effector modulates the activation of signaling molecules to cell-cell junctions following GnRH receptor activation. We first confirmed the involvemet of many cytoskeleton and cell-cell junctions elements, such as Rac1, Cdc42, E-Cadherin, N-Cadherin, β-Catenin, and F-Actin. Then, we evaluated the activation of these elements when knockdown IQGAP1 using pre-designed siRNA silencer. Afterthat, we investigated the level of the GnRH receptor-dependent gene expression in αT3-1 and LβT2 gonadotropes, especially after the IQGAP1 knockdown to evaluate the involvement of IQGAP1 in gene expression in response to GnRH receptor activation.

Together, we found that ICC, Flow Cytometry, and RT-PCR data revealed a significant role of IQGAP1 mediating cytoskeleton remodeling by regulating the activation of signaling molecules to cell-cell junctions, as well as the gene expression level of primary and tertiary genes that respond to GnRH receptor activation in αT3-1 and LβT2 gonadotropes. Our analysis futher supports our hypothesis that IQGAP1 represent a novel regulatory proteins downstream of the GnRH recepotor and further cooroborate our SILAC and LC- MS/MS analysis and identification of GnRH-responsive proteins dynamically regulated at the cell membrane.

The activation of signaling molecules to cell-cell junctions following GnRH receptor activation

IQGAP1 is localized at the plasma membrane at cell-cell adhesion and associated with small Rho GTPases Rac1 or Cdc42 to regulate the adherens junction complex through the interaction with β-catenin. Moreover, it has demonstrated that IQGAP1 associates directly with E-cadherin and affects its function (Noritake et al., 2005). Notably, the mediators of cell-cell adhesion E- and N-cadherin requires the interaction and association of IQGAP1/Cdc42/Rac1/α-catenin/β-catenin complexes (Fukata et al., 2001a; Kaibuchi et al., 1999a; Kuroda et al., 1999).

Our data showed an upstream activation and association of Rac1, Cdc42, E-Cadherin, N-Cadherin, and β-catenin in response to GnRH. Our indirect immunocytochemistry combined with confocal microscopy data shows redistribution of these proteins, especially, at the cell-cell adhesion positions where the signal shows more accumulation using primary antibodies conjugated to Alexa Fluor fluorescence secondary antibodies in αT3-1 gonadotropes in response to 20 UM GnRH (Fig. 4. 1A, B, & C).

A

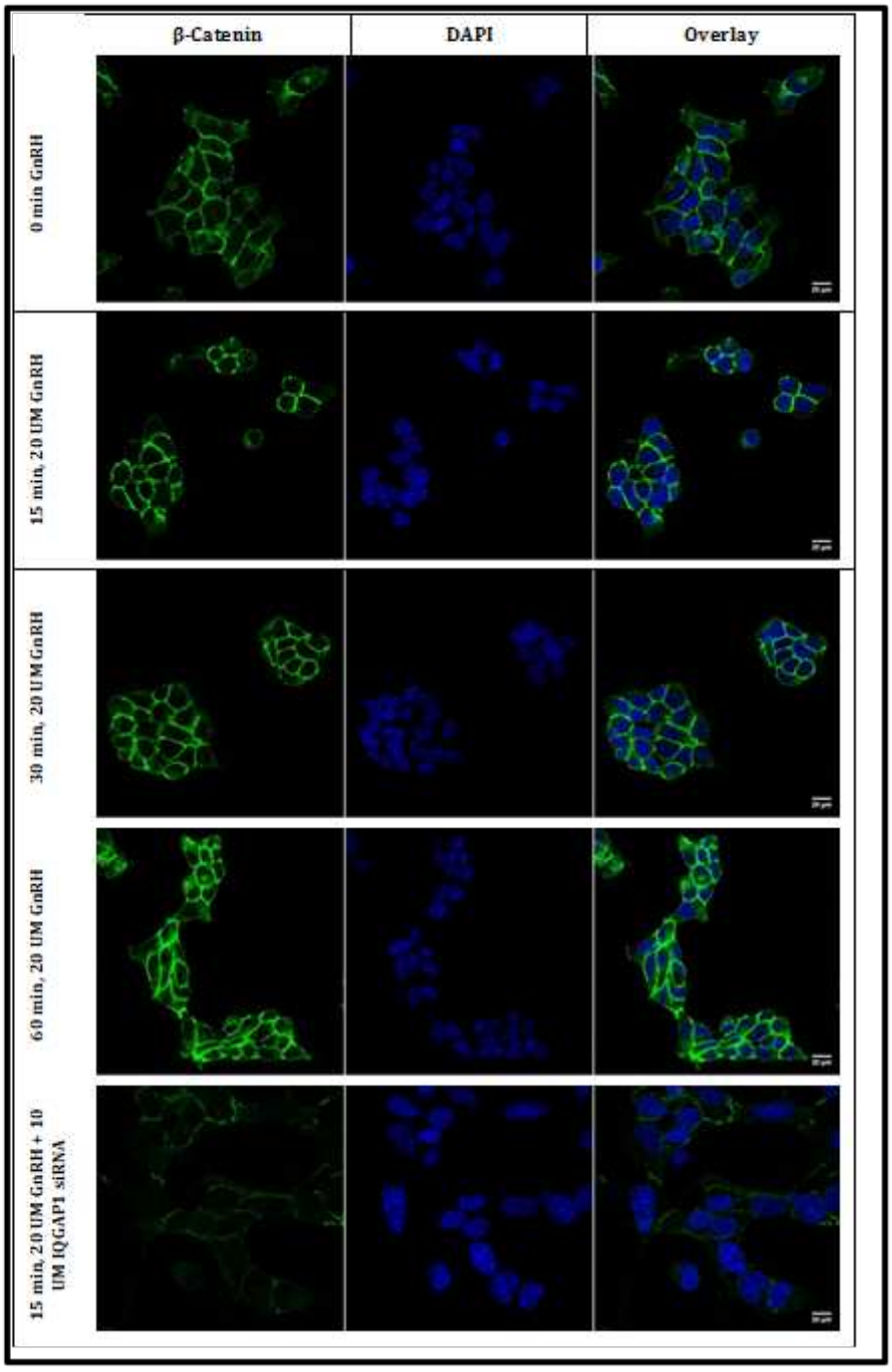
β-Catenin
DAPI
Overlay
0 min GnRH
15 min, 20 UM GnRH
30 min, 20 UM GnRH
60 min, 20 UM GnRH
15 min, 20 UM GnRH + 10 UM IQGAP1 siRNA

B

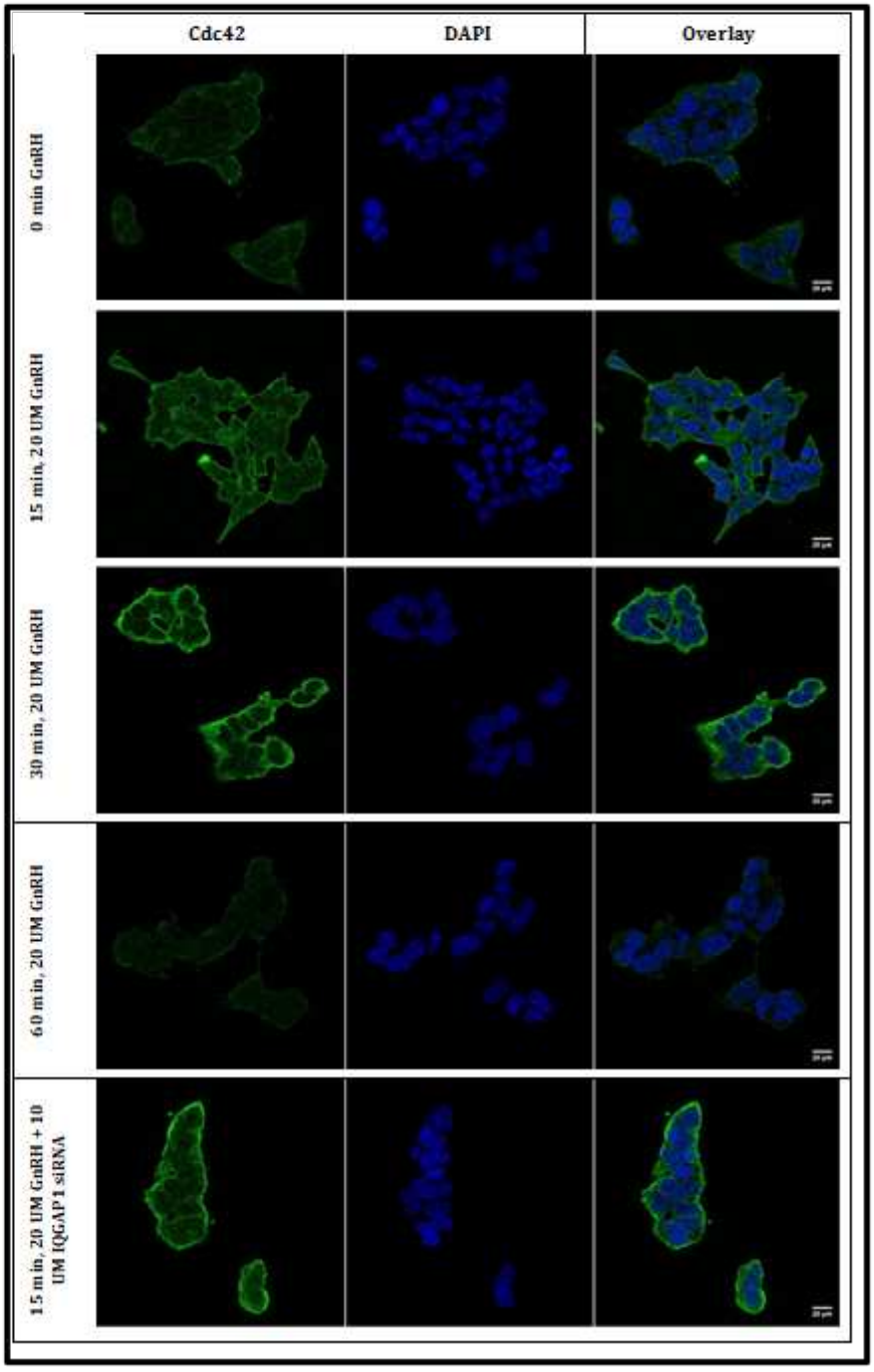
Cdc42
DAPI
Overlay
0 min GnRH
15 min, 20 UM GnRH
30 min, 20 UM GnRH
60 min, 20 UM GnRH
15 min, 20 UM GnRH + 10 UM IQGAP1 siRNA

C

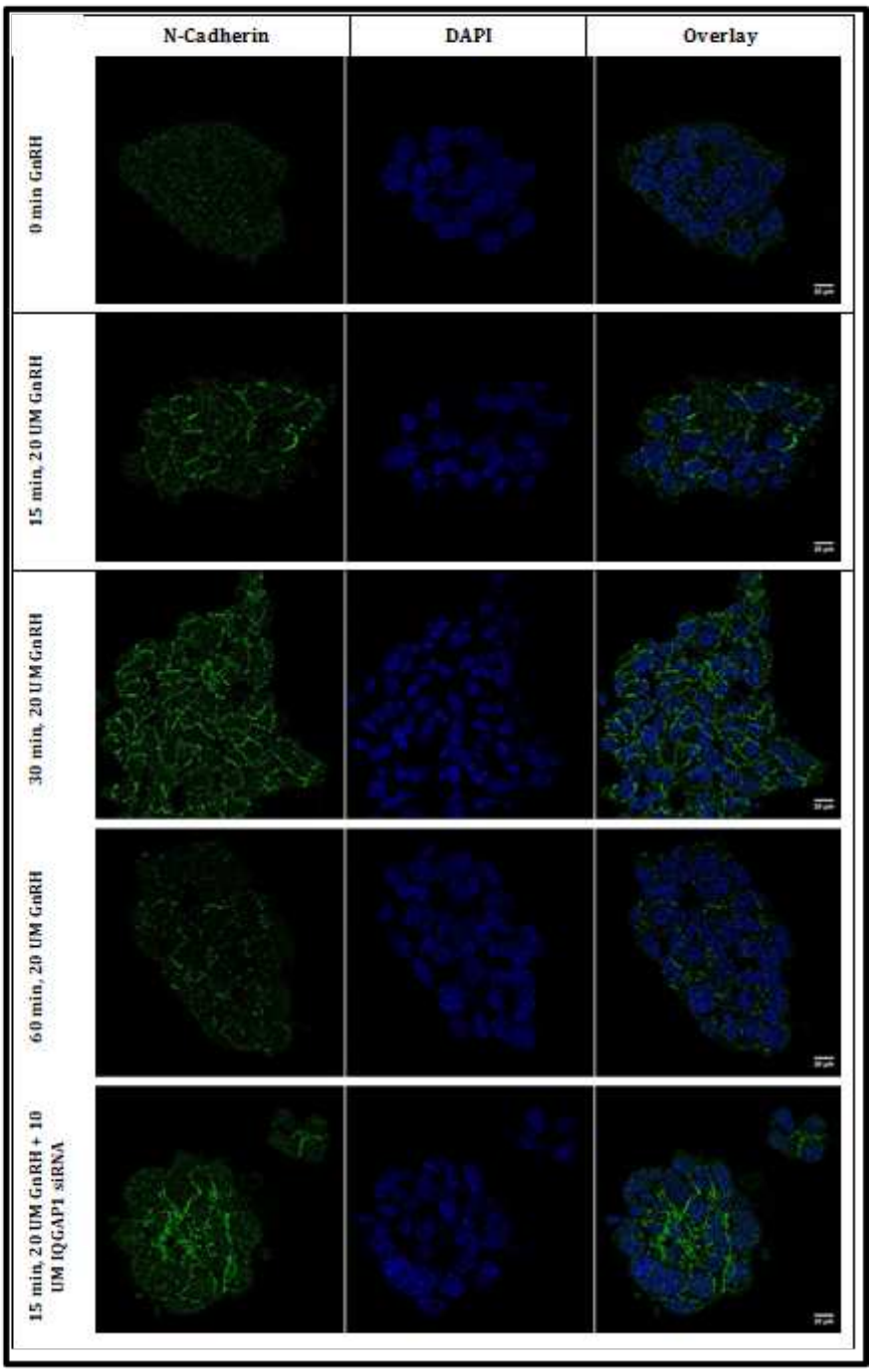

Fig. 4. 1: Representative confocal images of αT3-1 cells cultured in glass-bottom microwell dishes for 24 hrs. A group of cells were transfected with IQGAP1 pre-designed silencer siRNA for another 24 hrs. All cell groups were, then, incubated with either GnRH (10 nM) or water (control) for different time points (0 min, 15 min, 30 min, 60 min), fixed with 4% paraformaldehyde and permeabilized with 0.1% Triton. Dishes were sequentially stained with: A, Anti-β-Catenin antibody (1ug/ml) followed by Alexa Fluor 488-conjugated secondary antibody (2ug/ml), B, Anti-Cdc42 antibody (1ug/ml) followed by Alexa Fluor 488-conjugated secondary antibody (2ug/ml), and C, Anti-N-Cadherin antibody (1ug/ml) followed by Alexa Fluor 488-conjugated secondary antibody (2ug/ml). All cells were counterstained with DAPI to label nuclei and imaged under a 63x oil objective of a Zeiss LSM 800 confocal microscope.

To quantify the fluorescent intensity, we used the Flow Cytometry approach to evaluate this activation. We ran 250,000 events (cells) in triplicate for each sample using 96 well plate. Cells viability were measured using Ghost dye 510, and all dead cells were excluded, and the signal was measured in only live cells. Significantly, and indicating functional relevance, activation of GnRH receptor in αT3-1 gonadotropes increases the fluorescent intensity level of Anti- β-catenin -AF 594 conjugated antibody (Fig. 4. 2A), Anti-Rac1-AF 594 conjugated antibody (Fig. 4. 2B), Anti-Cdc42-AF 647 conjugated antibody (Fig. 4. 2C), Anti-E-Cadherin-AF 647 conjugated antibody (Fig. 4. 2E), and Anti-N-Cadherin-AF 790 conjugated antibody (Fig. 4. 2F).

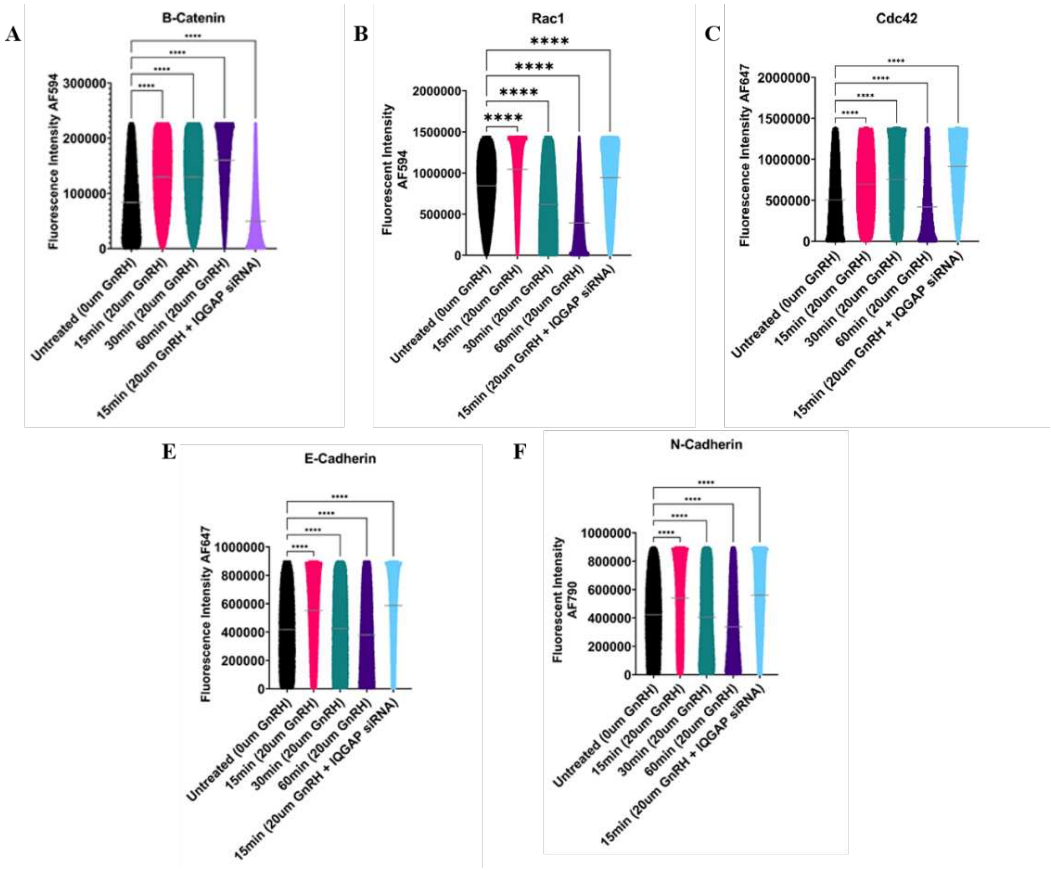

Fig. 4. 2: The florescent intensity level of A, Anti- β-catenin -AF 594 conjugated antibody (1ug/ml), B, Anti-Rac1-AF 594 conjugated antibody (1ug/ml), C, Anti-Cdc42-AF 647 conjugated antibody (1ug/ml), E. Anti-E-Cadherin-AF 647 conjugated antibody (1ug/ml), and F, Anti-N-Cadherin-AF 790 conjugated antibody (1ug/ml) in control and transfected αT3-1 gonadotropes with IQGAP1 pre-designed silencer siRNA, then, treated with 20 UM GnRH for different tie points (0, 15, 30 , 60 minutes), and prepared for the signal quantification through the Cytec Aurora Flow Cytometry system. Data was analyzed by FloJo software. Data shows a significant increase in the florescent intensity in response to GnRH.

Moreover, a further examination for the gene expression level of Rac1, Cdc42, and N-Cadherin was performed using RT-PCR in αT3-1 gonadotropes. RT-PCR data shows a significant increase in Rac1, Cdc42, and N-Cadherin expression level in response to GnRH receptor activation (Fig. 4. 3A, B, & C). Together, these data indicate the activation of signaling molecules to cell-cell junctions following GnRH receptor activation.

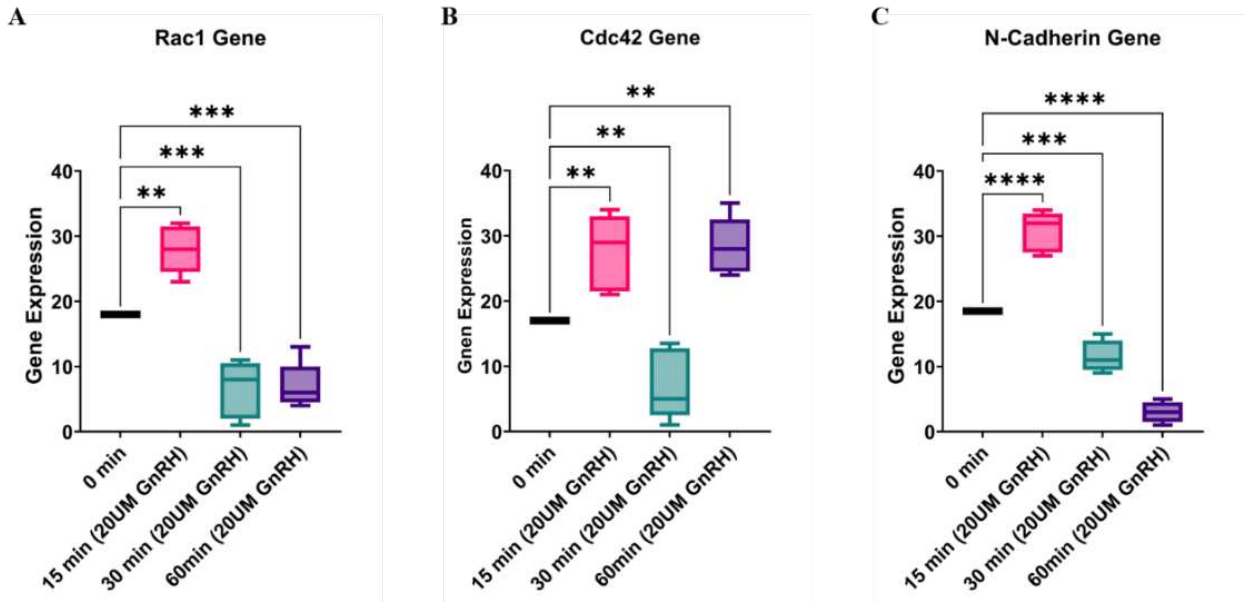

Fig. 4. 3: RT-PCR analysis showing the level of gene expression of target genes A, Rac1, B, Cdc42, and C, N-Cadherin in αT3-1 gonadotropes treated with GnRH for different time points, indicating a significant change in the expression level in response to GnRH.

IQGAP1 targets signaling molecules to cell-cell junctions following GnRH receptor activation

Overexpression of IQGAP1 (Kuroda et al., 1998b) and its translocation to sites of cell-cell contact (Li et al., 1999b) reduce the interaction between E-cadherin and the actin cytoskeleton, leading to weakening cell-cell attachment. Furthermore, in human endothelial cells, IQGAP1 co-localizes with VE-cadherin at sites of cell-cell contact, and knockdown of IQGAP1 using siRNA inhibits the localization of VE-cadherin at adherens junctions, as well as its phosphorylation through reactive oxygen species (Yamaoka-Tojo et al., 2006). Thus, in this specific objective, we investigated the role of IQGAP1 in mediating cell-cell junctions and influencing Junctional adhesion proteins in αT3-1 gonadotropes when

transfected with IQGAP1 Pre-designed silencer siRNA and treated with GnRH. Cells were maintained until they reached 80% confluency, then passaged into 6 well dish in low confluency allowing them to grow after the transfection for 48 hrs. After 2 hrs., cells were transfected with IQGAP1 pre-designed silencer siRNA, then, incubated for 48 hrs. in 5% Co2 and 37 temperature. After 2 hrs. of serum starving, cells were treated with 20 UM GnRH for different time points; then, proceeded for further preparations to perform immunocytochemistry, Flow Cytometry, and RT-PCR.

Our data shows a significant change following the GnRH receptor activation in transfected αT3-1 gonadotropes. We observed a greater increased signal accumulation using indirect immunocytochemistry combined to confocal microscopy in transfected αT3-1 gonadotropes stained with Anti-Cdc42 antibody, Anti-E-Cadherin antibody, and Anti-N-Cadherin antibody followed by Alexa Fluor secondary antibody staining (Fig. 4. 1B & C), whereas the level of Anti-β-Catenin antibody conjugated to Alexa Fluor secondary antibody shows a reduction in the signal accumulation (Fig. 4. 1A), indicating the effect of IQGAP1 knockdown that reflects the role that might IGAP1 play to regulate cell-cell junctions and influencing Junctional adhesion proteins in αT3-1 gonadotropes when treated with GnRH. This data comes compatible with the Flow Cytometry data that shows a significant increase in the level of the fluorescent intensity in transfected αT3-1 gonadotropes treated with 20 UM GnRH for 15 minutes and stained with Anti-Cdc42-AF 647 conjugated antibody, Anti-E-Cadherin-AF 647 conjugated antibody, Anti-N-Cadherin-AF 790 conjugated antibody (Fig. 4. 4B, E, & F). However, Anti- β-catenin-AF 594 conjugated antibody and Anti-Rac1-AF 594 conjugated antibody show a significant decrease in the level of the fluorescent intensity (Fig. 4. 4A & C) compared to control αT3-1 gonadotropes treated with 20 UM GnRH for 15 minutes.

In addition, the level of the expression of Rac1 and Cdc42 genes show a significant increase in transfected αT3-1 gonadotropes treated with 20 UM GnRH for 15 minutes (Fig. 4. 5A & B), while the expression level of N-Cadherin gene doesn't change significantly after treated the transfected cells with GnRH for 15 min (Fig. 4. 5C) However, the expression level of N-Cadherin genes changed significantly

in transfected αT3-1 gonadotropes treated with 20 UM GnRH for 30 and 60 minutes, as well as the expression level without GnRH treatment. These data suggest further level of regulation mediated by IQGAP1 as transcriptional effector that may control the activation of some genes involved in the signaling pathway of gonadotropes in response to GnRH.

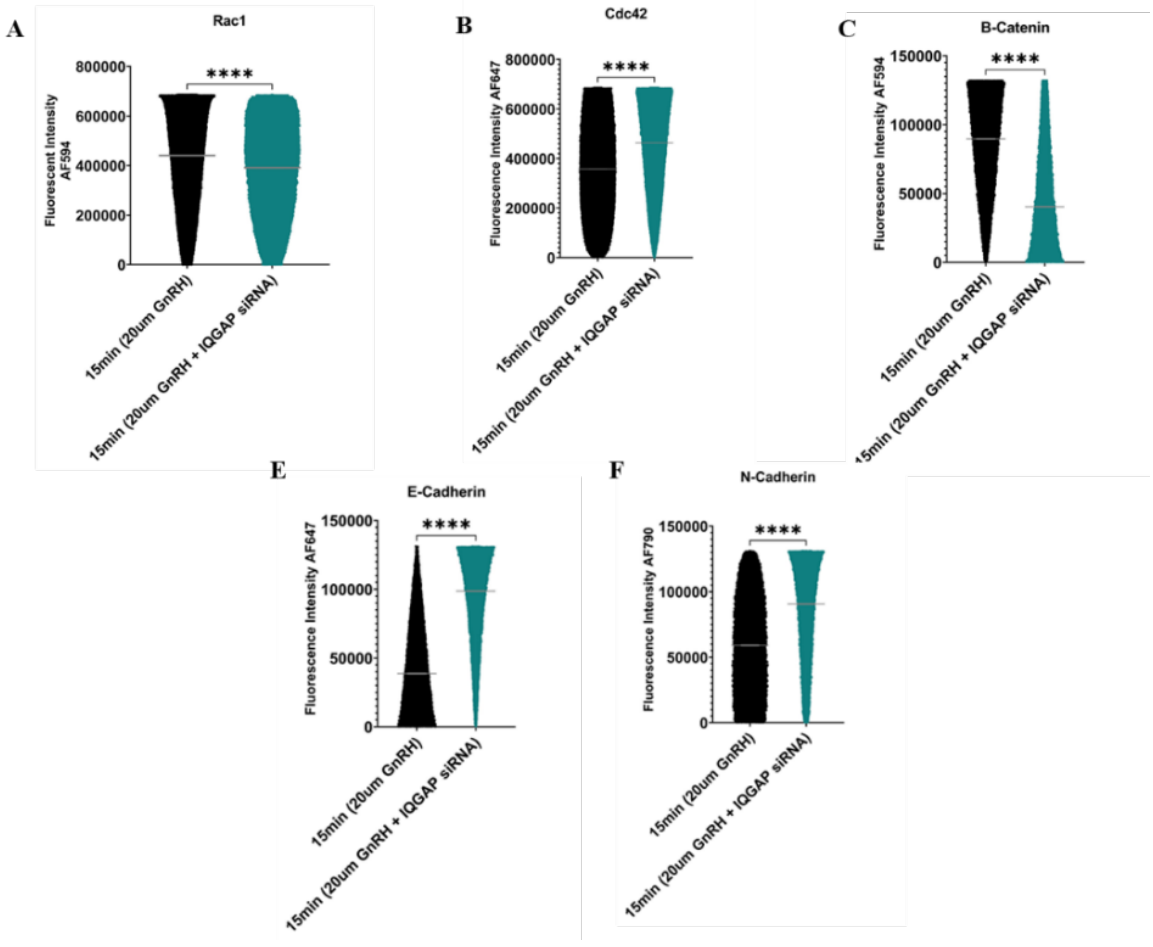

Fig. 4. 4: Flow Cytometry data indicating the level of the fluorescent intensity in transfected αT3-1 gonadotropes treated with 20 UM GnRH for 15 minutes and stained with A, Anti-Rac1-AF 594 conjugated antibody, B, Anti-Cdc42-AF 647 conjugated antibody, C, Anti- β-catenin-AF 594 conjugated antibody, E, Anti-E-Cadherin-AF 647 conjugated antibody, and F, Anti-N-Cadherin-AF 790 conjugated antibody.

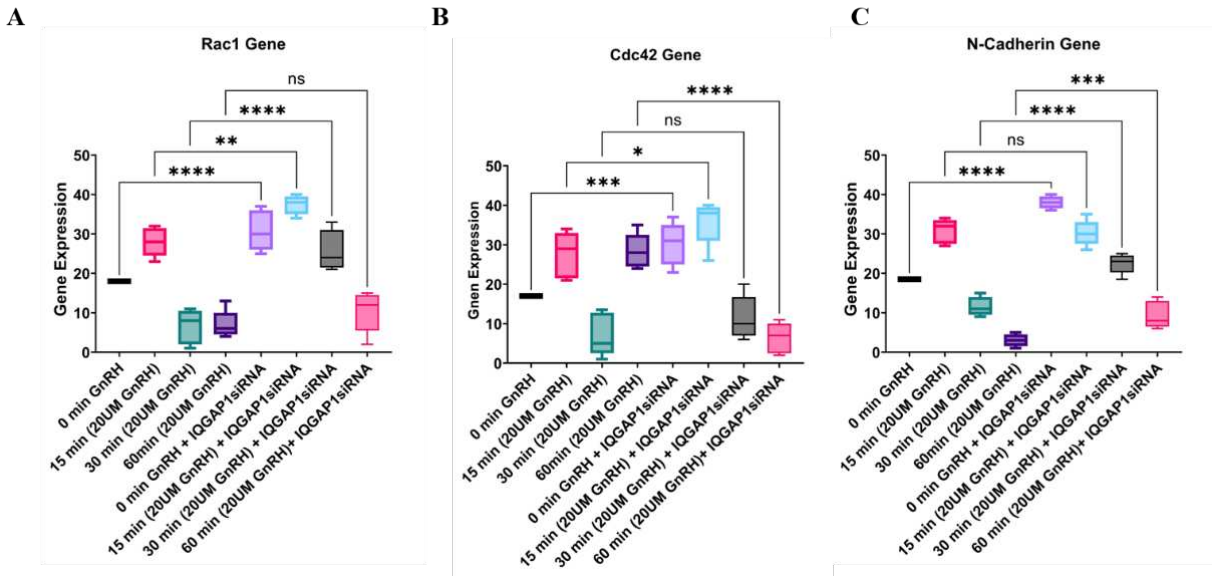

Fig. 4. 5: RT-PCR analysis showing the level of gene expression of target genes A, Rac1, B, Cdc42, and C, N-Cadherin in control and transfected αT3-1 gonadotropes using IQGAP1 pre-designed silencer siRNA and treated with GnRH for different time points. Data shows a significant change in the expression level in response to GnRH.

IQGAP1 promotes GnRH receptor-dependent cytoskeletal remodeling and cell mobility leading to functional interactions between gonadotropes

The actin cytoskeleton controls signaling and is essential for cell viability. Important functions for IQGAP1 have been identified in the regulation of cell adhesion, microtubule networks, and the actin cytoskeleton (Briggs and Sacks, 2003b; Mateer et al., 2003; Noritake et al., 2005). Over the last several years, it has been shown that IQGAP1 binds directly or in a complex with several other cytoskeleton-related proteins. IQGAP1 has been shown to interact with F-actin directly, controlling the assembly of actin meshwork (Boyer et al., 2011; Brill et al., 1996; Brown et al., 2007; Fukata et al., 2002a; Ho et al., 1999b; Mateer et al., 2002; Weissbach et al., 1998). In addition, IQGAP1 may interact with other proteins that have roles in reorganizing the cytoskeleton (Bielak-Zmijewska et al., 2008; Fukata et al., 2002a; Mateer et al., 2004). Cdc42 and Rac1 are among those mentioned (Bashour et al., 1997b; Fukata et al., 1997a; Hart et al., 1996), as well as APC (Tirnauer, 2004), CLIP-170 (Gundersen, 2002), Clasp2 (Watanabe et al., 2009), and EB1 (Zhang et al., 2009). Thus, we hypothesized that IQGAP1 mediates the cytoskeleton remodeling by regulating actin filament in the GnRH signaling pathway in gonadotropes.

We initiated our examination by directly observing the effects of IQGAP1 on actin filament barbed end growth using immunocytochemistry combined to confocal microscopy assays. Our confocal immunofluorescence data shows that 1X CellMask Green Actin Tracker signal increased in αT3-1 gonadotropes treated with 20 UM GnRH (Fig. 4. 6). The signal shows an accumulation at cell contacts, as well as colocalization with IQGAP1 in response to GnRH receptor activation. We further investigated the contribution of IQGAP1 in mediating the F-Actin network after the GnRH receptor activation by transfecting αT3-1 gonadotropes with IQGAP1 pre-designed silencer siRNA following with 15 minutes of GnRH treatment. Imaging using confocal microscopy, we noticed a reduction in cell extension when inhibited IQGAP1 activity, as well as a reduction in the signal (Fig. 4. 7A), indicating that IQGAP1, when sequestered in adhesions, enables regulation of F-actin involved in the generation of cell extensions.

In addition, we assessed the actin filament interaction when we treated αT3-1 gonadotropes with Nicardipine that shows high affinity for the dihydropyridine binding site (pKi = 9.7) and inhibits the L-type calcium ion channel as demonstrated by its ability to decrease the calcium ion-dependent action potential dose-dependently in ventricular papillary muscle (pIC50 = 7.15). We used GFP-UtrCH that can track the level of F-actin in αT3-1 gonadotropes in response to GnRH receptor activation. Data shows that GnRH-dependent cell junctions are enriched with actin and require L-type calcium channel function in gonadotropes (Fig. 4. 7B).

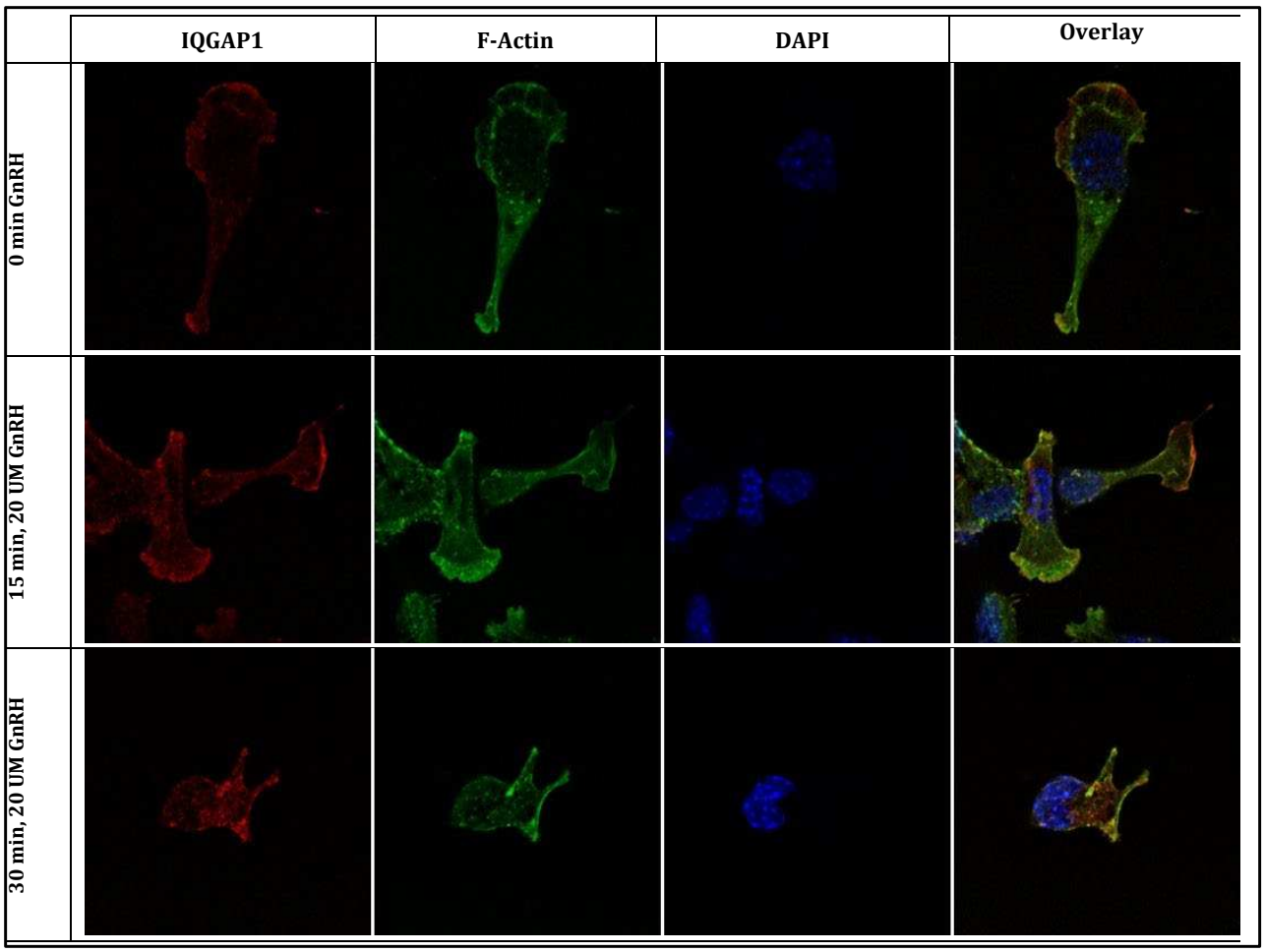

Fig. 4. 6: Representative confocal images of αT3-1 cells cultured in glass-bottom microwell dishes for 24 hrs., then, incubated with either GnRH (10 nM) or water (control) for different time points (0 min, 15 min, 30 min), fixed with 4% paraformaldehyde and permeabilized with 0.1% Triton. Dishes were sequentially stained first with Anti-IQGAP1 antibody (1ug/ml) followed by Alexa Fluor 586-conjugated secondary antibody (2ug/ml), then, stained with 1X CellMask Green Actin Tracker. All cells were counterstained with DAPI to label nuclei and imaged under a 63x oil objective of a Zeiss LSM 800 confocal microscope.

A

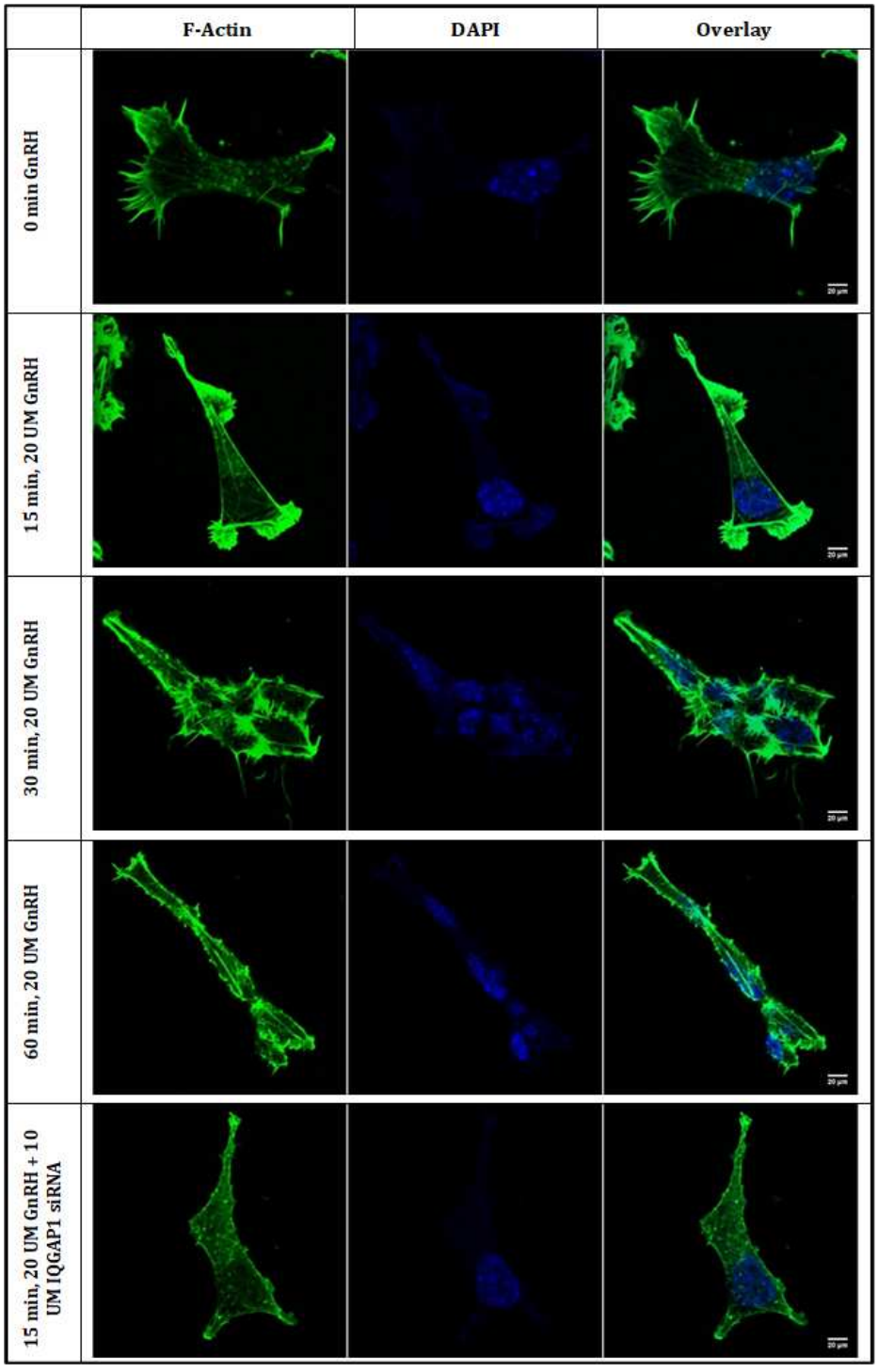
F-Actin
DAPI
Overlay
0 min GnRH
15 min, 20 UM GnRH
30 min, 20 UM GnRH
60 min, 20 UM GnRH
15 min, 20 UM GnRH + 10 UM IQGAP1 siRNA

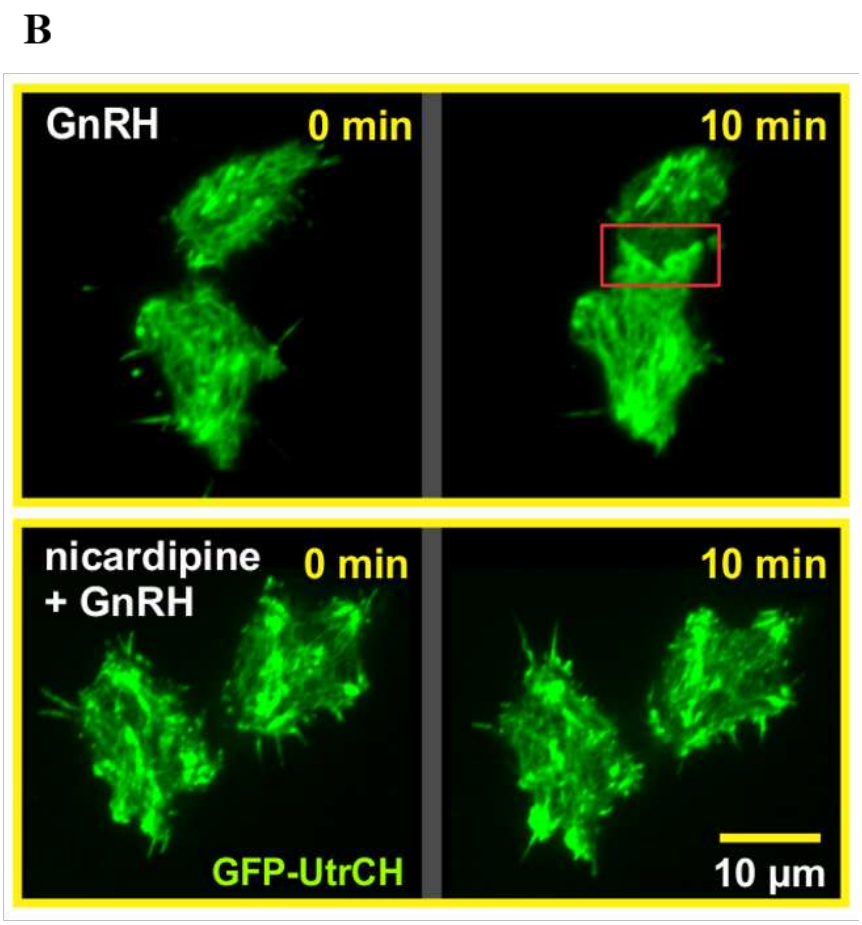

Fig. 4. 7: A, Representative confocal images of αT3-1 cells cultured in glass-bottom microwell dishes for 24 hrs., then, incubated with either GnRH (20 nM) or water (control) for different time points (0 min, 10 min, 15 min, 30 min), fixed with 4% paraformaldehyde and permeabilized with 0.1% Triton. Dishes were stained with1X CellMask Green Actin Tracker. B, TIRF images of control and transfected αT3-1 cells with GFP-UtrCH treated with GnRH. Cells were treated with nicardipine to investigate the role L-type calcium ion channel mediating the actin filaments interaction.

Gonadotropes respond to GnRH with an increase in phosphoinositide (PI), lead to a rise in the concentration of intracellular free Ca2+ and activation of protein kinase C (PKC) (Horn et al., 1991; Iida et al., 1991; Leong, 1991; Naor, 1990; Shangold et al., 1988). In a study using a rat, LH secretion is found not to require extracellular Ca2+ at the initial phase under GnRH stimulation, whereas the later phase does and is reduced when used dihydropyridine Ca2+ channel blockers (Chang et al., 1986). Furthermore, it has demonstrated that GnRH enhances voltage-gated Ca2+ currents (Naor, 2009), which may be mediated by a PKC-dependent mechanism in a gonadotrope cell line (Bosma and Hille, 1992). Importantly, in a study using pituitary gonadotropes, it has shown that treating cells with a GnRH-

antagonist analog led to abolishing spontaneous [Ca2+]i oscillations in pituitary gonadotrophs, as well as decreasing both basal and agonist-stimulated LH release. In addition, this led to converting the pulsatile pattern of endogenous GnRH release to a monotonic non-pulsatile profile (Martinez-Fuentes et al., 2004). Thus, Ca2+ signaling and cell junctions may serve as autocrine mechanisms that modulate cell signaling processes and functional interactions between gonadotropes. Many factors might regulate these mechanisms. Studying the role of IQGAP1 as mediator facilitating the interaction between gonadotropes may shed light on a new mechanism that may help understand the means of communication between gonadotropes.

Our data demonstrates that αT3-1 gonadotropes fired signals in response to GnRH when measuring GnRH-dependent GCaMP calcium transients, GCaMP6s-CAAX is Plasma membrane targeted GCaMP6s that is calcium sensor. Imaging cell surface was performed using TIRF microscopy (Fig. 4. 8A). Holding ROI location constant, intensity was measured for ROI 1&2 for each frame for ~60 frames or ~16 seconds. Observe, in the absence of GnRH two large whole cell calcium bursts constrained to a single cell (cell 2). Images represent the corresponding time in the scatter plot above. Below, images of same cells 1 and 2 at two different times, as indicated. Fluorescence was quantified as above except two ROIs (1 & 1', 2 & 2') for cells 1 and 2, respectively for each frame measured. Observe, after GnRH, both cells become equally active as indicated by the GCamp6s indicator and are synchronously oscillating. Collectively, this data suggests that Ca2+ - and cAMP - GnRH-dependent signaling may act as a mechanism providing the structural basis of interactions between gonadotropes.

Moreover, we investigated the IQGAP1role in Ca+ activity by applying another experiment using Fluo-3, AM, Ca+ indicator in αT3-1 gonadotropes treated with different concentration of GnRH (0. 20 UM, 50 UM, 100 UM) for 15-20 minutes. Cells were incubated in live cell imaging solution during the GnRH treatment, and for imaging step. Using confocal microscopy, we observed an increased signal between cells in response to GnRH, and this signal was increased when applied more GnRH concentration (Fig. 4. 8B). To further evaluate the regulatory role of IQGAP1 that may control the

activity of Ca+, we used IQGAP1 pre-designed silencer siRNA in αT3-1 gonadotropes, then, treated cells with 20 UM GnRH. In a comparison to the control, the transfected αT3-1 gonadotropes shows higher signal in response to GnRH receptor activation, indicating the role that IQGAP1 might have to control the Ca+ activation mediating the cell-junctions in gonadotropes.

A

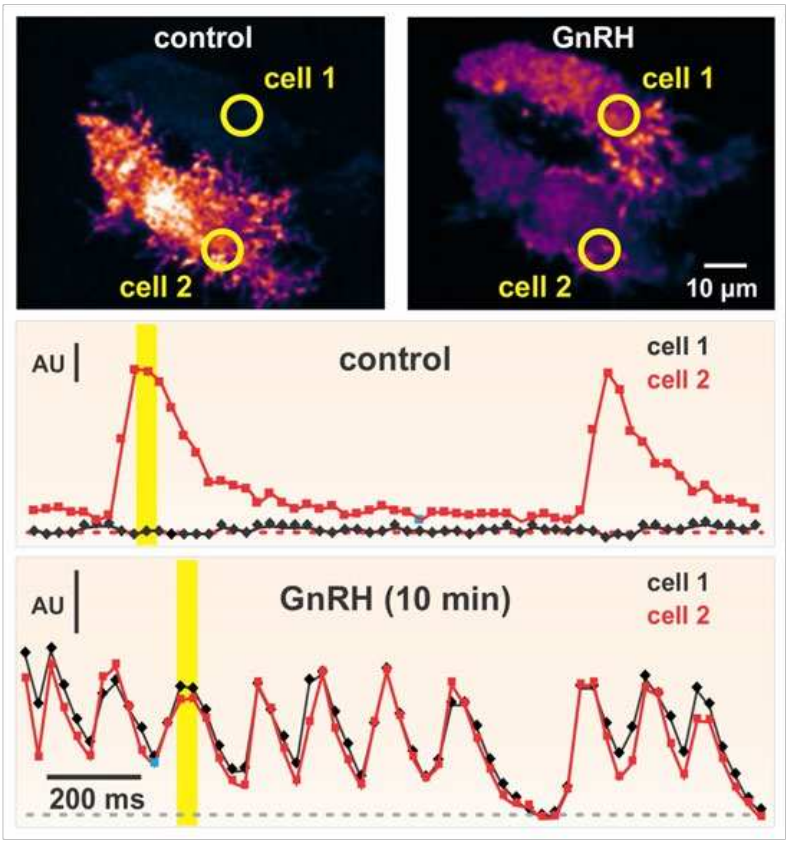

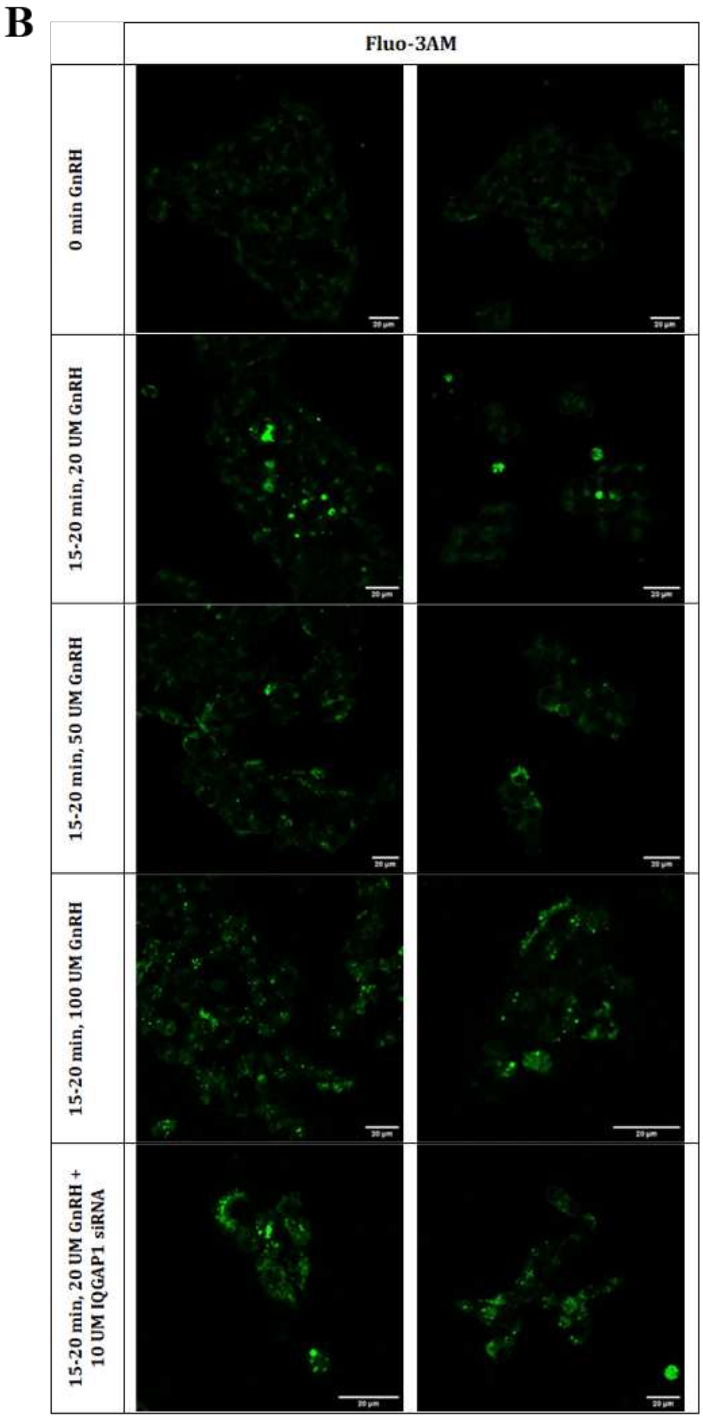

Fig. 4. 8: GnRH-dependent Ca activation in αT3-1 Gonadotropes. A, TIRF microscopy images show the relative intensity of Cell 1 & 2, ROI 1&2, respectively for unstimulated cells. B, Representative confocal images of αT3-1 cells cultured in glass-bottom microwell dishes for 24 hrs., then, the first group was incubated with either GnRH (0, 20, 50, 100 nM) or water (control) for 15-20 minutes. The second group was transfected with IQGAP1 pre-designed silencer siRNA before treating cells with 20 nM GnRH.

GnRH receptor-dependent gene expression in αT3-1 and LβT2 gonadotropes

IQGAP1 has been reported to have a regulatory role in certain nuclear events. It has shown that IQGAP1 associates nuclear-cytoplasmic shuttling proteins, including β-catenin and ERK, and participates in the MEK/ERK cascade, which leads to Elk-1-mediated transcription activation (Bourguignon et al., 2005; Roy et al., 2004). It also has been reported that IQGAP1 may also trigger nuclear localization and signaling of β-catenin (Briggs et al., 2002a; Wang et al., 2008). Furthermore, it has shown that many IQGAP1 binding partners, including actin (Hofmann, 2009), Rac1 (Michaelson et al., 2008), N-WASp (Yoo et al., 2007), and APC (Brocardo and Henderson, 2008), have been linked to nuclear functions. Moreover, in nuclei of murine oocytes and cleaving embryos, IQGAP1 has been found to envelop nucleoli (Bielak-Zmijewska et al., 2008), indicating that IQGAP1 has possible nuclear functions.

In a study using microarray in the LβT2 cell line, the immediate early genes respond to GnRH stimulation. The response reveals a significant upregulation of 28 immediate-early genes within 60 minutes of GnRH stimulation (Roberson et al., 1999). We stated our investigation by directly evaluating the expression level of immediate early genes including Egr1, Atf3, and Jun in αT3-1 gonadotropes in response to GnRH using RT-PCR approach. The data analysis shows that the expression of these genes peak after 15 min of 20 UM GnRH treatment (Fig. 4. 9A, B, & C). We further investigated gonadotrope gene expression in response to GnRH receptor using LβT2 murine gonadotrope derived cell line expresses the β subunits of LH and FSH (Aoki and Taketo, 2007) to study the response of the tertiary genes to GnRH stimulation including Lhb, Cga, Fshb, and Gnrhr. Parallel experiments were applied to evaluate the level of the expression for these genes using RT-PCR. We found that LHb expression shows a significant upregulation after 15 min treatment with 20 UM GnRH (Fig. 4. 10A). However, following this increase, LHb expression drops after 30 and 60 min of GnRH treatment in LβT2 gonadotropes. On the other hand, FSHb expression peaks after 15 min of 20 UM GnRH treatment and continues upregulated for the following 30 and 60 min in response to GnRH (Fig. 4. 10B). Collectively, this data

provides a validation of GnRH receptor-dependent gene expression activation in αT3-1 and LβT2 gonadotropes.

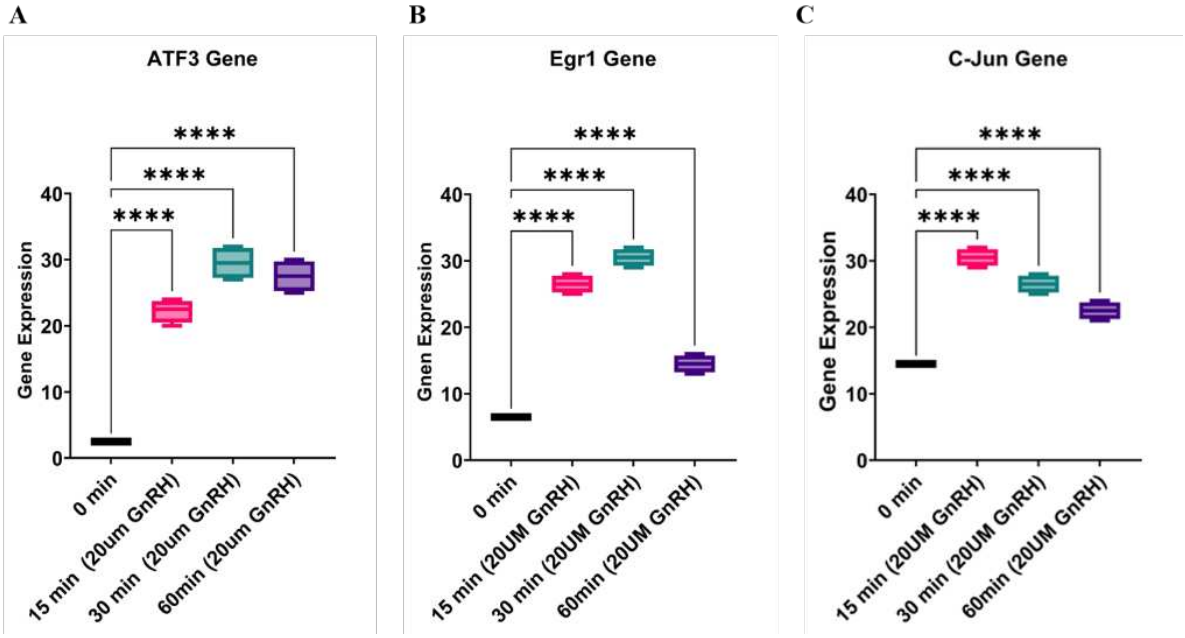

Fig. 4. 9: RT-PCR analysis showing the level of immediate early genes including A, Atf3, B, Egr1, and C, C-Jun in αT3-1 gonadotropes treated with GnRH for different time points, indicating a significant change in the expression level in response to GnRH.

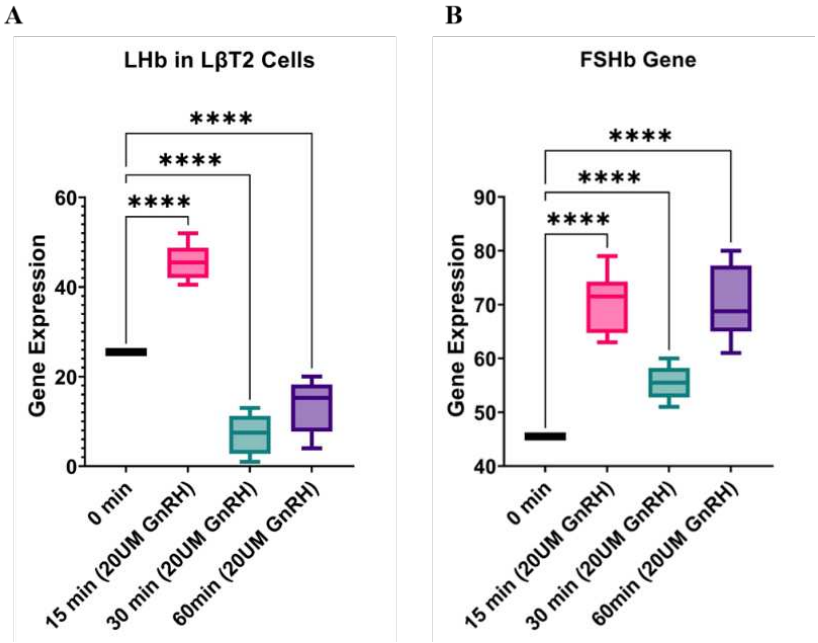

Fig. 4. 10: RT-PCR analysis showing the level of tertiary genes A, LHb, B, FSHb in LβT2 gonadotropes treated with GnRH for different time points, indicating a significant change in the expression level in response to GnRH.

IQGAP1 contributes to GnRH receptor-dependent regulation of gonadotropin gene expression and hormone secretion

To in investigate the correlation between adherens junction proteins (e.g., IQGAP1) and gonadotrope gene expression. Using RT-PCR, we transfected αT3-1 gonadotropes using IQGAP1pre-designed silencer siRNA, then, we evaluated the gene expression level for the immediate early genes, Atf3, Egr1, and C-Jun, that are shown to be significantly downregulated within 15 minutes of GnRH exposure when compared to control, which may indicate the role of IQGAP1 as a transcriptional regulator of the immediate early genes (Fig. 4. 11A, B, & C). In parallel experiments using RT-PCR, LHb expression level shows a constant significant increase in transfected LβT2 gonadotropes during the different time points of GnRH treatment (Fig. 4. 12A). Whereas, FSHb expression level shows a constant significant reduction compared to the control LβT2 gonadotropes after GnRH treatment for different time points (Fig. 4. 12A). Our findings indicate the transcriptional regulation of IQGAP1 in gonadotropes in response to GnRH.

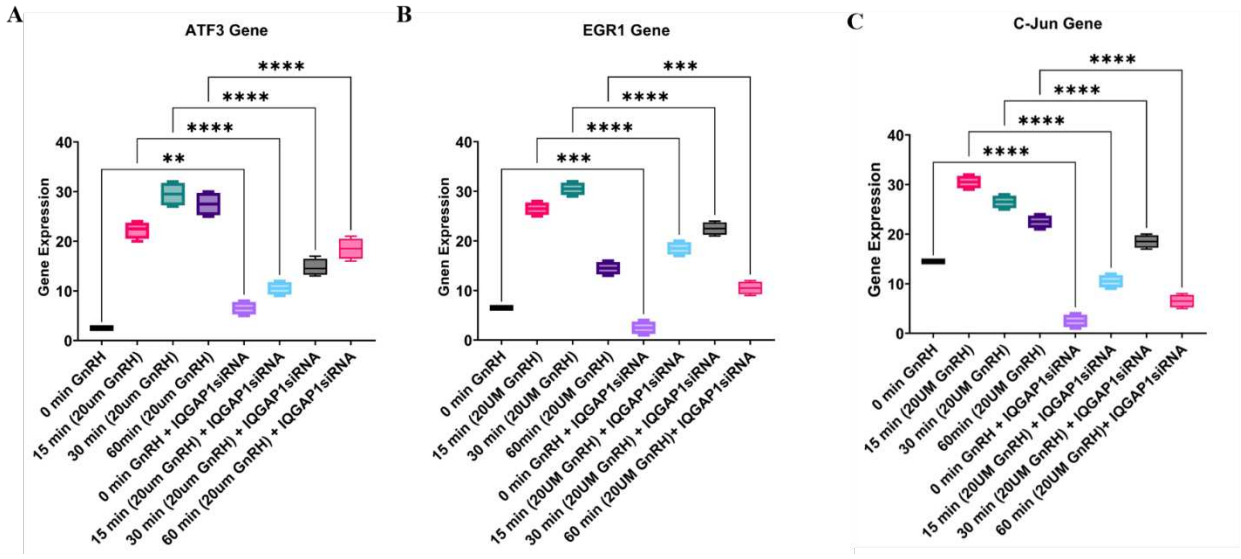

Fig. 4. 11: RT-PCR analysis showing the level of immediate early genes including A, Atf3, B, Egr1, and C, C-Jun in control and transfected αT3-1 gonadotropes using IQGAP1 pre-designed silencer siRNA and treated with GnRH for different time points, indicating a significant change in the expression level in response to GnRH and IQGAP1 inhibition.

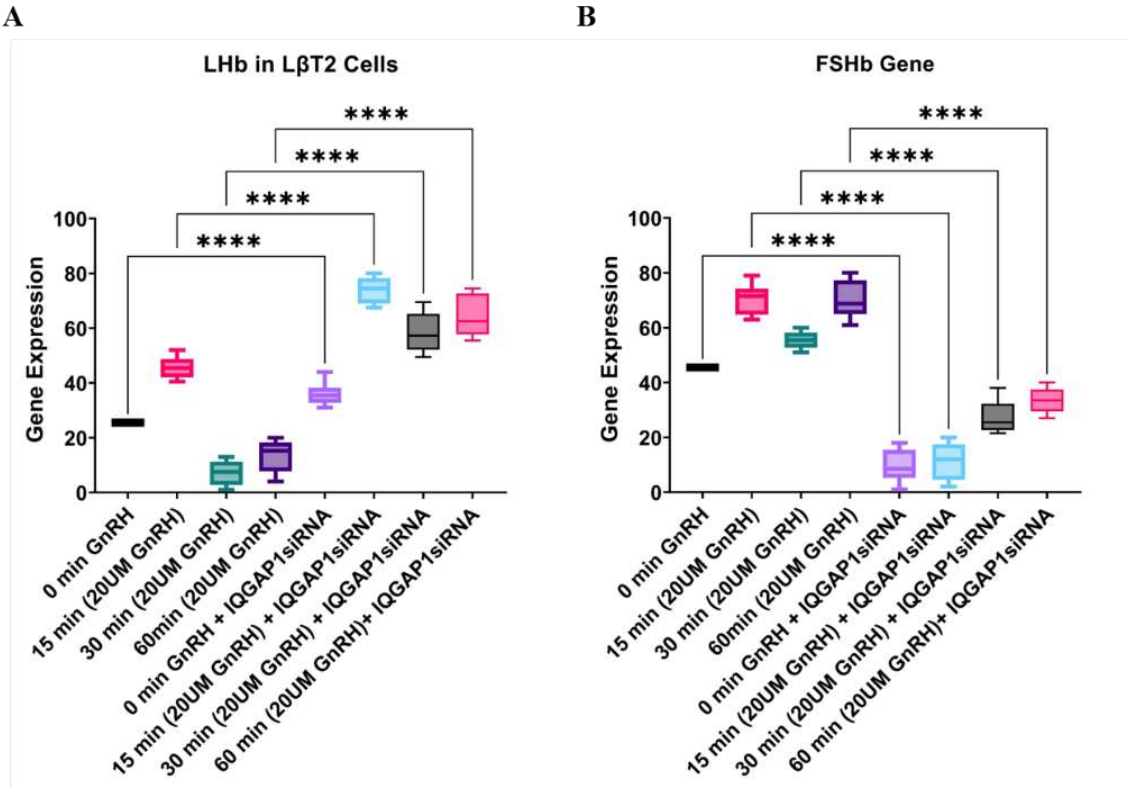

Fig. 4. 12: RT-PCR analysis showing the level of tertiary genes A, LHb, B, FSHb in control and transfected LβT2 gonadotropes using IQGAP1 pre-designed silencer siRNA and treated with GnRH for different time points, indicating a significant change in the expression level in response to GnRH and IQGAP1 inhibition.

Discussion

The reproductive system is regulated by the neurohormone GnRH, which is produced in the hypothalamus. This hormone activates the heptahelical transmembrane GnRH receptor, which is found on the surface of pituitary gonadotrope cells. Activation of GnRH receptor causes the production and release of the two gonadotropin hormones, luteinizing hormone (LH) and follicle-stimulating hormone (FSH). These hormones are responsible for regulating gametogenesis and steroidogenesis in the gonads. GnRH receptor is accountable for activating a complicated signaling network that includes many pathways, most notably calcium and cyclic AMP (cAMP). GnRH receptor is primarily connected to phospholipase C through Gq/11, which results in an immediate rise in intracellular calcium concentrations and the

activation of a number of different PKC isoforms (Naor, 2009). Either directly or indirectly, PKC controls gene transcription by activating the MAPK cascade. GnRH's recruitment of the cAMP/PKA pathway contributes, in addition, to the control of a select group of genes' expression, one of which is Gnrhr (Avet et al., 2013; Cohen-Tannoudji et al., 2012).

G-protein-coupled receptors (GPCR) engage in interactions with GPCR interacting proteins (GIP), which in turn regulate signal transmission from receptor to G proteins, receptor trafficking between plasma membrane and intracellular compartments, or subcellular localization (Bockaert et al., 2004; Sato et al., 2006). In our data, the proteomic screen of αT3-1 gonadotrope revealed GnRH-responsive PCP and cell-cell adhesion associated proteins as potential candidates involved with communication between gonadotropes. We investigated the role of PTK7 and IQGAP1 in GnRH-dependent transcellular gonadotrope communication. We also included an examination of β-catenin, a multifunctional PCP protein associated with cell junctions that interacts with PTK7 and IQGAP1, as well as other different cascades (Golubkov and Strongin, 2014; Goto et al., 2013a; Hu et al., 2019; Lichtig et al., 2019; Smith et al., 2015). Our data provides evidence of the involvement of IQGAP1 and PTK7 proteins as components mediating cell-cell contacts, as well as other cascades activated in response to GnRH in gonadotropes. Therefore, in this work, we broaden our investigation to include IQGAP1's participation in regulating several distinct proteins belonging to a variety of classes. These proteins connect the cytoskeleton to the plasma membrane and the extracellular matrix to create complexes that mediate cell communication along a variety of signaling pathways. In our case, GnRH signaling pathway in gonadotropes. These proteins activate signal transduction cascades, which in turn drive the essential cytoskeletal rearrangements for cellular activities such as changing shape and movement (Ridley et al., 2003; Vicente-Manzanares and Horwitz, 2011). The endocytic uptake and recycling of components of these complexes, notably the integrin molecules that bind their extracellular matrix ligands to the actin cytoskeleton (De Franceschi et al., 2015), is considered to be the most essential step in this process. These events are regulated by the Rho-GTPase signaling cascades and their many effectors (Hanna and El-Sibai, 2013), which in turn are activated by families

of small GTPases (ARFs, Rabs, etc.), their regulators, GAPs (GTPase-activating proteins), and GEFs (guanine exchange factors (Cherfils and Zeghouf, 2013). Our study focuses on studying Rac1, Cdc42, E-Cadherin, N-Cadherin, β-Catenin, F-Actin, and Ca+2 level in gonadotropes treated with GnRH. Rac1, Cdec4, and β-Catenin were shown in our proteomic screen of αT3-1 gonadotrope among the GnRH-responsive PCP and cell-cell adhesion associated proteins, considering them potential candidates involved with communication between gonadotropes. Our data shows an upstream activation of these components in response to GnRH. This activation is influenced by the inhibition of IQGAP1. Moreover, our data provides a validation of GnRH receptor-dependent gene expression activation in αT3-1 and LβT2 gonadotropes. We also observed changes in the gene expression level following IQGAP1 knockdown in gonadotropes. Together, our data shed the light on the contribution of IQGAP1 in the functional interactions between gonadotropes and their production following GnRH receptor activation.

IQGAP1's multiple domains allow the interaction with many different signaling and structural proteins, including actin, calmodulin, members of the Rho GTPase family (such as Rac1 and Cdc42), -catenin, and parts of the phosphoinositide 3-kinase (PI3K) /AKT pathway, and adenomatous poly-posis coli (Choi et al., 2016; Hedman et al., 2015). IQGAP1 controls a wide variety of cellular functions through binding to a wide variety of other proteins. These functions include cytoskeletal organization, cell-cell adhesion, cell motility, transcription, and signal transduction (Hedman et al., 2015; Smith et al., 2015).

Activated CDC42 and RAC1 are responsible for modulating actin filament rearrangement, which is important for a wide variety of biological activities, including cell polarity, cell adhesion, the production of lamellipodia and filopodia, as well as cell migration (Nobes and Hall, 1999; Ridley, 2015). For the proper regulation of IQGAP's functions, RAC1 and CDC42 (Briggs and Sacks, 2003a; Brown and Sacks, 2006; Watanabe et al., 2015) are important components. It has been established that RAC1 and CDC42 promote the action of IQGAP1 in intercellular adhesion sites in epithelial cells, in actin-crosslinking, and in defining its subcellular location. These three processes all take place in

epithelial cells (Kuroda et al., 1996; Watanabe et al., 2015). It has been shown that overexpression of IQGAP1 in epithelial cells causes a reduction in E-cadherin-mediated cell-cell adhesion. This occurs because IQGAP1 interacts with b-catenin, which in turn causes a-catenin to become detached from the cadherin-catenin complex. IQGAP1 is found in the places where cells are in touch with one another (Kuroda et al., 1998b). Positive regulation of E-cadherin-mediated cell-cell adhesion may be achieved by active versions of RAC1 and CDC42 via the inhibition of the interaction between IQGAP1 and b-catenin (Noritake et al., 2005). Increased levels of active RAC1 and CDC42 crosslink actin filaments via an interaction with IQGAP1. Strong adhesion occurs because IQGAP1 is prevented from binding b-catenin and thereby dissociating a-catenin from the cadherin-catenin complex. However, poor adhesion is caused by an increase in GDP-bound inactive RAC1/CDC42, which causes the release of IQGAP1 from RAC1/CDC42 and subsequent interactions with b-catenin to detach a-catenin from the cadherin-catenin complex.

The actin filament-binding protein IQGAP1 has also been demonstrated to crosslink actin filaments (Bashour et al., 1997b). IQGAP1 dimerization and/or oligomerization is required for this crosslinking capacity (Fukata et al., 1997a). Active CDC42 and RAC1 have been demonstrated to bind and promote IQGAP1 dimerization and oligomerization (Fukata et al., 1997a; LeCour et al., 2016b). Through its N-terminal CHD, IQGAP1 attaches to actin filaments in a direct manner. Multiple CHDs are used by the IQGAP1 dimer or IQGAP1 oligomer mediated by CDC42 and RAC1 to crosslink and bundle actin filaments.

Although it was first considered that IQGAP1's association with RHO proteins only served to modulate the cytoskeletal architecture, it is now obvious that they have crucial physiological functions outside the cytoskeleton (Hedman et al., 2015). IQGAP1 is widely distributed in neurons, including at the growth cone, along neuritis, in the growing axon, and at the axon initial segment (Li et al., 2005b). IQGAP1 has been found to interact with protein-tyrosine phosphatase PTPm, which is required for neurite outgrowth in ganglion cells. PTPm interacts with IQGAP1, N-cadherin, E-cadherin, and b-catenin to create a complex (Phillips-Mason et al., 2006). Through its association with IQGAP1, active

GTP-bound CDC42 stimulates actin remodeling and, ultimately, neurite outgrowth by encouraging PTPm to engage with IQGAP1 (Hedman et al., 2015; Li et al., 2005b).

Additionally, IQGAP1 binds to E-cadherin and modulates its activity (Noritake et al., 2005). Reduced E-cadherin interaction with the actin cytoskeleton results from overexpression of IQGAP1 (Kuroda et al., 1998b) and subsequent translocation to cell-cell contact sites (Li et al., 1999b). There is mounting evidence that IQGAP1 binds to and controls the activity of cadherins besides calmodulin. Memory formation is linked to synaptic remodeling, which may be facilitated by IQGAP1's binding to neuronal- (N-) cadherin in a complex with ERK (Schrick et al., 2007). Furthermore, IQGAP1 colocalizes with VE-cadherin at sites of cell-cell contact in human endothelial cells; knockdown of IQGAP1 with siRNA decreases localization of VE-cadherin at adherens junctions and its phosphorylation by reactive oxygen species (Yamaoka-Tojo et al., 2006). VE-cadherin has been demonstrated to form a ternary complex with β-catenin, which in turn binds to α-catenin. Later, α-catenin contributes to cross-linking actin and establishing a firm connection between neighboring cells (García-Ponce et al., 2015; Mateer et al., 2003; Meng and Takeichi, 2009; Pokutta et al., 2008). Permeability-increasing drugs target the VE-cadherin-catenin complex because of its crucial function in vascular permeability in endothelial cells (Angst et al., 2001). After vascular damage, during angiogenesis or chronic inflammatory disease, IQGAP1 expression is greatly enhanced in the endothelial cell layers, where it inhibits cell-cell adhesion mediated by the cadherin-catenin complex (Kuroda et al., 1998b). These two processes have been linked to IQGAP1, suggesting its role in the angiogenesis of capillary tube creation (Urao et al., 2010).

Together, previous studies in a compatible with our data suggest that IQGAP1 may function as a molecular scaffold, integrating and linking various cytoskeletal components; it also has the potential to combine with cell signal transduction molecules, forming the complex signal transduction cellular network in gonadotropes. Our examination using αT3-1 gonadotropes with additional evaluation of Rac1 and β-Catenin activity, as well as the interaction of Cdc42, E-Cadherin, and N-Cadherin in gonadotropes in response to GnRH shows a significant upstream activation and

association of Rac1, Cdc42, E-Cadherin, N-Cadherin, and β-catenin in response to GnRH. Our indirect immunocytochemistry combined with confocal microscopy data shows redistribution of these proteins, especially, at the cell-cell adhesion positions where the signal shows more accumulation using primary antibodies conjugated to Alexa Fluor fluorescence secondary antibodies in αT3-1 gonadotropes in response to 20 UM GnRH (Fig. 4. 1A, B, & C). The quantitative data using flow cytometry shwos a compatible analysis with the immunofluorescence data. Significantly, and indicating functional relevance, activation of GnRH receptor in αT3-1 gonadotropes increases the fluorescent intensity level of Anti- β-catenin -AF 594 conjugated antibody (Fig. 4. 2A), Anti-Rac1-AF 594 conjugated antibody (Fig. 4. 2B), Anti-Cdc42-AF 647 conjugated antibody (Fig. 3. 2C), Anti-E-Cadherin-AF 647 conjugated antibody (Fig. 4. 2E), and Anti-N-Cadherin-AF 790 conjugated antibody (Fig. 4. 2F). Further examination using RT-PCR, data shows a significant increase in Rac1, Cdc42, and N-Cadherin expression level in response to GnRH receptor activation (Fig. 4. 3A, B, & C). Together, these data indicate the activation of signaling molecules to cell-cell junctions following GnRH receptor activation. Our data also shows a significant change following the GnRH receptor activation in transfected αT3-1 gonadotropes. IQGAP1 inhibition using pre-design silencer siRNA triggers a greater increased signal accumulation using indirect immunocytochemistry combined to confocal microscopy in transfected αT3-1 gonadotropes stained with Anti-Cdc42 antibody, Anti-E-Cadherin antibody, and Anti-N-Cadherin antibody followed by Alexa Fluor secondary antibody staining (Fig. 4. 1B & C), whereas the level of Anti-β-Catenin antibody conjugated to Alexa Fluor secondary antibody shows a reduction in the signal accumulation (Fig. 4. 1A), indicating the effect of IQGAP1 knockdown that reflects the role that might IGAP1 play to regulate cell-cell junctions and influencing Junctional adhesion proteins in αT3-1 gonadotropes when treated with GnRH. This data comes compatible with the Flow Cytometry data that shows a significant increase in the level of the fluorescent intensity in transfected αT3-1 gonadotropes treated with 20 UM GnRH for 15 minutes and stained with Anti-Cdc42-AF 647 conjugated antibody, Anti-E-Cadherin-AF 647 conjugated antibody, Anti-N-Cadherin-AF 790 conjugated antibody (Fig. 4. 4B, E, & F). However, Anti- β-catenin-AF 594

conjugated antibody and Anti-Rac1-AF 594 conjugated antibody show a significant decrease in the level of the fluorescent intensity (Fig. 4. 4A & C) compared to control αT3-1 gonadotropes treated with 20 UM GnRH for 15 minutes. In addition, the level of the expression of Rac1 and Cdc42 genes show a significant increase in transfected αT3-1 gonadotropes treated with 20 UM GnRH for 15 minutes (Fig. 4. 5A & B), while the expression level of N-Cadherin gene doesn't change significantly after treated the transfected cells with GnRH for 15 min (Fig. 4. 5C) However, the expression level of N-Cadherin genes changed significantly in transfected αT3-1 gonadotropes treated with 20 UM GnRH for 30 and 60 minutes, as well as the expression level without GnRH treatment. These data suggest further level of regulation mediated by IQGAP1 as transcriptional effector that may control the activation of some genes involved in the signaling pathway of gonadotropes in response to GnRH.

Our confocal immunofluorescence data also shows that 1X CellMask Green Actin Tracker signal increased in αT3-1 gonadotropes treated with 20 UM GnRH (Fig. 4. 6). The signal shows an accumulation at cell contacts, as well as colocalization with IQGAP1 in response to GnRH receptor activation. However, the analysis exhibits a reduction in cell extension when IQGAP1 activity was inhibited, as well as a reduction in the signal (Fig. 4. 7A), indicating that IQGAP1, when sequestered in adhesions, enables regulation of F-actin involved in the generation of cell extensions. In addition, data shows that GnRH-dependent cell junctions are enriched with actin and require L-type calcium channel function in gonadotropes (Fig. 4. 7B).

In gonadotropes, GnRH receptor activation produces two distinct intracellular Ca2+ signals: Ca2+ release from the endoplasmic reticulum (ER) through inositol-1,4,5-trisphosphate (IP3) receptors and Ca2+ influx through the plasma membrane via L-type Ca2+ channels (Grosse et al., 2000b). These two Ca2+ signals increase mitogen-activated protein (MAP) kinase signaling (Mulvaney and Roberson, 2000; Mulvaney et al., 1999). Specifically, Ca2+ release from the ER promotes c-Jun N-terminal kinase (JNK) activity, which increases in FSH expression, while Ca2+ influx through L-type Ca2+ channels promotes extracellular signal-regulated kinase (ERK) activity, which increases LH expression (Mulvaney

and Roberson, 2000; Mulvaney et al., 1999). Our data demonstrates that αT3-1 gonadotropes fired signals in response to GnRH when measuring GnRH-dependent GCaMP calcium transients using GCaMP6s-CAAX (Fig. 4. 8A), suggesting that Ca2+ - and cAMP - GnRH-dependent signaling may act as a mechanism providing the structural basis of interactions between gonadotropes. Moreover, our confocal analysis shows an increase in the signal of Fluo-3, AM, Ca+ indicator in αT3-1 gonadotropes treated with GnRH, and this signal shows a cumulative increase when apply more GnRH concentration (Fig. 4. 8B). In a comparison to the control, the IQGAP1 knockdown triggers higher signal in response to GnRH receptor activation in transfected αT3-1 gonadotropes, indicating the role that IQGAP1 might have to control the Ca+ activation mediating the cell-junctions in gonadotropes.

The expression of *Cga*, *Lhb*, and *Fshb* genes is essential for the synthesis of LH and FSH. Cga encodes a general α-subunit for all hormones, while Lhb and Fshb encode hormone-specific β-subunits. GnRH controls LH and FSH synthesis mainly at the transcriptional level (Gharib et al., 1990; Jorgensen et al., 2004). Transduction of the transcriptional signal occurs when GnRH binds to its receptor, and several kinase families phosphorylate a variety of downstream targets, including some DNA-binding proteins (Mulvaney and Roberson, 2000; Mulvaney et al., 1999; Naor et al., 2000; Roberson et al., 1995; Roberson et al., 1999; Xie et al., 2005). The aggregation of GnRH-regulated mRNAs and their encoded proteins occurs in three waves: primary, secondary, and tertiary (Ruf et al., 2003; Ruf and Sealfon, 2004; Salisbury et al., 2007; Wurmbach et al., 2001; Yuen et al., 2002). The tertiary network of GnRH-responsive genes includes Cga, Lhb, Fshb, and Gnrhr. Since changes in their transcription are dependent on proteins encoded by the primary and secondary response genes, they respond to GnRH more slowly (Salisbury et al., 2008). In a study using microarray in the LβT2 cell line, the immediate early genes respond to GnRH stimulation. The response reveals a significant upregulation of 28 immediate-early genes within 60 minutes of GnRH stimulation (Roberson et al., 1999). Our data show that the expression of immediate early genes including Egr1, Atf3, and Jun peaks after 15 min in αT3-1 cell line when treated with 20 nM GnRH (Fig. 4. 9A, B, & C). Moreover, using LβT2 murine gonadotrope derived cell line

expresses the β subunits of LH and FSH [86], analysis demonstrates that LHb expression shows a significant upregulation after 15 min treatment with 20 UM GnRH (Fig. 4. 10A). However, following this increase, LHb expression drops after 30 and 60 min of GnRH treatment in LβT2 gonadotropes. On the other hand, FSHb expression peaks after 15 min of 20 UM GnRH treatment and continues upregulated for the following 30 and 60 min in response to GnRH (Fig. 4. 10B). Collectively, this data provides a validation of GnRH receptor-dependent gene expression activation in αT3-1 and LβT2 gonadotropes.

IQGAP1 has been reported to have a regulatory role in certain nuclear events. It has shown that IQGAP1 associates nuclear-cytoplasmic shuttling proteins, including β-catenin and ERK, and participates in the MEK/ERK cascade, which leads to Elk-1-mediated transcription activation (Bourguignon et al., 2005; Roy et al., 2004). It also has been reported that IQGAP1 may also trigger nuclear localization and signaling of β-catenin (Briggs et al., 2002a; Wang et al., 2008). Furthermore, it has shown that many IQGAP1 binding partners, including actin (Hofmann, 2009), Rac1 (Michaelson et al., 2008), N-WASp (Yoo et al., 2007), and APC (Brocardo and Henderson, 2008), have been linked to nuclear functions. Moreover, in nuclei of murine oocytes and cleaving embryos, IQGAP1 has been found to envelop nucleoli (Bielak-Zmijewska et al., 2008), indicating that IQGAP1 has possible nuclear functions. Our data indicates a correlation between IQGAP1 and gonadotrope gene expression using RT-PCR. The inhibition of IQGAP1 activity using IQGAP1pre-designed silencer siRNA in αT3-1 gonadotropes impacts the expression level for the immediate early genes, Atf3, Egr1, and C-Jun, that are shown to be significantly downregulated within 15 minutes of GnRH exposure when compared to control (Fig. 4. 11A, B, & C). In parallel experiments using RT-PCR, LHb expression level shows a constant significant increase in transfected LβT2 gonadotropes during the different time points of GnRH treatment (Fig. 4. 12A). Whereas FSHb expression level shows a constant significant reduction compared to the control LβT2 gonadotropes after GnRH treatment for different time points (Fig. 4. 12A). Our observations suggest that IQGAP1 has a transcriptional regulatory role in expressing primary, secondary, and tertiary genes that regulate the synthesis of LH and FSH in gonadotropes in response to GnRH.

GnRH-responsive planer cell polarity and adherens junction-related proteins such as IQGAP1 contribute to intergonadotrope communication and interactions resulting in the signaling pathway that leads to the gonadotropes productions. The primary objective of this study is to investigate the molecular role of IQGAP1 in mediating the GnRH signaling network in gonadotropes. Our data improves our fundamental understanding of gonadotrope biology by directly addressing the patent knowledge gap regarding intergonadotrope-related phenomena. Our observations reveal novel molecular targets potentially useful for experimental and clinical manipulation of gonadotrope function. After all, our results may have ramifications in various biomedical fields, including embryology and oncology, as our planer cell polarity and adherens junction-related proteins of interest influence intercellular communication during fetal development and tumorigenesis (Gärtner et al., 2014; Golubkov and Strongin, 2014; Lei et al., 2019; Mattes and Scholpp, 2018; Shin et al., 2015). However, this study has several limitations, and further research is necessary to investigate the level of complexity of IQGAP1 function that is provided by the crosstalk among signaling pathways in gonadotropes following GnRH receptor activation.

The majority of data presented in this study are based on experiments that used immortalized gonadotropic cells, αT3-1 and LβT2 cells. These cell lines considerably facilitate the investigations of the hormonal signaling pathways that mediate the expression of the gonadotropin genes. αT3-1 cells are thought to represent immature gonadotropes since they only express a limited number of gonadotrope-associated proteins. These proteins include Cga, Gnrhr, and Nr5a1 (encoding SF-1), but they do not express Fshb or Lhb (Windle et al., 1990). By contrast, LβT2 cells have a more advanced gonadotropic phenotype since they release LH and FSH in response to hormonal stimulation (Graham et al., 1999; Pernasetti et al., 2001; Turgeon et al., 1996). These features establish the LβT2 cell line as a reliable model for researching gonadotrope physiology. In addition to steroid hormone receptors, LβT2 cells express activin, follistatin, and inhibin (Lewis et al., 2000; Takeda et al., 2007; Thackray et al., 2006). The effects of paracrine factors generated by other pituitary cells may not be accounted for in studies

using LβT2 cells and other gonadotrope-derived cell lines. Furthermore, the expression profile of LβT2 cells is slightly distinct from that of primary gonadotropes, despite the fact that they represent more developed gonadotropes than the αT3-1 cell line (Yuen et al., 2012). While several regulated genes were unique, the vast majority were the same. changes in gene expression might be the consequence of species-specific variables, changes in experimental design, microarray technology, sensitivity, or variations in paracrine factors. Despite these limitations, LβT2 cells are the prevailing in vitro cellular model for investigating gonadotrope signaling.

Primary cultures, On the other hand, primary culture which are made up of mixed pituitary cells and are created by dispersing fresh pituitary tissue, are often used. It is important to note, however, that these models do have some significant caveats. To begin, the anterior pituitary gland contains a wide variety of secretory cells, including but not limited to gonadotropes, thyrotropes, somatotropes, lactotropes, corticotropes, and folliculostellate cells, all of which produce their own unique hormones. Only 10-15% of the cell populations of the adenohypophyseal glands are gonadotropes (Ooi et al., 2004). Second, in certain species, the gonadotropes and lactotropes are concentrated at the intermediate lobe, which may indicate a paracrine link (Bliss et al., 2010; Denef, 2008). Paracrine substances, such as follistatin and PACAP, produced by folliculostellate cells (Kawakami et al., 2002; Thackray et al., 2010; Winters and Moore, 2007) might influence gonadotrope responses and hence impact experimental results. Dispersed pituitary cultures may have a breakdown in the paracrine connections between them. To conclude, the endocrine milieu at the time of pituitary harvest, such as the estrous stage of female mice, should be taken into account since it may alter experimental outcomes (Fallest and Schwartz, 1991).

Researchers have devised new methods for isolating and purifying gonadotropes in transgenic mice models in order to circumvent these restrictions. Transgenic cell surface antigens (H-2Kk) have been used in vivo to tag FSH-producing gonadotropes, allowing for in vitro purification of these cells by immunologically based cell enrichment utilizing H-2Kk-specific antibodies (Wu et al., 2004). One further

method utilized to assist in the detection and identification of gonadotropes was the expression of yellow fluorescent protein (YFP) in these cells using a gene-targeted technique.

Finally, researchers have employed a wide variety of in vivo animal models to learn more about gonadotropin production, secretion, and action, such as gonadectomized rats (Dalkin et al., 1989; Haisenleder et al., 1991) and gain- and loss-of-function mice models (Kumar, 2016). Mice with a gonadotrope-specific deletion of genes expressing transcription factors, such as cFos and steroidogenic factor 1 (SF-1) (Tran et al., 2013; Xie et al., 2015a; Zhao et al., 2001b; Zhao et al., 2001c), or other factors that are important in the control of Fshb and Lhb transcription, such as ERK1/2, (Bliss et al., 2009), have been created. These animal models have allowed researchers to examine the consequences of inhibiting individual signaling pathways in a living organism. Using Mice with a gonadotrope-specific deletion of IQGAP1, as an important effector in cell-cell adhesion and cell transcription in gonadotropes, will support our hypothesis, enabling us to shed the light on a novel tool that can be assisting not only to understand the mechanism that regulate the gonadotrope production at the basic scientific level, but also to reveal a new promising protein that may has significant therapeutic implications for the future of reproductive health at the clinical level.

References

Abdul-Manan, N., Aghazadeh, B., Liu, G.A., Majumdar, A., Ouerfelli, O., Siminovitch, K.A., and Rosen, M.K. (1999). Structure of Cdc42 in complex with the GTPase-binding domain of the 'Wiskott-Aldrich syndrome' protein. Nature *399*, 379-383.
Abel, A.M., Schuldt, K.M., Rajasekaran, K., Hwang, D., Riese, M.J., Rao, S., Thakar, M.S., and Malarkannan, S. (2015a). IQGAP1: Insights into the function of a molecular puppeteer. Molecular Immunology *65*, 336-349.
Abel, A.M., Schuldt, K.M., Rajasekaran, K., Hwang, D., Riese, M.J., Rao, S., Thakar, M.S., and Malarkannan, S. (2015b). IQGAP1: insights into the function of a molecular puppeteer. Mol Immunol *65*, 336-349.
Abraham, M., Sandri, C., and Akert, K. (1979). Freeze-etch study of the teleostean pituitary. Cell and Tissue Research *199*, 397-407.
Adams, T.E., and Nett, T.M. (1979). Interaction of GnRH with anterior pituitary. III. Role of divalent cations, microtubules and microfilaments in the GnRH activated gonadotroph. Biology of reproduction *21*, 1073-1086.
Adamson, E.D., Yu, J., and Mustelin, T. (2005). Co-factors p300 and CBP catch Egr1 in their network. The Prostate *63*, 407-410.
Alim, Z., Hartshorn, C., Mai, O., Stitt, I., Clay, C., Tobet, S., and Boehm, U. (2012). Gonadotrope plasticity at cellular and population levels. Endocrinology *153*, 4729-4739.
Allaerts, W., and Vankelecom, H. (2005). History and perspectives of pituitary folliculo-stellate cell research. European journal of endocrinology *153*, 1-12.
Allen-Worthington, K., Xie, J., Brown, J.L., Edmunson, A.M., Dowling, A., Navratil, A.M., Scavelli, K., Yoon, H., Kim, D.G., Bynoe, M.S.*, et al.* (2016). The F0F1 ATP Synthase Complex Localizes to Membrane Rafts in Gonadotrope Cells. Molecular endocrinology (Baltimore, Md) *30*, 996-1011.
Ammer, A.G., and Weed, S.A. (2008). Cortactin branches out: roles in regulating protrusive actin dynamics. Cell motility and the cytoskeleton *65*, 687-707.
Ando, H., Hew, C.L., and Urano, A. (2001). Signal transduction pathways and transcription factors involved in the gonadotropin-releasing hormone-stimulated gonadotropin subunit gene expression. Comparative biochemistry and physiology Part B, Biochemistry & molecular biology *129*, 525-532.
Andreeva, A., Lee, J., Lohia, M., Wu, X., Macara, I.G., and Lu, X. (2014). PTK7-Src signaling at epithelial cell contacts mediates spatial organization of actomyosin and planar cell polarity. Developmental cell *29*, 20-33.
Angel, P., Hattori, K., Smeal, T., and Karin, M. (1988). The jun proto-oncogene is positively autoregulated by its product, Jun/AP-1. Cell *55*, 875-885.
Angst, B.D., Marcozzi, C., and Magee, A.I. (2001). The cadherin superfamily: diversity in form and function. Journal of cell science *114*, 629-641.
Aoki, K., and Taketo, M.M. (2007). Adenomatous polyposis coli (APC): a multi-functional tumor suppressor gene. Journal of cell science *120*, 3327-3335.
Armstrong, S.P., Caunt, C.J., Fowkes, R.C., Tsaneva-Atanasova, K., and McArdle, C.A. (2010). Pulsatile and sustained gonadotropin-releasing hormone (GnRH) receptor signaling: does the ERK signaling pathway decode GnRH pulse frequency? The Journal of biological chemistry *285*, 24360-24371.
Arora, P., Nakajima, K., Nanda, A., Plaha, A., Wilde, A., Sacks, D., and McCulloch, C. (2020). Flightless anchors IQGAP1 and R-ras to mediate cell extension formation and matrix remodeling. Molecular biology of the cell *31*, 1595-1610.
Arora, P.D., Di Gregorio, M., He, P., and McCulloch, C.A. (2017). TRPV4 mediates the Ca(2+) influx required for the interaction between flightless-1 and non-muscle myosin, and collagen remodeling. Journal of cell science *130*, 2196-2208.

Arora, P.D., Wang, Y., Bresnick, A., Janmey, P.A., and McCulloch, C.A. (2015). Flightless I interacts with NMMIIA to promote cell extension formation, which enables collagen remodeling. Molecular biology of the cell *26*, 2279-2297.
Avet, C., Garrel, G., Denoyelle, C., Laverrière, J.N., Counis, R., Cohen-Tannoudji, J., and Simon, V. (2013). SET protein interacts with intracellular domains of the gonadotropin-releasing hormone receptor and differentially regulates receptor signaling to cAMP and calcium in gonadotrope cells. The Journal of biological chemistry *288*, 2641-2654.
Awasthi, A., Samarakoon, A., Chu, H., Kamalakannan, R., Quilliam, L.A., Chrzanowska-Wodnicka, M., White, G.C., 2nd, and Malarkannan, S. (2010). Rap1b facilitates NK cell functions via IQGAP1-mediated signalosomes. The Journal of experimental medicine *207*, 1923-1938.
Bañón-Rodríguez, I., Gálvez-Santisteban, M., Vergarajauregui, S., Bosch, M., Borreguero-Pascual, A., and Martín-Belmonte, F. (2014). EGFR controls IQGAP basolateral membrane localization and mitotic spindle orientation during epithelial morphogenesis. The EMBO journal *33*, 129-145.
Bardwell, A.J., Lagunes, L., Zebarjedi, R., and Bardwell, L. (2017). The WW domain of the scaffolding protein IQGAP1 is neither necessary nor sufficient for binding to the MAPKs ERK1 and ERK2. The Journal of biological chemistry *292*, 8750-8761.
Barker, N., Hurlstone, A., Musisi, H., Miles, A., Bienz, M., and Clevers, H. (2001). The chromatin remodelling factor Brg-1 interacts with beta-catenin to promote target gene activation. The EMBO journal *20*, 4935-4943.
Bashour, A.-M., Fullerton, A.T., Hart, M.J., and Bloom, G.S. (1997a). IQGAP1, a Rac-and Cdc42-binding protein, directly binds and cross-links microfilaments. The Journal of cell biology *137*, 1555-1566.
Bashour, A.M., Fullerton, A.T., Hart, M.J., and Bloom, G.S. (1997b). IQGAP1, a Rac- and Cdc42-binding protein, directly binds and cross-links microfilaments. The Journal of cell biology *137*, 1555-1566.
Bazzoni, G., Dejana, E., and Lampugnani, M.G. (1999). Endothelial adhesion molecules in the development of the vascular tree: the garden of forking paths. Current opinion in cell biology *11*, 573-581.
Beaty, B.T., and Condeelis, J. (2014). Digging a little deeper: the stages of invadopodium formation and maturation. European journal of cell biology *93*, 438-444.
Bédécarrats, G.Y., and Kaiser, U.B. (2003). Differential regulation of gonadotropin subunit gene promoter activity by pulsatile gonadotropin-releasing hormone (GnRH) in perifused L beta T2 cells: role of GnRH receptor concentration. Endocrinology *144*, 1802-1811.
Ben-Ze'ev, A., and Geiger, B. (1998). Differential molecular interactions of beta-catenin and plakoglobin in adhesion, signaling and cancer. Current opinion in cell biology *10*, 629-639.
Benard, O., Naor, Z., and Seger, R. (2017). Role of dynamin, Src, and Ras in the protein kinase C-mediated activation of ERK by gonadotropin-releasing hormone. The Journal of biological chemistry *292*, 8855.
Benard, V., Bohl, B.P., and Bokoch, G.M. (1999). Characterization of rac and cdc42 activation in chemoattractant-stimulated human neutrophils using a novel assay for active GTPases. The Journal of biological chemistry *274*, 13198-13204.
Berger, H., Breuer, M., Peradziryi, H., Podleschny, M., Jacob, R., and Borchers, A. (2017). PTK7 localization and protein stability is affected by canonical Wnt ligands. Journal of cell science *130*, 1890-1903.
Bernard, D.J., Fortin, J., Wang, Y., and Lamba, P. (2010). Mechanisms of FSH synthesis: what we know, what we don't, and why you should care. Fertility and sterility *93*, 2465-2485.
Bielak-Zmijewska, A., Kolano, A., Szczepanska, K., Maleszewski, M., and Borsuk, E. (2008). Cdc42 protein acts upstream of IQGAP1 and regulates cytokinesis in mouse oocytes and embryos. Developmental biology *322*, 21-32.
Bienz, M., and Clevers, H. (2000). Linking colorectal cancer to Wnt signaling. Cell *103*, 311-320.

Bilezikjian, L.M., Leal, A.M., Blount, A.L., Corrigan, A.Z., Turnbull, A.V., and Vale, W.W. (2003). Rat anterior pituitary folliculostellate cells are targets of interleukin-1beta and a major source of intrapituitary follistatin. Endocrinology *144*, 732-740.
Bin-Nun, N., Lichtig, H., Malyarova, A., Levy, M., Elias, S., and Frank, D. (2014). PTK7 modulates Wnt signaling activity via LRP6. Development (Cambridge, England) *141*, 410-421.
Bliss, S.P., Miller, A., Navratil, A.M., Xie, J., McDonough, S.P., Fisher, P.J., Landreth, G.E., and Roberson, M.S. (2009). ERK signaling in the pituitary is required for female but not male fertility. Molecular endocrinology (Baltimore, Md) *23*, 1092-1101.
Bliss, S.P., Navratil, A.M., Breed, M., Skinner, D.C., Clay, C.M., and Roberson, M.S. (2007). Signaling complexes associated with the type I gonadotropin-releasing hormone (GnRH) receptor: colocalization of extracellularly regulated kinase 2 and GnRH receptor within membrane rafts. Molecular endocrinology (Baltimore, Md) *21*, 538-549.
Bliss, S.P., Navratil, A.M., Xie, J., Miller, A., Baccarini, M., and Roberson, M.S. (2012). ERK signaling, but not c-Raf, is required for gonadotropin-releasing hormone (GnRH)-induced regulation of Nur77 in pituitary gonadotropes. Endocrinology *153*, 700-711.
Bliss, S.P., Navratil, A.M., Xie, J., and Roberson, M.S. (2010). GnRH signaling, the gonadotrope and endocrine control of fertility. Frontiers in neuroendocrinology *31*, 322-340.
Bockaert, J., Fagni, L., Dumuis, A., and Marin, P. (2004). GPCR interacting proteins (GIP). Pharmacology & therapeutics *103*, 203-221.
Bonello, T.T., and Peifer, M. (2019). Scribble: A master scaffold in polarity, adhesion, synaptogenesis, and proliferation. The Journal of cell biology *218*, 742-756.
Bonfil, D., Chuderland, D., Kraus, S., Shahbazian, D., Friedberg, I., Seger, R., and Naor, Z. (2004). Extracellular signal-regulated kinase, Jun N-terminal kinase, p38, and c-Src are involved in gonadotropin-releasing hormone-stimulated activity of the glycoprotein hormone follicle-stimulating hormone beta-subunit promoter. Endocrinology *145*, 2228-2244.
Borders, A.S., de Almeida, L., Van Eldik, L.J., and Watterson, D.M. (2008). The p38alpha mitogen-activated protein kinase as a central nervous system drug discovery target. BMC neuroscience *9 Suppl 2*, S12.
Borst, J.G., Lodder, J.C., Roubos, E.W., and Kits, K.S. (1996). In situ recordings of presumed folliculo-stellate cells in the intermediate lobe of the pituitary gland of Xenopus laevis. Neuroscience letters *209*, 61-64.
Bosma, M.M., and Hille, B. (1992). Electrophysiological properties of a cell line of the gonadotrope lineage. Endocrinology *130*, 3411-3420.
Bottone, F.G., Jr., Moon, Y., Alston-Mills, B., and Eling, T.E. (2005). Transcriptional regulation of activating transcription factor 3 involves the early growth response-1 gene. The Journal of pharmacology and experimental therapeutics *315*, 668-677.
Bourguignon, L.Y., Gilad, E., Rothman, K., and Peyrollier, K. (2005). Hyaluronan-CD44 interaction with IQGAP1 promotes Cdc42 and ERK signaling, leading to actin binding, Elk-1/estrogen receptor transcriptional activation, and ovarian cancer progression. The Journal of biological chemistry *280*, 11961-11972.
Bouwmeester, T., Bauch, A., Ruffner, H., Angrand, P.O., Bergamini, G., Croughton, K., Cruciat, C., Eberhard, D., Gagneur, J., Ghidelli, S.*, et al.* (2004). A physical and functional map of the human TNF-alpha/NF-kappa B signal transduction pathway. Nature cell biology *6*, 97-105.
Boyer, O., Benoit, G., Gribouval, O., Nevo, F., Tête, M.J., Dantal, J., Gilbert-Dussardier, B., Touchard, G., Karras, A., Presne, C.*, et al.* (2011). Mutations in INF2 are a major cause of autosomal dominant focal segmental glomerulosclerosis. Journal of the American Society of Nephrology : JASN *22*, 239-245.
Bozdagi, O., Shan, W., Tanaka, H., Benson, D.L., and Huntley, G.W. (2000). Increasing numbers of synaptic puncta during late-phase LTP: N-cadherin is synthesized, recruited to synaptic sites, and required for potentiation. Neuron *28*, 245-259.
Braga, V.M. (2002). Cell-cell adhesion and signalling. Current opinion in cell biology *14*, 546-556.

Brandt, D.T., and Grosse, R. (2007). Get to grips: steering local actin dynamics with IQGAPs. EMBO reports *8*, 1019-1023.
Brennan, D.F., Dar, A.C., Hertz, N.T., Chao, W.C., Burlingame, A.L., Shokat, K.M., and Barford, D. (2011). A Raf-induced allosteric transition of KSR stimulates phosphorylation of MEK. Nature *472*, 366-369.
Briggs, M.W., Li, Z., and Sacks, D.B. (2002a). IQGAP1-mediated stimulation of transcriptional co-activation by beta-catenin is modulated by calmodulin. The Journal of biological chemistry *277*, 7453-7465.
Briggs, M.W., Li, Z., and Sacks, D.B. (2002b). IQGAP1-mediated stimulation of transcriptional co-activation by β-catenin is modulated by calmodulin. Journal of Biological Chemistry *277*, 7453-7465.
Briggs, M.W., and Sacks, D.B. (2003a). IQGAP1 as signal integrator: Ca2+, calmodulin, Cdc42 and the cytoskeleton. FEBS letters *542*, 7-11.
Briggs, M.W., and Sacks, D.B. (2003b). IQGAP proteins are integral components of cytoskeletal regulation. EMBO reports *4*, 571-574.
Brill, S., Li, S., Lyman, C.W., Church, D.M., Wasmuth, J.J., Weissbach, L., Bernards, A., and Snijders, A.J. (1996). The Ras GTPase-activating-protein-related human protein IQGAP2 harbors a potential actin binding domain and interacts with calmodulin and Rho family GTPases. Molecular and cellular biology *16*, 4869-4878.
Brinkley, H.J. (1981). Endocrine signaling and female reproduction. Biology of reproduction *24*, 22-43.
Brocardo, M., and Henderson, B.R. (2008). APC shuttling to the membrane, nucleus and beyond. Trends in cell biology *18*, 587-596.
Brown, M.D., Bry, L., Li, Z., and Sacks, D.B. (2007). IQGAP1 regulates Salmonella invasion through interactions with actin, Rac1, and Cdc42. The Journal of biological chemistry *282*, 30265-30272.
Brown, M.D., and Sacks, D.B. (2006). IQGAP1 in cellular signaling: bridging the GAP. Trends in cell biology *16*, 242-249.
Bruzzaniti, A., Neff, L., Sanjay, A., Horne, W.C., De Camilli, P., and Baron, R. (2005). Dynamin forms a Src kinase-sensitive complex with Cbl and regulates podosomes and osteoclast activity. Molecular biology of the cell *16*, 3301-3313.
Budry, L., Lafont, C., El Yandouzi, T., Chauvet, N., Conéjero, G., Drouin, J., and Mollard, P. (2011). Related pituitary cell lineages develop into interdigitated 3D cell networks. Proceedings of the National Academy of Sciences of the United States of America *108*, 12515-12520.
Buggs, C., Weinberg, F., Kim, E., Wolfe, A., Radovick, S., and Wondisford, F. (2006). Insulin augments GnRH-stimulated LHbeta gene expression by Egr-1. Molecular and cellular endocrinology *249*, 99-106.
Burger, L.L., Haisenleder, D.J., Aylor, K.W., and Marshall, J.C. (2008). Regulation of intracellular signaling cascades by GNRH pulse frequency in the rat pituitary: roles for CaMK II, ERK, and JNK activation. Biology of reproduction *79*, 947-953.
Burger, L.L., Haisenleder, D.J., Dalkin, A.C., and Marshall, J.C. (2004). Regulation of gonadotropin subunit gene transcription. Journal of molecular endocrinology *33*, 559-584.
Call, G.B., and Wolfe, M.W. (2002). Species differences in GnRH activation of the LHbeta promoter: role of Egr1 and Sp1. Molecular and cellular endocrinology *189*, 85-96.
Calvo, F., Agudo-Ibáñez, L., and Crespo, P. (2010). The Ras-ERK pathway: understanding site-specific signaling provides hope of new anti-tumor therapies. BioEssays : news and reviews in molecular, cellular and developmental biology *32*, 412-421.
Cantley, L.C. (2002). The phosphoinositide 3-kinase pathway. Science (New York, NY) *296*, 1655-1657.
Carmon, K.S., Gong, X., Yi, J., Thomas, A., and Liu, Q. (2014). RSPO-LGR4 functions via IQGAP1 to potentiate Wnt signaling. Proceedings of the National Academy of Sciences of the United States of America *111*, E1221-1229.
Carmon, K.S., Gong, X., Yi, J., Wu, L., Thomas, A., Moore, C.M., Masuho, I., Timson, D.J., Martemyanov, K.A., and Liu, Q.J. (2017). LGR5 receptor promotes cell–cell adhesion in stem cells and colon cancer cells via the IQGAP1–Rac1 pathway. Journal of Biological Chemistry *292*, 14989-15001.

Casar, B., Arozarena, I., Sanz-Moreno, V., Pinto, A., Agudo-Ibáñez, L., Marais, R., Lewis, R.E., Berciano, M.T., and Crespo, P. (2009a). Ras subcellular localization defines extracellular signal-regulated kinase 1 and 2 substrate specificity through distinct utilization of scaffold proteins. Molecular and cellular biology *29*, 1338-1353.
Casar, B., Pinto, A., and Crespo, P. (2008). Essential role of ERK dimers in the activation of cytoplasmic but not nuclear substrates by ERK-scaffold complexes. Molecular cell *31*, 708-721.
Casar, B., Pinto, A., and Crespo, P. (2009b). ERK dimers and scaffold proteins: unexpected partners for a forgotten (cytoplasmic) task. Cell cycle (Georgetown, Tex) *8*, 1007-1013.
Caunt, C.J., Finch, A.R., Sedgley, K.R., and McArdle, C.A. (2006). Seven-transmembrane receptor signalling and ERK compartmentalization. Trends in endocrinology and metabolism: TEM *17*, 276-283.
Cereijido, M., Robbins, E.S., Dolan, W.J., Rotunno, C.A., and Sabatini, D.D. (1978). Polarized monolayers formed by epithelial cells on a permeable and translucent support. The Journal of cell biology *77*, 853-880.
Chang, J.P., McCoy, E.E., Graeter, J., Tasaka, K., and Catt, K.J. (1986). Participation of voltage-dependent calcium channels in the action of gonadotropin-releasing hormone. The Journal of biological chemistry *261*, 9105-9108.
Chang, L., and Karin, M. (2001). Mammalian MAP kinase signalling cascades. Nature *410*, 37-40.
Cherfils, J., and Zeghouf, M. (2013). Regulation of small GTPases by GEFs, GAPs, and GDIs. Physiological reviews *93*, 269-309.
Cheung, K.L., Lee, J.H., Shu, L., Kim, J.H., Sacks, D.B., and Kong, A.N. (2013). The Ras GTPase-activating-like protein IQGAP1 mediates Nrf2 protein activation via the mitogen-activated protein kinase/extracellular signal-regulated kinase (ERK) kinase (MEK)-ERK pathway. The Journal of biological chemistry *288*, 22378-22386.
Chichili, G.R., and Rodgers, W. (2009). Cytoskeleton-membrane interactions in membrane raft structure. Cellular and molecular life sciences : CMLS *66*, 2319-2328.
Childs, G.V. (1985). Shifts in gonadotropin storage in cultured gonadotropes following GnRH stimulation, in vitro. Peptides *6*, 103-107.
Childs, G.V., MacNicol, A.M., and MacNicol, M.C. (2020). Molecular Mechanisms of Pituitary Cell Plasticity. Frontiers in endocrinology *11*, 656.
Childs, G.V., Unabia, G., Lee, B.L., and Rougeau, D. (1992a). Heightened secretion by small and medium-sized luteinizing hormone (LH) gonadotropes late in the cycle suggests contributions to the LH surge or possible paracrine interactions. Endocrinology *130*, 345-352.
Childs, G.V., Unabia, G., and Lloyd, J. (1992b). Recruitment and maturation of small subsets of luteinizing hormone gonadotropes during the estrous cycle. Endocrinology *130*, 335-344.
Choi, S., Hedman, A.C., Sayedyahossein, S., Thapa, N., Sacks, D.B., and Anderson, R.A. (2016). Agonist-stimulated phosphatidylinositol-3,4,5-trisphosphate generation by scaffolded phosphoinositide kinases. Nature cell biology *18*, 1324-1335.
Chuang, H.-C., Chang, C.-C., Teng, C.-F., Hsueh, C.-H., Chiu, L.-L., Hsu, P.-M., Lee, M.-C., Hsu, C.-P., Chen, Y.-R., and Liu, Y.-C. (2019). MAP4K3/GLK promotes lung cancer metastasis by phosphorylating and activating IQGAP1. Cancer research *79*, 4978-4993.
Chuderland, D., and Seger, R. (2005). Protein-protein interactions in the regulation of the extracellular signal-regulated kinase. Molecular biotechnology *29*, 57-74.
Clayton, R.N., and Catt, K.J. (1981). Gonadotropin-releasing hormone receptors: characterization, physiological regulation, and relationship to reproductive function. Endocrine reviews *2*, 186-209.
Clevers, H. (2006). Wnt/beta-catenin signaling in development and disease. Cell *127*, 469-480.
Clevers, H., and Nusse, R. (2012). Wnt/β-catenin signaling and disease. Cell *149*, 1192-1205.
Cohen-Tannoudji, J., Avet, C., Garrel, G., Counis, R., and Simon, V. (2012). Decoding high Gonadotropin-releasing hormone pulsatility: a role for GnRH receptor coupling to the cAMP pathway? Frontiers in endocrinology *3*, 107.

Cornea, A., Janovick, J.A., Maya-Núñez, G., and Conn, P.M. (2001). Gonadotropin-releasing hormone receptor microaggregation. Rate monitored by fluorescence resonance energy transfer. The Journal of biological chemistry *276*, 2153-2158.
Cosen-Binker, L.I., and Kapus, A. (2006). Cortactin: the gray eminence of the cytoskeleton. Physiology (Bethesda, Md) *21*, 352-361.
Coss, D., Hand, C.M., Yaphockun, K.K., Ely, H.A., and Mellon, P.L. (2007). p38 mitogen-activated protein kinase is critical for synergistic induction of the FSH(beta) gene by gonadotropin-releasing hormone and activin through augmentation of c-Fos induction and Smad phosphorylation. Molecular endocrinology (Baltimore, Md) *21*, 3071-3086.
Coss, D., Jacobs, S.B., Bender, C.E., and Mellon, P.L. (2004). A novel AP-1 site is critical for maximal induction of the follicle-stimulating hormone beta gene by gonadotropin-releasing hormone. The Journal of biological chemistry *279*, 152-162.
Crespo, P., and León, J. (2000). Ras proteins in the control of the cell cycle and cell differentiation. Cellular and molecular life sciences : CMLS *57*, 1613-1636.
Dalkin, A.C., Haisenleder, D.J., Ortolano, G.A., Ellis, T.R., and Marshall, J.C. (1989). The frequency of gonadotropin-releasing-hormone stimulation differentially regulates gonadotropin subunit messenger ribonucleic acid expression. Endocrinology *125*, 917-924.
Dang, A.K., Murtazina, D.A., Magee, C., Navratil, A.M., Clay, C.M., and Amberg, G.C. (2014). GnRH evokes localized subplasmalemmal calcium signaling in gonadotropes. Molecular endocrinology (Baltimore, Md) *28*, 2049-2059.
Davey, C.F., and Moens, C.B. (2017). Planar cell polarity in moving cells: think globally, act locally. Development (Cambridge, England) *144*, 187-200.
Davidson, L., Pawson, A.J., Millar, R.P., and Maudsley, S. (2004). Cytoskeletal reorganization dependence of signaling by the gonadotropin-releasing hormone receptor. The Journal of biological chemistry *279*, 1980-1993.
De Franceschi, N., Hamidi, H., Alanko, J., Sahgal, P., and Ivaska, J. (2015). Integrin traffic - the update. Journal of cell science *128*, 839-852.
De la Llosa, P., and Jutisz, M. (1969). Reversible dissociation into subunits and biological activity of ovine luteinizing hormone. Biochimica et biophysica acta *181*, 426-436.
De Paul, A.L., Bonaterra, M., Aoki, A., and Torres, A.I. (2000). Cellular and functional interactions between gonadotrophs and lactotrophs in pituitary cell cultures. Medical electron microscopy : official journal of the Clinical Electron Microscopy Society of Japan *33*, 231-240.
Denef, C. (2008). Paracrinicity: the story of 30 years of cellular pituitary crosstalk. Journal of neuroendocrinology *20*, 1-70.
Deplazes, J., Fuchs, M., Rauser, S., Genth, H., Lengyel, E., Busch, R., and Luber, B. (2009). Rac1 and Rho contribute to the migratory and invasive phenotype associated with somatic E-cadherin mutation. Human Molecular Genetics *18*, 3632-3644.
Desaulniers, A.T., Cederberg, R.A., Lents, C.A., and White, B.R. (2017). Expression and Role of Gonadotropin-Releasing Hormone 2 and Its Receptor in Mammals. Frontiers in endocrinology *8*, 269.
Desclozeaux, M., Krylova, I.N., Horn, F., Fletterick, R.J., and Ingraham, H.A. (2002). Phosphorylation and intramolecular stabilization of the ligand binding domain in the nuclear receptor steroidogenic factor 1. Molecular and cellular biology *22*, 7193-7203.
Devenport, D. (2014). The cell biology of planar cell polarity. The Journal of cell biology *207*, 171-179.
Dhanasekaran, D.N., Kashef, K., Lee, C.M., Xu, H., and Reddy, E.P. (2007). Scaffold proteins of MAP-kinase modules. Oncogene *26*, 3185-3202.
Dimchev, G., Steffen, A., Kage, F., Dimchev, V., Pernier, J., Carlier, M.F., and Rottner, K. (2017). Efficiency of lamellipodia protrusion is determined by the extent of cytosolic actin assembly. Molecular biology of the cell *28*, 1311-1325.
Dixon, M.J., Gray, A., Boisvert, F.M., Agacan, M., Morrice, N.A., Gourlay, R., Leslie, N.R., Downes, C.P., and Batty, I.H. (2011). A screen for novel phosphoinositide 3-kinase effector proteins. Molecular & cellular proteomics : MCP *10*, M110.003178.

Dobkin-Bekman, M., Naidich, M., Pawson, A.J., Millar, R.P., Seger, R., and Naor, Z. (2006). Activation of mitogen-activated protein kinase (MAPK) by GnRH is cell-context dependent. Molecular and cellular endocrinology *252*, 184-190.
Dorn, C., Ou, Q., Svaren, J., Crawford, P.A., and Sadovsky, Y. (1999). Activation of luteinizing hormone beta gene by gonadotropin-releasing hormone requires the synergy of early growth response-1 and steroidogenic factor-1. The Journal of biological chemistry *274*, 13870-13876.
Doussau, F., and Augustine, G.J. (2000). The actin cytoskeleton and neurotransmitter release: an overview. Biochimie *82*, 353-363.
Duan, W.R., Ito, M., Park, Y., Maizels, E.T., Hunzicker-Dunn, M., and Jameson, J.L. (2002). GnRH regulates early growth response protein 1 transcription through multiple promoter elements. Molecular endocrinology (Baltimore, Md) *16*, 221-233.
Dudek, S.M., and Garcia, J.G. (2001). Cytoskeletal regulation of pulmonary vascular permeability. Journal of applied physiology (Bethesda, Md : 1985) *91*, 1487-1500.
Dumontier, M., Höcht, P., Mintert, U., and Faix, J. (2000). Rac1 GTPases control filopodia formation, cell motility, endocytosis, cytokinesis and development in Dictyostelium. Journal of cell science *113 (Pt 12)*, 2253-2265.
Durán-Pastén, M.L., and Fiordelisio, T. (2013). GnRH-Induced Ca(2+) Signaling Patterns and Gonadotropin Secretion in Pituitary Gonadotrophs. Functional Adaptations to Both Ordinary and Extraordinary Physiological Demands. Frontiers in endocrinology *4*, 127.
Dvorsky, R., and Ahmadian, M.R. (2004). Always look on the bright site of Rho: structural implications for a conserved intermolecular interface. EMBO reports *5*, 1130-1136.
Dvorsky, R., Blumenstein, L., Vetter, I.R., and Ahmadian, M.R. (2004). Structural insights into the interaction of ROCKI with the switch regions of RhoA. The Journal of biological chemistry *279*, 7098-7104.
Eblen, S.T. (2018). Extracellular-Regulated Kinases: Signaling From Ras to ERK Substrates to Control Biological Outcomes. Advances in cancer research *138*, 99-142.
Edwards, B.S., Clay, C.M., Ellsworth, B.S., and Navratil, A.M. (2017a). Functional Role of Gonadotrope Plasticity and Network Organization. Frontiers in endocrinology *8*, 223.
Edwards, B.S., Dang, A.K., Murtazina, D.A., Dozier, M.G., Whitesell, J.D., Khan, S.A., Cherrington, B.D., Amberg, G.C., Clay, C.M., and Navratil, A.M. (2015). Dynamin is required for GnRH signaling to L-type calcium channels and activation of ERK. Endocrinology, en20151575-en20151575.
Edwards, B.S., Dang, A.K., Murtazina, D.A., Dozier, M.G., Whitesell, J.D., Khan, S.A., Cherrington, B.D., Amberg, G.C., Clay, C.M., and Navratil, A.M. (2016). Dynamin Is Required for GnRH Signaling to L-Type Calcium Channels and Activation of ERK. Endocrinology *157*, 831-843.
Edwards, B.S., Isom, W.J., and Navratil, A.M. (2017b). Gonadotropin releasing hormone activation of the mTORC2/Rictor complex regulates actin remodeling and ERK activity in LβT2 cells. Molecular and cellular endocrinology *439*, 346-353.
Elliott, S.F., Allen, G., and Timson, D.J. (2012a). Biochemical analysis of the interactions of IQGAP1 C-terminal domain with CDC42. World journal of biological chemistry *3*, 53-60.
Elliott, S.F., Allen, G., and Timson, D.J. (2012b). Biochemical analysis of the interactions of IQGAP1 C-terminal domain with CDC42. World journal of biological chemistry *3*, 53-60.
Ellsworth, B.S., White, B.R., Burns, A.T., Cherrington, B.D., Otis, A.M., and Clay, C.M. (2003). c-Jun N-terminal kinase activation of activator protein-1 underlies homologous regulation of the gonadotropin-releasing hormone receptor gene in alpha T3-1 cells. Endocrinology *144*, 839-849.
Emadali, A., Muscatelli-Groux, B., Delom, F., Jenna, S., Boismenu, D., Sacks, D.B., Metrakos, P.P., and Chevet, E. (2006). Proteomic Analysis of Ischemia-Reperfusion Injury upon Human Liver Transplantation Reveals the Protective Role of IQGAP1* S. Molecular & cellular proteomics *5*, 1300-1313.
Eng, K., Naqvi, N.I., Wong, K.C., and Balasubramanian, M.K. (1998). Rng2p, a protein required for cytokinesis in fission yeast, is a component of the actomyosin ring and the spindle pole body. Current biology : CB *8*, 611-621.

Epp, J.A., and Chant, J. (1997). An IQGAP-related protein controls actin-ring formation and cytokinesis in yeast. Current biology : CB *7*, 921-929.
Erdemir, H.H., Li, Z., and Sacks, D.B. (2014). IQGAP1 binds to estrogen receptor-α and modulates its function. The Journal of biological chemistry *289*, 9100-9112.
Erickson, J.W., Cerione, R.A., and Hart, M.J. (1997). Identification of an actin cytoskeletal complex that includes IQGAP and the Cdc42 GTPase. The Journal of biological chemistry *272*, 24443-24447.
Essers, M.A., de Vries-Smits, L.M., Barker, N., Polderman, P.E., Burgering, B.M., and Korswagen, H.C. (2005). Functional interaction between beta-catenin and FOXO in oxidative stress signaling. Science (New York, NY) *308*, 1181-1184.
Fallest, P.C., and Schwartz, N.B. (1991). Acute inhibitory effects of 17 beta-estradiol are observed on gonadotropin secretion from perifused pituitary fragments of metestrous, but not proestrous, rats. Endocrinology *128*, 273-279.
Fauquier, T., Guérineau, N.C., McKinney, R.A., Bauer, K., and Mollard, P. (2001). Folliculostellate cell network: a route for long-distance communication in the anterior pituitary. Proceedings of the National Academy of Sciences of the United States of America *98*, 8891-8896.
Featherstone, K., Hey, K., Momiji, H., McNamara, A.V., Patist, A.L., Woodburn, J., Spiller, D.G., Christian, H.C., McNeilly, A.S., Mullins, J.J.*, et al.* (2016). Spatially coordinated dynamic gene transcription in living pituitary tissue. eLife *5*, e08494.
Feigin, M.E., Xue, B., Hammell, M.C., and Muthuswamy, S.K. (2014). G-protein-coupled receptor GPR161 is overexpressed in breast cancer and is a promoter of cell proliferation and invasion. Proceedings of the National Academy of Sciences of the United States of America *111*, 4191-4196.
Ferri, N., Bernini, S.K., Corsini, A., Clerici, F., Erba, E., Stragliotto, S., and Contini, A. (2013). 3-Aryl-N-aminoylsulfonylphenyl-1H-pyrazole-5-carboxamides: a new class of selective Rac inhibitors. MedChemComm *4*, 537-541.
Ferris, H.A., and Shupnik, M.A. (2006). Mechanisms for pulsatile regulation of the gonadotropin subunit genes by GNRH1. Biology of reproduction *74*, 993-998.
Filić, V., Marinović, M., Faix, J., and Weber, I. (2012). A dual role for Rac1 GTPases in the regulation of cell motility. Journal of cell science *125*, 387-398.
Fletcher, W.H., Anderson, N.C., Jr., and Everett, J.W. (1975). Intercellular communication in the rat anterior pituitary gland. An in vivo and in vitro study. The Journal of cell biology *67*, 469-476.
Fontaine, R., Ciani, E., Haug, T.M., Hodne, K., Ager-Wick, E., Baker, D.M., and Weltzien, F.A. (2020). Gonadotrope plasticity at cellular, population and structural levels: A comparison between fishes and mammals. General and comparative endocrinology *287*, 113344.
Foroutannejad, S., Rohner, N., Reimer, M., Kwon, G., and Schober, J.M. (2014). A novel role for IQGAP1 protein in cell motility through cell retraction. Biochemical and biophysical research communications *448*, 39-44.
Fortin, J., Lamba, P., Wang, Y., and Bernard, D.J. (2009). Conservation of mechanisms mediating gonadotrophin-releasing hormone 1 stimulation of human luteinizing hormone beta subunit transcription. Molecular human reproduction *15*, 77-87.
Foster, W.G., and Younglai, E.V. (1991). An immunohistochemical study of the GnRH neuron morphology and topography in the adult female rabbit hypothalamus. The American journal of anatomy *191*, 293-300.
Fowkes, R.C., King, P., and Burrin, J.M. (2002). Regulation of human glycoprotein hormone alpha-subunit gene transcription in LbetaT2 gonadotropes by protein kinase C and extracellular signal-regulated kinase 1/2. Biology of reproduction *67*, 725-734.
Frame, S., and Cohen, P. (2001). GSK3 takes centre stage more than 20 years after its discovery. The Biochemical journal *359*, 1-16.
Franklin, C.C., and Kraft, A.S. (1997). Conditional expression of the mitogen-activated protein kinase (MAPK) phosphatase MKP-1 preferentially inhibits p38 MAPK and stress-activated protein kinase in U937 cells. The Journal of biological chemistry *272*, 16917-16923.

Fu, Y., Westenbroek, R.E., Yu, F.H., Clark, J.P., 3rd, Marshall, M.R., Scheuer, T., and Catterall, W.A. (2011). Deletion of the distal C terminus of $Ca_V1.2$ channels leads to loss of b-adrenergic regulation and heart failure *in vivo*. J Biol Chem *286*, 12617-12626.
Fukata, M., Kuroda, S., Fujii, K., Nakamura, T., Shoji, I., Matsuura, Y., Okawa, K., Iwamatsu, A., Kikuchi, A., and Kaibuchi, K. (1997a). Regulation of cross-linking of actin filament by IQGAP1, a target for Cdc42. The Journal of biological chemistry *272*, 29579-29583.
Fukata, M., Kuroda, S., Fujii, K., Nakamura, T., Shoji, I., Matsuura, Y., Okawa, K., Iwamatsu, A., Kikuchi, A., and Kaibuchi, K. (1997b). Regulation of cross-linking of actin filament by IQGAP1, a target for Cdc42. Journal of Biological Chemistry *272*, 29579-29583.
Fukata, M., Kuroda, S., Nakagawa, M., Kawajiri, A., Itoh, N., Shoji, I., Matsuura, Y., Yonehara, S., Fujisawa, H., and Kikuchi, A. (1999a). Cdc42 and Rac1 regulate the interaction of IQGAP1 with β-catenin. Journal of Biological Chemistry *274*, 26044-26050.
Fukata, M., Kuroda, S., Nakagawa, M., Kawajiri, A., Itoh, N., Shoji, I., Matsuura, Y., Yonehara, S., Fujisawa, H., Kikuchi, A*., et al.* (1999b). Cdc42 and Rac1 regulate the interaction of IQGAP1 with beta-catenin. The Journal of biological chemistry *274*, 26044-26050.
Fukata, M., Nakagawa, M., Itoh, N., Kawajiri, A., Yamaga, M., Kuroda, S., and Kaibuchi, K. (2001a). Involvement of IQGAP1, an effector of Rac1 and Cdc42 GTPases, in cell-cell dissociation during cell scattering. Molecular and cellular biology *21*, 2165-2183.
Fukata, M., Nakagawa, M., Itoh, N., Kawajiri, A., Yamaga, M., Kuroda, S., and Kaibuchi, K. (2001b). Involvement of IQGAP1, an effector of Rac1 and Cdc42 GTPases, in cell-cell dissociation during cell scattering. Molecular and cellular biology *21*, 2165-2183.
Fukata, M., Watanabe, T., Noritake, J., Nakagawa, M., Yamaga, M., Kuroda, S., Matsuura, Y., Iwamatsu, A., Perez, F., and Kaibuchi, K. (2002a). Rac1 and Cdc42 capture microtubules through IQGAP1 and CLIP-170. Cell *109*, 873-885.
Fukata, M., Watanabe, T., Noritake, J., Nakagawa, M., Yamaga, M., Kuroda, S., Matsuura, Y., Iwamatsu, A., Perez, F., and Kaibuchi, K. (2002b). Rac1 and Cdc42 capture microtubules through IQGAP1 and CLIP-170. Cell *109*, 873-885.
Garbett, D., and Bretscher, A. (2014). The surprising dynamics of scaffolding proteins. Molecular biology of the cell *25*, 2315-2319.
García-Ponce, A., Citalán-Madrid, A.F., Velázquez-Avila, M., Vargas-Robles, H., and Schnoor, M. (2015). The role of actin-binding proteins in the control of endothelial barrier integrity. Thrombosis and haemostasis *113*, 20-36.
Gardner, S., Maudsley, S., Millar, R.P., and Pawson, A.J. (2007). Nuclear stabilization of beta-catenin and inactivation of glycogen synthase kinase-3beta by gonadotropin-releasing hormone: targeting Wnt signaling in the pituitary gonadotrope. Molecular endocrinology (Baltimore, Md) *21*, 3028-3038.
Gardner, S., and Pawson, A.J. (2009). Emerging targets of the GnRH receptor: novel interactions with Wnt signalling mediators. Neuroendocrinology *89*, 241-251.
Gärtner, S., Gunesch, A., Knyazeva, T., Wolf, P., Högel, B., Eiermann, W., Ullrich, A., Knyazev, P., and Ataseven, B. (2014). PTK 7 is a transforming gene and prognostic marker for breast cancer and nodal metastasis involvement. PloS one *9*, e84472.
Gault, P.M., Maudsley, S., and Lincoln, G.A. (2003). Evidence that gonadotropin-releasing hormone II is not a physiological regulator of gonadotropin secretion in mammals. Journal of neuroendocrinology *15*, 831-839.
Gharib, S.D., Wierman, M.E., Shupnik, M.A., and Chin, W.W. (1990). Molecular biology of the pituitary gonadotropins. Endocrine reviews *11*, 177-199.
Godoy, J., Nishimura, M., and Webster, N.J. (2011). Gonadotropin-releasing hormone induces miR-132 and miR-212 to regulate cellular morphology and migration in immortalized LbetaT2 pituitary gonadotrope cells. Molecular endocrinology (Baltimore, Md) *25*, 810-820.
Golan, M., Hollander-Cohen, L., and Levavi-Sivan, B. (2016a). Stellate Cell Networks in the Teleost Pituitary. Scientific reports *6*, 24426.

Golan, M., Martin, A.O., Mollard, P., and Levavi-Sivan, B. (2016b). Anatomical and functional gonadotrope networks in the teleost pituitary. Scientific reports *6*, 23777.
Golub, T., and Caroni, P. (2005). PI(4,5)P2-dependent microdomain assemblies capture microtubules to promote and control leading edge motility. The Journal of cell biology *169*, 151-165.
Golubkov, V.S., and Strongin, A.Y. (2014). Downstream signaling and genome-wide regulatory effects of PTK7 pseudokinase and its proteolytic fragments in cancer cells. Cell communication and signaling : CCS *12*, 15.
Göngrich, C., García-González, D., Le Magueresse, C., Roth, L.C., Watanabe, Y., Burks, D.J., Grinevich, V., and Monyer, H. (2016). Electrotonic Coupling in the Pituitary Supports the Hypothalamic-Pituitary-Gonadal Axis in a Sex Specific Manner. Frontiers in molecular neuroscience *9*, 65.
Gordon, M.D., and Nusse, R. (2006). Wnt signaling: multiple pathways, multiple receptors, and multiple transcription factors. The Journal of biological chemistry *281*, 22429-22433.
Gorisse, L., Li, Z., Wagner, C.D., Worthylake, D.K., Zappacosta, F., Hedman, A.C., Annan, R.S., and Sacks, D.B. (2020). Ubiquitination of the scaffold protein IQGAP1 diminishes its interaction with and activation of the Rho GTPase CDC42. The Journal of biological chemistry *295*, 4822-4835.
Goto, T., Sato, A., Adachi, S., Iemura, S., Natsume, T., and Shibuya, H. (2013a). IQGAP1 protein regulates nuclear localization of β-catenin via importin-β5 protein in Wnt signaling. The Journal of biological chemistry *288*, 36351-36360.
Goto, T., Sato, A., Shimizu, M., Adachi, S., Satoh, K., Iemura, S., Natsume, T., and Shibuya, H. (2013b). IQGAP1 functions as a modulator of dishevelled nuclear localization in Wnt signaling. PloS one *8*, e60865.
Gracia-Navarro, F., Gonzalez-Reyes, J.A., Guerrero-Callejas, F., and Garcia-Herdugo, G. (1983). An electron microscopic study of stellate cells and cavities in the pars distalis of frog pituitary. Tissue & cell *15*, 729-736.
Graham, K.E., Nusser, K.D., and Low, M.J. (1999). LbetaT2 gonadotroph cells secrete follicle stimulating hormone (FSH) in response to active A. The Journal of endocrinology *162*, R1-5.
Gray, N.W., Kruchten, A.E., Chen, J., and McNiven, M.A. (2005). A dynamin-3 spliced variant modulates the actin/cortactin-dependent morphogenesis of dendritic spines. Journal of cell science *118*, 1279-1290.
Grimes, C.A., and Jope, R.S. (2001). The multifaceted roles of glycogen synthase kinase 3beta in cellular signaling. Progress in neurobiology *65*, 391-426.
Grohmanova, K., Schlaepfer, D., Hess, D., Gutierrez, P., Beck, M., and Kroschewski, R. (2004). Phosphorylation of IQGAP1 modulates its binding to Cdc42, revealing a new type of rho-GTPase regulator. The Journal of biological chemistry *279*, 48495-48504.
Grosse, R., Schmid, A., Schoneberg, T., Herrlich, A., Muhn, P., Schultz, G., and Gudermann, T. (2000a). Gonadotropin-releasing hormone receptor initiates multiple signaling pathways by exclusively coupling to $G_{q/11}$ proteins. J Biol Chem *275*, 9193-9200.
Grosse, R., Schmid, A., Schöneberg, T., Herrlich, A., Muhn, P., Schultz, G., and Gudermann, T. (2000b). Gonadotropin-releasing hormone receptor initiates multiple signaling pathways by exclusively coupling to G(q/11) proteins. The Journal of biological chemistry *275*, 9193-9200.
Guérineau, N.C., Bonnefont, X., Stoeckel, L., and Mollard, P. (1998). Synchronized spontaneous Ca2+ transients in acute anterior pituitary slices. The Journal of biological chemistry *273*, 10389-10395.
Gummow, B.M., Winnay, J.N., and Hammer, G.D. (2003). Convergence of Wnt signaling and steroidogenic factor-1 (SF-1) on transcription of the rat inhibin alpha gene. The Journal of biological chemistry *278*, 26572-26579.
Gundersen, G.G. (2002). Microtubule capture: IQGAP and CLIP-170 expand the repertoire. Current biology : CB *12*, R645-647.
Hagler, D.J., Jr., and Goda, Y. (1998). Synaptic adhesion: the building blocks of memory? Neuron *20*, 1059-1062.
Haisenleder, D.J., Burger, L.L., Walsh, H.E., Stevens, J., Aylor, K.W., Shupnik, M.A., and Marshall, J.C. (2008). Pulsatile gonadotropin-releasing hormone stimulation of gonadotropin subunit transcription in rat

pituitaries: evidence for the involvement of Jun N-terminal kinase but not p38. Endocrinology *149*, 139-145.
Haisenleder, D.J., Cox, M.E., Parsons, S.J., and Marshall, J.C. (1998). Gonadotropin-releasing hormone pulses are required to maintain activation of mitogen-activated protein kinase: role in stimulation of gonadotrope gene expression. Endocrinology *139*, 3104-3111.
Haisenleder, D.J., Dalkin, A.C., Ortolano, G.A., Marshall, J.C., and Shupnik, M.A. (1991). A pulsatile gonadotropin-releasing hormone stimulus is required to increase transcription of the gonadotropin subunit genes: evidence for differential regulation of transcription by pulse frequency in vivo. Endocrinology *128*, 509-517.
Hall, A. (2012). Rho family GTPases. Biochemical Society transactions *40*, 1378-1382.
Halvorson, L.M., Ito, M., Jameson, J.L., and Chin, W.W. (1998). Steroidogenic factor-1 and early growth response protein 1 act through two composite DNA binding sites to regulate luteinizing hormone beta-subunit gene expression. The Journal of biological chemistry *273*, 14712-14720.
Halvorson, L.M., Kaiser, U.B., and Chin, W.W. (1999). The protein kinase C system acts through the early growth response protein 1 to increase LHbeta gene expression in synergy with steroidogenic factor-1. Molecular endocrinology (Baltimore, Md) *13*, 106-116.
Hanna, S., and El-Sibai, M. (2013). Signaling networks of Rho GTPases in cell motility. Cellular signalling *25*, 1955-1961.
Harris, D., Bonfil, D., Chuderland, D., Kraus, S., Seger, R., and Naor, Z. (2002). Activation of MAPK cascades by GnRH: ERK and Jun N-terminal kinase are involved in basal and GnRH-stimulated activity of the glycoprotein hormone LHbeta-subunit promoter. Endocrinology *143*, 1018-1025.
Harris, D., Chuderland, D., Bonfil, D., Kraus, S., Seger, R., and Naor, Z. (2003). Extracellular signal-regulated kinase and c-Src, but not Jun N-terminal kinase, are involved in basal and gonadotropin-releasing hormone-stimulated activity of the glycoprotein hormone alpha-subunit promoter. Endocrinology *144*, 612-622.
Hart, M.J., Callow, M.G., Souza, B., and Polakis, P. (1996). IQGAP1, a calmodulin-binding protein with a rasGAP-related domain, is a potential effector for cdc42Hs. The EMBO journal *15*, 2997-3005.
Hartsock, A., and Nelson, W.J. (2008). Adherens and tight junctions: structure, function and connections to the actin cytoskeleton. Biochimica et biophysica acta *1778*, 660-669.
Harwood, N.E., and Batista, F.D. (2008). New insights into the early molecular events underlying B cell activation. Immunity *28*, 609-619.
Hattori, K., Shirasawa, N., Suzuki, H., Otsuka, T., Wada, I., Yashiro, T., Herbert, D.C., Soji, T., and Hashitani, H. (2013). Intercellular communication within the rat anterior pituitary gland. XV. Properties of spontaneous and LHRH-induced Ca2+ transients in the transitional zone of the rat anterior pituitary in situ. Endocrinology *154*, 400-409.
Hayes, M., Naito, M., Daulat, A., Angers, S., and Ciruna, B. (2013). Ptk7 promotes non-canonical Wnt/PCP-mediated morphogenesis and inhibits Wnt/β-catenin-dependent cell fate decisions during vertebrate development. Development (Cambridge, England) *140*, 1807-1818.
Hearn, M.T., and Gomme, P.T. (2000). Molecular architecture and biorecognition processes of the cystine knot protein superfamily: part I. The glycoprotein hormones. Journal of molecular recognition : JMR *13*, 223-278.
Hecht, A., Vleminckx, K., Stemmler, M.P., van Roy, F., and Kemler, R. (2000). The p300/CBP acetyltransferases function as transcriptional coactivators of beta-catenin in vertebrates. The EMBO journal *19*, 1839-1850.
Hedman, A.C., Smith, J.M., and Sacks, D.B. (2015). The biology of IQGAP proteins: beyond the cytoskeleton. EMBO reports *16*, 427-446.
Hemsath, L., Dvorsky, R., Fiegen, D., Carlier, M.F., and Ahmadian, M.R. (2005). An electrostatic steering mechanism of Cdc42 recognition by Wiskott-Aldrich syndrome proteins. Molecular cell *20*, 313-324.
Herbert, D.C. (1979). Intercellular junctions in the rhesus monkey pars distalis. The Anatomical record *195*, 1-5.

Herbison, A.E., Porteous, R., Pape, J.R., Mora, J.M., and Hurst, P.R. (2008). Gonadotropin-releasing hormone neuron requirements for puberty, ovulation, and fertility. Endocrinology *149*, 597-604.
Herrero, A., Pinto, A., Colón-Bolea, P., Casar, B., Jones, M., Agudo-Ibáñez, L., Vidal, R., Tenbaum, S.P., Nuciforo, P., Valdizán, E.M.*, et al.* (2015). Small Molecule Inhibition of ERK Dimerization Prevents Tumorigenesis by RAS-ERK Pathway Oncogenes. Cancer cell *28*, 170-182.
Heuberger, J., and Birchmeier, W. (2010). Interplay of cadherin-mediated cell adhesion and canonical Wnt signaling. Cold Spring Harbor perspectives in biology *2*, a002915.
Hino, S., Tanji, C., Nakayama, K.I., and Kikuchi, A. (2005). Phosphorylation of beta-catenin by cyclic AMP-dependent protein kinase stabilizes beta-catenin through inhibition of its ubiquitination. Molecular and cellular biology *25*, 9063-9072.
Ho, Y.-D., Joyal, J.L., Li, Z., and Sacks, D.B. (1999a). IQGAP1 integrates Ca2+/calmodulin and Cdc42 signaling. Journal of Biological Chemistry *274*, 464-470.
Ho, Y.D., Joyal, J.L., Li, Z., and Sacks, D.B. (1999b). IQGAP1 integrates Ca2+/calmodulin and Cdc42 signaling. The Journal of biological chemistry *274*, 464-470.
Hodson, D.J., Romanò, N., Schaeffer, M., Fontanaud, P., Lafont, C., Fiordelisio, T., and Mollard, P. (2012a). Coordination of calcium signals by pituitary endocrine cells in situ. Cell calcium *51*, 222-230.
Hodson, D.J., Schaeffer, M., Romanò, N., Fontanaud, P., Lafont, C., Birkenstock, J., Molino, F., Christian, H., Lockey, J., Carmignac, D.*, et al.* (2012b). Existence of long-lasting experience-dependent plasticity in endocrine cell networks. Nature communications *3*, 605.
Hoesel, B., and Schmid, J.A. (2013). The complexity of NF-κB signaling in inflammation and cancer. Molecular cancer *12*, 86.
Hofmann, W.A. (2009). Cell and molecular biology of nuclear actin. International review of cell and molecular biology *273*, 219-263.
Horn, F., Bilezikjian, L.M., Perrin, M.H., Bosma, M.M., Windle, J.J., Huber, K.S., Blount, A.L., Hille, B., Vale, W., and Mellon, P.L. (1991). Intracellular responses to gonadotropin-releasing hormone in a clonal cell line of the gonadotrope lineage. Molecular endocrinology (Baltimore, Md) *5*, 347-355.
Horvat, R.D., Roess, D.A., Nelson, S.E., Barisas, B.G., and Clay, C.M. (2001). Binding of agonist but not antagonist leads to fluorescence resonance energy transfer between intrinsically fluorescent gonadotropin-releasing hormone receptors. Molecular endocrinology (Baltimore, Md) *15*, 695-703.
Hu, Q., Milenkovic, L., Jin, H., Scott, M.P., Nachury, M.V., Spiliotis, E.T., and Nelson, W.J. (2010). A septin diffusion barrier at the base of the primary cilium maintains ciliary membrane protein distribution. Science (New York, NY) *329*, 436-439.
Hu, W., Wang, Z., Zhang, S., Lu, X., Wu, J., Yu, K., Ji, A., Lu, W., Wang, Z., Wu, J.*, et al.* (2019). IQGAP1 promotes pancreatic cancer progression and epithelial-mesenchymal transition (EMT) through Wnt/β-catenin signaling. Scientific reports *9*, 7539.
Huang da, W., Sherman, B.T., and Lempicki, R.A. (2009). Systematic and integrative analysis of large gene lists using DAVID bioinformatics resources. Nature protocols *4*, 44-57.
Husi, H., Ward, M.A., Choudhary, J.S., Blackstock, W.P., and Grant, S.G. (2000). Proteomic analysis of NMDA receptor-adhesion protein signaling complexes. Nat Neurosci *3*, 661-669.
Iida, T., Stojilković, S.S., Izumi, S., and Catt, K.J. (1991). Spontaneous and agonist-induced calcium oscillations in pituitary gonadotrophs. Molecular endocrinology (Baltimore, Md) *5*, 949-958.
Ikeda, Y., Luo, X., Abbud, R., Nilson, J.H., and Parker, K.L. (1995). The nuclear receptor steroidogenic factor 1 is essential for the formation of the ventromedial hypothalamic nucleus. Molecular endocrinology (Baltimore, Md) *9*, 478-486.
Itoh, J., Kawai, K., Serizawa, A., Yasumura, K., Ogawa, K., and Osamura, R.Y. (2000). A new approach to three-dimensional reconstructed imaging of hormone-secreting cells and their microvessel environments in rat pituitary glands by confocal laser scanning microscopy. The journal of histochemistry and cytochemistry : official journal of the Histochemistry Society *48*, 569-578.
Itoh, J., Serizawa, A., Kawai, K., Ishii, Y., Teramoto, A., and Osamura, R.Y. (2003). Vascular networks and endothelial cells in the rat experimental pituitary glands and in the human pituitary adenomas. Microscopy research and technique *60*, 231-235.

Itoh, N., Nagai, T., Watanabe, T., Taki, K., Nabeshima, T., Kaibuchi, K., and Yamada, K. (2017). Valosin-containing protein (VCP) is a novel IQ motif-containing GTPase activating protein 1 (IQGAP1)-interacting protein. Biochemical and biophysical research communications *493*, 1384-1389.
Izumi, G., Sakisaka, T., Baba, T., Tanaka, S., Morimoto, K., and Takai, Y. (2004). Endocytosis of E-cadherin regulated by Rac and Cdc42 small G proteins through IQGAP1 and actin filaments. The Journal of cell biology *166*, 237-248.
Jacinto, E., Loewith, R., Schmidt, A., Lin, S., Rüegg, M.A., Hall, A., and Hall, M.N. (2004). Mammalian TOR complex 2 controls the actin cytoskeleton and is rapamycin insensitive. Nature cell biology *6*, 1122-1128.
Jacquemet, G., and Humphries, M.J. (2013). IQGAP1 is a key node within the small GTPase network. Small GTPases *4*, 199-207.
Jaiswal, M., Fansa, E.K., Dvorsky, R., and Ahmadian, M.R. (2013). New insight into the molecular switch mechanism of human Rho family proteins: shifting a paradigm. Biological chemistry *394*, 89-95.
Jameson, K.L., Mazur, P.K., Zehnder, A.M., Zhang, J., Zarnegar, B., Sage, J., and Khavari, P.A. (2013). IQGAP1 scaffold-kinase interaction blockade selectively targets RAS-MAP kinase-driven tumors. Nature medicine *19*, 626-630.
Janjic, M.M., Stojilkovic, S.S., and Bjelobaba, I. (2017). Intrinsic and Regulated Gonadotropin-Releasing Hormone Receptor Gene Transcription in Mammalian Pituitary Gonadotrophs. Frontiers in endocrinology *8*, 221.
Jausoro, I., Mestres, I., Quassollo, G., Masseroni, L., Heredia, F., and Caceres, A. (2013). Regulation of spine density and morphology by IQGAP1 protein domains. PloS one *8*, e56574.
Jeong, H.W., Li, Z., Brown, M.D., and Sacks, D.B. (2007). IQGAP1 binds Rap1 and modulates its activity. The Journal of biological chemistry *282*, 20752-20762.
Johnson, M., Sharma, M., Brocardo, M.G., and Henderson, B.R. (2011). IQGAP1 translocates to the nucleus in early S-phase and contributes to cell cycle progression after DNA replication arrest. The international journal of biochemistry & cell biology *43*, 65-73.
Johnson, M., Sharma, M., and Henderson, B.R. (2009). IQGAP1 regulation and roles in cancer. Cellular signalling *21*, 1471-1478.
Johnson, M.A., Sharma, M., Mok, M.T., and Henderson, B.R. (2013). Stimulation of in vivo nuclear transport dynamics of actin and its co-factors IQGAP1 and Rac1 in response to DNA replication stress. Biochimica et Biophysica Acta (BBA)-Molecular Cell Research *1833*, 2334-2347.
Jope, R.S., and Johnson, G.V. (2004). The glamour and gloom of glycogen synthase kinase-3. Trends in biochemical sciences *29*, 95-102.
Jorgensen, J.S., Quirk, C.C., and Nilson, J.H. (2004). Multiple and overlapping combinatorial codes orchestrate hormonal responsiveness and dictate cell-specific expression of the genes encoding luteinizing hormone. Endocrine reviews *25*, 521-542.
Joyal, J.L., Annan, R.S., Ho, Y.-D., Huddleston, M.E., Carr, S.A., Hart, M.J., and Sacks, D.B. (1997a). Calmodulin modulates the interaction between IQGAP1 and Cdc42: identification of IQGAP1 by nanoelectrospray tandem mass spectrometry. Journal of Biological Chemistry *272*, 15419-15425.
Joyal, J.L., Annan, R.S., Ho, Y.D., Huddleston, M.E., Carr, S.A., Hart, M.J., and Sacks, D.B. (1997b). Calmodulin modulates the interaction between IQGAP1 and Cdc42. Identification of IQGAP1 by nanoelectrospray tandem mass spectrometry. The Journal of biological chemistry *272*, 15419-15425.
Junghans, D., Haas, I.G., and Kemler, R. (2005). Mammalian cadherins and protocadherins: about cell death, synapses and processing. Current opinion in cell biology *17*, 446-452.
Kaibuchi, K., Kuroda, S., and Amano, M. (1999a). Regulation of the cytoskeleton and cell adhesion by the Rho family GTPases in mammalian cells. Annual review of biochemistry *68*, 459-486.
Kaibuchi, K., Kuroda, S., Fukata, M., and Nakagawa, M. (1999b). Regulation of cadherin-mediated cell-cell adhesion by the Rho family GTPases. Current opinion in cell biology *11*, 591-596.
Kaiser, U.B., Halvorson, L.M., and Chen, M.T. (2000). Sp1, steroidogenic factor 1 (SF-1), and early growth response protein 1 (egr-1) binding sites form a tripartite gonadotropin-releasing hormone response

element in the rat luteinizing hormone-beta gene promoter: an integral role for SF-1. Molecular endocrinology (Baltimore, Md) *14*, 1235-1245.
Kaiser, U.B., Jakubowiak, A., Steinberger, A., and Chin, W.W. (1997). Differential effects of gonadotropin-releasing hormone (GnRH) pulse frequency on gonadotropin subunit and GnRH receptor messenger ribonucleic acid levels in vitro. Endocrinology *138*, 1224-1231.
Kaiser, U.B., Sabbagh, E., Chen, M.T., Chin, W.W., and Saunders, B.D. (1998). Sp1 binds to the rat luteinizing hormone beta (LHbeta) gene promoter and mediates gonadotropin-releasing hormone-stimulated expression of the LHbeta subunit gene. The Journal of biological chemistry *273*, 12943-12951.
Käll, L., Storey, J.D., MacCoss, M.J., and Noble, W.S. (2008). Assigning significance to peptides identified by tandem mass spectrometry using decoy databases. Journal of proteome research *7*, 29-34.
Kanasaki, H., Bedecarrats, G.Y., Kam, K.Y., Xu, S., and Kaiser, U.B. (2005). Gonadotropin-releasing hormone pulse frequency-dependent activation of extracellular signal-regulated kinase pathways in perifused LbetaT2 cells. Endocrinology *146*, 5503-5513.
Kanasaki, H., Purwana, I., Oride, A., Mijiddorj, T., and Miyazaki, K. (2012). Extracellular Signal-Regulated Kinase (ERK) Activation and Mitogen-Activated Protein Kinase Phosphatase 1 Induction by Pulsatile Gonadotropin-Releasing Hormone in Pituitary Gonadotrophs. Journal of signal transduction *2012*, 198527.
Kawakami, S., Fujii, Y., Okada, Y., and Winters, S.J. (2002). Paracrine regulation of FSH by follistatin in folliculostellate cell-enriched primate pituitary cell cultures. Endocrinology *143*, 2250-2258.
Keely, P.J., Rusyn, E.V., Cox, A.D., and Parise, L.V. (1999). R-Ras signals through specific integrin alpha cytoplasmic domains to promote migration and invasion of breast epithelial cells. The Journal of cell biology *145*, 1077-1088.
Keller, A., Nesvizhskii, A.I., Kolker, E., and Aebersold, R. (2002). Empirical statistical model to estimate the accuracy of peptide identifications made by MS/MS and database search. Analytical chemistry *74*, 5383-5392.
Kelly, C., McClenaghan, N.H., and Flatt, P.R. (2011). Role of islet structure and cellular interactions in the control of insulin secretion. Islets *3*, 41-47.
Keshet, Y., and Seger, R. (2010). The MAP kinase signaling cascades: a system of hundreds of components regulates a diverse array of physiological functions. Methods in molecular biology (Clifton, NJ) *661*, 3-38.
Khokhlatchev, A.V., Canagarajah, B., Wilsbacher, J., Robinson, M., Atkinson, M., Goldsmith, E., and Cobb, M.H. (1998). Phosphorylation of the MAP kinase ERK2 promotes its homodimerization and nuclear translocation. Cell *93*, 605-615.
Kholmanskikh, S.S., Koeller, H.B., Wynshaw-Boris, A., Gomez, T., Letourneau, P.C., and Ross, M.E. (2006). Calcium-dependent interaction of Lis1 with IQGAP1 and Cdc42 promotes neuronal motility. Nature neuroscience *9*, 50-57.
Kikuchi, A., Kishida, S., and Yamamoto, H. (2006). Regulation of Wnt signaling by protein-protein interaction and post-translational modifications. Experimental & molecular medicine *38*, 1-10.
Kim, H., White, C.D., and Sacks, D.B. (2011). IQGAP1 in microbial pathogenesis: Targeting the actin cytoskeleton. FEBS letters *585*, 723-729.
Kim, J.H., Xu, E.Y., Sacks, D.B., Lee, J., Shu, L., Xia, B., and Kong, A.N. (2013). Identification and functional studies of a new Nrf2 partner IQGAP1: a critical role in the stability and transactivation of Nrf2. Antioxidants & redox signaling *19*, 89-101.
Kim, S.H., Li, Z., and Sacks, D.B. (2000). E-cadherin-mediated cell-cell attachment activates Cdc42. The Journal of biological chemistry *275*, 36999-37005.
Kim, T.J., Kim, M., Kim, H.M., Lim, S.A., Kim, E.O., Kim, K., Song, K.H., Kim, J., Kumar, V., Yee, C., *et al.* (2014). Homotypic NK cell-to-cell communication controls cytokine responsiveness of innate immune NK cells. Scientific reports *4*, 7157.
Kishimoto, A., Mikawa, K., Hashimoto, K., Yasuda, I., Tanaka, S., Tominaga, M., Kuroda, T., and Nishizuka, Y. (1989). Limited proteolysis of protein kinase C subspecies by calcium-dependent neutral protease (calpain). The Journal of biological chemistry *264*, 4088-4092.

Knobil, E. (1974). On the control of gonadotropin secretion in the rhesus monkey. Recent progress in hormone research *30*, 1-46.
Kolch, W. (2005). Coordinating ERK/MAPK signalling through scaffolds and inhibitors. Nature reviews Molecular cell biology *6*, 827-837.
Kondoh, K., and Nishida, E. (2007). Regulation of MAP kinases by MAP kinase phosphatases. Biochimica et biophysica acta *1773*, 1227-1237.
Kortum, R.L., Costanzo, D.L., Haferbier, J., Schreiner, S.J., Razidlo, G.L., Wu, M.H., Volle, D.J., Mori, T., Sakaue, H., Chaika, N.V.*, et al.* (2005). The molecular scaffold kinase suppressor of Ras 1 (KSR1) regulates adipogenesis. Molecular and cellular biology *25*, 7592-7604.
Kortum, R.L., Johnson, H.J., Costanzo, D.L., Volle, D.J., Razidlo, G.L., Fusello, A.M., Shaw, A.S., and Lewis, R.E. (2006). The molecular scaffold kinase suppressor of Ras 1 is a modifier of RasV12-induced and replicative senescence. Molecular and cellular biology *26*, 2202-2214.
Koziel, K., Lebiedzinska, M., Szabadkai, G., Onopiuk, M., Brutkowski, W., Wierzbicka, K., Wilczynski, G., Pinton, P., Duszynski, J., Zablocki, K.*, et al.* (2009). Plasma membrane associated membranes (PAM) from Jurkat cells contain STIM1 protein is PAM involved in the capacitative calcium entry? Int J Biochem Cell Biol *41*, 2440-2449.
Kumar, T.R. (2016). Mouse Models for the Study of Synthesis, Secretion, and Action of Pituitary Gonadotropins. Progress in molecular biology and translational science *143*, 49-84.
Kurella, V.B., Richard, J.M., Parke, C.L., LeCour, L.F., Bellamy, H.D., and Worthylake, D.K. (2009a). Crystal structure of the GTPase-activating protein-related domain from IQGAP1. Journal of Biological Chemistry *284*, 14857-14865.
Kurella, V.B., Richard, J.M., Parke, C.L., Lecour, L.F., Jr., Bellamy, H.D., and Worthylake, D.K. (2009b). Crystal structure of the GTPase-activating protein-related domain from IQGAP1. The Journal of biological chemistry *284*, 14857-14865.
Kuroda, S., Fukata, M., Kobayashi, K., Nakafuku, M., Nomura, N., Iwamatsu, A., and Kaibuchi, K. (1996). Identification of IQGAP as a putative target for the small GTPases, Cdc42 and Rac1. The Journal of biological chemistry *271*, 23363-23367.
Kuroda, S., Fukata, M., Nakagawa, M., Fujii, K., Nakamura, T., Ookubo, T., Izawa, I., Nagase, T., Nomura, N., and Tani, H. (1998a). Role of IQGAP1, a target of the small GTPases Cdc42 and Rac1, in regulation of E-cadherin-mediated cell-cell adhesion. Science (New York, NY) *281*, 832-835.
Kuroda, S., Fukata, M., Nakagawa, M., Fujii, K., Nakamura, T., Ookubo, T., Izawa, I., Nagase, T., Nomura, N., Tani, H.*, et al.* (1998b). Role of IQGAP1, a target of the small GTPases Cdc42 and Rac1, in regulation of E-cadherin- mediated cell-cell adhesion. Science (New York, NY) *281*, 832-835.
Kuroda, S., Fukata, M., Nakagawa, M., and Kaibuchi, K. (1999). Cdc42, Rac1, and their effector IQGAP1 as molecular switches for cadherin-mediated cell-cell adhesion. Biochemical and biophysical research communications *262*, 1-6.
Kwiatkowski, D.J., Janmey, P.A., and Yin, H.L. (1989). Identification of critical functional and regulatory domains in gelsolin. The Journal of cell biology *108*, 1717-1726.
Kwong, L., Wozniak, M.A., Collins, A.S., Wilson, S.D., and Keely, P.J. (2003). R-Ras promotes focal adhesion formation through focal adhesion kinase and p130(Cas) by a novel mechanism that differs from integrins. Molecular and cellular biology *23*, 933-949.
Kyriakis, J.M., and Avruch, J. (2001). Mammalian mitogen-activated protein kinase signal transduction pathways activated by stress and inflammation. Physiological reviews *81*, 807-869.
Lamkin, W.M., Fujino, M., Mayfield, J.D., Holcomb, G.N., and Ward, D.N. (1970). Separation of the subunits of ovine luteinizing hormone by a chromatographic procedure and comparison with a countercurrent distribution procedure. Biochimica et biophysica acta *214*, 290-298.
Lampugnani, M.G., Zanetti, A., Breviario, F., Balconi, G., Orsenigo, F., Corada, M., Spagnuolo, R., Betson, M., Braga, V., and Dejana, E. (2002). VE-cadherin regulates endothelial actin activating Rac and increasing membrane association of Tiam. Molecular biology of the cell *13*, 1175-1189.
Lapthorn, A.J., Harris, D.C., Littlejohn, A., Lustbader, J.W., Canfield, R.E., Machin, K.J., Morgan, F.J., and Isaacs, N.W. (1994). Crystal structure of human chorionic gonadotropin. Nature *369*, 455-461.

Lavoie, H., Sahmi, M., Maisonneuve, P., Marullo, S.A., Thevakumaran, N., Jin, T., Kurinov, I., Sicheri, F., and Therrien, M. (2018). MEK drives BRAF activation through allosteric control of KSR proteins. Nature *554*, 549-553.
Lawrence, P.A., and Casal, J. (2018). Planar cell polarity: two genetic systems use one mechanism to read gradients. Development (Cambridge, England) *145*.
Lawson, M.A., Tsutsumi, R., Zhang, H., Talukdar, I., Butler, B.K., Santos, S.J., Mellon, P.L., and Webster, N.J. (2007). Pulse sensitivity of the luteinizing hormone beta promoter is determined by a negative feedback loop Involving early growth response-1 and Ngfi-A binding protein 1 and 2. Molecular endocrinology (Baltimore, Md) *21*, 1175-1191.
Le Clainche, C., Schlaepfer, D., Ferrari, A., Klingauf, M., Grohmanova, K., Veligodskiy, A., Didry, D., Le, D., Egile, C., Carlier, M.F*., et al.* (2007). IQGAP1 stimulates actin assembly through the N-WASP-Arp2/3 pathway. The Journal of biological chemistry *282*, 426-435.
Le Tissier, P., Campos, P., Lafont, C., Romanò, N., Hodson, D.J., and Mollard, P. (2017). An updated view of hypothalamic-vascular-pituitary unit function and plasticity. Nature reviews Endocrinology *13*, 257-267.
Lebiedzinska, M., Szabadkai, G., Jones, A.W., Duszynski, J., and Wieckowski, M.R. (2009). Interactions between the endoplasmic reticulum, mitochondria, plasma membrane and other subcellular organelles. The international journal of biochemistry & cell biology *41*, 1805-1816.
LeCour, L., Boyapati, V.K., Liu, J., Li, Z., Sacks, D.B., and Worthylake, D.K. (2016a). The structural basis for Cdc42-induced dimerization of IQGAPs. Structure (London, England : 1993) *24*, 1499-1508.
LeCour, L., Jr., Boyapati, V.K., Liu, J., Li, Z., Sacks, D.B., and Worthylake, D.K. (2016b). The Structural Basis for Cdc42-Induced Dimerization of IQGAPs. Structure (London, England : 1993) *24*, 1499-1508.
Lee, J., Andreeva, A., Sipe, C.W., Liu, L., Cheng, A., and Lu, X. (2012). PTK7 regulates myosin II activity to orient planar polarity in the mammalian auditory epithelium. Current biology : CB *22*, 956-966.
Lee, S.L., Sadovsky, Y., Swirnoff, A.H., Polish, J.A., Goda, P., Gavrilina, G., and Milbrandt, J. (1996). Luteinizing hormone deficiency and female infertility in mice lacking the transcription factor NGFI-A (Egr-1). Science (New York, NY) *273*, 1219-1221.
Lee, S.L., Tourtellotte, L.C., Wesselschmidt, R.L., and Milbrandt, J. (1995). Growth and differentiation proceeds normally in cells deficient in the immediate early gene NGFI-A. The Journal of biological chemistry *270*, 9971-9977.
Lei, Y., Kim, S.E., Chen, Z., Cao, X., Zhu, H., Yang, W., Shaw, G.M., Zheng, Y., Zhang, T., Wang, H.Y*., et al.* (2019). Variants identified in PTK7 associated with neural tube defects. Molecular genetics & genomic medicine *7*, e00584.
Leong, D.A. (1991). A model for intracellular calcium signaling and the coordinate regulation of hormone biosynthesis, receptors and secretion. Cell calcium *12*, 255-268.
Leong, D.A., and Thorner, M.O. (1991). A potential code of luteinizing hormone-releasing hormone-induced calcium ion responses in the regulation of luteinizing hormone secretion among individual gonadotropes. The Journal of biological chemistry *266*, 9016-9022.
Levavi-Sivan, B., Bloch, C.L., Gutnick, M.J., and Fleidervish, I.A. (2005). Electrotonic coupling in the anterior pituitary of a teleost fish. Endocrinology *146*, 1048-1052.
Levi, N.L., Hanoch, T., Benard, O., Rozenblat, M., Harris, D., Reiss, N., Naor, Z., and Seger, R. (1998a). Stimulation of Jun N-terminal kinase (JNK) by gonadotropin-releasing hormone in pituitary alpha T3-1 cell line is mediated by protein kinase C, c-Src, and CDC42. Molecular endocrinology (Baltimore, Md) *12*, 815-824.
Levi, N.L., Hanoch, T., Benard, O., Rozenblat, M., Harris, D., Reiss, N., Naor, Z., and Seger, R. (1998b). Stimulation of Jun N-terminal kinase (JNK) by gonadotropin-releasing hormone in pituitary aT3-1 cell line is mediated by protein kinase C, c-Src, and CDC42. Molecular endocrinology *12*, 815-824.
Lewis, K.A., Gray, P.C., Blount, A.L., MacConell, L.A., Wiater, E., Bilezikjian, L.M., and Vale, W. (2000). Betaglycan binds inhibin and can mediate functional antagonism of activin signalling. Nature *404*, 411-414.

Lhoumeau, A.C., Puppo, F., Prébet, T., Kodjabachian, L., and Borg, J.P. (2011). PTK7: a cell polarity receptor with multiple facets. Cell cycle (Georgetown, Tex) *10*, 1233-1236.
Li, C.H., and Starman, B. (1964). MOLECULAR WEIGHT OF SHEEP PITUITARY INTERSTITIAL CELL-STIMULATING HORMONE. Nature *202*, 291-292.
Li, Q., and Stuenkel, E.L. (2004). Calcium negatively modulates calmodulin interaction with IQGAP1. Biochemical and biophysical research communications *317*, 787-795.
Li, R., Debreceni, B., Jia, B., Gao, Y., Tigyi, G., and Zheng, Y. (1999a). Localization of the PAK1-, WASP-, and IQGAP1-specifying regions of Cdc42. The Journal of biological chemistry *274*, 29648-29654.
Li, Z., Kim, S.H., Higgins, J.M., Brenner, M.B., and Sacks, D.B. (1999b). IQGAP1 and calmodulin modulate E-cadherin function. The Journal of biological chemistry *274*, 37885-37892.
Li, Z., Kim, S.H., Higgins, J.M., Brenner, M.B., and Sacks, D.B. (1999c). IQGAP1 and calmodulin modulate E-cadherin function. Journal of Biological Chemistry *274*, 37885-37892.
Li, Z., McNulty, D.E., Marler, K.J., Lim, L., Hall, C., Annan, R.S., and Sacks, D.B. (2005a). IQGAP1 promotes neurite outgrowth in a phosphorylation-dependent manner. Journal of Biological Chemistry *280*, 13871-13878.
Li, Z., McNulty, D.E., Marler, K.J., Lim, L., Hall, C., Annan, R.S., and Sacks, D.B. (2005b). IQGAP1 promotes neurite outgrowth in a phosphorylation-dependent manner. The Journal of biological chemistry *280*, 13871-13878.
Liao, T.H., and Pierce, J.G. (1970). The presence of a common type of subunit in bovine thyroid-stimulating and luteinizing hormones. The Journal of biological chemistry *245*, 3275-3281.
Lichtig, H., Cohen, Y., Bin-Nun, N., Golubkov, V., and Frank, D. (2019). PTK7 proteolytic fragment proteins function during early Xenopus development. Developmental biology *453*, 48-55.
Lilien, J., and Balsamo, J. (2005). The regulation of cadherin-mediated adhesion by tyrosine phosphorylation/dephosphorylation of beta-catenin. Current opinion in cell biology *17*, 459-465.
Lippincott, J., and Li, R. (1998). Sequential assembly of myosin II, an IQGAP-like protein, and filamentous actin to a ring structure involved in budding yeast cytokinesis. The Journal of cell biology *140*, 355-366.
Liu, F., Austin, D.A., Mellon, P.L., Olefsky, J.M., and Webster, N.J. (2002). GnRH activates ERK1/2 leading to the induction of c-fos and LHbeta protein expression in LbetaT2 cells. Molecular endocrinology (Baltimore, Md) *16*, 419-434.
Liu, J., Guidry, J.J., and Worthylake, D.K. (2014). Conserved sequence repeats of IQGAP1 mediate binding to Ezrin. Journal of proteome research *13*, 1156-1166.
Liu, Z., Liu, D., Bojdani, E., El-Naggar, A.K., Vasko, V., and Xing, M. (2010). IQGAP1 plays an important role in the invasiveness of thyroid cancer. Clinical cancer research : an official journal of the American Association for Cancer Research *16*, 6009-6018.
Logan, C.Y., and Nusse, R. (2004). The Wnt signaling pathway in development and disease. Annual review of cell and developmental biology *20*, 781-810.
Logue, J.S., Whiting, J.L., Tunquist, B., Sacks, D.B., Langeberg, L.K., Wordeman, L., and Scott, J.D. (2011a). AKAP220 protein organizes signaling elements that impact cell migration. Journal of Biological Chemistry *286*, 39269-39281.
Logue, J.S., Whiting, J.L., Tunquist, B., Sacks, D.B., Langeberg, L.K., Wordeman, L., and Scott, J.D. (2011b). AKAP220 protein organizes signaling elements that impact cell migration. The Journal of biological chemistry *286*, 39269-39281.
Lu, X., Borchers, A.G., Jolicoeur, C., Rayburn, H., Baker, J.C., and Tessier-Lavigne, M. (2004). PTK7/CCK-4 is a novel regulator of planar cell polarity in vertebrates. Nature *430*, 93-98.
Lui, W.Y., Mruk, D.D., and Cheng, C.Y. (2005). Interactions among IQGAP1, Cdc42, and the cadherin/catenin protein complex regulate Sertoli-germ cell adherens junction dynamics in the testis. Journal of cellular physiology *202*, 49-66.
Lyles, D., Tien, J.H., McCobb, D.P., and Zeeman, M.L. (2010). Pituitary network connectivity as a mechanism for the luteinising hormone surge. Journal of neuroendocrinology *22*, 1267-1278.

Mabuchi, Y., Shirasawa, N., Sakuma, E., Hashimoto, Y., Kuno, M., Coombs, R.J., Herbert, D.C., and Soji, T. (2004). Intercellular communication within the rat anterior pituitary: relationship between LH-RH neurons and folliculo-stellate cells in the pars tuberalis. Cell Tissue Res *317*, 79-90.
MacDonald, B.T., Tamai, K., and He, X. (2009). Wnt/beta-catenin signaling: components, mechanisms, and diseases. Developmental cell *17*, 9-26.
Machesky, L.M. (1998). Cytokinesis: IQGAPs find a function. Current biology : CB *8*, R202-205.
Malarkannan, S., Awasthi, A., Rajasekaran, K., Kumar, P., Schuldt, K.M., Bartoszek, A., Manoharan, N., Goldner, N.K., Umhoefer, C.M., and Thakar, M.S. (2012). IQGAP1: a regulator of intracellular spacetime relativity. Journal of immunology (Baltimore, Md : 1950) *188*, 2057-2063.
Mann, B., Gelos, M., Siedow, A., Hanski, M.L., Gratchev, A., Ilyas, M., Bodmer, W.F., Moyer, M.P., Riecken, E.O., Buhr, H.J*., et al.* (1999). Target genes of beta-catenin-T cell-factor/lymphoid-enhancer-factor signaling in human colorectal carcinomas. Proceedings of the National Academy of Sciences of the United States of America *96*, 1603-1608.
Marambaud, P., Wen, P.H., Dutt, A., Shioi, J., Takashima, A., Siman, R., and Robakis, N.K. (2003). A CBP binding transcriptional repressor produced by the PS1/epsilon-cleavage of N-cadherin is inhibited by PS1 FAD mutations. Cell *114*, 635-645.
Marshall, C.J. (1995). Specificity of receptor tyrosine kinase signaling: transient versus sustained extracellular signal-regulated kinase activation. Cell *80*, 179-185.
Marshall, M.R., Clark, J.P., 3rd, Westenbroek, R., Yu, F.H., Scheuer, T., and Catterall, W.A. (2011). Functional roles of a C-terminal signaling complex of CaV1 channels and A-kinase anchoring protein 15 in brain neurons. The Journal of biological chemistry *286*, 12627-12639.
Martín-Vega, A., Ruiz-Peinado, L., García-Gómez, R., Herrero, A., de la Fuente-Vivas, D., Parvathaneni, S., Caloto, R., Morante, M., von Kriegsheim, A., Bustelo, X.R*., et al.* (2023). Scaffold coupling: ERK activation by trans-phosphorylation across different scaffold protein species. Science advances *9*, eadd7969.
Martinez-Fuentes, A.J., Hu, L., Krsmanovic, L.Z., and Catt, K.J. (2004). Gonadotropin-releasing hormone (GnRH) receptor expression and membrane signaling in early embryonic GnRH neurons: role in pulsatile neurosecretion. Molecular endocrinology (Baltimore, Md) *18*, 1808-1817.
Mataraza, J.M., Briggs, M.W., Li, Z., Entwistle, A., Ridley, A.J., and Sacks, D.B. (2003a). IQGAP1 promotes cell motility and invasion. The Journal of biological chemistry *278*, 41237-41245.
Mataraza, J.M., Briggs, M.W., Li, Z., Frank, R., and Sacks, D.B. (2003b). Identification and characterization of the Cdc42-binding site of IQGAP1. Biochemical and biophysical research communications *305*, 315-321.
Mataraza, J.M., Briggs, M.W., Li, Z., Frank, R., and Sacks, D.B. (2003c). Identification and characterization of the Cdc42-binding site of IQGAP1. Biochemical and biophysical research communications *305*, 315-321.
Mataraza, J.M., Li, Z., Jeong, H.W., Brown, M.D., and Sacks, D.B. (2007). Multiple proteins mediate IQGAP1-stimulated cell migration. Cellular signalling *19*, 1857-1865.
Mateer, S.C., McDaniel, A.E., Nicolas, V., Habermacher, G.M., Lin, M.J., Cromer, D.A., King, M.E., and Bloom, G.S. (2002). The mechanism for regulation of the F-actin binding activity of IQGAP1 by calcium/calmodulin. The Journal of biological chemistry *277*, 12324-12333.
Mateer, S.C., Morris, L.E., Cromer, D.A., Benseñor, L.B., and Bloom, G.S. (2004). Actin filament binding by a monomeric IQGAP1 fragment with a single calponin homology domain. Cell motility and the cytoskeleton *58*, 231-241.
Mateer, S.C., Wang, N., and Bloom, G.S. (2003). IQGAPs: integrators of the cytoskeleton, cell adhesion machinery, and signaling networks. Cell motility and the cytoskeleton *55*, 147-155.
Matter, K., and Balda, M.S. (2003). Signalling to and from tight junctions. Nature reviews Molecular cell biology *4*, 225-236.
Mattes, B., and Scholpp, S. (2018). Emerging role of contact-mediated cell communication in tissue development and diseases. Histochemistry and cell biology *150*, 431-442.

Maudsley, S., Naor, Z., Bonfil, D., Davidson, L., Karali, D., Pawson, A.J., Larder, R., Pope, C., Nelson, N., Millar, R.P*., et al.* (2007). Proline-rich tyrosine kinase 2 mediates gonadotropin-releasing hormone signaling to a specific extracellularly regulated kinase-sensitive transcriptional locus in the luteinizing hormone beta-subunit gene. Molecular endocrinology (Baltimore, Md) *21*, 1216-1233.
McCallum, S.J., Wu, W.J., and Cerione, R.A. (1996). Identification of a putative effector for Cdc42Hs with high sequence similarity to the RasGAP-related protein IQGAP1 and a Cdc42Hs binding partner with similarity to IQGAP2. The Journal of biological chemistry *271*, 21732-21737.
McCubrey, J.A., Abrams, S.L., Stadelman, K., Chappell, W.H., Lahair, M., Ferland, R.A., and Steelman, L.S. (2010). Targeting signal transduction pathways to eliminate chemotherapeutic drug resistance and cancer stem cells. Advances in enzyme regulation *50*, 285-307.
McKay, M.M., Ritt, D.A., and Morrison, D.K. (2011). RAF inhibitor-induced KSR1/B-RAF binding and its effects on ERK cascade signaling. Current biology : CB *21*, 563-568.
McNiven, M.A., Kim, L., Krueger, E.W., Orth, J.D., Cao, H., and Wong, T.W. (2000). Regulated interactions between dynamin and the actin-binding protein cortactin modulate cell shape. The Journal of cell biology *151*, 187-198.
McNulty, D.E., Li, Z., White, C.D., Sacks, D.B., and Annan, R.S. (2011a). MAPK scaffold IQGAP1 binds the EGF receptor and modulates its activation. Journal of biological chemistry *286*, 15010-15021.
McNulty, D.E., Li, Z., White, C.D., Sacks, D.B., and Annan, R.S. (2011b). MAPK scaffold IQGAP1 binds the EGF receptor and modulates its activation. The Journal of biological chemistry *286*, 15010-15021.
Meiri, K.F. (2004). Membrane/cytoskeleton communication. Sub-cellular biochemistry *37*, 247-282.
Melamed, P., Haj, M., Yosefzon, Y., Rudnizky, S., Wijeweera, A., Pnueli, L., and Kaplan, A. (2018). Multifaceted Targeting of the Chromatin Mediates Gonadotropin-Releasing Hormone Effects on Gene Expression in the Gonadotrope. Frontiers in endocrinology *9*, 58.
Mellman, I., and Nelson, W.J. (2008). Coordinated protein sorting, targeting and distribution in polarized cells. Nature reviews Molecular cell biology *9*, 833-845.
Meng, W., and Takeichi, M. (2009). Adherens junction: molecular architecture and regulation. Cold Spring Harbor perspectives in biology *1*, a002899.
Michaelson, D., Abidi, W., Guardavaccaro, D., Zhou, M., Ahearn, I., Pagano, M., and Philips, M.R. (2008). Rac1 accumulates in the nucleus during the G2 phase of the cell cycle and promotes cell division. The Journal of cell biology *181*, 485-496.
Millar, R.P. (2005). GnRHs and GnRH receptors. Animal reproduction science *88*, 5-28.
Miyamoto, K., Hasegawa, Y., Nomura, M., Igarashi, M., Kangawa, K., and Matsuo, H. (1984). Identification of the second gonadotropin-releasing hormone in chicken hypothalamus: evidence that gonadotropin secretion is probably controlled by two distinct gonadotropin-releasing hormones in avian species. Proceedings of the National Academy of Sciences of the United States of America *81*, 3874-3878.
Miyoshi, T., Shirakusa, T., Ishikawa, Y., Iwasaki, A., Shiraishi, T., Makimoto, Y., Iwasaki, H., and Nabeshima, K. (2005). Possible mechanism of metastasis in lung adenocarcinomas with a micropapillary pattern. Pathology international *55*, 419-424.
Mizusaki, H., Kawabe, K., Mukai, T., Ariyoshi, E., Kasahara, M., Yoshioka, H., Swain, A., and Morohashi, K. (2003). Dax-1 (dosage-sensitive sex reversal-adrenal hypoplasia congenita critical region on the X chromosome, gene 1) gene transcription is regulated by wnt4 in the female developing gonad. Molecular endocrinology (Baltimore, Md) *17*, 507-519.
Momiji, H., Hassall, K.L., Featherstone, K., McNamara, A.V., Patist, A.L., Spiller, D.G., Christian, H.C., White, M.R.H., Davis, J.R.E., Finkenstädt, B.F*., et al.* (2019). Disentangling juxtacrine from paracrine signalling in dynamic tissue. PLoS computational biology *15*, e1007030.
Montcouquiol, M., Crenshaw, E.B., 3rd, and Kelley, M.W. (2006). Noncanonical Wnt signaling and neural polarity. Annual review of neuroscience *29*, 363-386.

Monteleon, C.L., McNeal, A., Duperret, E.K., Oh, S.J., Schapira, E., and Ridky, T.W. (2015). IQGAP1 and IQGAP3 Serve Individually Essential Roles in Normal Epidermal Homeostasis and Tumor Progression. The Journal of investigative dermatology *135*, 2258-2265.
Mooren, O.L., Kotova, T.I., Moore, A.J., and Schafer, D.A. (2009). Dynamin2 GTPase and cortactin remodel actin filaments. The Journal of biological chemistry *284*, 23995-24005.
Morand, I., Fonlupt, P., Guerrier, A., Trouillas, J., Calle, A., Remy, C., Rousset, B., and Munari-Silem, Y. (1996). Cell-to-cell communication in the anterior pituitary: evidence for gap junction-mediated exchanges between endocrine cells and folliculostellate cells. Endocrinology *137*, 3356-3367.
Morgan, F.J., and Canfield, R.E. (1971). Nature of the subunits of human chorionic gonadotropin. Endocrinology *88*, 1045-1053.
Morreale, A., Venkatesan, M., Mott, H.R., Owen, D., Nietlispach, D., Lowe, P.N., and Laue, E.D. (2000). Structure of Cdc42 bound to the GTPase binding domain of PAK. Nature structural biology *7*, 384-388.
Morrison, D.K., and Davis, R.J. (2003). Regulation of MAP kinase signaling modules by scaffold proteins in mammals. Annual review of cell and developmental biology *19*, 91-118.
Mosaddeghzadeh, N., and Ahmadian, M.R. (2021). The RHO Family GTPases: Mechanisms of Regulation and Signaling. Cells *10*.
Mosaddeghzadeh, N., Nouri, K., Krumbach, O.H.F., Amin, E., Dvorsky, R., and Ahmadian, M.R. (2021). Selectivity Determinants of RHO GTPase Binding to IQGAPs. International journal of molecular sciences *22*.
Mosaddeghzadeh, N., Pudewell, S., Bazgir, F., Kazemein Jasemi, N.S., Krumbach, O.H.F., Gremer, L., Willbold, D., Dvorsky, R., and Ahmadian, M.R. (2022). CDC42-IQGAP Interactions Scrutinized: New Insights into the Binding Properties of the GAP-Related Domain. International journal of molecular sciences *23*.
Mott, H.R., and Owen, D. (2015). Structures of Ras superfamily effector complexes: What have we learnt in two decades? Critical reviews in biochemistry and molecular biology *50*, 85-133.
Mott, H.R., Owen, D., Nietlispach, D., Lowe, P.N., Manser, E., Lim, L., and Laue, E.D. (1999). Structure of the small G protein Cdc42 bound to the GTPase-binding domain of ACK. Nature *399*, 384-388.
Mouillet, J.F., Sonnenberg-Hirche, C., Yan, X., and Sadovsky, Y. (2004). p300 regulates the synergy of steroidogenic factor-1 and early growth response-1 in activating luteinizing hormone-beta subunit gene. The Journal of biological chemistry *279*, 7832-7839.
Müller, M.R., and Rao, A. (2010). NFAT, immunity and cancer: a transcription factor comes of age. Nature reviews Immunology *10*, 645-656.
Mulvaney, J.M., and Roberson, M.S. (2000). Divergent signaling pathways requiring discrete calcium signals mediate concurrent activation of two mitogen-activated protein kinases by gonadotropin-releasing hormone. The Journal of biological chemistry *275*, 14182-14189.
Mulvaney, J.M., Zhang, T., Fewtrell, C., and Roberson, M.S. (1999). Calcium influx through L-type channels is required for selective activation of extracellular signal-regulated kinase by gonadotropin-releasing hormone. The Journal of biological chemistry *274*, 29796-29804.
Murase, S., and Schuman, E.M. (1999). The role of cell adhesion molecules in synaptic plasticity and memory. Current opinion in cell biology *11*, 549-553.
Murphy, L.O., and Blenis, J. (2006). MAPK signal specificity: the right place at the right time. Trends in biochemical sciences *31*, 268-275.
Murphy, L.O., MacKeigan, J.P., and Blenis, J. (2004). A network of immediate early gene products propagates subtle differences in mitogen-activated protein kinase signal amplitude and duration. Molecular and cellular biology *24*, 144-153.
Na, H.W., Shin, W.S., Ludwig, A., and Lee, S.T. (2012). The cytosolic domain of protein-tyrosine kinase 7 (PTK7), generated from sequential cleavage by a disintegrin and metalloprotease 17 (ADAM17) and γ-secretase, enhances cell proliferation and migration in colon cancer cells. The Journal of biological chemistry *287*, 25001-25009.
Nakajima, K., Arora, P.D., Plaha, A., and McCulloch, C.A. (2021). Role of the small GTPase activating protein IQGAP1 in collagen phagocytosis. Journal of cellular physiology *236*, 1270-1280.

Nakhaei-Nejad, M., Zhang, Q.X., and Murray, A.G. (2010). Endothelial IQGAP1 regulates efficient lymphocyte transendothelial migration. European journal of immunology *40*, 204-213.
Naor, Z. (1990). Signal transduction mechanisms of Ca2+ mobilizing hormones: the case of gonadotropin-releasing hormone. Endocrine reviews *11*, 326-353.
Naor, Z. (2009). Signaling by G-protein-coupled receptor (GPCR): studies on the GnRH receptor. Frontiers in neuroendocrinology *30*, 10-29.
Naor, Z., Benard, O., and Seger, R. (2000). Activation of MAPK cascades by G-protein-coupled receptors: the case of gonadotropin-releasing hormone receptor. Trends in endocrinology and metabolism: TEM *11*, 91-99.
Naor, Z., and Huhtaniemi, I. (2013). Interactions of the GnRH receptor with heterotrimeric G proteins. Frontiers in neuroendocrinology *34*, 88-94.
Nassar, N., Hoffman, G.R., Manor, D., Clardy, J.C., and Cerione, R.A. (1998). Structures of Cdc42 bound to the active and catalytically compromised forms of Cdc42GAP. Nature structural biology *5*, 1047-1052.
Nateri, A.S., Spencer-Dene, B., and Behrens, A. (2005). Interaction of phosphorylated c-Jun with TCF4 regulates intestinal cancer development. Nature *437*, 281-285.
Navratil, A.M., Bliss, S.P., Berghorn, K.A., Haughian, J.M., Farmerie, T.A., Graham, J.K., Clay, C.M., and Roberson, M.S. (2003). Constitutive localization of the gonadotropin-releasing hormone (GnRH) receptor to low density membrane microdomains is necessary for GnRH signaling to ERK. The Journal of biological chemistry *278*, 31593-31602.
Navratil, A.M., Bliss, S.P., and Roberson, M.S. (2010). Membrane rafts and GnRH receptor signaling. Brain research *1364*, 53-61.
Navratil, A.M., Dozier, M.G., Whitesell, J.D., Clay, C.M., and Roberson, M.S. (2014). Role of cortactin in dynamic actin remodeling events in gonadotrope cells. Endocrinology *155*, 548-557.
Navratil, A.M., Knoll, J.G., Whitesell, J.D., Tobet, S.A., and Clay, C.M. (2007). Neuroendocrine plasticity in the anterior pituitary: gonadotropin-releasing hormone-mediated movement in vitro and in vivo. Endocrinology *148*, 1736-1744.
Neilsen, B.K., Frodyma, D.E., Lewis, R.E., and Fisher, K.W. (2017). KSR as a therapeutic target for Ras-dependent cancers. Expert opinion on therapeutic targets *21*, 499-509.
Nesvizhskii, A.I., Keller, A., Kolker, E., and Aebersold, R. (2003). A statistical model for identifying proteins by tandem mass spectrometry. Analytical chemistry *75*, 4646-4658.
Neudauer, C.L., Joberty, G., Tatsis, N., and Macara, I.G. (1998). Distinct cellular effects and interactions of the Rho-family GTPase TC10. Current biology : CB *8*, 1151-1160.
Nguyen, K.A., Intriago, R.E., Upadhyay, H.C., Santos, S.J., Webster, N.J., and Lawson, M.A. (2010). Modulation of gonadotropin-releasing hormone-induced extracellular signal-regulated kinase activation by dual-specificity protein phosphatase 1 in LbetaT2 gonadotropes. Endocrinology *151*, 4882-4893.
Niehrs, C. (2012). The complex world of WNT receptor signalling. Nature reviews Molecular cell biology *13*, 767-779.
Nishimura, S., Yamashita, M., Kaneko, T., Kawabata, F., and Tabata, S. (2017). Cytokeratin-positive folliculo-stellate cells in chicken adenohypophysis. Animal science journal = Nihon chikusan Gakkaiho *88*, 1835-1841.
Nobes, C.D., and Hall, A. (1999). Rho GTPases control polarity, protrusion, and adhesion during cell movement. The Journal of cell biology *144*, 1235-1244.
Noritake, J., Fukata, M., Sato, K., Nakagawa, M., Watanabe, T., Izumi, N., Wang, S., Fukata, Y., and Kaibuchi, K. (2004a). Positive role of IQGAP1, an effector of Rac1, in actin-meshwork formation at sites of cell-cell contact. Molecular biology of the cell *15*, 1065-1076.
Noritake, J., Fukata, M., Sato, K., Nakagawa, M., Watanabe, T., Izumi, N., Wang, S., Fukata, Y., and Kaibuchi, K. (2004b). Positive role of IQGAP1, an effector of Rac1, in actin-meshwork formation at sites of cell-cell contact. Molecular biology of the cell *15*, 1065-1076.
Noritake, J., Watanabe, T., Sato, K., Wang, S., and Kaibuchi, K. (2005). IQGAP1: a key regulator of adhesion and migration. Journal of cell science *118*, 2085-2092.

Norwitz, E.R., Xu, S., Xu, J., Spiryda, L.B., Park, J.S., Jeong, K.H., McGee, E.A., and Kaiser, U.B. (2002). Direct binding of AP-1 (Fos/Jun) proteins to a SMAD binding element facilitates both gonadotropin-releasing hormone (GnRH)- and activin-mediated transcriptional activation of the mouse GnRH receptor gene. The Journal of biological chemistry *277*, 37469-37478.
Nouri, K., Fansa, E.K., Amin, E., Dvorsky, R., Gremer, L., Willbold, D., Schmitt, L., Timson, D.J., and Ahmadian, M.R. (2016a). IQGAP1 interaction with RHO family proteins revisited: kinetic and equilibrium evidence for multiple distinct binding sites. Journal of Biological Chemistry *291*, 26364-26376.
Nouri, K., Fansa, E.K., Amin, E., Dvorsky, R., Gremer, L., Willbold, D., Schmitt, L., Timson, D.J., and Ahmadian, M.R. (2016b). IQGAP1 Interaction with RHO Family Proteins Revisited: KINETIC AND EQUILIBRIUM EVIDENCE FOR MULTIPLE DISTINCT BINDING SITES. The Journal of biological chemistry *291*, 26364-26376.
Nouri, K., Timson, D.J., and Ahmadian, M.R. (2020). New model for the interaction of IQGAP1 with CDC42 and RAC1. Small GTPases *11*, 16-22.
Oblander, S.A., and Brady-Kalnay, S.M. (2010). Distinct PTPmu-associated signaling molecules differentially regulate neurite outgrowth on E-, N-, and R-cadherin. Molecular and Cellular Neuroscience *44*, 78-93.
Ochoa, G.C., Slepnev, V.I., Neff, L., Ringstad, N., Takei, K., Daniell, L., Kim, W., Cao, H., McNiven, M., Baron, R.*, et al.* (2000). A functional link between dynamin and the actin cytoskeleton at podosomes. The Journal of cell biology *150*, 377-389.
Odle, A.K., Akhter, N., Syed, M.M., Allensworth-James, M.L., Beneš, H., Melgar Castillo, A.I., MacNicol, M.C., MacNicol, A.M., and Childs, G.V. (2017). Leptin Regulation of Gonadotrope Gonadotropin-Releasing Hormone Receptors As a Metabolic Checkpoint and Gateway to Reproductive Competence. Frontiers in endocrinology *8*, 367.
Okubo, K., and Nagahama, Y. (2008). Structural and functional evolution of gonadotropin-releasing hormone in vertebrates. Acta physiologica (Oxford, England) *193*, 3-15.
Oliveria, S.F., Dell'Acqua, M.L., and Sather, W.A. (2007). AKAP79/150 anchoring of calcineurin controls neuronal L-type Ca2+ channel activity and nuclear signaling. Neuron *55*, 261-275.
Olson, L.E., Tollkuhn, J., Scafoglio, C., Krones, A., Zhang, J., Ohgi, K.A., Wu, W., Taketo, M.M., Kemler, R., Grosschedl, R.*, et al.* (2006). Homeodomain-mediated beta-catenin-dependent switching events dictate cell-lineage determination. Cell *125*, 593-605.
Ong, S.E., Blagoev, B., Kratchmarova, I., Kristensen, D.B., Steen, H., Pandey, A., and Mann, M. (2002). Stable isotope labeling by amino acids in cell culture, SILAC, as a simple and accurate approach to expression proteomics. Molecular & cellular proteomics : MCP *1*, 376-386.
Ooi, G.T., Tawadros, N., and Escalona, R.M. (2004). Pituitary cell lines and their endocrine applications. Molecular and cellular endocrinology *228*, 1-21.
Orth, J.D., Krueger, E.W., Cao, H., and McNiven, M.A. (2002). The large GTPase dynamin regulates actin comet formation and movement in living cells. Proceedings of the National Academy of Sciences of the United States of America *99*, 167-172.
Orth, J.D., and McNiven, M.A. (2003). Dynamin at the actin-membrane interface. Current opinion in cell biology *15*, 31-39.
Osman, M. (2010). An emerging role for IQGAP1 in regulating protein traffic. TheScientificWorldJournal *10*, 944-953.
Osman, M.A., and Cerione, R.A. (1998). Iqg1p, a yeast homologue of the mammalian IQGAPs, mediates cdc42p effects on the actin cytoskeleton. The Journal of cell biology *142*, 443-455.
Osman, M.A., Sarkar, F.H., and Rodriguez-Boulan, E. (2013). A molecular rheostat at the interface of cancer and diabetes. Biochimica et biophysica acta *1836*, 166-176.
Owen, D., Campbell, L.J., Littlefield, K., Evetts, K.A., Li, Z., Sacks, D.B., Lowe, P.N., and Mott, H.R. (2008a). The IQGAP1-Rac1 and IQGAP1-Cdc42 interactions: interfaces differ between the complexes. Journal of Biological Chemistry *283*, 1692-1704.

Owen, D., Campbell, L.J., Littlefield, K., Evetts, K.A., Li, Z., Sacks, D.B., Lowe, P.N., and Mott, H.R. (2008b). The IQGAP1-Rac1 and IQGAP1-Cdc42 interactions: interfaces differ between the complexes. The Journal of biological chemistry *283*, 1692-1704.
Owen, D., and Mott, H.R. (2018). CRIB effector disorder: exquisite function from chaos. Biochemical Society transactions *46*, 1289-1302.
Ozdemir, E.S., Jang, H., Gursoy, A., Keskin, O., Li, Z., Sacks, D.B., and Nussinov, R. (2018). Unraveling the molecular mechanism of interactions of the Rho GTPases Cdc42 and Rac1 with the scaffolding protein IQGAP2. The Journal of biological chemistry *293*, 3685-3699.
Palani, S., Ghosh, S., Ivorra-Molla, E., Clarke, S., Suchenko, A., Balasubramanian, M.K., and Köster, D.V. (2021). Calponin-homology domain mediated bending of membrane-associated actin filaments. eLife *10*.
Pan, C.Q., Sudol, M., Sheetz, M., and Low, B.C. (2012). Modularity and functional plasticity of scaffold proteins as p(l)acemakers in cell signaling. Cellular signalling *24*, 2143-2165.
Papkoff, H., and Samy, T.S. (1967). Isolation and partial characterization of the polypeptide chains of ovine interstitial cell-stimulating hormone. Biochimica et biophysica acta *147*, 175-177.
Parakh, T.N., Hernandez, J.A., Grammer, J.C., Weck, J., Hunzicker-Dunn, M., Zeleznik, A.J., and Nilson, J.H. (2006). Follicle-stimulating hormone/cAMP regulation of aromatase gene expression requires beta-catenin. Proceedings of the National Academy of Sciences of the United States of America *103*, 12435-12440.
Patterson, K.I., Brummer, T., O'Brien, P.M., and Daly, R.J. (2009). Dual-specificity phosphatases: critical regulators with diverse cellular targets. The Biochemical journal *418*, 475-489.
Paudyal, A., Damrau, C., Patterson, V.L., Ermakov, A., Formstone, C., Lalanne, Z., Wells, S., Lu, X., Norris, D.P., Dean, C.H.*, et al.* (2010). The novel mouse mutant, chuzhoi, has disruption of Ptk7 protein and exhibits defects in neural tube, heart and lung development and abnormal planar cell polarity in the ear. BMC developmental biology *10*, 87.
Pearson, G., Robinson, F., Beers Gibson, T., Xu, B.E., Karandikar, M., Berman, K., and Cobb, M.H. (2001). Mitogen-activated protein (MAP) kinase pathways: regulation and physiological functions. Endocrine reviews *22*, 153-183.
Peng, X., Wang, T., Gao, H., Yue, X., Bian, W., Mei, J., and Zhang, Y. (2021). The interplay between IQGAP1 and small GTPases in cancer metastasis. Biomedicine & pharmacotherapy = Biomedecine & pharmacotherapie *135*, 111243.
Peradziryi, H., Kaplan, N.A., Podleschny, M., Liu, X., Wehner, P., Borchers, A., and Tolwinski, N.S. (2011). PTK7/Otk interacts with Wnts and inhibits canonical Wnt signalling. The EMBO journal *30*, 3729-3740.
Peradziryi, H., Tolwinski, N.S., and Borchers, A. (2012). The many roles of PTK7: a versatile regulator of cell-cell communication. Archives of biochemistry and biophysics *524*, 71-76.
Pernasetti, F., Vasilyev, V.V., Rosenberg, S.B., Bailey, J.S., Huang, H.J., Miller, W.L., and Mellon, P.L. (2001). Cell-specific transcriptional regulation of follicle-stimulating hormone-beta by activin and gonadotropin-releasing hormone in the LbetaT2 pituitary gonadotrope cell model. Endocrinology *142*, 2284-2295.
Perron, J.C., and Bixby, J.L. (1999). Distinct neurite outgrowth signaling pathways converge on ERK activation. Molecular and cellular neurosciences *13*, 362-378.
Petersen, C.P., and Reddien, P.W. (2009). Wnt signaling and the polarity of the primary body axis. Cell *139*, 1056-1068.
Phillips-Mason, P.J., Gates, T.J., Major, D.L., Sacks, D.B., and Brady-Kalnay, S.M. (2006). The receptor protein-tyrosine phosphatase PTPmu interacts with IQGAP1. The Journal of biological chemistry *281*, 4903-4910.
Pichler, H., Gaigg, B., Hrastnik, C., Achleitner, G., Kohlwein, S.D., Zellnig, G., Perktold, A., and Daum, G. (2001). A subfraction of the yeast endoplasmic reticulum associates with the plasma membrane and has a high capacity to synthesize lipids. European journal of biochemistry *268*, 2351-2361.

Pierce, J.G., Liao, T., Howard, S.M., Shome, B., and Cornell, J.S. (1971). Studies on the structure of thyrotropin: its relationship to luteinizing hormone. Recent progress in hormone research *27*, 165-212.
Plotnikov, A., Zehorai, E., Procaccia, S., and Seger, R. (2011). The MAPK cascades: signaling components, nuclear roles and mechanisms of nuclear translocation. Biochimica et biophysica acta *1813*, 1619-1633.
Podleschny, M., Grund, A., Berger, H., Rollwitz, E., and Borchers, A. (2015). A PTK7/Ror2 Co-Receptor Complex Affects Xenopus Neural Crest Migration. PloS one *10*, e0145169.
Pokutta, S., Drees, F., Yamada, S., Nelson, W.J., and Weis, W.I. (2008). Biochemical and structural analysis of alpha-catenin in cell-cell contacts. Biochemical Society transactions *36*, 141-147.
Pollard, T.D., and Cooper, J.A. (2009). Actin, a central player in cell shape and movement. Science (New York, NY) *326*, 1208-1212.
Porat-Shliom, N., Milberg, O., Masedunskas, A., and Weigert, R. (2013). Multiple roles for the actin cytoskeleton during regulated exocytosis. Cellular and molecular life sciences : CMLS *70*, 2099-2121.
Puppo, F., Thomé, V., Lhoumeau, A.C., Cibois, M., Gangar, A., Lembo, F., Belotti, E., Marchetto, S., Lécine, P., Prébet, T.*, et al.* (2011). Protein tyrosine kinase 7 has a conserved role in Wnt/β-catenin canonical signalling. EMBO reports *12*, 43-49.
Purwana, I.N., Kanasaki, H., Mijiddorj, T., Oride, A., and Miyazaki, K. (2011). Induction of dual-specificity phosphatase 1 (DUSP1) by pulsatile gonadotropin-releasing hormone stimulation: role for gonadotropin subunit expression in mouse pituitary LbetaT2 cells. Biology of reproduction *84*, 996-1004.
Quirk, C.C., Lozada, K.L., Keri, R.A., and Nilson, J.H. (2001). A single Pitx1 binding site is essential for activity of the LHbeta promoter in transgenic mice. Molecular endocrinology (Baltimore, Md) *15*, 734-746.
Rahamim-Ben Navi, L., Tsukerman, A., Feldman, A., Melamed, P., Tomić, M., Stojilkovic, S.S., Boehm, U., Seger, R., and Naor, Z. (2017). GnRH Induces ERK-Dependent Bleb Formation in Gonadotrope Cells, Involving Recruitment of Members of a GnRH Receptor-Associated Signalosome to the Blebs. Frontiers in endocrinology *8*, 113.
Redies, C. (2000). Cadherins in the central nervous system. Progress in neurobiology *61*, 611-648.
Reiss, N., Llevi, L.N., Shacham, S., Harris, D., Seger, R., and Naor, Z. (1997). Mechanism of mitogen-activated protein kinase activation by gonadotropin-releasing hormone in the pituitary of alphaT3-1 cell line: differential roles of calcium and protein kinase C. Endocrinology *138*, 1673-1682.
Ren, J.-G., Li, Z., Crimmins, D.L., and Sacks, D.B. (2005). Self-association of IQGAP1: characterization and functional sequelae. Journal of Biological Chemistry *280*, 34548-34557.
Ren, J.-G., Li, Z., and Sacks, D.B. (2008). IQGAP1 integrates Ca2+/calmodulin and B-Raf signaling. Journal of Biological Chemistry *283*, 22972-22982.
Ren, J.G., Li, Z., and Sacks, D.B. (2007). IQGAP1 modulates activation of B-Raf. Proceedings of the National Academy of Sciences of the United States of America *104*, 10465-10469.
Ren, Y., Meng, S., Mei, L., Zhao, Z.J., Jove, R., and Wu, J. (2004). Roles of Gab1 and SHP2 in paxillin tyrosine dephosphorylation and Src activation in response to epidermal growth factor. The Journal of biological chemistry *279*, 8497-8505.
Ridley, A.J. (2015). Rho GTPase signalling in cell migration. Current opinion in cell biology *36*, 103-112.
Ridley, A.J., Schwartz, M.A., Burridge, K., Firtel, R.A., Ginsberg, M.H., Borisy, G., Parsons, J.T., and Horwitz, A.R. (2003). Cell migration: integrating signals from front to back. Science (New York, NY) *302*, 1704-1709.
Rittmeyer, E.N., Daniel, S., Hsu, S.-C., and Osman, M.A. (2008a). A dual role for IQGAP1 in regulating exocytosis. Journal of cell science *121*, 391-403.
Rittmeyer, E.N., Daniel, S., Hsu, S.C., and Osman, M.A. (2008b). A dual role for IQGAP1 in regulating exocytosis. Journal of cell science *121*, 391-403.
Roberson, M.S., Bliss, S.P., Xie, J., Navratil, A.M., Farmerie, T.A., Wolfe, M.W., and Clay, C.M. (2005). Gonadotropin-releasing hormone induction of extracellular-signal regulated kinase is blocked by inhibition of calmodulin. Molecular endocrinology (Baltimore, Md) *19*, 2412-2423.

Roberson, M.S., Misra-Press, A., Laurance, M.E., Stork, P.J., and Maurer, R.A. (1995). A role for mitogen-activated protein kinase in mediating activation of the glycoprotein hormone alpha-subunit promoter by gonadotropin-releasing hormone. Molecular and cellular biology *15*, 3531-3539.
Roberson, M.S., Zhang, T., Li, H.L., and Mulvaney, J.M. (1999). Activation of the p38 mitogen-activated protein kinase pathway by gonadotropin-releasing hormone. Endocrinology *140*, 1310-1318.
Rose, R., Weyand, M., Lammers, M., Ishizaki, T., Ahmadian, M.R., and Wittinghofer, A. (2005). Structural and mechanistic insights into the interaction between Rho and mammalian Dia. Nature *435*, 513-518.
Roskoski, R., Jr. (2012). ERK1/2 MAP kinases: structure, function, and regulation. Pharmacological research *66*, 105-143.
Roy, M., Li, Z., and Sacks, D.B. (2004). IQGAP1 binds ERK2 and modulates its activity. The Journal of biological chemistry *279*, 17329-17337.
Roy, M., Li, Z., and Sacks, D.B. (2005). IQGAP1 is a scaffold for mitogen-activated protein kinase signaling. Molecular and cellular biology *25*, 7940-7952.
Ruf-Zamojski, F., Fribourg, M., Ge, Y., Nair, V., Pincas, H., Zaslavsky, E., Nudelman, G., Tuminello, S.J., Watanabe, H., Turgeon, J.L*., et al.* (2018). Regulatory Architecture of the LβT2 Gonadotrope Cell Underlying the Response to Gonadotropin-Releasing Hormone. Frontiers in endocrinology *9*, 34.
Ruf, F., Fink, M.Y., and Sealfon, S.C. (2003). Structure of the GnRH receptor-stimulated signaling network: insights from genomics. Frontiers in neuroendocrinology *24*, 181-199.
Ruf, F., and Sealfon, S.C. (2004). Genomics view of gonadotrope signaling circuits. Trends in endocrinology and metabolism: TEM *15*, 331-338.
Ruiz-Velasco, R., Lanning, C.C., and Williams, C.L. (2002). The activation of Rac1 by M3 muscarinic acetylcholine receptors involves the translocation of Rac1 and IQGAP1 to cell junctions and changes in the composition of protein complexes containing Rac1, IQGAP1, and actin. The Journal of biological chemistry *277*, 33081-33091.
Sabio, G., and Davis, R.J. (2014). TNF and MAP kinase signalling pathways. Seminars in immunology *26*, 237-245.
Saci, A., Cantley, L.C., and Carpenter, C.L. (2011). Rac1 regulates the activity of mTORC1 and mTORC2 and controls cellular size. Molecular cell *42*, 50-61.
Sakurai-Yageta, M., Recchi, C., Le Dez, G., Sibarita, J.B., Daviet, L., Camonis, J., D'Souza-Schorey, C., and Chavrier, P. (2008). The interaction of IQGAP1 with the exocyst complex is required for tumor cell invasion downstream of Cdc42 and RhoA. The Journal of cell biology *181*, 985-998.
Salisbury, T.B., Binder, A.K., Grammer, J.C., and Nilson, J.H. (2007). Maximal activity of the luteinizing hormone beta-subunit gene requires beta-catenin. Molecular endocrinology (Baltimore, Md) *21*, 963-971.
Salisbury, T.B., Binder, A.K., Grammer, J.C., and Nilson, J.H. (2009). GnRH-regulated expression of Jun and JUN target genes in gonadotropes requires a functional interaction between TCF/LEF family members and beta-catenin. Molecular endocrinology (Baltimore, Md) *23*, 402-411.
Salisbury, T.B., Binder, A.K., and Nilson, J.H. (2008). Welcoming beta-catenin to the gonadotropin-releasing hormone transcriptional network in gonadotropes. Molecular endocrinology (Baltimore, Md) *22*, 1295-1303.
Sanchez-Laorden, B., Viros, A., and Marais, R. (2013). Mind the IQGAP. Cancer cell *23*, 715-717.
Sato, M., Blumer, J.B., Simon, V., and Lanier, S.M. (2006). Accessory proteins for G proteins: partners in signaling. Annual review of pharmacology and toxicology *46*, 151-187.
Savage, J.J., Yaden, B.C., Kiratipranon, P., and Rhodes, S.J. (2003). Transcriptional control during mammalian anterior pituitary development. Gene *319*, 1-19.
Sbroggiò, M., Carnevale, D., Bertero, A., Cifelli, G., De Blasio, E., Mascio, G., Hirsch, E., Bahou, W.F., Turco, E., Silengo, L*., et al.* (2011). IQGAP1 regulates ERK1/2 and AKT signalling in the heart and sustains functional remodelling upon pressure overload. Cardiovascular research *91*, 456-464.
Schaeffer, M., Hodson, D.J., Meunier, A.C., Lafont, C., Birkenstock, J., Carmignac, D., Murray, J.F., Gavois, E., Robinson, I.C., Le Tissier, P*., et al.* (2011). Influence of estrogens on GH-cell network dynamics in females: a live in situ imaging approach. Endocrinology *152*, 4789-4799.

Schafer, D.A., Weed, S.A., Binns, D., Karginov, A.V., Parsons, J.T., and Cooper, J.A. (2002). Dynamin2 and cortactin regulate actin assembly and filament organization. Current biology : CB *12*, 1852-1857.
Schally, A.V. (2000). Use of GnRH in preference to LH-RH terminology in scientific papers. Human reproduction (Oxford, England) *15*, 2059-2061.
Schally, A.V., Arimura, A., Baba, Y., Nair, R.M., Matsuo, H., Redding, T.W., and Debeljuk, L. (1971a). Isolation and properties of the FSH and LH-releasing hormone. Biochemical and biophysical research communications *43*, 393-399.
Schally, A.V., Arimura, A., Kastin, A.J., Matsuo, H., Baba, Y., Redding, T.W., Nair, R.M., Debeljuk, L., and White, W.F. (1971b). Gonadotropin-releasing hormone: one polypeptide regulates secretion of luteinizing and follicle-stimulating hormones. Science (New York, NY) *173*, 1036-1038.
Schauer, K.L., Freund, D.M., Prenni, J.E., and Curthoys, N.P. (2013). Proteomic profiling and pathway analysis of the response of rat renal proximal convoluted tubules to metabolic acidosis. American journal of physiology Renal physiology *305*, F628-640.
Scheffzek, K., Ahmadian, M.R., Kabsch, W., Wiesmüller, L., Lautwein, A., Schmitz, F., and Wittinghofer, A. (1997). The Ras-RasGAP complex: structural basis for GTPase activation and its loss in oncogenic Ras mutants. Science (New York, NY) *277*, 333-338.
Schiefermeier, N., Scheffler, J.M., de Araujo, M.E., Stasyk, T., Yordanov, T., Ebner, H.L., Offterdinger, M., Munck, S., Hess, M.W., Wickström, S.A.*, et al.* (2014). The late endosomal p14-MP1 (LAMTOR2/3) complex regulates focal adhesion dynamics during cell migration. The Journal of cell biology *205*, 525-540.
Schrick, C., Fischer, A., Srivastava, D.P., Tronson, N.C., Penzes, P., and Radulovic, J. (2007). N-cadherin regulates cytoskeletally associated IQGAP1/ERK signaling and memory formation. Neuron *55*, 786-798.
Searle, B.C., Turner, M., and Nesvizhskii, A.I. (2008). Improving sensitivity by probabilistically combining results from multiple MS/MS search methodologies. The Journal of Proteome Research *7*, 245-253.
Seternes, O.M., Kidger, A.M., and Keyse, S.M. (2019). Dual-specificity MAP kinase phosphatases in health and disease. Biochimica et biophysica acta Molecular cell research *1866*, 124-143.
Shangold, G.A., Murphy, S.N., and Miller, R.J. (1988). Gonadotropin-releasing hormone-induced Ca2+ transients in single identified gonadotropes require both intracellular Ca2+ mobilization and Ca2+ influx. Proceedings of the National Academy of Sciences of the United States of America *85*, 6566-6570.
Shapiro, L., and Colman, D.R. (1998). Structural biology of cadherins in the nervous system. Current opinion in neurobiology *8*, 593-599.
Sharma, S., Findlay, G.M., Bandukwala, H.S., Oberdoerffer, S., Baust, B., Li, Z., Schmidt, V., Hogan, P.G., Sacks, D.B., and Rao, A. (2011). Dephosphorylation of the nuclear factor of activated T cells (NFAT) transcription factor is regulated by an RNA-protein scaffold complex. Proceedings of the National Academy of Sciences of the United States of America *108*, 11381-11386.
Shaul, Y.D., and Seger, R. (2007). The MEK/ERK cascade: from signaling specificity to diverse functions. Biochimica et biophysica acta *1773*, 1213-1226.
Sheldon, R., Moy, A., Lindsley, K., Shasby, S., and Shasby, D.M. (1993). Role of myosin light-chain phosphorylation in endothelial cell retraction. The American journal of physiology *265*, L606-612.
Shin, W.S., Na, H.W., and Lee, S.T. (2015). Biphasic effect of PTK7 on KDR activity in endothelial cells and angiogenesis. Biochimica et biophysica acta *1853*, 2251-2260.
Shirasawa, N., Kihara, H., Yamaguchi, S., and Yoshimura, F. (1983). Pituitary folliculo-stellate cells immunostained with S-100 protein antiserum in postnatal, castrated and thyroidectomized rats. Cell Tissue Res *231*, 235-249.
Shirasawa, N., Mabuchi, Y., Sakuma, E., Horiuchi, O., Yashiro, T., Kikuchi, M., Hashimoto, Y., Tsuruo, Y., Herbert, D.C., and Soji, T. (2004). Intercellular communication within the rat anterior pituitary gland: X. Immunohistocytochemistry of S-100 and connexin 43 of folliculo-stellate cells in the rat anterior pituitary gland. The anatomical record Part A, Discoveries in molecular, cellular, and evolutionary biology *278*, 462-473.

Shirasawa, N., Sakuma, E., Wada, I., Naito, A., Horiuchi, O., Mabuchi, Y., Kanai, M., Herbert, D.C., and Soji, T. (2007). Intercellular communication within the rat anterior pituitary: XIV electron microscopic and immunohistochemical study on the relationship between the agranular cells and GnRH neurons in the dorsal pars tuberalis of the pituitary gland. Anatomical record (Hoboken, NJ : 2007) *290*, 1388-1398.
Smith, J.M., Hedman, A.C., and Sacks, D.B. (2015). IQGAPs choreograph cellular signaling from the membrane to the nucleus. Trends in cell biology *25*, 171-184.
Soji, T., and Herbert, D.C. (1989). Intercellular communication between rat anterior pituitary cells. The Anatomical record *224*, 523-533.
Soji, T., and Herbert, D.C. (1990). Intercellular communication within the rat anterior pituitary gland. II. Castration effects and changes after injection of luteinizing hormone-releasing hormone (LH-RH) or testosterone. The Anatomical record *226*, 342-346.
Soji, T., Mabuchi, Y., Kurono, C., and Herbert, D.C. (1997). Folliculo-stellate cells and intercellular communication within the rat anterior pituitary gland. Microscopy research and technique *39*, 138-149.
Song, L.N., Herrell, R., Byers, S., Shah, S., Wilson, E.M., and Gelmann, E.P. (2003). Beta-catenin binds to the activation function 2 region of the androgen receptor and modulates the effects of the N-terminal domain and TIF2 on ligand-dependent transcription. Molecular and cellular biology *23*, 1674-1687.
Staal, F.J., Weerkamp, F., Baert, M.R., van den Burg, C.M., van Noort, M., de Haas, E.F., and van Dongen, J.J. (2004). Wnt target genes identified by DNA microarrays in immature CD34+ thymocytes regulate proliferation and cell adhesion. Journal of immunology (Baltimore, Md : 1950) *172*, 1099-1108.
Stevens, T., Garcia, J.G., Shasby, D.M., Bhattacharya, J., and Malik, A.B. (2000). Mechanisms regulating endothelial cell barrier function. American journal of physiology Lung cellular and molecular physiology *279*, L419-422.
Stinchcombe, J.C., Majorovits, E., Bossi, G., Fuller, S., and Griffiths, G.M. (2006). Centrosome polarization delivers secretory granules to the immunological synapse. Nature *443*, 462-465.
Stinchcombe, J.C., Randzavola, L.O., Angus, K.L., Mantell, J.M., Verkade, P., and Griffiths, G.M. (2015). Mother Centriole Distal Appendages Mediate Centrosome Docking at the Immunological Synapse and Reveal Mechanistic Parallels with Ciliogenesis. Current biology : CB *25*, 3239-3244.
Stoddart, A., Fleming, H.E., and Paige, C.J. (2001). The role of homotypic interactions in the differentiation of B cell precursors. European journal of immunology *31*, 1160-1172.
Stojilkovic, S.S., Bjelobaba, I., and Zemkova, H. (2017). Ion Channels of Pituitary Gonadotrophs and Their Roles in Signaling and Secretion. Frontiers in endocrinology *8*, 126.
Strahl, B.D., Huang, H.J., Sebastian, J., Ghosh, B.R., and Miller, W.L. (1998). Transcriptional activation of the ovine follicle-stimulating hormone beta-subunit gene by gonadotropin-releasing hormone: involvement of two activating protein-1-binding sites and protein kinase C. Endocrinology *139*, 4455-4465.
Stuart, D.D., and Sellers, W.R. (2013). Targeting RAF-MEK-ERK kinase-scaffold interactions in cancer. Nature medicine *19*, 538-540.
Subauste, M.C., Von Herrath, M., Benard, V., Chamberlain, C.E., Chuang, T.H., Chu, K., Bokoch, G.M., and Hahn, K.M. (2000). Rho family proteins modulate rapid apoptosis induced by cytotoxic T lymphocytes and Fas. The Journal of biological chemistry *275*, 9725-9733.
Suski, J.M., Lebiedzinska, M., Wojtala, A., Duszynski, J., Giorgi, C., Pinton, P., and Wieckowski, M.R. (2014). Isolation of plasma membrane-associated membranes from rat liver. Nature protocols *9*, 312-322.
Suzuki, K., Chikamatsu, Y., and Takahashi, K. (2005). Requirement of protein phosphatase 2A for recruitment of IQGAP1 to Rac-bound beta1 integrin. Journal of cellular physiology *203*, 487-492.
Suzuki, K., and Takahashi, K. (2008). Regulation of lamellipodia formation and cell invasion by CLIP-170 in invasive human breast cancer cells. Biochemical and biophysical research communications *368*, 199-204.
Swaminathan, N., and Bahl, O.P. (1970). Dissociation and recombination of the subunits of human chorionic gonadotropin. Biochemical and biophysical research communications *40*, 422-427.
Swart-Mataraza, J.M., Li, Z., and Sacks, D.B. (2002). IQGAP1 is a component of Cdc42 signaling to the cytoskeleton. The Journal of biological chemistry *277*, 24753-24763.

Swiech, L., Blazejczyk, M., Urbanska, M., Pietruszka, P., Dortland, B.R., Malik, A.R., Wulf, P.S., Hoogenraad, C.C., and Jaworski, J. (2011). CLIP-170 and IQGAP1 cooperatively regulate dendrite morphology. The Journal of neuroscience : the official journal of the Society for Neuroscience *31*, 4555-4568.
Takahashi, K., Nakajima, E., and Suzuki, K. (2006a). Involvement of protein phosphatase 2A in the maintenance of E-cadherin-mediated cell-cell adhesion through recruitment of IQGAP1. Journal of cellular physiology *206*, 814-820.
Takahashi, K., Nakajima, E., and Suzuki, K. (2006b). Involvement of protein phosphatase 2A in the maintenance of E-cadherin-mediated cell–cell adhesion through recruitment of IQGAP1. Journal of cellular physiology *206*, 814-820.
Takahashi, K., and Suzuki, K. (2008). Requirement of kinesin-mediated membrane transport of WAVE2 along microtubules for lamellipodia formation promoted by hepatocyte growth factor. Experimental cell research *314*, 2313-2322.
Takeda, M., Otsuka, F., Otani, H., Inagaki, K., Miyoshi, T., Suzuki, J., Mimura, Y., Ogura, T., and Makino, H. (2007). Effects of peroxisome proliferator-activated receptor activation on gonadotropin transcription and cell mitosis induced by bone morphogenetic proteins in mouse gonadotrope LbetaT2 cells. The Journal of endocrinology *194*, 87-99.
Tang, L., Hung, C.P., and Schuman, E.M. (1998). A role for the cadherin family of cell adhesion molecules in hippocampal long-term potentiation. Neuron *20*, 1165-1175.
Tanos, B.E., Perez Bay, A.E., Salvarezza, S., Vivanco, I., Mellinghoff, I., Osman, M., Sacks, D.B., and Rodriguez-Boulan, E. (2015). IQGAP1 controls tight junction formation through differential regulation of claudin recruitment. Journal of cell science *128*, 853-862.
Tanos, B.E., Yeaman, C., and Rodriguez-Boulan, E. (2018). An emerging role for IQGAP1 in tight junction control. Small GTPases *9*, 375-383.
Taurin, S., Sandbo, N., Qin, Y., Browning, D., and Dulin, N.O. (2006). Phosphorylation of beta-catenin by cyclic AMP-dependent protein kinase. The Journal of biological chemistry *281*, 9971-9976.
Terasaka, T., Adakama, M.E., Li, S., Kim, T., Terasaka, E., Li, D., and Lawson, M.A. (2017). Reactive Oxygen Species Link Gonadotropin-Releasing Hormone Receptor Signaling Cascades in the Gonadotrope. Frontiers in endocrinology *8*, 286.
Thackray, V.G., McGillivray, S.M., and Mellon, P.L. (2006). Androgens, progestins, and glucocorticoids induce follicle-stimulating hormone beta-subunit gene expression at the level of the gonadotrope. Molecular endocrinology (Baltimore, Md) *20*, 2062-2079.
Thackray, V.G., Mellon, P.L., and Coss, D. (2010). Hormones in synergy: regulation of the pituitary gonadotropin genes. Molecular and cellular endocrinology *314*, 192-203.
Thomanetz, V., Angliker, N., Cloëtta, D., Lustenberger, R.M., Schweighauser, M., Oliveri, F., Suzuki, N., and Rüegg, M.A. (2013). Ablation of the mTORC2 component rictor in brain or Purkinje cells affects size and neuron morphology. The Journal of cell biology *201*, 293-308.
Thompson, I.R., Ciccone, N.A., Zhou, Q., Xu, S., Khogeer, A., Carroll, R.S., and Kaiser, U.B. (2016). GnRH Pulse Frequency Control of Fshb Gene Expression Is Mediated via ERK1/2 Regulation of ICER. Molecular endocrinology (Baltimore, Md) *30*, 348-360.
Tirnauer, J.S. (2004). A new cytoskeletal connection for APC: linked to actin through IQGAP. Developmental cell *7*, 778-780.
To, C., Kulkarni, S., Pawson, T., Honda, T., Gribble, G.W., Sporn, M.B., Wrana, J.L., and Di Guglielmo, G.M. (2008). The synthetic triterpenoid 2-cyano-3, 12-dioxooleana-1, 9-dien-28-oic acid-imidazolide alters transforming growth factor β-dependent signaling and cell migration by affecting the cytoskeleton and the polarity complex. Journal of Biological Chemistry *283*, 11700-11713.
Tocker, A.M., Durocher, E., Jacob, K.D., Trieschman, K.E., Talento, S.M., Rechnitzer, A.A., Roberts, D.M., and Davis, B.K. (2017). The Scaffolding Protein IQGAP1 Interacts with NLRC3 and Inhibits Type I IFN Production. Journal of immunology (Baltimore, Md : 1950) *199*, 2896-2909.

Topilko, P., Schneider-Maunoury, S., Levi, G., Trembleau, A., Gourdji, D., Driancourt, M.A., Rao, C.V., and Charnay, P. (1998). Multiple pituitary and ovarian defects in Krox-24 (NGFI-A, Egr-1)-targeted mice. Molecular endocrinology (Baltimore, Md) *12*, 107-122.
Toualbi, K., Güller, M.C., Mauriz, J.L., Labalette, C., Buendia, M.A., Mauviel, A., and Bernuau, D. (2007). Physical and functional cooperation between AP-1 and beta-catenin for the regulation of TCF-dependent genes. Oncogene *26*, 3492-3502.
Tran, S., Zhou, X., Lafleur, C., Calderon, M.J., Ellsworth, B.S., Kimmins, S., Boehm, U., Treier, M., Boerboom, D., and Bernard, D.J. (2013). Impaired fertility and FSH synthesis in gonadotrope-specific Foxl2 knockout mice. Molecular endocrinology (Baltimore, Md) *27*, 407-421.
Tremblay, J.J., and Drouin, J. (1999). Egr-1 is a downstream effector of GnRH and synergizes by direct interaction with Ptx1 and SF-1 to enhance luteinizing hormone beta gene transcription. Molecular and cellular biology *19*, 2567-2576.
Tremblay, J.J., Marcil, A., Gauthier, Y., and Drouin, J. (1999). Ptx1 regulates SF-1 activity by an interaction that mimics the role of the ligand-binding domain. The EMBO journal *18*, 3431-3441.
Trenton, N.J., McLaughlin, R.T., Bellamkonda, S.K., Tsao, D.S., Rodzinski, A., Mace, E.M., Orange, J.S., Schweikhard, V., and Diehl, M.R. (2020). Membrane and Actin Tethering Transitions Help IQGAP1 Coordinate GTPase and Lipid Messenger Signaling. Biophysical journal *118*, 586-599.
Tsukita, S., Oishi, K., Sato, N., Sagara, J., Kawai, A., and Tsukita, S. (1994). ERM family members as molecular linkers between the cell surface glycoprotein CD44 and actin-based cytoskeletons. The Journal of cell biology *126*, 391-401.
Tsutsumi, R., and Webster, N.J. (2009). GnRH pulsatility, the pituitary response and reproductive dysfunction. Endocrine journal *56*, 729-737.
Turgeon, J.L., Kimura, Y., Waring, D.W., and Mellon, P.L. (1996). Steroid and pulsatile gonadotropin-releasing hormone (GnRH) regulation of luteinizing hormone and GnRH receptor in a novel gonadotrope cell line. Molecular endocrinology (Baltimore, Md) *10*, 439-450.
Urao, N., Razvi, M., Oshikawa, J., McKinney, R.D., Chavda, R., Bahou, W.F., Fukai, T., and Ushio-Fukai, M. (2010). IQGAP1 is involved in post-ischemic neovascularization by regulating angiogenesis and macrophage infiltration. PloS one *5*, e13440.
Uruno, T., Liu, J., Zhang, P., Fan, Y., Egile, C., Li, R., Mueller, S.C., and Zhan, X. (2001). Activation of Arp2/3 complex-mediated actin polymerization by cortactin. Nature cell biology *3*, 259-266.
Vasilyev, V.V., Lawson, M.A., Dipaolo, D., Webster, N.J., and Mellon, P.L. (2002). Different signaling pathways control acute induction versus long-term repression of LHbeta transcription by GnRH. Endocrinology *143*, 3414-3426.
Venturelli, C.R., Kuznetsov, S., Salgado, L.M., and Bosch, T.C. (2000). An IQGAP-related gene is activated during tentacle formation in the simple metazoan Hydra. Development genes and evolution *210*, 458-463.
Vicente-Manzanares, M., and Horwitz, A.R. (2011). Adhesion dynamics at a glance. Journal of cell science *124*, 3923-3927.
Villacé, P., Marión, R.M., and Ortín, J. (2004). The composition of Staufen-containing RNA granules from human cells indicates their role in the regulated transport and translation of messenger RNAs. Nucleic acids research *32*, 2411-2420.
Viola, A., and Gupta, N. (2007). Tether and trap: regulation of membrane-raft dynamics by actin-binding proteins. Nature reviews Immunology *7*, 889-896.
Vodicska, B., Cerikan, B., Schiebel, E., and Hoffmann, I. (2018). MISP regulates the IQGAP1/Cdc42 complex to collectively orchestrate spindle orientation and mitotic progression. Scientific reports *8*, 6330.
Vomastek, T., Schaeffer, H.J., Tarcsafalvi, A., Smolkin, M.E., Bissonette, E.A., and Weber, M.J. (2004). Modular construction of a signaling scaffold: MORG1 interacts with components of the ERK cascade and links ERK signaling to specific agonists. Proceedings of the National Academy of Sciences of the United States of America *101*, 6981-6986.
Wada, I., Sakuma, E., Shirasawa, N., Wakabayashi, K., Otsuka, T., Hattori, K., Yashiro, T., Herbert, D.C., and Soji, T. (2014). Intercellular communications within the rat anterior pituitary. XVI: postnatal

changes of distribution of S-100 protein positive cells, connexin 43 and LH-RH positive sites in the pars tuberalis of the rat pituitary gland. An immunohistochemical and electron microscopic study. Tissue & cell *46*, 33-39.
Wainstein, E., and Seger, R. (2016). The dynamic subcellular localization of ERK: mechanisms of translocation and role in various organelles. Current opinion in cell biology *39*, 15-20.
Wallrabe, H., Sun, Y., Fang, X., Periasamy, A., and Bloom, G.S. (2015). Three-color confocal Förster (or fluorescence) resonance energy transfer microscopy: Quantitative analysis of protein interactions in the nucleation of actin filaments in live cells. Cytometry Part A : the journal of the International Society for Analytical Cytology *87*, 580-588.
Wang, J.-B., Sonn, R., Tekletsadik, Y.K., Samorodnitsky, D., and Osman, M.A. (2009). IQGAP1 regulates cell proliferation through a novel CDC42-mTOR pathway. Journal of cell science *122*, 2024-2033.
Wang, M., De Marco, P., Merello, E., Drapeau, P., Capra, V., and Kibar, Z. (2015). Role of the planar cell polarity gene Protein tyrosine kinase 7 in neural tube defects in humans. Birth defects research Part A, Clinical and molecular teratology *103*, 1021-1027.
Wang, S., Watanabe, T., Noritake, J., Fukata, M., Yoshimura, T., Itoh, N., Harada, T., Nakagawa, M., Matsuura, Y., Arimura, N.*, et al.* (2007). IQGAP3, a novel effector of Rac1 and Cdc42, regulates neurite outgrowth. Journal of cell science *120*, 567-577.
Wang, Y., Wang, A., Wang, F., Wang, M., Zhu, M., Ma, Y., and Wu, R. (2008). IQGAP1 activates Tcf signal independent of Rac1 and Cdc42 in injury and repair of bronchial epithelial cells. Experimental and molecular pathology *85*, 122-128.
Ward, D., Fujino, M., and Lamkin, W. (1966). EVIDENCE FOR 2 CARBOHYDRATE MOIETIES IN OVINE LUTEINIZING HORMONE (LH). Paper presented at: FEDERATION PROCEEDINGS (FEDERATION AMER SOC EXP BIOL 9650 ROCKVILLE PIKE, BETHESDA, MD 20814-3998).
Ward, D.N., Bousfield, G. R., and Moore, K. H (1991). Gonadotropins. In Reproduction in Domestic Animals (P. T.

Cupps, Ed.).
WARD, D.N., SWEENEY, C.M., HOLCOMB, G.N., LAMKIN, W.M., and FUJINO, M. (1969). Recent studies on the structure of ovine luteinizing hormone. Progress in Endocrinology, edited by C Gual Amsterdam: Excerpta Medica Foundation Excerpta Med Found Intern Congr Ser *184*, 385-393.
Watanabe, T., Noritake, J., Kakeno, M., Matsui, T., Harada, T., Wang, S., Itoh, N., Sato, K., Matsuzawa, K., Iwamatsu, A.*, et al.* (2009). Phosphorylation of CLASP2 by GSK-3beta regulates its interaction with IQGAP1, EB1 and microtubules. Journal of cell science *122*, 2969-2979.
Watanabe, T., Wang, S., and Kaibuchi, K. (2015). IQGAPs as Key Regulators of Actin-cytoskeleton Dynamics. Cell structure and function *40*, 69-77.
Watanabe, T., Wang, S., Noritake, J., Sato, K., Fukata, M., Takefuji, M., Nakagawa, M., Izumi, N., Akiyama, T., and Kaibuchi, K. (2004a). Interaction with IQGAP1 links APC to Rac1, Cdc42, and actin filaments during cell polarization and migration. Developmental cell *7*, 871-883.
Watanabe, T., Wang, S., Noritake, J., Sato, K., Fukata, M., Takefuji, M., Nakagawa, M., Izumi, N., Akiyama, T., and Kaibuchi, K. (2004b). Interaction with IQGAP1 links APC to Rac1, Cdc42, and actin filaments during cell polarization and migration. Developmental cell *7*, 871-883.
Weaver, A.M., Karginov, A.V., Kinley, A.W., Weed, S.A., Li, Y., Parsons, J.T., and Cooper, J.A. (2001). Cortactin promotes and stabilizes Arp2/3-induced actin filament network formation. Current biology : CB *11*, 370-374.
Weck, J., Anderson, A.C., Jenkins, S., Fallest, P.C., and Shupnik, M.A. (2000). Divergent and composite gonadotropin-releasing hormone-responsive elements in the rat luteinizing hormone subunit genes. Molecular endocrinology (Baltimore, Md) *14*, 472-485.
Wehner, P., Shnitsar, I., Urlaub, H., and Borchers, A. (2011). RACK1 is a novel interaction partner of PTK7 that is required for neural tube closure. Development (Cambridge, England) *138*, 1321-1327.

Weissbach, L., Bernards, A., and Herion, D.W. (1998). Binding of myosin essential light chain to the cytoskeleton-associated protein IQGAP1. Biochemical and biophysical research communications *251*, 269-276.
Weissbach, L., Settleman, J., Kalady, M.F., Snijders, A.J., Murthy, A.E., Yan, Y.X., and Bernards, A. (1994). Identification of a human rasGAP-related protein containing calmodulin-binding motifs. The Journal of biological chemistry *269*, 20517-20521.
Wheelock, M.J., and Johnson, K.R. (2003a). Cadherin-mediated cellular signaling. Current opinion in cell biology *15*, 509-514.
Wheelock, M.J., and Johnson, K.R. (2003b). Cadherins as modulators of cellular phenotype. Annual review of cell and developmental biology *19*, 207-235.
White, B.R., Duval, D.L., Mulvaney, J.M., Roberson, M.S., and Clay, C.M. (1999). Homologous regulation of the gonadotropin-releasing hormone receptor gene is partially mediated by protein kinase C activation of an activator protein-1 element. Molecular endocrinology (Baltimore, Md) *13*, 566-577.
White, C.D., Brown, M.D., and Sacks, D.B. (2009). IQGAPs in cancer: a family of scaffold proteins underlying tumorigenesis. FEBS letters *583*, 1817-1824.
White, C.D., Erdemir, H.H., and Sacks, D.B. (2012). IQGAP1 and its binding proteins control diverse biological functions. Cellular signalling *24*, 826-834.
White, C.D., Li, Z., Dillon, D.A., and Sacks, D.B. (2011). IQGAP1 protein binds human epidermal growth factor receptor 2 (HER2) and modulates trastuzumab resistance. The Journal of biological chemistry *286*, 29734-29747.
White, S.A., Bond, C.T., Francis, R.C., Kasten, T.L., Fernald, R.D., and Adelman, J.P. (1994). A second gene for gonadotropin-releasing hormone: cDNA and expression pattern in the brain. Proceedings of the National Academy of Sciences of the United States of America *91*, 1423-1427.
Widelitz, R. (2005). Wnt signaling through canonical and non-canonical pathways: recent progress. Growth factors (Chur, Switzerland) *23*, 111-116.
Wilfinger, W.W., Larsen, W.J., Downs, T.R., and Wilbur, D.L. (1984). An in vitro model for studies of intercellular communication in cultured rat anterior pituitary cells. Tissue & cell *16*, 483-497.
Williams, M., Yen, W., Lu, X., and Sutherland, A. (2014). Distinct apical and basolateral mechanisms drive planar cell polarity-dependent convergent extension of the mouse neural plate. Developmental cell *29*, 34-46.
Windle, J.J., Weiner, R.I., and Mellon, P.L. (1990). Cell lines of the pituitary gonadotrope lineage derived by targeted oncogenesis in transgenic mice. Molecular endocrinology (Baltimore, Md) *4*, 597-603.
Winters, S.J., and Moore, J.P. (2007). Paracrine control of gonadotrophs. Seminars in reproductive medicine *25*, 379-387.
Witzel, F., Maddison, L., and Blüthgen, N. (2012). How scaffolds shape MAPK signaling: what we know and opportunities for systems approaches. Frontiers in physiology *3*, 475.
Wolfe, M.W., and Call, G.B. (1999). Early growth response protein 1 binds to the luteinizing hormone-beta promoter and mediates gonadotropin-releasing hormone-stimulated gene expression. Molecular endocrinology (Baltimore, Md) *13*, 752-763.
Wong, W., and Scott, J.D. (2004). AKAP signalling complexes: focal points in space and time. Nature reviews Molecular cell biology *5*, 959-970.
Wortzel, I., and Seger, R. (2011). The ERK Cascade: Distinct Functions within Various Subcellular Organelles. Genes & cancer *2*, 195-209.
Wu, H., Lustbader, J.W., Liu, Y., Canfield, R.E., and Hendrickson, W.A. (1994). Structure of human chorionic gonadotropin at 2.6 A resolution from MAD analysis of the selenomethionyl protein. Structure (London, England : 1993) *2*, 545-558.
Wu, J.C., Su, P., Safwat, N.W., Sebastian, J., and Miller, W.L. (2004). Rapid, efficient isolation of murine gonadotropes and their use in revealing control of follicle-stimulating hormone by paracrine pituitary factors. Endocrinology *145*, 5832-5839.
Wu, T., and Mohan, C. (2009). The AKT axis as a therapeutic target in autoimmune diseases. Endocrine, metabolic & immune disorders drug targets *9*, 145-150.

Wu, Y., Chen, Y.-C., Sang, J.-R., and Xu, W.-R. (2011). RhoC protein stimulates migration of gastric cancer cells through interaction with scaffold protein IQGAP1. Molecular Medicine Reports *4*, 697-703.
Wu, Y., and Chen, Y.C. (2014). Structure and function of IQ-domain GTPase-activating protein 1 and its association with tumor progression (Review). Biomedical reports *2*, 3-6.
Wurmbach, E., Yuen, T., Ebersole, B.J., and Sealfon, S.C. (2001). Gonadotropin-releasing hormone receptor-coupled gene network organization. The Journal of biological chemistry *276*, 47195-47201.
Xie, C., Jonak, C.R., Kauffman, A.S., and Coss, D. (2015a). Gonadotropin and kisspeptin gene expression, but not GnRH, are impaired in cFOS deficient mice. Molecular and cellular endocrinology *411*, 223-231.
Xie, J., Allen, K.H., Marguet, A., Berghorn, K.A., Bliss, S.P., Navratil, A.M., Guan, J.L., and Roberson, M.S. (2008). Analysis of the calcium-dependent regulation of proline-rich tyrosine kinase 2 by gonadotropin-releasing hormone. Molecular endocrinology (Baltimore, Md) *22*, 2322-2335.
Xie, J., Bliss, S.P., Nett, T.M., Ebersole, B.J., Sealfon, S.C., and Roberson, M.S. (2005). Transcript profiling of immediate early genes reveals a unique role for activating transcription factor 3 in mediating activation of the glycoprotein hormone alpha-subunit promoter by gonadotropin-releasing hormone. Molecular endocrinology (Baltimore, Md) *19*, 2624-2638.
Xie, Y., Kapoor, A., Peng, H., Cutz, J.-C., Tao, L., and Tang, D. (2015b). Iqgap2 displays tumor suppression functions. Journal of Analytical Oncology *4*, 86-93.
Yamaguchi, K., Lee, S.H., Kim, J.S., Wimalasena, J., Kitajima, S., and Baek, S.J. (2006). Activating transcription factor 3 and early growth response 1 are the novel targets of LY294002 in a phosphatidylinositol 3-kinase-independent pathway. Cancer research *66*, 2376-2384.
Yamaoka-Tojo, M., Tojo, T., Kim, H.W., Hilenski, L., Patrushev, N.A., Zhang, L., Fukai, T., and Ushio-Fukai, M. (2006). IQGAP1 mediates VE-cadherin-based cell-cell contacts and VEGF signaling at adherence junctions linked to angiogenesis. Arteriosclerosis, thrombosis, and vascular biology *26*, 1991-1997.
Yamaoka-Tojo, M., Ushio-Fukai, M., Hilenski, L., Dikalov, S.I., Chen, Y.E., Tojo, T., Fukai, T., Fujimoto, M., Patrushev, N.A., Wang, N.*, et al.* (2004). IQGAP1, a novel vascular endothelial growth factor receptor binding protein, is involved in reactive oxygen species--dependent endothelial migration and proliferation. Circulation research *95*, 276-283.
Yang, F., Li, X., Sharma, M., Sasaki, C.Y., Longo, D.L., Lim, B., and Sun, Z. (2002). Linking beta-catenin to androgen-signaling pathway. The Journal of biological chemistry *277*, 11336-11344.
Yao, Z., and Seger, R. (2009). The ERK signaling cascade--views from different subcellular compartments. BioFactors (Oxford, England) *35*, 407-416.
Yap, A.S., Gomez, G.A., and Parton, R.G. (2015). Adherens Junctions Revisualized: Organizing Cadherins as Nanoassemblies. Developmental cell *35*, 12-20.
Yen, W.W., Williams, M., Periasamy, A., Conaway, M., Burdsal, C., Keller, R., Lu, X., and Sutherland, A. (2009). PTK7 is essential for polarized cell motility and convergent extension during mouse gastrulation. Development (Cambridge, England) *136*, 2039-2048.
Yin, H.L. (1987). Gelsolin: calcium- and polyphosphoinositide-regulated actin-modulating protein. BioEssays : news and reviews in molecular, cellular and developmental biology *7*, 176-179.
Yonemura, S. (2017). Actin filament association at adherens junctions. The journal of medical investigation : JMI *64*, 14-19.
Yoo, Y., Wu, X., and Guan, J.L. (2007). A novel role of the actin-nucleating Arp2/3 complex in the regulation of RNA polymerase II-dependent transcription. The Journal of biological chemistry *282*, 7616-7623.
Yu, J., de Belle, I., Liang, H., and Adamson, E.D. (2004). Coactivating factors p300 and CBP are transcriptionally crossregulated by Egr1 in prostate cells, leading to divergent responses. Molecular cell *15*, 83-94.
Yuen, T., Choi, S.G., Pincas, H., Waring, D.W., Sealfon, S.C., and Turgeon, J.L. (2012). Optimized amplification and single-cell analysis identify GnRH-mediated activation of Rap1b in primary rat gonadotropes. Molecular and cellular endocrinology *350*, 10-19.

Yuen, T., Wurmbach, E., Ebersole, B.J., Ruf, F., Pfeffer, R.L., and Sealfon, S.C. (2002). Coupling of GnRH concentration and the GnRH receptor-activated gene program. Molecular endocrinology (Baltimore, Md) *16*, 1145-1153.
Zhang, B., Chernoff, J., and Zheng, Y. (1998). Interaction of Rac1 with GTPase-activating proteins and putative effectors. A comparison with Cdc42 and RhoA. The Journal of biological chemistry *273*, 8776-8782.
Zhang, B., Wang, Z.X., and Zheng, Y. (1997). Characterization of the interactions between the small GTPase Cdc42 and its GTPase-activating proteins and putative effectors. Comparison of kinetic properties of Cdc42 binding to the Cdc42-interactive domains. The Journal of biological chemistry *272*, 21999-22007.
Zhang, P., and Hinshaw, J.E. (2001). Three-dimensional reconstruction of dynamin in the constricted state. Nature cell biology *3*, 922-926.
Zhang, T., Mulvaney, J.M., and Roberson, M.S. (2001a). Activation of mitogen-activated protein kinase phosphatase 2 by gonadotropin-releasing hormone. Molecular and cellular endocrinology *172*, 79-89.
Zhang, T., and Roberson, M.S. (2006). Role of MAP kinase phosphatases in GnRH-dependent activation of MAP kinases. Journal of molecular endocrinology *36*, 41-50.
Zhang, T., Wolfe, M.W., and Roberson, M.S. (2001b). An early growth response protein (Egr) 1 cis-element is required for gonadotropin-releasing hormone-induced mitogen-activated protein kinase phosphatase 2 gene expression. The Journal of biological chemistry *276*, 45604-45613.
Zhang, T., Zaal, K.J., Sheridan, J., Mehta, A., Gundersen, G.G., and Ralston, E. (2009). Microtubule plus-end binding protein EB1 is necessary for muscle cell differentiation, elongation and fusion. Journal of cell science *122*, 1401-1409.
Zhao, L., Bakke, M., Krimkevich, Y., Cushman, L.J., Parlow, A.F., Camper, S.A., and Parker, K.L. (2001a). Hypomorphic phenotype in mice with pituitary-specific knockout of steroidogenic factor 1. Genesis (New York, NY : 2000) *30*, 65-69.
Zhao, L., Bakke, M., Krimkevich, Y., Cushman, L.J., Parlow, A.F., Camper, S.A., and Parker, K.L. (2001b). Steroidogenic factor 1 (SF1) is essential for pituitary gonadotrope function. Development (Cambridge, England) *128*, 147-154.
Zhao, L., Bakke, M., and Parker, K.L. (2001c). Pituitary-specific knockout of steroidogenic factor 1. Molecular and cellular endocrinology *185*, 27-32.
Zhou, B., Wang, Z.X., Zhao, Y., Brautigan, D.L., and Zhang, Z.Y. (2002). The specificity of extracellular signal-regulated kinase 2 dephosphorylation by protein phosphatases. The Journal of biological chemistry *277*, 31818-31825.
Zorn, A.M., Barish, G.D., Williams, B.O., Lavender, P., Klymkowsky, M.W., and Varmus, H.E. (1999). Regulation of Wnt signaling by Sox proteins: XSox17 alpha/beta and XSox3 physically interact with beta-catenin. Molecular cell *4*, 487-498.

Appendix

Table S1: PAM Fraction Proteins identified by LC-MS/MS

Exclusive Unique Peptide Count

#	Identified Proteins (537/833)	Accession Number	Molecular Weight	Protein Grouping Ambiguity	Taxonomy	Golgi apparatus	cytoskeleton	cytosol	endoplasmic reticulum	lysosome	mitochondrion	nucleus	plasma membrane	S1-8/6/2020	S2-8/9/2020	S3-8/13/2020	S4-8/18/2020
460	Spectrin alpha chain, non-erythrocytic 1 OS=Mus musculus GN=Sptan1 PE=2 SV=1	A3KGU7_MOUSE	285 kDa	TRUE	Mus musculus		microtubule cytoskeleton						lateral plasma membrane	89	90	148	47
134	Clathrin heavy chain 1 OS=Mus musculus GN=Cltc PE=1 SV=3	CLH1_MOUSE (+1)	192 kDa		Mus musculus	clathrin coat of trans-Golgi network vesicle	spindle				mitochondrion		clathrin coat of coated pit	79	83	93	38
461	Spectrin beta chain, non-erythrocytic 1 OS=Mus musculus GN=Sptbn1 PE=1 SV=2	sp|Q62261|SPTB2_MOUSE	274 kDa	TRUE	Mus musculus		spectrin					nucleus	plasma membrane	71	67	105	42
149	Cytoplasmic dynein 1 heavy chain 1 OS=Mus musculus GN=Dync1h1 PE=1 SV=2	DYHC1_MOUSE	532 kDa		Mus musculus		microtubule							113	66	117	6
451	Sodium/potassium-transporting ATPase subunit alpha-1 OS=Mus musculus GN=Atp1a1 PE=1 SV=1	AT1A1_MOUSE	113 kDa	TRUE	Mus musculus	Golgi apparatus			endoplasmic reticulum				plasma membrane	43	45	51	37
395	Protein Utrn OS=Mus musculus GN=Utrn PE=2 SV=1	E9Q6R7_MOUSE	393 kDa		Mus musculus							nucleus	sarcolemma	71	51	98	8
178	Endoplasmin OS=Mus musculus GN=Hsp90b1 PE=1 SV=2	ENPL_MOUSE	92 kDa	TRUE	Mus musculus			cytosol	endoplasmic reticulum membrane			nucleus	plasma membrane	44	49	41	23
235	Hypoxia up-regulated protein 1 OS=Mus musculus GN=Hyou1 PE=1 SV=1	HYOU1_MOUSE	111 kDa		Mus musculus				endoplasmic reticulum					38	44	32	15
51	78 kDa glucose-regulated protein OS=Mus musculus GN=Hspa5 PE=1 SV=3	GRP78_MOUSE	72 kDa	TRUE	Mus musculus				endoplasmic reticulum membrane			signalosome	plasma membrane	35	41	31	20
332	Myosin-10 OS=Mus musculus GN=Myh10 PE=1 SV=2	MYH10_MOUSE (+2)	229 kDa	TRUE	Mus musculus		spindle	cytosol				nucleus	plasma membrane	45	40	69	26
198	Filamin, alpha OS=Mus musculus GN=Flna PE=4 SV=1	B7FAU9_MOUSE (+1)	280 kDa	TRUE	Mus musculus	trans-Golgi network								48	38	69	23
199	Filamin-B OS=Mus musculus GN=Flnb PE=1 SV=3	FLNB_MOUSE	278 kDa	TRUE	Mus musculus		stress fiber						focal adhesion	52	39	75	14
331	Myosin-9 OS=Mus musculus GN=Myh9 PE=1 SV=4	MYH9_MOUSE	226 kDa	TRUE	Mus musculus		spindle	cytosol				nucleus	integrin complex	38	33	51	21
77	Actin, cytoplasmic 1 OS=Mus musculus GN=Actb PE=1 SV=1	ACTB_MOUSE (+1)	42 kDa	TRUE	Mus musculus		cortical cytoskeleton	cytosol				NuA4 histone acetyltransferase complex		22	19	22	21
196	Fatty acid synthase OS=Mus musculus GN=Fasn PE=1 SV=2	FAS_MOUSE	272 kDa		Mus musculus	Golgi apparatus					mitochondrion		plasma membrane	42	33	50	7
128	Cation-independent mannose-6-phosphate receptor OS=Mus musculus GN=Igf2r PE=1 SV=1	MPRI_MOUSE	274 kDa		Mus musculus	trans-Golgi network transport vesicle				lysosome		nuclear envelope lumen	plasma membrane	50	47	46	10

324	Microtubule-associated protein 1B OS=Mus musculus GN=Map1b PE=1 SV=2	MAP1B_MOUSE	270 kDa		Mus musculus		microtubule associated complex	cytosol					cell junction	40	35	45	3
534	sp|G5E829|AT2B1_MOUSE	sp|G5E829|AT2B1_MOUSE	?	TRUE	Mus musculus								integral to plasma membrane	27	30	44	21
481	Talin-1 OS=Mus musculus GN=Tln1 PE=1 SV=2	TLN1_MOUSE	270 kDa	TRUE	Mus musculus		actin cytoskeleton						plasma membrane	28	25	53	14
491	Transitional endoplasmic reticulum ATPase OS=Mus musculus GN=Vcp PE=1 SV=4	TERA_MOUSE	89 kDa		Mus musculus			cytosol	Hrd1p ubiquitin ligase complex			nucleus		27	25	31	19
339	Neural cell adhesion molecule 1 OS=Mus musculus GN=Ncam1 PE=1 SV=3	sp|P13595|NCAM1_MOUSE	119 kDa	TRUE	Mus musculus								plasma membrane	20	25	33	14
397	Protein disulfide-isomerase A3 OS=Mus musculus GN=Pdia3 PE=1 SV=2	PDIA3_MOUSE	57 kDa		Mus musculus				endoplasmic reticulum			nucleus		24	26	21	18
434	Sarcoplasmic/endoplasmic reticulum calcium ATPase 2 OS=Mus musculus GN=Atp2a2 PE=3 SV=1	J3KMM5_MOUSE (+1)	110 kDa		Mus musculus				sarcoplasmic reticulum					25	28	25	3
3	4F2 cell-surface antigen heavy chain OS=Mus musculus GN=Slc3a2 PE=1 SV=1	4F2_MOUSE (+1)	58 kDa		Mus musculus								plasma membrane	18	17	23	17
258	Isoform 2 of Neutral alpha-glucosidase AB OS=Mus musculus GN=Ganab	sp|Q8BHN3-2|GANAB_MOUSE (+1)	109 kDa		unknown									29	41	26	3
497	Tubulin beta-5 chain OS=Mus musculus GN=Tubb5 PE=1 SV=1	TBB5_MOUSE	50 kDa	TRUE	Mus musculus		microtubule	cytosol				nuclear envelope lumen		21	20	21	10
400	Protein disulfide-isomerase OS=Mus musculus GN=P4hb PE=1 SV=2	PDIA1_MOUSE	57 kDa		Mus musculus				endoplasmic reticulum				plasma membrane	24	29	23	11
64	ATP synthase subunit beta, mitochondrial OS=Mus musculus GN=Atp5b PE=1 SV=2	ATPB_MOUSE	56 kDa		Mus musculus						mitochondrial nucleoid	nucleus	plasma membrane	23	24	11	6
503	UDP-glucose:glycoprotein glucosyltransferase 1 OS=Mus musculus GN=Uggt1 PE=1 SV=4	UGGG1_MOUSE	176 kDa		Mus musculus									28	32	20	3
459	Sortilin-related receptor OS=Mus musculus GN=Sorl1 PE=1 SV=3	SORL_MOUSE	247 kDa		Mus musculus	trans-Golgi network			endoplasmic reticulum			nuclear envelope lumen		30	24	28	0
511	V-type proton ATPase 116 kDa subunit a isoform 1 OS=Mus musculus GN=Atp6v0a1 PE=4 SV=1	K3W4T3_MOUSE (+2)	96 kDa	TRUE	Mus musculus									15	17	23	11
320	Melanoma inhibitory activity protein 3 OS=Mus musculus GN=Mia3 PE=1 SV=2	sp|Q8BI84|MIA3_MOUSE	214 kDa	TRUE	Mus musculus				endoplasmic reticulum membrane					25	32	16	0
175	Elongation factor 2 OS=Mus musculus GN=Eef2 PE=1 SV=2	EF2_MOUSE	95 kDa		Mus musculus							nucleus		16	20	24	11
172	Elongation factor 1-alpha 1 OS=Mus musculus GN=Eef1a1 PE=1 SV=3	EF1A1_MOUSE	50 kDa	TRUE	Mus musculus							nucleolus	plasma membrane	16	15	18	13
452	Sodium/potassium-transporting ATPase subunit alpha-3 OS=Mus musculus GN=Atp1a3 PE=1 SV=1	AT1A3_MOUSE (+1)	112 kDa	TRUE	Mus musculus	Golgi apparatus			endoplasmic reticulum			nucleus	plasma membrane	17	16	24	14
223	Heat shock cognate 71 kDa protein OS=Mus musculus GN=Hspa8 PE=1 SV=1	HSP7C_MOUSE	71 kDa	TRUE	Mus musculus			cytosol				nucleus	plasma membrane	17	17	20	16
330	Myo1b protein OS=Mus musculus GN=Myo1b PE=2 SV=1	Q7TQD7_MOUSE (+1)	132 kDa		Mus musculus	trans-Golgi network membrane	actin filament							13	16	33	20
314	MCG115602 OS=Mus musculus GN=Dnajc13 PE=4 SV=1	G3X922_MOUSE (+1)	254 kDa		Mus musculus					lysosomal membrane				24	16	39	6
406	Pyruvate kinase PKM OS=Mus musculus GN=Pkm PE=1 SV=4	sp|P52480|KPYM_MOUSE	58 kDa	TRUE	Mus musculus						mitochondrion	nucleus	plasma membrane	18	20	22	7

262	Isoform 2 of Protein scribble homolog OS=Mus musculus GN=Scrib	sp|Q80U72-2|SCRIB_MOUSE (+2)	177 kDa	TRUE	unknown									14	12	29	9
107	Bifunctional glutamate/proline--tRNA ligase OS=Mus musculus GN=Eprs PE=1 SV=4	SYEP_MOUSE	170 kDa		Mus musculus									29	32	15	0
164	Dolichyl-diphosphooligosaccharide--protein glycosyltransferase subunit 1 OS=Mus musculus GN=Rpn1 PE=2 SV=1	RPN1_MOUSE	69 kDa		Mus musculus				endoplasmic reticulum membrane					21	24	13	8
63	ATP synthase subunit alpha, mitochondrial OS=Mus musculus GN=Atp5a1 PE=1 SV=1	ATPA_MOUSE	60 kDa		Mus musculus						mitochondrial inner membrane	signalosome	plasma membrane	20	21	14	5
323	Microtubule-actin cross-linking factor 1 (Fragment) OS=Mus musculus GN=Macf1 PE=2 SV=1	F7ACR9_MOUSE	608 kDa	TRUE	Mus musculus		microtubule cytoskeleton							32	7	42	0
124	Catenin beta-1 OS=Mus musculus GN=Ctnnb1 PE=1 SV=1	CTNB1_MOUSE	85 kDa	TRUE	Mus musculus		centrosome	cytosol				transcription factor complex	plasma membrane	11	11	17	11
117	Calnexin OS=Mus musculus GN=Canx PE=1 SV=1	CALX_MOUSE	67 kDa	TRUE	Mus musculus				endoplasmic reticulum					16	23	16	4
190	Extended synaptotagmin-1 OS=Mus musculus GN=Esyt1 PE=2 SV=2	sp|Q3U7R1|ESYT1_MOUSE	122 kDa		Mus musculus				integral to endoplasmic reticulum membrane				plasma membrane	17	23	17	2
525	Vesicle-fusing ATPase OS=Mus musculus GN=Nsf PE=1 SV=2	NSF_MOUSE	83 kDa		Mus musculus					lysosomal membrane			plasma membrane	14	17	22	11
225	Heat shock protein HSP 90-beta OS=Mus musculus GN=Hsp90ab1 PE=1 SV=3	HS90B_MOUSE	83 kDa	TRUE	Mus musculus			cytosol			mitochondrion	signalosome	basolateral plasma membrane	20	14	15	12
215	Guanine nucleotide-binding protein G(I)/G(S)/G(T) subunit beta-2 OS=Mus musculus GN=Gnb2 PE=2 SV=1	E9QKR0_MOUSE (+1)	41 kDa	TRUE	Mus musculus								heterotrimeric G-protein complex	12	15	16	4
488	Transferrin receptor protein 1 OS=Mus musculus GN=Tfrc PE=1 SV=1	TFR1_MOUSE	86 kDa		Mus musculus								plasma membrane	13	14	26	8
165	Dolichyl-diphosphooligosaccharide--protein glycosyltransferase subunit 2 OS=Mus musculus GN=Rpn2 PE=2 SV=1	RPN2_MOUSE	69 kDa		Mus musculus				oligosaccharyltransferase complex			nucleus		18	15	13	0
269	Isoform 2 of Teneurin-4 OS=Mus musculus GN=Tenm4	sp|Q3UHK6-2|TEN4_MOUSE (+3)	313 kDa		unknown									16	14	32	2
399	Protein disulfide-isomerase A6 OS=Mus musculus GN=Pdia6 PE=1 SV=3	PDIA6_MOUSE	48 kDa		Mus musculus				endoplasmic reticulum				plasma membrane	16	16	12	10
472	Syntaxin-binding protein 1 OS=Mus musculus GN=Stxbp1 PE=1 SV=2	sp|O08599|STXB1_MOUSE	68 kDa		Mus musculus						mitochondrion		plasma membrane	11	12	19	13
535	sp|P70704-2|AT8A1_MOUSE	sp|P70704-2|AT8A1_MOUSE	?		unknown									17	15	24	5
216	Guanine nucleotide-binding protein G(i) subunit alpha-2 OS=Mus musculus GN=Gnai2 PE=1 SV=5	GNAI2_MOUSE	40 kDa	TRUE	Mus musculus		centrosome	cytosol				nucleus	plasma membrane	11	16	18	12
385	Protein Gcn1l1 OS=Mus musculus GN=Gcn1l1 PE=2 SV=1	E9PVA8_MOUSE	293 kDa		Mus musculus									10	9	30	2
123	Catenin alpha-1 OS=Mus musculus GN=Ctnna1 PE=1 SV=1	CTNA1_MOUSE	100 kDa	TRUE	Mus musculus		actin cytoskeleton						plasma membrane	9	11	21	14
202	Fructose-bisphosphate aldolase OS=Mus musculus GN=Aldoa PE=2 SV=1	A6ZI44_MOUSE (+1)	45 kDa		Mus musculus						mitochondrion			6	5	21	15
367	Plexin-B2 OS=Mus musculus GN=Plxnb2 PE=1 SV=1	PLXB2_MOUSE	206 kDa		Mus musculus								integral to plasma membrane	10	13	25	7

496	Tubulin alpha-1B chain OS=Mus musculus GN=Tuba1b PE=1 SV=2	TBA1B_MOUSE	50 kDa	TRUE	Mus musculus		microtubule	cytosol						16	16	0	7
381	Prolow-density lipoprotein receptor-related protein 1 OS=Mus musculus GN=Lrp1 PE=1 SV=1	LRP1_MOUSE	505 kDa		Mus musculus					lysosomal membrane		nucleus	coated pit	26	18	24	0
382	Protein 4.1 OS=Mus musculus GN=Epb4.1 PE=2 SV=1	A2A841_MOUSE (+1)	97 kDa		Mus musculus		actin cytoskeleton							10	13	20	11
219	Guanine nucleotide-binding protein G(s) subunit alpha isoforms XLas OS=Mus musculus GN=Gnas PE=2 SV=1	sp|Q6R0H7|GNAS1_MOUSE	122 kDa	TRUE	Mus musculus								heterotrimeric G-protein complex	10	11	12	8
168	Dystonin OS=Mus musculus GN=Dst PE=4 SV=1	S4R1P5_MOUSE	871 kDa	TRUE	Mus musculus		microtubule cytoskeleton						hemidesmosome	25	11	32	0
280	Isoform Alpha-2 of Guanine nucleotide-binding protein G(o) subunit alpha OS=Mus musculus GN=Gnao1	sp|P18872-2|GNAO_MOUSE	40 kDa	TRUE	unknown									8	10	12	10
239	Integrin beta-1 OS=Mus musculus GN=Itgb1 PE=1 SV=1	ITB1_MOUSE	88 kDa		Mus musculus								plasma membrane	11	14	16	5
432	Ribosome-binding protein 1 OS=Mus musculus GN=Rrbp1 PE=2 SV=1	A2AVJ7_MOUSE (+1)	158 kDa		Mus musculus				integral to endoplasmic reticulum membrane					16	26	9	0
462	Staphylococcal nuclease domain-containing protein 1 OS=Mus musculus GN=Snd1 PE=1 SV=1	SND1_MOUSE	102 kDa		Mus musculus						mitochondrion	nucleus		16	13	15	6
340	Neural cell adhesion molecule 2 OS=Mus musculus GN=Ncam2 PE=1 SV=1	sp|O35136|NCAM2_MOUSE	93 kDa		Mus musculus								plasma membrane	7	10	16	7
281	Isoform Alpha-6X1A of Integrin alpha-6 OS=Mus musculus GN=Itga6	sp|Q61739-2|ITA6_MOUSE	120 kDa		unknown									12	14	16	12
402	Protein sidekick-1 OS=Mus musculus GN=Sdk1 PE=2 SV=1	sp|Q3UH53|SDK1_MOUSE	240 kDa		Mus musculus									8	7	19	3
125	Catenin delta-1 OS=Mus musculus GN=Ctnnd1 PE=2 SV=1	E9Q8Z6_MOUSE (+3)	107 kDa		Mus musculus								tight junction	8	9	20	14
328	Moesin OS=Mus musculus GN=Msn PE=1 SV=3	MOES_MOUSE	68 kDa	TRUE	Mus musculus		cytoskeleton						apical plasma membrane	9	11	21	12
512	V-type proton ATPase catalytic subunit A OS=Mus musculus GN=Atp6v1a PE=1 SV=2	sp|P50516|VATA_MOUSE	68 kDa		Mus musculus			cytosol		lysosomal membrane	mitochondrion		plasma membrane	8	12	10	8
58	AP-2 complex subunit alpha-2 OS=Mus musculus GN=Ap2a2 PE=1 SV=2	AP2A2_MOUSE	104 kDa	TRUE	Mus musculus								plasma membrane	11	15	23	4
294	KxDL motif-containing protein 1 (Fragment) OS=Mus musculus GN=Kxd1 PE=2 SV=1	E9Q4P0_MOUSE (+9)	22 kDa		unknown									4	4	4	7
150	Cytoskeleton-associated protein 4 OS=Mus musculus GN=Ckap4 PE=2 SV=2	CKAP4_MOUSE	64 kDa		Mus musculus		cytoskeleton		endoplasmic reticulum				plasma membrane	19	18	8	2
247	Isoform 2 of AP-2 complex subunit beta OS=Mus musculus GN=Ap2b1	sp|Q9DBG3-2|AP2B1_MOUSE (+1)	106 kDa	TRUE	Mus musculus									5	10	17	2
20	60 kDa heat shock protein, mitochondrial OS=Mus musculus GN=Hspd1 PE=1 SV=1	sp|P63038|CH60_MOUSE	61 kDa		Mus musculus			cytosol			mitochondrial inner membrane	cyclin-dependent protein kinase activating kinase holoenzyme complex	coated pit	12	14	0	0
251	Isoform 2 of Catenin alpha-2 OS=Mus musculus GN=Ctnna2	sp|Q61301-2|CTNA2_MOUSE (+1)	100 kDa	TRUE	unknown									7	9	15	4

309	Lysosomal alpha-glucosidase OS=Mus musculus GN=Gaa PE=1 SV=2	LYAG_MOUSE	106 kDa		Mus musculus					lysosomal membrane				13	12	10	4
88	Alpha-internexin OS=Mus musculus GN=Ina PE=1 SV=2	AINX_MOUSE	56 kDa	TRUE	Mus musculus		neurofilament							18	17	0	6
83	Alpha-1,3/1,6-mannosyltransferase ALG2 OS=Mus musculus GN=Alg2 PE=2 SV=2	ALG2_MOUSE	47 kDa		Mus musculus							nucleus		11	11	7	2
272	Isoform 2 of Unconventional myosin-Ic OS=Mus musculus GN=Myo1c	sp|Q9WTI7-2|MYO1C_MOUSE (+2)	118 kDa		unknown									9	10	20	7
207	Glyceraldehyde-3-phosphate dehydrogenase OS=Mus musculus GN=Gapdh PE=1 SV=2	G3P_MOUSE (+1)	36 kDa		Mus musculus		microtubule cytoskeleton	cytosol				nucleus		11	9	8	8
140	Contactin-1 OS=Mus musculus GN=Cntn1 PE=1 SV=1	CNTN1_MOUSE	113 kDa		Mus musculus								plasma membrane	11	13	18	5
537	tr|A0A0A6YX40|A0A0A6YX40_MOUSE	tr|A0A0A6YX40|A0A0A6YX40_MOUSE	?		unknown									10	9	19	0
348	Nodal modulator 1 OS=Mus musculus GN=Nomo1 PE=1 SV=1	NOMO1_MOUSE	133 kDa		Mus musculus									16	22	9	0
100	Atrial natriuretic peptide receptor 2 OS=Mus musculus GN=Npr2 PE=2 SV=2	sp|Q6VVW5|ANPRB_MOUSE	117 kDa		Mus musculus								plasma membrane	8	10	14	5
292	Kinectin OS=Mus musculus GN=Ktn1 PE=2 SV=1	F8VQC7_MOUSE (+5)	153 kDa		Mus musculus				endoplasmic reticulum					19	20	4	0
218	Guanine nucleotide-binding protein G(q) subunit alpha OS=Mus musculus GN=Gnaq PE=1 SV=4	GNAQ_MOUSE	42 kDa	TRUE	Mus musculus					lysosomal membrane		nucleus	plasma membrane	6	10	10	9
365	Plasma membrane calcium-transporting ATPase 2 OS=Mus musculus GN=Atp2b2 PE=2 SV=1	F8WHB1_MOUSE	137 kDa	TRUE	Mus musculus				endoplasmic reticulum				plasma membrane	5	5	12	3
428	Reticulon-4 OS=Mus musculus GN=Rtn4 PE=1 SV=2	sp|Q99P72|RTN4_MOUSE	127 kDa		Mus musculus				integral to endoplasmic reticulum membrane			nuclear envelope		12	14	11	2
398	Protein disulfide-isomerase A4 OS=Mus musculus GN=Pdia4 PE=1 SV=3	PDIA4_MOUSE	72 kDa		Mus musculus				endoplasmic reticulum					10	18	5	5
529	Voltage-dependent calcium channel subunit alpha-2/delta-1 OS=Mus musculus GN=Cacna2d1 PE=4 SV=2	E9Q1X8_MOUSE (+5)	123 kDa		Mus musculus				sarcoplasmic reticulum				T-tubule	6	11	16	8
22	60S ribosomal protein L4 OS=Mus musculus GN=Rpl4 PE=1 SV=3	RL4_MOUSE	47 kDa		Mus musculus			cytosolic large ribosomal subunit				nucleolus		8	9	8	10
283	Isoform E2 of Drebrin OS=Mus musculus GN=Dbn1	sp|Q9QXS6-3|DREB_MOUSE (+1)	72 kDa		unknown									6	9	13	6
81	Afadin OS=Mus musculus GN=Mllt4 PE=4 SV=2	E9Q852_MOUSE (+3)	205 kDa		Mus musculus								cell-cell adherens junction	8	8	19	7
298	Large neutral amino acids transporter small subunit 1 OS=Mus musculus GN=Slc7a5 PE=1 SV=2	LAT1_MOUSE	56 kDa		Mus musculus							nucleolus	plasma membrane	5	6	6	7
343	Neutral amino acid transporter ASCT2 OS=Mus musculus GN=Slc1a5 PE=2 SV=1	Q9ESU7_MOUSE	58 kDa		Mus musculus	Golgi apparatus							plasma membrane	8	7	9	6
108	Brefeldin A-inhibited guanine nucleotide-exchange protein 3 OS=Mus musculus GN=Arfgef3 PE=1 SV=1	BIG3_MOUSE	240 kDa		Mus musculus	trans-Golgi network								21	15	13	2
102	Band 4.1-like protein 2 OS=Mus musculus GN=Epb41l2 PE=1 SV=2	E41L2_MOUSE	110 kDa		Mus musculus		actin cytoskeleton					signalosome	plasma membrane	2	6	22	8

513	V-type proton ATPase subunit B, brain isoform OS=Mus musculus GN=Atp6v1b2 PE=1 SV=1	VATB2_MOUSE	57 kDa		Mus musculus			cytosol		lysosomal membrane			plasma membrane	5	12	9	3
118	Calreticulin OS=Mus musculus GN=Calr PE=1 SV=1	CALR_MOUSE	48 kDa	TRUE	Mus musculus	Golgi apparatus		cytosol	MHC class I peptide loading complex			nucleus	external side of plasma membrane	12	13	7	3
313	MCG13402, isoform CRA_a OS=Mus musculus GN=Ptbp1 PE=2 SV=1	Q8BGJ5_MOUSE (+1)	57 kDa		Mus musculus							nucleus		5	6	6	3
21	60S ribosomal protein L3 OS=Mus musculus GN=Rpl3 PE=2 SV=3	RL3_MOUSE	46 kDa		Mus musculus			cytosolic large ribosomal subunit				nucleolus		6	10	11	4
518	Valine--tRNA ligase OS=Mus musculus GN=Vars PE=2 SV=1	SYVC_MOUSE	140 kDa		Mus musculus						mitochondrion			8	10	8	0
163	Dolichyl-diphosphooligosaccharide--protein glycosyltransferase 48 kDa subunit OS=Mus musculus GN=Ddost PE=1 SV=2	OST48_MOUSE	49 kDa		Mus musculus				oligosaccharyltransferase complex					11	12	8	0
413	Ras-related protein Rab-2A OS=Mus musculus GN=Rab2a PE=1 SV=1	RAB2A_MOUSE	24 kDa		Mus musculus	Golgi apparatus			endoplasmic reticulum	lysosomal membrane		nucleus		9	9	9	3
194	Fatty acid desaturase 1 OS=Mus musculus GN=Fads1 PE=2 SV=1	FADS1_MOUSE	52 kDa		Mus musculus				endoplasmic reticulum		mitochondrion	nucleus		10	11	8	0
24	60S ribosomal protein L6 OS=Mus musculus GN=Rpl6 PE=1 SV=3	RL6_MOUSE	34 kDa		Mus musculus							nucleolus		7	9	9	6
136	Coatomer subunit alpha OS=Mus musculus GN=Copa PE=1 SV=2	COPA_MOUSE (+1)	138 kDa		Mus musculus	COPI vesicle coat								7	4	21	2
474	T-complex protein 1 subunit beta OS=Mus musculus GN=Cct2 PE=1 SV=4	TCPB_MOUSE	57 kDa		Mus musculus		microtubule	chaperonin-containing T-complex						6	5	6	7
442	Serine/threonine-protein kinase MRCK alpha OS=Mus musculus GN=Cdc42bpa PE=2 SV=1	D3YYN8_MOUSE (+2)	193 kDa	TRUE	Mus musculus									9	6	20	3
54	ADP/ATP translocase 1 OS=Mus musculus GN=Slc25a4 PE=1 SV=4	ADT1_MOUSE	33 kDa	TRUE	Mus musculus						mitochondrion	nucleus		14	14	9	0
121	Carboxypeptidase E OS=Mus musculus GN=Cpe PE=1 SV=2	CBPE_MOUSE	53 kDa		Mus musculus	Golgi apparatus								8	8	11	10
300	Leucine-rich repeat-containing protein 59 OS=Mus musculus GN=Lrrc59 PE=2 SV=1	LRC59_MOUSE	35 kDa		Mus musculus				endoplasmic reticulum		mitochondrial nucleoid	nucleus		11	12	5	3
73	ATP-dependent RNA helicase DDX3X OS=Mus musculus GN=Ddx3x PE=1 SV=3	DDX3X_MOUSE	73 kDa	TRUE	Mus musculus			cytosolic small ribosomal subunit			mitochondrial outer membrane	nucleus		8	9	7	2
416	Ras-related protein Rab-7a OS=Mus musculus GN=Rab7a PE=1 SV=2	RAB7A_MOUSE	23 kDa		Mus musculus	Golgi apparatus				lysosome				8	8	8	4
315	Malate dehydrogenase, mitochondrial OS=Mus musculus GN=Mdh2 PE=1 SV=3	MDHM_MOUSE	36 kDa		Mus musculus						mitochondrion	nucleus	plasma membrane	13	15	4	0
411	Ras-related protein Rab-1A OS=Mus musculus GN=Rab1A PE=1 SV=3	RAB1A_MOUSE	23 kDa	TRUE	Mus musculus	Golgi apparatus			endoplasmic reticulum					6	9	10	0
127	Cathepsin D OS=Mus musculus GN=Ctsd PE=1 SV=1	CATD_MOUSE	45 kDa		Mus musculus					lysosome	mitochondrion			8	7	6	5
510	Unconventional myosin-Va OS=Mus musculus GN=Myo5a PE=2 SV=1	D3YZ62_MOUSE (+2)	212 kDa		Mus musculus	Golgi apparatus	myosin complex							10	13	20	0
122	Cartilage acidic protein 1 OS=Mus musculus GN=Crtac1 PE=2 SV=1	CRAC1_MOUSE	70 kDa		Mus musculus									5	5	10	8
220	Guanine nucleotide-binding protein subunit alpha-11 OS=Mus musculus GN=Gna11 PE=1 SV=1	GNA11_MOUSE	42 kDa	TRUE	Mus musculus					lysosomal membrane			heterotrimeric G-protein complex	4	4	5	6

392	Protein Pi4ka OS=Mus musculus GN=Pi4ka PE=4 SV=1	E9Q3L2_MOUSE	231 kDa		Mus musculus	Golgi-associated vesicle membrane							plasma membrane	5	5	14	2
92	Annexin A2 OS=Mus musculus GN=Anxa2 PE=1 SV=2	ANXA2_MOUSE	39 kDa		Mus musculus					lysosomal membrane		nucleus	Schmidt-Lanterman cleft	13	13	0	9
255	Isoform 2 of Inositol 1,4,5-trisphosphate receptor type 1 OS=Mus musculus GN=Itpr1	sp|P11881-2|ITPR1_MOUSE (+7)	311 kDa	TRUE	unknown									17	9	7	0
334	NAC-alpha domain-containing protein 1 OS=Mus musculus GN=Nacad PE=1 SV=1	NACAD_MOUSE	157 kDa		Mus musculus							nucleus		16	14	3	0
407	RAS-related C3 botulinum substrate 1, isoform CRA_a OS=Mus musculus GN=Rac1 PE=2 SV=1	Q3TLP8_MOUSE (+1)	23 kDa	TRUE	Mus musculus								extrinsic to plasma membrane	7	6	8	6
286	Isoform PLEC-1D of Plectin OS=Mus musculus GN=Plec	sp|Q9QXS1-10|PLEC_MOUSE (+15)	514 kDa	TRUE	unknown									15	6	25	0
166	Dolichyl-diphosphooligosaccharide--protein glycosyltransferase subunit STT3A OS=Mus musculus GN=Stt3a PE=1 SV=1	STT3A_MOUSE	81 kDa		Mus musculus				oligosaccharyltransferase complex					9	12	4	0
509	Unconventional myosin-VI OS=Mus musculus GN=Myo6 PE=2 SV=1	E9PVU0_MOUSE (+1)	146 kDa		Mus musculus		myosin complex						plasma membrane	10	12	8	0
69	ATP-binding cassette sub-family B member 6, mitochondrial OS=Mus musculus GN=Abcb6 PE=1 SV=1	ABCB6_MOUSE	94 kDa		Mus musculus	Golgi apparatus			endoplasmic reticulum		mitochondrion		plasma membrane	6	7	9	0
84	Alpha-actinin-4 OS=Mus musculus GN=Actn4 PE=1 SV=1	ACTN4_MOUSE	105 kDa	TRUE	Mus musculus		stress fiber					nucleus	cell-cell junction	3	5	18	5
234	Histone H4 OS=Mus musculus GN=Hist1h4a PE=1 SV=2	H4_MOUSE	11 kDa		Mus musculus							nucleoplasm		7	8	5	4
25	60S ribosomal protein L7 OS=Mus musculus GN=Rpl7 PE=2 SV=2	RL7_MOUSE	31 kDa		Mus musculus			cytosolic large ribosomal subunit				nucleus		5	7	7	6
468	Surfeit locus protein 4 OS=Mus musculus GN=Surf4 PE=2 SV=1	SURF4_MOUSE	30 kDa		Mus musculus	Golgi apparatus			endoplasmic reticulum					4	4	4	0
115	Calcium-binding mitochondrial carrier protein Aralar1 OS=Mus musculus GN=Slc25a12 PE=1 SV=1	CMC1_MOUSE	75 kDa	TRUE	Mus musculus						mitochondrial inner membrane			8	12	3	0
363	Phospholipase C beta 4 OS=Mus musculus GN=Plcb4 PE=2 SV=1	Q91UZ1_MOUSE	135 kDa		Mus musculus		postsynaptic density		smooth endoplasmic reticulum			nucleus		4	6	13	5
154	Dedicator of cytokinesis protein 7 OS=Mus musculus GN=Dock7 PE=2 SV=1	A2A9M5_MOUSE (+3)	241 kDa	TRUE	Mus musculus							signalosome		4	3	8	3
68	ATP-binding cassette sub-family A member 7 OS=Mus musculus GN=Abca7 PE=2 SV=1	E9Q6G4_MOUSE	238 kDa		Mus musculus	Golgi apparatus							apical plasma membrane	7	5	20	4
279	Isoform Alpha of MAGUK p55 subfamily member 6 OS=Mus musculus GN=Mpp6	sp|Q9JLB0-2|MPP6_MOUSE	61 kDa	TRUE	unknown									4	5	8	5
358	Phosphate carrier protein, mitochondrial OS=Mus musculus GN=Slc25a3 PE=1 SV=1	MPCP_MOUSE	40 kDa		Mus musculus						mitochondrial inner membrane			9	12	4	0
37	60S ribosomal protein L21 OS=Mus musculus GN=Rpl21 PE=2 SV=1	Q9CQM8_MOUSE (+1)	19 kDa		Mus musculus			cytosolic large ribosomal subunit				nucleolus		3	2	3	3
410	Ras GTPase-activating-like protein IQGAP1 OS=Mus musculus GN=Iqgap1 PE=1 SV=2	IQGA1_MOUSE	189 kDa		Mus musculus		microtubule cytoskeleton					nucleus	lateral plasma membrane	6	7	10	0

35	60S ribosomal protein L18 OS=Mus musculus GN=Rpl18 PE=2 SV=3	RL18_MOUSE	22 kDa		Mus musculus			cytosolic large ribosomal subunit				nucleolus		5	9	6	5
290	Isoleucine--tRNA ligase, cytoplasmic OS=Mus musculus GN=Iars PE=2 SV=2	SYIC_MOUSE	144 kDa		Mus musculus									10	15	6	0
26	60S ribosomal protein L7a OS=Mus musculus GN=Rpl7a PE=2 SV=2	RL7A_MOUSE	30 kDa		Mus musculus									7	7	6	6
87	Alpha-enolase OS=Mus musculus GN=Eno1 PE=1 SV=3	ENOA_MOUSE	47 kDa		Mus musculus			phosphopyruvate hydratase complex					plasma membrane	2	6	10	4
288	Isoform Short of Tripeptidyl-peptidase 2 OS=Mus musculus GN=Tpp2	sp|Q64514-2|TPP2_MOUSE	138 kDa		unknown									9	9	13	2
148	Cytoplasmic FMR1-interacting protein 2 OS=Mus musculus GN=Cyfip2 PE=1 SV=2	CYFP2_MOUSE	146 kDa	TRUE	Mus musculus								cell junction	5	9	13	2
489	Transforming protein RhoA OS=Mus musculus GN=Rhoa PE=1 SV=1	RHOA_MOUSE	22 kDa	TRUE	Mus musculus		cytoskeleton	cytosol			mitochondrion	nucleus	apical junction complex	5	7	7	0
174	Elongation factor 1-gamma OS=Mus musculus GN=Eef1g PE=1 SV=3	EF1G_MOUSE	50 kDa		Mus musculus							nucleus		5	7	6	3
167	Dolichyl-diphosphooligosaccharide--protein glycosyltransferase subunit STT3B OS=Mus musculus GN=Stt3b PE=1 SV=2	STT3B_MOUSE	93 kDa		Mus musculus				oligosaccharyltransferase complex					6	8	7	0
232	Histone H2B type 1-B OS=Mus musculus GN=Hist1h2bb PE=1 SV=3	H2B1B_MOUSE (+9)	14 kDa		Mus musculus							nucleoplasm		2	3	5	0
299	Leucine--tRNA ligase, cytoplasmic OS=Mus musculus GN=Lars PE=2 SV=2	SYLC_MOUSE	134 kDa		Mus musculus							nucleus		8	15	4	0
424	Ras-related protein Rap-1A OS=Mus musculus GN=Rap1a PE=2 SV=1	RAP1A_MOUSE	21 kDa		Mus musculus								plasma membrane	3	4	7	3
99	Atlastin-2 OS=Mus musculus GN=Atl2 PE=1 SV=1	sp|Q6PA06|ATLA2_MOUSE	66 kDa		Mus musculus				endoplasmic reticulum					3	7	5	0
130	Cell division control protein 42 homolog OS=Mus musculus GN=Cdc42 PE=1 SV=2	sp|P60766|CDC42_MOUSE	21 kDa	TRUE	Mus musculus	Golgi membrane	spindle midzone	cytosol					cell-cell junction	3	3	4	3
27	60S ribosomal protein L8 OS=Mus musculus GN=Rpl8 PE=2 SV=2	RL8_MOUSE	28 kDa		Mus musculus			cytosolic large ribosomal subunit						6	7	4	0
457	Solute carrier family 12 member 4 OS=Mus musculus GN=Slc12a4 PE=4 SV=2	F8WIJ0_MOUSE (+1)	121 kDa		Mus musculus									6	5	14	0
180	Enhancer of mRNA decapping 4, isoform CRA_b OS=Mus musculus GN=Edc4 PE=4 SV=1	G5E896_MOUSE	152 kDa		Mus musculus							nucleus		13	13	0	0
152	DNA fragmentation factor subunit beta OS=Mus musculus GN=Cad PE=2 SV=1	E9QAI5_MOUSE (+1)	236 kDa		Mus musculus									8	4	8	0
214	Guanine nucleotide-binding protein G(I)/G(S)/G(T) subunit beta-1 OS=Mus musculus GN=Gnb1 PE=1 SV=3	GBB1_MOUSE	37 kDa	TRUE	Mus musculus					lysosomal membrane			plasma membrane	4	4	4	3
254	Isoform 2 of Glucosidase 2 subunit beta OS=Mus musculus GN=Prkcsh	sp|O08795-2|GLU2B_MOUSE (+1)	60 kDa		unknown									9	9	3	2
521	Very-long-chain enoyl-CoA reductase OS=Mus musculus GN=Tecr PE=1 SV=1	TECR_MOUSE	36 kDa		Mus musculus				integral to endoplasmic reticulum membrane					6	8	6	0
230	High affinity cationic amino acid transporter 1 OS=Mus musculus GN=Slc7a1 PE=2 SV=1	CTR1_MOUSE	67 kDa		Mus musculus									4	4	5	3
329	Monocarboxylate transporter 1 OS=Mus musculus GN=Slc16a1 PE=1 SV=1	MOT1_MOUSE	53 kDa		Mus musculus		centrosome				mitochondrion		plasma membrane	4	4	7	5
505	Ubiquitin-like modifier-activating enzyme 1 OS=Mus musculus GN=Uba1 PE=1 SV=1	UBA1_MOUSE	118 kDa		Mus musculus			cytosol	rough endoplasmic reticulum membrane	lysosomal	mitochondrion	nucleus	desmosome	4	5	5	0

										membrane							
171	ER membrane protein complex subunit 1 OS=Mus musculus GN=Emc1 PE=1 SV=1	sp|Q8C7X2|EMC1_MOUSE	112 kDa		Mus musculus									5	10	6	0
374	Probable cation-transporting ATPase 13A1 OS=Mus musculus GN=Atp13a1 PE=1 SV=2	AT131_MOUSE	132 kDa		Mus musculus				endoplasmic reticulum					8	12	6	0
373	Probable ATP-dependent RNA helicase DDX6 OS=Mus musculus GN=Ddx6 PE=1 SV=1	DDX6_MOUSE	54 kDa		Mus musculus									6	5	3	0
355	Peroxidasin homolog OS=Mus musculus GN=Pxdn PE=2 SV=2	PXDN_MOUSE	165 kDa		Mus musculus				endoplasmic reticulum					6	10	7	0
453	Sodium/potassium-transporting ATPase subunit beta-1 OS=Mus musculus GN=Atp1b1 PE=1 SV=1	AT1B1_MOUSE	35 kDa		Mus musculus								plasma membrane	4	4	5	5
420	Ras-related protein Rab-14 OS=Mus musculus GN=Rab14 PE=1 SV=3	RAB14_MOUSE	24 kDa		Mus musculus	Golgi apparatus				lysosomal membrane				6	6	6	3
151	Cytoskeleton-associated protein 5 OS=Mus musculus GN=Ckap5 PE=4 SV=1	K3W4R5_MOUSE (+2)	226 kDa		Mus musculus		centrosome							8	6	9	0
90	Angiotensin-converting enzyme OS=Mus musculus GN=Ace PE=1 SV=3	sp|P09470|ACE_MOUSE	151 kDa		Mus musculus								plasma membrane	3	4	10	3
456	Solute carrier family 12 member 2 OS=Mus musculus GN=Slc12a2 PE=4 SV=1	E9QM38_MOUSE	131 kDa		Mus musculus								apical plasma membrane	4	3	11	3
419	Ras-related protein Rab-11B OS=Mus musculus GN=Rab11b PE=1 SV=3	RB11B_MOUSE	24 kDa		Mus musculus						mitochondrion		cell junction	7	7	5	0
217	Guanine nucleotide-binding protein G(k) subunit alpha OS=Mus musculus GN=Gnai3 PE=1 SV=3	GNAI3_MOUSE	41 kDa	TRUE	Mus musculus	Golgi apparatus	centrosome			lysosomal membrane			plasma membrane	4	5	4	3
515	V-type proton ATPase subunit d 1 OS=Mus musculus GN=Atp6v0d1 PE=1 SV=2	VA0D1_MOUSE	40 kDa		Mus musculus		centrosome			lysosomal membrane			apical plasma membrane	4	4	4	4
480	T-complex protein 1 subunit zeta OS=Mus musculus GN=Cct6a PE=1 SV=3	TCPZ_MOUSE	58 kDa		Mus musculus			chaperonin-containing T-complex						5	7	5	2
249	Isoform 2 of CD97 antigen OS=Mus musculus GN=Cd97	sp|Q9Z0M6-2|CD97_MOUSE (+3)	80 kDa		unknown									5	5	8	2
438	Septin-7 OS=Mus musculus GN=Sept7 PE=3 SV=2	E9Q1G8_MOUSE (+2)	51 kDa		Mus musculus		septin complex							0	0	6	7
464	Steryl-sulfatase OS=Mus musculus GN=Sts PE=2 SV=1	STS_MOUSE	67 kDa		Mus musculus				endoplasmic reticulum					4	4	3	0
357	Peroxisomal multifunctional enzyme type 2 OS=Mus musculus GN=Hsd17b4 PE=1 SV=3	DHB4_MOUSE	79 kDa		Mus musculus						mitochondrion			7	14	3	0
285	Isoform Mt-VDAC1 of Voltage-dependent anion-selective channel protein 1 OS=Mus musculus GN=Vdac1	sp|Q60932-2|VDAC1_MOUSE (+1)	31 kDa		unknown									7	9	0	0
268	Isoform 2 of Synaptotagmin-like protein 4 OS=Mus musculus GN=Sytl4	sp|Q9R0Q1-2|SYTL4_MOUSE (+2)	57 kDa		unknown									3	4	8	6
30	60S ribosomal protein L12 OS=Mus musculus GN=Rpl12 PE=1 SV=2	RL12_MOUSE	18 kDa		Mus musculus									4	6	5	2
322	Methionine--tRNA ligase, cytoplasmic OS=Mus musculus GN=Mars PE=2 SV=1	E9QB02_MOUSE (+1)	102 kDa		Mus musculus						mitochondrion			5	8	4	0
506	Uncharacterized protein OS=Mus musculus GN=Gm8730 PE=2 SV=1	E9Q070_MOUSE	34 kDa		Mus musculus									6	8	7	4

31	60S ribosomal protein L13 OS=Mus musculus GN=Rpl13 PE=2 SV=3	RL13_MOUSE	24 kDa		Mus musculus									7	6	3	3
10	40S ribosomal protein S8 OS=Mus musculus GN=Rps8 PE=1 SV=2	RS8_MOUSE	24 kDa		Mus musculus			cytosolic small ribosomal subunit				nucleus		5	7	6	2
176	Endoplasmic reticulum metallopeptidase 1 OS=Mus musculus GN=Ermp1 PE=1 SV=2	sp|Q3UVK0|ERMP1_MOUSE	100 kDa		Mus musculus				endoplasmic reticulum					5	6	3	0
403	Protein transport protein Sec61 subunit alpha isoform 1 OS=Mus musculus GN=Sec61a1 PE=2 SV=2	S61A1_MOUSE	52 kDa		Mus musculus				rough endoplasmic reticulum					3	6	2	0
352	Peptidyl-prolyl cis-trans isomerase A OS=Mus musculus GN=Ppia PE=1 SV=2	PPIA_MOUSE	18 kDa		Mus musculus			cytosol				nucleus		3	4	5	3
231	Histone H2A type 1-F OS=Mus musculus GN=Hist1h2af PE=1 SV=3	H2A1F_MOUSE (+6)	14 kDa		Mus musculus							nucleus		3	4	3	2
56	AP-1 complex subunit beta-1 OS=Mus musculus GN=Ap1b1 PE=1 SV=2	AP1B1_MOUSE (+2)	104 kDa	TRUE	Mus musculus	trans-Golgi network								2	3	5	0
519	Very low-density lipoprotein receptor OS=Mus musculus GN=Vldlr PE=2 SV=1	F8WGI9_MOUSE (+2)	89 kDa		Mus musculus									2	6	7	0
138	Coatomer subunit gamma-1 OS=Mus musculus GN=Copg1 PE=2 SV=1	COPG1_MOUSE	98 kDa		Mus musculus	COPI vesicle coat								4	5	5	4
193	FERM, RhoGEF and pleckstrin domain-containing protein 1 OS=Mus musculus GN=Farp1 PE=1 SV=1	FARP1_MOUSE	119 kDa		Mus musculus		cytoskeleton	cytosol					cell junction	3	5	9	3
526	Vesicle-trafficking protein SEC22b OS=Mus musculus GN=Sec22b PE=1 SV=3	SC22B_MOUSE	25 kDa		Mus musculus	Golgi membrane			endoplasmic reticulum membrane					6	8	4	0
203	G protein-regulated inducer of neurite outgrowth 1 OS=Mus musculus GN=Gprin1 PE=1 SV=2	GRIN1_MOUSE	95 kDa		Mus musculus								plasma membrane	0	3	13	5
470	Synaptophysin OS=Mus musculus GN=Syp PE=1 SV=2	SYPH_MOUSE	34 kDa		Mus musculus								cell junction	2	2	2	4
200	Flotillin 2, isoform CRA_a OS=Mus musculus GN=Flot2 PE=4 SV=1	Q5SS83_MOUSE (+3)	47 kDa		Mus musculus								caveola	3	5	7	2
353	Peptidyl-prolyl cis-trans isomerase B OS=Mus musculus GN=Ppib PE=2 SV=2	PPIB_MOUSE	24 kDa		Mus musculus				endoplasmic reticulum			nucleus		5	9	2	0
29	60S ribosomal protein L10 (Fragment) OS=Mus musculus GN=Rpl10 PE=4 SV=1	I7HLV2_MOUSE (+1)	23 kDa		Mus musculus									3	5	4	0
80	Adenylyl cyclase-associated protein 1 OS=Mus musculus GN=Cap1 PE=1 SV=4	CAP1_MOUSE	52 kDa		Mus musculus		cortical actin cytoskeleton	cytosol					plasma membrane	2	2	2	0
156	Dedicator of cytokinesis protein 11 OS=Mus musculus GN=Dock11 PE=2 SV=1	A2AF67_MOUSE	218 kDa	TRUE	Mus musculus									2	2	10	0
41	60S ribosomal protein L24 OS=Mus musculus GN=Rpl24 PE=2 SV=2	RL24_MOUSE	18 kDa		Mus musculus			cytosolic large ribosomal subunit						2	4	4	2
120	Carboxypeptidase D OS=Mus musculus GN=Cpd PE=1 SV=2	CBPD_MOUSE	152 kDa		Mus musculus									4	5	6	0
310	Lysosome membrane protein 2 OS=Mus musculus GN=Scarb2 PE=1 SV=3	SCRB2_MOUSE	54 kDa		Mus musculus					lysosomal membrane				4	5	6	2
335	NADH-cytochrome b5 reductase 3 OS=Mus musculus GN=Cyb5r3 PE=2 SV=1	F2Z456_MOUSE (+2)	35 kDa		Mus musculus						mitochondrial inner membrane			6	8	4	0
62	ATP synthase subunit O, mitochondrial OS=Mus musculus GN=Atp5o PE=1 SV=1	ATPO_MOUSE	23 kDa		Mus musculus						mitochondrial proton-transporting ATP			7	7	0	0

											synthase complex						
179	Endothelin-converting enzyme-like 1 OS=Mus musculus GN=Ecel1 PE=2 SV=2	ECEL1_MOUSE	88 kDa		Mus musculus								integral to plasma membrane	4	8	5	2
8	40S ribosomal protein S4, X isoform OS=Mus musculus GN=Rps4x PE=2 SV=2	RS4X_MOUSE	30 kDa		Mus musculus									5	9	4	0
126	Cathepsin B OS=Mus musculus GN=Ctsb PE=1 SV=2	CATB_MOUSE	37 kDa		Mus musculus					lysosome	mitochondrion	nucleolus		6	7	2	0
169	E3 ubiquitin-protein ligase HUWE1 OS=Mus musculus GN=Huwe1 PE=2 SV=1	A2AFQ0_MOUSE (+2)	483 kDa		Mus musculus							nucleus		8	0	6	0
475	T-complex protein 1 subunit delta OS=Mus musculus GN=Cct4 PE=2 SV=1	G5E839_MOUSE (+1)	55 kDa		Mus musculus			chaperonin-containing T-complex						3	3	6	2
23	60S ribosomal protein L5 OS=Mus musculus GN=Rpl5 PE=1 SV=3	RL5_MOUSE	34 kDa		Mus musculus			cytosolic large ribosomal subunit				nucleolus		2	2	8	3
408	Radixin OS=Mus musculus GN=Rdx PE=1 SV=3	RADI_MOUSE	69 kDa	TRUE	Mus musculus		cytoskeleton						T-tubule	5	3	8	0
276	Isoform 3 of Sec1 family domain-containing protein 1 OS=Mus musculus GN=Scfd1	sp|Q8BRF7-3|SCFD1_MOUSE (+1)	67 kDa		unknown									6	5	6	0
137	Coatomer subunit beta' OS=Mus musculus GN=Copb2 PE=2 SV=2	COPB2_MOUSE	102 kDa		Mus musculus	COPI vesicle coat								2	4	11	0
253	Isoform 2 of Electroneutral sodium bicarbonate exchanger 1 OS=Mus musculus GN=Slc4a8	sp|Q8JZR6-2|S4A8_MOUSE (+1)	117 kDa		unknown									0	3	7	0
477	T-complex protein 1 subunit eta OS=Mus musculus GN=Cct7 PE=1 SV=1	TCPH_MOUSE	60 kDa		Mus musculus		microtubule	chaperonin-containing T-complex			mitochondrion			4	2	4	3
430	Ribosomal protein L15 OS=Mus musculus GN=Gm10020 PE=3 SV=1	E9QAZ2_MOUSE (+1)	24 kDa		Mus musculus			cytosolic large ribosomal subunit				nucleus		5	6	7	2
142	Coronin-1C OS=Mus musculus GN=Coro1c PE=1 SV=2	COR1C_MOUSE	53 kDa		Mus musculus		cytoskeleton						plasma membrane	3	6	8	2
405	Pyruvate carboxylase OS=Mus musculus GN=Pcx PE=2 SV=1	E9QPD7_MOUSE (+1)	130 kDa		Mus musculus						mitochondrial inner membrane			10	8	0	0
387	Protein Gm10320 OS=Mus musculus GN=Gm10320 PE=4 SV=1	E9PW43_MOUSE (+1)	12 kDa		unknown									3	3	3	3
270	Isoform 2 of UPF0577 protein KIAA1324 OS=Mus musculus GN=Kiaa1324	sp|A2AFS3-2|K1324_MOUSE (+2)	100 kDa		unknown									5	6	9	0
391	Protein Nbas OS=Mus musculus GN=Nbas PE=2 SV=1	E9Q411_MOUSE	266 kDa		Mus musculus									12	5	3	0
144	Cytochrome P450 2S1 OS=Mus musculus GN=Cyp2s1 PE=2 SV=1	CP2S1_MOUSE (+1)	56 kDa		Mus musculus				endoplasmic reticulum					3	4	0	0
478	T-complex protein 1 subunit gamma OS=Mus musculus GN=Cct3 PE=2 SV=1	E9Q133_MOUSE (+1)	57 kDa		Mus musculus			chaperonin-containing T-complex						3	3	6	5
370	Polyadenylate-binding protein 1 OS=Mus musculus GN=Pabpc1 PE=1 SV=2	PABP1_MOUSE	71 kDa		Mus musculus							spliceosome		8	6	5	0
384	Protein Atp2b4 OS=Mus musculus GN=Atp2b4 PE=2 SV=1	E9Q828_MOUSE (+3)	129 kDa	TRUE	Mus musculus								integral to plasma membrane	0	2	3	2
291	Junction plakoglobin OS=Mus musculus GN=Jup PE=1 SV=3	PLAK_MOUSE	82 kDa	TRUE	Mus musculus		actin cytoskeleton	cytosol					lateral plasma membrane	5	0	6	7
349	Nucleolin OS=Mus musculus GN=Ncl PE=1 SV=2	NUCL_MOUSE	77 kDa		Mus musculus							nucleolus		7	4	4	0
229	Hexokinase 1, isoform CRA_f OS=Mus musculus GN=Hk1 PE=3 SV=1	G3UVV4_MOUSE (+3)	102 kDa		Mus musculus			cytosol			mitochondrion			5	8	0	0

494	Trifunctional enzyme subunit alpha, mitochondrial OS=Mus musculus GN=Hadha PE=1 SV=1	ECHA_MOUSE	83 kDa		Mus musculus						mitochondrion			5	5	0	0
265	Isoform 2 of Seizure 6-like protein 2 OS=Mus musculus GN=Sez6l2	sp|Q4V9Z5-2|SE6L2_MOUSE (+1)	99 kDa		unknown									0	3	7	2
59	AP-2 complex subunit mu OS=Mus musculus GN=Ap2m1 PE=1 SV=1	AP2M1_MOUSE (+1)	50 kDa		Mus musculus						mitochondrion		plasma membrane	3	4	5	0
306	Long-chain-fatty-acid--CoA ligase 3 OS=Mus musculus GN=Acsl3 PE=2 SV=2	ACSL3_MOUSE	80 kDa	TRUE	Mus musculus	Golgi apparatus			endoplasmic reticulum		mitochondrial outer membrane			6	7	3	0
492	Translocation protein SEC63 homolog OS=Mus musculus GN=Sec63 PE=1 SV=4	SEC63_MOUSE	88 kDa		Mus musculus				endoplasmic reticulum					4	6	5	0
243	Isoform 1 of Neurofibromin OS=Mus musculus GN=Nf1	sp|Q04690-2|NF1_MOUSE (+1)	317 kDa		unknown									3	3	6	0
91	Ankyrin-2 OS=Mus musculus GN=Ank2 PE=4 SV=1	S4R1F9_MOUSE (+2)	428 kDa	TRUE	Mus musculus								plasma membrane	2	0	12	0
532	cAMP-dependent protein kinase type I-alpha regulatory subunit OS=Mus musculus GN=Prkar1a PE=1 SV=3	KAP0_MOUSE	43 kDa	TRUE	Mus musculus								plasma membrane	2	5	5	4
524	Vesicle-associated membrane protein-associated protein A OS=Mus musculus GN=Vapa PE=1 SV=2	VAPA_MOUSE	28 kDa	TRUE	Mus musculus		microtubule cytoskeleton		endoplasmic reticulum				plasma membrane	4	7	2	0
393	Protein Slc8a2 OS=Mus musculus GN=Slc8a2 PE=2 SV=1	Q8K596_MOUSE	101 kDa		Mus musculus									3	2	5	0
182	Erlin-2 OS=Mus musculus GN=Erlin2 PE=1 SV=1	ERLN2_MOUSE	38 kDa	TRUE	Mus musculus				endoplasmic reticulum membrane					5	6	3	0
465	Stress-70 protein, mitochondrial OS=Mus musculus GN=Hspa9 PE=1 SV=3	GRP75_MOUSE	73 kDa		Mus musculus						mitochondrion	nucleus		8	9	0	0
469	Synaptic vesicle glycoprotein 2A OS=Mus musculus GN=Sv2a PE=1 SV=1	SV2A_MOUSE	83 kDa		Mus musculus				endoplasmic reticulum				cell-cell junction	2	3	7	2
446	Serine/threonine-protein phosphatase PP1-alpha catalytic subunit OS=Mus musculus GN=Ppp1ca PE=1 SV=1	PP1A_MOUSE	38 kDa		Mus musculus							nucleoplasm		3	4	3	0
191	Ezrin OS=Mus musculus GN=Ezr PE=1 SV=3	EZRI_MOUSE	69 kDa	TRUE	Mus musculus		actin filament	cytosol				nucleolus	plasma membrane	2	2	9	0
162	DnaJ homolog subfamily C member 10 OS=Mus musculus GN=Dnajc10 PE=1 SV=2	DJC10_MOUSE	91 kDa		Mus musculus				endoplasmic reticulum chaperone complex					4	10	4	0
316	Malectin OS=Mus musculus GN=Mlec PE=2 SV=2	MLEC_MOUSE	32 kDa		Mus musculus				endoplasmic reticulum					5	5	4	0
119	Caprin-1 OS=Mus musculus GN=Caprin1 PE=1 SV=2	CAPR1_MOUSE	78 kDa		Mus musculus									3	3	3	0
536	sp|Q8K2B3|SDHA_MOUSE	sp|Q8K2B3|SDHA_MOUSE	?		Mus musculus						mitochondrion			6	7	0	0
341	Neurofilament medium polypeptide OS=Mus musculus GN=Nefm PE=1 SV=4	NFM_MOUSE	96 kDa	TRUE	Mus musculus									6	11	0	0
184	Eukaryotic initiation factor 4A-I OS=Mus musculus GN=Eif4a1 PE=1 SV=1	IF4A1_MOUSE	46 kDa	TRUE	Mus musculus									4	5	3	2
275	Isoform 3 of Peripheral plasma membrane protein CASK OS=Mus musculus GN=Cask	sp|O70589-3|CSKP_MOUSE (+4)	102 kDa		unknown									4	6	8	0
204	GPI transamidase component PIG-S OS=Mus musculus GN=Pigs PE=1 SV=3	PIGS_MOUSE	62 kDa		Mus musculus				GPI-anchor transamidase complex					3	3	2	0
318	Mannosyl-oligosaccharide glucosidase OS=Mus musculus GN=Mogs PE=2 SV=1	MOGS_MOUSE	92 kDa		Mus musculus				endoplasmic reticulum					2	7	2	0

181	Erbb2ip protein OS=Mus musculus GN=Erbb2ip PE=2 SV=1	B7ZNX6_MOUSE (+4)	158 kDa		Mus musculus								basolateral plasma membrane	2	2	3	0
437	Septin-2 OS=Mus musculus GN=Sept2 PE=1 SV=2	SEPT2_MOUSE	42 kDa		Mus musculus		microtubule cytoskeleton					nucleolus	cilium membrane	0	0	4	4
520	Very-long-chain (3R)-3-hydroxyacyl-[acyl-carrier protein] dehydratase 3 OS=Mus musculus GN=ptplad1 PE=1 SV=2	HACD3_MOUSE	43 kDa		Mus musculus				endoplasmic reticulum					5	6	4	0
379	Prohibitin OS=Mus musculus GN=Phb PE=1 SV=1	PHB_MOUSE	30 kDa		Mus musculus						mitochondrial inner membrane	nucleus	integral to plasma membrane	7	8	0	0
44	60S ribosomal protein L27a OS=Mus musculus GN=Rpl27a PE=2 SV=5	RL27A_MOUSE	17 kDa		Mus musculus									4	6	5	2
7	40S ribosomal protein S3 OS=Mus musculus GN=Rps3 PE=1 SV=1	RS3_MOUSE	27 kDa		Mus musculus			cytosolic small ribosomal subunit				nucleus	ruffle membrane	2	6	5	0
38	60S ribosomal protein L22 OS=Mus musculus GN=Rpl22 PE=2 SV=2	RL22_MOUSE	15 kDa		Mus musculus			cytosolic large ribosomal subunit				nucleus		2	3	4	0
70	ATP-binding cassette sub-family D member 3 OS=Mus musculus GN=Abcd3 PE=1 SV=2	ABCD3_MOUSE	75 kDa		Mus musculus						mitochondrial inner membrane			5	9	0	0
487	Transcriptional activator protein Pur-beta OS=Mus musculus GN=Purb PE=1 SV=3	PURB_MOUSE	34 kDa		Mus musculus							DNA replication factor A complex		3	4	2	0
302	Lipase maturation factor 2 OS=Mus musculus GN=Lmf2 PE=2 SV=1	LMF2_MOUSE	80 kDa		Mus musculus				endoplasmic reticulum					4	4	5	0
282	Isoform B of FK506-binding protein 15 OS=Mus musculus GN=Fkbp15	sp|Q6P9Q6-2|FKB15_MOUSE (+1)	137 kDa		unknown									2	5	4	0
287	Isoform Short of Delta-1-pyrroline-5-carboxylate synthase OS=Mus musculus GN=Aldh18a1	sp|Q9Z110-2|P5CS_MOUSE (+1)	87 kDa		unknown									4	8	0	0
146	Cytochrome b-c1 complex subunit 2, mitochondrial OS=Mus musculus GN=Uqcrc2 PE=1 SV=1	QCR2_MOUSE	48 kDa		Mus musculus						mitochondrial inner membrane			6	7	0	0
4	7-dehydrocholesterol reductase OS=Mus musculus GN=Dhcr7 PE=2 SV=1	DHCR7_MOUSE	54 kDa		Mus musculus				endoplasmic reticulum			nuclear outer membrane		2	4	4	0
65	ATP synthase subunit d, mitochondrial OS=Mus musculus GN=Atp5h PE=1 SV=3	ATP5H_MOUSE (+1)	19 kDa		Mus musculus						mitochondrion			4	5	0	0
448	Signal sequence receptor, delta OS=Mus musculus GN=Ssr4 PE=2 SV=1	Q9D8L3_MOUSE (+1)	19 kDa		Mus musculus				endoplasmic reticulum					3	5	2	0
161	Disco-interacting protein 2 homolog B OS=Mus musculus GN=Dip2b PE=1 SV=1	sp|Q3UH60|DIP2B_MOUSE	171 kDa		Mus musculus							nucleus		0	2	9	0
347	Nischarin OS=Mus musculus GN=Nisch PE=1 SV=2	sp|Q80TM9|NISCH_MOUSE	175 kDa		Mus musculus			cytosol					plasma membrane	9	3	4	0
135	Cleft lip and palate transmembrane protein 1 homolog OS=Mus musculus GN=Clptm1 PE=1 SV=1	CLPT1_MOUSE	75 kDa		Mus musculus								external side of plasma membrane	7	8	3	0
14	40S ribosomal protein S15a OS=Mus musculus GN=Rps15a PE=2 SV=2	RS15A_MOUSE	15 kDa		Mus musculus									2	6	5	0
289	Isoform Smooth muscle of Myosin light polypeptide 6 OS=Mus musculus GN=Myl6	sp|Q60605-2|MYL6_MOUSE (+1)	17 kDa		unknown									2	4	0	2
454	Sodium/potassium-transporting ATPase subunit beta-3 OS=Mus musculus GN=Atp1b3 PE=1 SV=1	AT1B3_MOUSE	32 kDa		Mus musculus								sodium:potassium-exchanging ATPase complex	3	3	7	2

75	Acid sphingomyelinase-like phosphodiesterase 3b OS=Mus musculus GN=Smpdl3b PE=1 SV=1	ASM3B_MOUSE	52 kDa		Mus musculus									2	2	4	2
240	Interleukin-6 receptor subunit beta OS=Mus musculus GN=Il6st PE=1 SV=2	IL6RB_MOUSE	102 kDa		Mus musculus								external side of plasma membrane	2	3	6	4
307	Long-chain-fatty-acid--CoA ligase 4 OS=Mus musculus GN=Acsl4 PE=2 SV=2	sp|Q9QUJ7|ACSL4_MOUSE	79 kDa	TRUE	Mus musculus				endoplasmic reticulum		mitochondrial outer membrane			4	6	3	0
5	14-3-3 protein zeta/delta OS=Mus musculus GN=Ywhaz PE=1 SV=1	1433Z_MOUSE	28 kDa	TRUE	Mus musculus		postsynaptic density	cytosol		mast cell granule	mitochondrion	nucleus		3	3	3	0
356	Peroxiredoxin-4 OS=Mus musculus GN=Prdx4 PE=1 SV=1	PRDX4_MOUSE	31 kDa		Mus musculus			cytosol	endoplasmic reticulum		mitochondrion	nucleus		4	7	2	0
33	60S ribosomal protein L14 OS=Mus musculus GN=Rpl14 PE=2 SV=3	RL14_MOUSE	24 kDa		Mus musculus			cytosolic large ribosomal subunit						4	4	6	2
263	Isoform 2 of Rab GDP dissociation inhibitor beta OS=Mus musculus GN=Gdi2	sp|Q61598-2|GDIB_MOUSE (+1)	47 kDa		unknown									3	3	2	2
267	Isoform 2 of Sodium-coupled neutral amino acid transporter 5 OS=Mus musculus GN=Slc38a5	sp|Q3U1J0-2|S38A5_MOUSE (+1)	52 kDa		unknown									3	0	6	0
185	Eukaryotic translation initiation factor 3 subunit A OS=Mus musculus GN=Eif3a PE=1 SV=5	EIF3A_MOUSE	162 kDa		Mus musculus		cytoskeleton					nucleolus		6	7	2	0
143	Cullin-associated NEDD8-dissociated protein 1 OS=Mus musculus GN=Cand1 PE=2 SV=2	CAND1_MOUSE	136 kDa		Mus musculus							nucleus		4	5	4	0
311	Lysosome-associated membrane glycoprotein 1 OS=Mus musculus GN=Lamp1 PE=1 SV=2	LAMP1_MOUSE	44 kDa		Mus musculus					lysosome			sarcolemma	3	3	3	0
139	Cofilin-1 OS=Mus musculus GN=Cfl1 PE=1 SV=3	COF1_MOUSE (+1)	19 kDa		Mus musculus		cortical actin cytoskeleton	cytosol				nucleus	plasma membrane	3	4	3	2
479	T-complex protein 1 subunit theta OS=Mus musculus GN=Cct8 PE=2 SV=1	H3BL49_MOUSE (+1)	53 kDa		Mus musculus			chaperonin-containing T-complex						3	2	4	4
39	60S ribosomal protein L23 OS=Mus musculus GN=Rpl23 PE=1 SV=1	RL23_MOUSE	15 kDa		Mus musculus			cytosolic ribosome				nucleolus		3	3	2	2
86	Alpha-centractin OS=Mus musculus GN=Actr1a PE=2 SV=1	ACTZ_MOUSE	43 kDa		Mus musculus		centrosome							2	2	2	3
501	Tyrosine-protein kinase receptor OS=Mus musculus GN=Igf1r PE=2 SV=1	E9QNX9_MOUSE (+1)	155 kDa		Mus musculus								caveola	2	4	8	2
414	Ras-related protein Rab-5C OS=Mus musculus GN=Rab5c PE=1 SV=2	RAB5C_MOUSE	23 kDa	TRUE	Mus musculus								plasma membrane	2	5	2	0
61	ATP synthase F(0) complex subunit B1, mitochondrial OS=Mus musculus GN=Atp5f1 PE=1 SV=1	AT5F1_MOUSE	29 kDa		Mus musculus						mitochondrial proton-transporting ATP synthase complex, coupling factor F(o)	nucleus		4	3	2	0
377	Procollagen-lysine,2-oxoglutarate 5-dioxygenase 2 OS=Mus musculus GN=Plod2 PE=2 SV=1	E9Q718_MOUSE (+1)	87 kDa		Mus musculus				endoplasmic reticulum					2	4	2	0
321	Membrane-associated progesterone receptor component 2 OS=Mus musculus GN=Pgrmc2 PE=1 SV=2	PGRC2_MOUSE	23 kDa		Mus musculus									4	4	2	0
113	CLIP-associating protein 1 OS=Mus musculus GN=Clasp1 PE=4 SV=1	J3QP81_MOUSE (+7)	161 kDa	TRUE	Mus musculus		kinetochore microtubule							2	5	5	0
380	Prohibitin-2 OS=Mus musculus GN=Phb2 PE=1 SV=1	PHB2_MOUSE	33 kDa		Mus musculus						mitochondrial inner membrane	nuclear matrix		6	5	0	0

224	Heat shock protein HSP 90-alpha OS=Mus musculus GN=Hsp90aa1 PE=1 SV=4	HS90A_MOUSE	85 kDa	TRUE	Mus musculus			cytosol			mitochondrion	nucleus	basolateral plasma membrane	3	0	7	2
346	Niemann-Pick C1 protein OS=Mus musculus GN=Npc1 PE=1 SV=2	NPC1_MOUSE	143 kDa		Mus musculus	Golgi apparatus			endoplasmic reticulum	lysosomal membrane		nuclear envelope	plasma membrane	3	4	4	0
18	40S ribosomal protein S27 OS=Mus musculus GN=Rps27 PE=1 SV=3	RS27_MOUSE (+1)	9 kDa		Mus musculus									2	3	3	0
375	Probable phospholipid-transporting ATPase IIA OS=Mus musculus GN=Atp9a PE=2 SV=1	A2AQC3_MOUSE (+3)	124 kDa		Mus musculus	trans-Golgi network								4	3	6	0
105	Beta-hexosaminidase subunit beta OS=Mus musculus GN=Hexb PE=2 SV=2	HEXB_MOUSE	61 kDa		Mus musculus					lysosome				4	5	2	0
2	3-ketoacyl-CoA thiolase A, peroxisomal OS=Mus musculus GN=Acaa1a PE=2 SV=1	THIKA_MOUSE	44 kDa		Mus musculus						mitochondrion			4	5	2	0
284	Isoform LAMP-2B of Lysosome-associated membrane glycoprotein 2 OS=Mus musculus GN=Lamp2	sp|P17047-2|LAMP2_MOUSE (+2)	46 kDa		unknown									3	3	4	0
297	Lanosterol synthase OS=Mus musculus GN=Lss PE=2 SV=2	ERG7_MOUSE	83 kDa		Mus musculus				endoplasmic reticulum					4	8	5	0
443	Serine/threonine-protein kinase MRCK beta OS=Mus musculus GN=Cdc42bpb PE=1 SV=2	MRCKB_MOUSE	195 kDa	TRUE	Mus musculus		actomyosin						cell-cell junction	4	3	8	0
248	Isoform 2 of Acetyl-CoA carboxylase 1 OS=Mus musculus GN=Acaca	sp|Q5SWU9-2|ACACA_MOUSE (+1)	270 kDa		unknown									4	2	7	0
67	ATP synthase subunit gamma, mitochondrial OS=Mus musculus GN=Atp5c1 PE=1 SV=1	ATPG_MOUSE (+1)	33 kDa		Mus musculus						mitochondrial inner membrane			3	7	0	0
295	L-lactate dehydrogenase OS=Mus musculus GN=Ldha PE=3 SV=1	G5E8N5_MOUSE (+1)	40 kDa		Mus musculus			cytosol			mitochondrion	nucleus		2	3	3	0
55	ADP/ATP translocase 2 OS=Mus musculus GN=Slc25a5 PE=1 SV=3	ADT2_MOUSE	33 kDa	TRUE	Mus musculus						mitochondrial nucleoid	nucleus		4	5	2	0
74	Acetyl-CoA acetyltransferase, mitochondrial OS=Mus musculus GN=Acat1 PE=1 SV=1	THIL_MOUSE	45 kDa		Mus musculus						mitochondrial matrix			5	6	0	0
386	Protein Gm9493 OS=Mus musculus GN=Gm9493 PE=4 SV=1	F6SVV1_MOUSE (+1)	22 kDa		Mus musculus			cytosolic small ribosomal subunit						4	3	3	2
6	40S ribosomal protein S2 OS=Mus musculus GN=Rps2 PE=1 SV=3	RS2_MOUSE	31 kDa		Mus musculus			cytosolic small ribosomal subunit						3	5	4	2
236	IgE-binding protein OS=Mus musculus GN=Iap PE=2 SV=1	IGEB_MOUSE	63 kDa		Mus musculus									6	7	2	0
484	Thioredoxin-related transmembrane protein 1 OS=Mus musculus GN=Tmx1 PE=1 SV=1	TMX1_MOUSE	31 kDa		Mus musculus				endoplasmic reticulum			nucleolus		2	4	3	0
305	Long-chain-fatty-acid--CoA ligase 1 OS=Mus musculus GN=Acsl1 PE=1 SV=2	ACSL1_MOUSE (+1)	78 kDa	TRUE	Mus musculus				endoplasmic reticulum		mitochondrial outer membrane		plasma membrane	2	6	2	0
449	Sodium- and chloride-dependent taurine transporter OS=Mus musculus GN=Slc6a6 PE=1 SV=2	SC6A6_MOUSE	70 kDa	TRUE	Mus musculus								integral to plasma membrane	2	3	5	0
104	Beta-hexosaminidase subunit alpha OS=Mus musculus GN=Hexa PE=2 SV=2	HEXA_MOUSE	61 kDa		Mus musculus					lysosome				3	3	3	2
418	Ras-related protein Rab-10 OS=Mus musculus GN=Rab10 PE=1 SV=1	RAB10_MOUSE	23 kDa	TRUE	Mus musculus	Golgi apparatus			endoplasmic reticulum membrane				plasma membrane	2	2	2	0
482	Thioredoxin domain-containing protein 5 OS=Mus musculus GN=Txndc5 PE=2 SV=1	E9PXX7_MOUSE (+1)	39 kDa		Mus musculus									3	6	0	0
256	Isoform 2 of Integrin alpha-3 OS=Mus musculus GN=Itga3	sp|Q62470-2|ITA3_MOUSE (+1)	119 kDa		unknown									0	3	6	2

422	Ras-related protein Rab-35 OS=Mus musculus GN=Rab35 PE=1 SV=1	RAB35_MOUSE	23 kDa		Mus musculus						mitochondrion		coated pit	2	3	5	0
103	Beta-glucuronidase OS=Mus musculus GN=Gusb PE=2 SV=2	BGLR_MOUSE	74 kDa		Mus musculus				endoplasmic reticulum	lysosome				2	5	2	0
508	Uncharacterized protein OS=Mus musculus GN=Gm10260 PE=3 SV=2	F6YVP7_MOUSE (+1)	18 kDa		Mus musculus									2	5	3	0
226	Heterogeneous nuclear ribonucleoprotein K OS=Mus musculus GN=Hnrnpk PE=2 SV=1	B2M1R6_MOUSE (+3)	49 kDa		Mus musculus									5	4	2	0
394	Protein Sptbn2 OS=Mus musculus GN=Sptbn2 PE=2 SV=1	Q68FG2_MOUSE	271 kDa	TRUE	Mus musculus		spectrin						plasma membrane	0	0	5	2
72	ATP-dependent RNA helicase A OS=Mus musculus GN=Dhx9 PE=2 SV=1	E9QNN1_MOUSE (+1)	150 kDa		Mus musculus		centrosome					nucleolus		2	0	6	0
326	Mitochondrial inner membrane protein OS=Mus musculus GN=Immt PE=2 SV=1	E9Q800_MOUSE (+4)	76 kDa		Mus musculus						mitochondrion			4	7	0	0
423	Ras-related protein Ral-B OS=Mus musculus GN=Ralb PE=2 SV=1	RALB_MOUSE	23 kDa	TRUE	Mus musculus								plasma membrane	2	3	2	4
11	40S ribosomal protein S9 OS=Mus musculus GN=Rps9 PE=2 SV=3	RS9_MOUSE	23 kDa		Mus musculus			cytosolic small ribosomal subunit				nucleolus		3	7	4	0
445	Serine/threonine-protein phosphatase 2A 65 kDa regulatory subunit A alpha isoform OS=Mus musculus GN=Ppp2r1a PE=1 SV=3	2AAA_MOUSE	65 kDa		Mus musculus			cytosol						4	2	2	0
238	Inactive tyrosine-protein kinase 7 OS=Mus musculus GN=Ptk7 PE=1 SV=1	PTK7_MOUSE	118 kDa		Mus musculus								plasma membrane	0	2	4	2
390	Protein Kif13b OS=Mus musculus GN=Kif13b PE=2 SV=1	E9Q4K7_MOUSE	205 kDa		Mus musculus		kinesin complex							4	3	5	0
271	Isoform 2 of UPF0577 protein KIAA1324-like homolog OS=Mus musculus	sp|Q3UZV7-2|K132L_MOUSE (+1)	112 kDa		unknown									3	5	8	0
28	60S ribosomal protein L9 OS=Mus musculus GN=Rpl9 PE=2 SV=2	RL9_MOUSE (+1)	22 kDa		Mus musculus			cytosolic large ribosomal subunit						4	3	4	0
141	Copper-transporting ATPase 2 OS=Mus musculus GN=Atp7b PE=1 SV=2	ATP7B_MOUSE	157 kDa		Mus musculus	trans-Golgi network							basolateral plasma membrane	4	2	7	0
325	Minor histocompatibility antigen H13 (Fragment) OS=Mus musculus GN=H13 PE=2 SV=1	A3KGR9_MOUSE (+2)	38 kDa		Mus musculus				endoplasmic reticulum membrane					2	2	2	0
98	Aspartate aminotransferase, mitochondrial OS=Mus musculus GN=Got2 PE=1 SV=1	AATM_MOUSE	47 kDa		Mus musculus						mitochondrial inner membrane		plasma membrane	5	4	0	0
96	Arginine-rich, mutated in early stage tumors, isoform CRA_b OS=Mus musculus GN=Manf PE=2 SV=1	Q3TMX5_MOUSE (+1)	20 kDa		Mus musculus							nucleus		5	6	0	0
110	CD81 antigen OS=Mus musculus GN=Cd81 PE=1 SV=2	CD81_MOUSE	26 kDa		Mus musculus								integral to plasma membrane	2	2	2	0
531	XK-related protein 7 OS=Mus musculus GN=Xkr7 PE=2 SV=1	XKR7_MOUSE	64 kDa		Mus musculus									0	0	4	2
517	Vacuolar protein sorting-associated protein 35 OS=Mus musculus GN=Vps35 PE=1 SV=1	VPS35_MOUSE	92 kDa		Mus musculus			cytosol		lysosomal membrane				0	2	7	3
97	Aspartate aminotransferase, cytoplasmic OS=Mus musculus GN=Got1 PE=1 SV=3	AATC_MOUSE	46 kDa		Mus musculus			cytosol		lysosome		nucleus		0	0	3	2
233	Histone H3.2 OS=Mus musculus GN=Hist1h3b PE=1 SV=2	H32_MOUSE	15 kDa	TRUE	Mus musculus							nucleoplasm		5	4	3	0

337	NADPH--cytochrome P450 reductase OS=Mus musculus GN=Por PE=1 SV=2	NCPR_MOUSE	77 kDa		Mus musculus			cytosol	endoplasmic reticulum		mitochondrion			3	7	2	0
296	Lanosterol 14-alpha demethylase OS=Mus musculus GN=Cyp51a1 PE=2 SV=1	CP51A_MOUSE	57 kDa		Mus musculus				endoplasmic reticulum					3	6	2	0
205	Ganglioside-induced differentiation-associated protein 1-like 1 OS=Mus musculus GN=Gdap1l1 PE=2 SV=1	GD1L1_MOUSE (+1)	42 kDa		Mus musculus									3	3	0	0
260	Isoform 2 of Pericentriolar material 1 protein OS=Mus musculus GN=Pcm1	sp|Q9R0L6-2|PCM1_MOUSE (+1)	233 kDa		unknown									8	4	0	0
476	T-complex protein 1 subunit epsilon OS=Mus musculus GN=Cct5 PE=1 SV=1	TCPE_MOUSE	60 kDa		Mus musculus		microtubule	chaperonin-containing T-complex				nucleolus		3	2	3	3
261	Isoform 2 of Poly(rC)-binding protein 2 OS=Mus musculus GN=Pcbp2	sp|Q61990-2|PCBP2_MOUSE (+2)	35 kDa	TRUE	unknown									2	3	2	2
293	Kinesin heavy chain isoform 5C OS=Mus musculus GN=Kif5c PE=1 SV=3	KIF5C_MOUSE	109 kDa	TRUE	Mus musculus		kinesin complex							3	2	5	2
507	Uncharacterized protein OS=Mus musculus GN=Gm10036 PE=3 SV=1	E9PYL9_MOUSE (+2)	20 kDa		Mus musculus									2	4	0	2
345	Nicastrin OS=Mus musculus GN=Ncstn PE=1 SV=3	NICA_MOUSE	78 kDa		Mus musculus	Golgi apparatus			endoplasmic reticulum	lysosomal membrane			plasma membrane	3	3	3	0
36	60S ribosomal protein L18a OS=Mus musculus GN=Rpl18a PE=1 SV=1	RL18A_MOUSE	21 kDa		Mus musculus			cytosolic large ribosomal subunit						4	5	4	0
257	Isoform 2 of Microtubule-associated protein 4 OS=Mus musculus GN=Map4	sp|P27546-2|MAP4_MOUSE (+3)	117 kDa		unknown									2	0	6	3
301	Leucyl-cystinyl aminopeptidase OS=Mus musculus GN=Lnpep PE=1 SV=1	LCAP_MOUSE	117 kDa		Mus musculus					lysosomal membrane			plasma membrane	4	4	7	0
421	Ras-related protein Rab-18 OS=Mus musculus GN=Rab18 PE=2 SV=2	RAB18_MOUSE	23 kDa		Mus musculus								plasma membrane	3	5	2	0
264	Isoform 2 of Regulator of nonsense transcripts 1 OS=Mus musculus GN=Upf1	sp|Q9EPU0-2|RENT1_MOUSE (+1)	123 kDa		unknown									3	5	2	0
514	V-type proton ATPase subunit H OS=Mus musculus GN=Atp6v1h PE=1 SV=1	VATH_MOUSE (+1)	56 kDa		Mus musculus					lysosomal membrane				2	4	3	0
188	Excitatory amino acid transporter 2 OS=Mus musculus GN=Slc1a2 PE=4 SV=1	A2APL5_MOUSE (+3)	61 kDa		Mus musculus								axolemma	3	0	6	0
93	Annexin A6 OS=Mus musculus GN=Anxa6 PE=1 SV=3	ANXA6_MOUSE (+1)	76 kDa		Mus musculus					lysosomal membrane				0	0	7	6
415	Ras-related protein Rab-6B OS=Mus musculus GN=Rab6b PE=1 SV=1	RAB6B_MOUSE	23 kDa		Mus musculus	Golgi apparatus								0	2	2	0
500	Tyrosine-protein kinase Yes OS=Mus musculus GN=Yes1 PE=1 SV=3	YES_MOUSE	61 kDa	TRUE	Mus musculus	Golgi apparatus	actin filament						plasma membrane	0	0	3	4
85	Alpha-adducin OS=Mus musculus GN=Add1 PE=2 SV=1	F8WGR0_MOUSE (+3)	73 kDa		Mus musculus		cytoskeleton							0	3	3	2
1	1-acyl-sn-glycerol-3-phosphate acyltransferase delta OS=Mus musculus GN=Agpat4 PE=2 SV=1	PLCD_MOUSE	44 kDa		Mus musculus									4	7	4	0
17	40S ribosomal protein S23 OS=Mus musculus GN=Rps23 PE=2 SV=3	RS23_MOUSE	16 kDa		Mus musculus			cytosolic small ribosomal subunit				nucleolus		3	2	2	0
522	Vesicle transport protein GOT1B OS=Mus musculus GN=Golt1b PE=2 SV=1	GOT1B_MOUSE	15 kDa		Mus musculus	Golgi apparatus			endoplasmic reticulum					2	2	3	0

46	60S ribosomal protein L30 OS=Mus musculus GN=Rpl30 PE=2 SV=2	RL30_MOUSE	13 kDa		Mus musculus			cytosolic large ribosomal subunit				nucleus		2	4	3	0
499	Tyrosine-protein kinase OS=Mus musculus GN=Jak1 PE=3 SV=1	B1ASP2_MOUSE (+1)	133 kDa		Mus musculus		cytoskeleton					nucleus		0	3	4	2
473	T-complex protein 1 subunit alpha OS=Mus musculus GN=Tcp1 PE=1 SV=3	sp|P11983|TCPA_MOUSE	60 kDa		Mus musculus	Golgi apparatus	microtubule organizing center	chaperonin-containing T-complex				nuclear heterochromatin		3	2	7	2
429	Rho-related GTP-binding protein RhoG OS=Mus musculus GN=Rhog PE=2 SV=1	RHOG_MOUSE	21 kDa	TRUE	Mus musculus								plasma membrane	0	2	2	0
252	Isoform 2 of E3 UFM1-protein ligase 1 OS=Mus musculus GN=Ufl1	sp|Q8CCJ3-1|UFL1_MOUSE (+1)	80 kDa		unknown									2	3	2	0
237	Importin subunit beta-1 OS=Mus musculus GN=Kpnb1 PE=1 SV=2	IMB1_MOUSE	97 kDa		Mus musculus							nuclear membrane		2	3	5	2
523	Vesicle-associated membrane protein 3 OS=Mus musculus GN=Vamp3 PE=1 SV=1	VAMP3_MOUSE	11 kDa	TRUE	Mus musculus								apical plasma membrane	2	4	2	2
495	Tubulin alpha-1A chain OS=Mus musculus GN=Tuba1a PE=1 SV=1	TBA1A_MOUSE	50 kDa	TRUE	Mus musculus		cytoplasmic microtubule					nucleus		2	2	2	0
412	Ras-related protein Rab-1B OS=Mus musculus GN=Rab1b PE=1 SV=1	RAB1B_MOUSE	22 kDa	TRUE	Mus musculus	Golgi apparatus					mitochondrion			4	4	3	0
378	Procollagen-lysine,2-oxoglutarate 5-dioxygenase 3 OS=Mus musculus GN=Plod3 PE=1 SV=1	PLOD3_MOUSE	85 kDa		Mus musculus				endoplasmic reticulum					2	5	3	0
244	Isoform 2 of 2-oxoglutarate dehydrogenase, mitochondrial OS=Mus musculus GN=Ogdh	sp|Q60597-2|ODO1_MOUSE (+4)	115 kDa		unknown									5	6	0	0
40	60S ribosomal protein L23a OS=Mus musculus GN=Rpl23a PE=1 SV=1	RL23A_MOUSE	18 kDa		Mus musculus							nucleus		2	3	2	2
116	Calcium/calmodulin-dependent protein kinase type II subunit beta OS=Mus musculus GN=Camk2b PE=1 SV=2	KCC2B_MOUSE (+8)	60 kDa		Mus musculus		spindle midzone	cytosol	sarcoplasmic reticulum					2	5	3	0
435	Secretory carrier-associated membrane protein 1 OS=Mus musculus GN=Scamp1 PE=1 SV=1	SCAM1_MOUSE	38 kDa		Mus musculus	trans-Golgi network								2	2	2	0
45	60S ribosomal protein L28 OS=Mus musculus GN=Rpl28 PE=1 SV=2	RL28_MOUSE	16 kDa		Mus musculus									2	5	4	0
463	Sterol-4-alpha-carboxylate 3-dehydrogenase, decarboxylating OS=Mus musculus GN=Nsdhl PE=2 SV=1	NSDHL_MOUSE	41 kDa		Mus musculus				endoplasmic reticulum					2	6	3	0
197	Fatty-acid amide hydrolase 1 OS=Mus musculus GN=Faah PE=2 SV=1	FAAH1_MOUSE	63 kDa		Mus musculus	Golgi apparatus			endoplasmic reticulum					2	0	2	0
433	Saccharopine dehydrogenase-like oxidoreductase OS=Mus musculus GN=Sccpdh PE=2 SV=1	SCPDL_MOUSE	47 kDa		Mus musculus						mitochondrion	nucleus		2	6	0	0
60	AP-3 complex subunit delta-1 OS=Mus musculus GN=Ap3d1 PE=1 SV=1	AP3D1_MOUSE	135 kDa		Mus musculus	trans-Golgi network				lysosomal membrane				0	3	2	0
274	Isoform 3 of E3 ubiquitin-protein ligase UBR4 OS=Mus musculus GN=Ubr4	sp|A2AN08-3|UBR4_MOUSE (+2)	570 kDa		unknown									4	0	8	0
277	Isoform 4 of Fatty acyl-CoA reductase 1 OS=Mus musculus GN=Far1	sp|Q922J9-4|FACR1_MOUSE (+1)	60 kDa		unknown									4	4	3	0
79	Adenylate cyclase type 8 OS=Mus musculus GN=Adcy8 PE=2 SV=2	ADCY8_MOUSE	140 kDa		Mus musculus									0	0	10	2
350	PRA1 family protein 3 OS=Mus musculus GN=Arl6ip5 PE=1 SV=2	PRAF3_MOUSE	22 kDa		Mus musculus		cytoskeleton		endoplasmic reticulum					3	3	3	0

417	Ras-related protein Rab-8A OS=Mus musculus GN=Rab8a PE=1 SV=2	RAB8A_MOUSE	24 kDa	TRUE	Mus musculus									3	2	4	0
338	Nck-associated protein 1 OS=Mus musculus GN=Nckap1 PE=2 SV=1	A2AS98_MOUSE (+1)	130 kDa		Mus musculus									2	2	7	0
213	Guanine nucleotide-binding protein G(I)/G(S)/G(O) subunit gamma-3 OS=Mus musculus GN=Gng3 PE=1 SV=1	GBG3_MOUSE	8 kDa		Mus musculus								heterotrimeric G-protein complex	0	2	2	0
76	Aconitate hydratase, mitochondrial OS=Mus musculus GN=Aco2 PE=1 SV=1	ACON_MOUSE	85 kDa		Mus musculus						mitochondrion	nucleus		5	9	0	0
273	Isoform 2B of GTPase KRas OS=Mus musculus GN=Kras	sp|P32883-2|RASK_MOUSE	21 kDa	TRUE	Mus musculus									0	4	3	2
458	Solute carrier family 12 member 9 OS=Mus musculus GN=Slc12a9 PE=1 SV=2	S12A9_MOUSE	96 kDa		Mus musculus								plasma membrane	4	2	3	0
388	Protein Gm20425 OS=Mus musculus GN=Gm20425 PE=4 SV=1	E9Q035_MOUSE	108 kDa		Mus musculus									2	3	0	0
447	Sideroflexin-1 OS=Mus musculus GN=Sfxn1 PE=1 SV=3	SFXN1_MOUSE	36 kDa	TRUE	Mus musculus						mitochondrial inner membrane			3	3	0	0
242	Isocitrate dehydrogenase [NAD] subunit alpha, mitochondrial OS=Mus musculus GN=Idh3a PE=1 SV=1	sp|Q9D6R2|IDH3A_MOUSE	40 kDa		Mus musculus						mitochondrion	nucleus		3	4	0	0
201	Flotillin-1 OS=Mus musculus GN=Flot1 PE=1 SV=1	FLOT1_MOUSE	48 kDa		Mus musculus		centriolar satellite			lysosomal membrane		signalosome	plasma membrane	2	2	6	0
431	Ribosomal protein L19 OS=Mus musculus GN=Rpl19 PE=2 SV=1	A2A547_MOUSE (+1)	23 kDa		Mus musculus			cytosolic large ribosomal subunit				nucleolus		2	2	2	0
133	Clathrin coat assembly protein AP180 OS=Mus musculus GN=Snap91 PE=4 SV=2	E9Q9A3_MOUSE (+6)	86 kDa	TRUE	Mus musculus									2	2	2	0
114	Cadherin-2 OS=Mus musculus GN=Cdh2 PE=1 SV=2	CADH2_MOUSE (+1)	100 kDa		Mus musculus								apical plasma membrane	3	0	3	0
34	60S ribosomal protein L17 OS=Mus musculus GN=Rpl17 PE=2 SV=1	Q6ZWZ7_MOUSE (+1)	21 kDa		Mus musculus									2	4	2	0
209	Glycerophosphoinositol inositolphosphodiesterase GDPD2 OS=Mus musculus GN=Gdpd2 PE=1 SV=1	GDPD2_MOUSE	61 kDa		Mus musculus		cytoskeleton						plasma membrane	0	2	3	2
245	Isoform 2 of 40S ribosomal protein S24 OS=Mus musculus GN=Rps24	sp|P62849-2|RS24_MOUSE (+2)	15 kDa		unknown									2	2	2	0
436	Secretory carrier-associated membrane protein 3 OS=Mus musculus GN=Scamp3 PE=2 SV=1	E9Q855_MOUSE (+1)	35 kDa		Mus musculus	Golgi membrane								3	0	4	0
369	Poly(rC)-binding protein 1 OS=Mus musculus GN=Pcbp1 PE=1 SV=1	PCBP1_MOUSE	37 kDa	TRUE	Mus musculus							nucleus		4	4	0	0
427	Reticulon-1 OS=Mus musculus GN=Rtn1 PE=1 SV=1	RTN1_MOUSE	84 kDa		Mus musculus				endoplasmic reticulum					2	5	4	0
195	Fatty acid desaturase 2 OS=Mus musculus GN=Fads2 PE=2 SV=1	FADS2_MOUSE	52 kDa		Mus musculus				endoplasmic reticulum					4	2	2	0
354	Peptidyl-tRNA hydrolase 2, mitochondrial OS=Mus musculus GN=Ptrh2 PE=2 SV=1	PTH2_MOUSE	20 kDa		Mus musculus			cytosol			mitochondrion			3	3	2	0
211	Golgi apparatus protein 1 (Fragment) OS=Mus musculus GN=Glg1 PE=2 SV=1	F8WHM5_MOUSE (+1)	132 kDa		Mus musculus	Golgi apparatus								5	6	0	0
440	Serine hydroxymethyltransferase OS=Mus musculus GN=Shmt2 PE=2 SV=1	Q9CZN7_MOUSE	56 kDa		Mus musculus		microtubule cytoskeleton				mitochondrial nucleoid			4	3	0	0

95	Arginine--tRNA ligase, cytoplasmic OS=Mus musculus GN=Rars PE=2 SV=2	SYRC_MOUSE	76 kDa		Mus musculus						mitochondrion	nucleus		5	7	0	0
266	Isoform 2 of Septin-11 OS=Mus musculus GN=Sept11	sp|Q8C1B7-2|SEP11_MOUSE (+2)	49 kDa		unknown									0	0	4	2
361	Phosphatidylinositol 4-kinase type 2-alpha OS=Mus musculus GN=Pi4k2a PE=1 SV=1	P4K2A_MOUSE	54 kDa		Mus musculus	Golgi apparatus		BLOC-1 complex		lysosomal membrane	mitochondrion		integral to plasma membrane	3	3	3	0
78	Actin-related protein 3 OS=Mus musculus GN=Actr3 PE=1 SV=3	ARP3_MOUSE	47 kDa		Mus musculus	Golgi membrane	podosome						cell-cell junction	0	3	6	0
48	60S ribosomal protein L34 OS=Mus musculus GN=Rpl34 PE=3 SV=2	RL34_MOUSE	13 kDa		Mus musculus			cytosolic large ribosomal subunit				nucleolus		2	4	4	0
155	Dedicator of cytokinesis protein 10 OS=Mus musculus GN=Dock10 PE=2 SV=1	E9QM99_MOUSE (+5)	250 kDa		Mus musculus									2	0	4	0
493	Transmembrane emp24 domain-containing protein 10 OS=Mus musculus GN=Tmed10 PE=2 SV=1	sp|Q9D1D4|TMEDA_MOUSE	25 kDa		Mus musculus	COPI-coated vesicle			endoplasmic reticulum				plasma membrane	3	4	0	0
259	Isoform 2 of Peptidyl-prolyl cis-trans isomerase FKBP8 OS=Mus musculus GN=Fkbp8	sp|O35465-2|FKBP8_MOUSE (+1)	44 kDa		unknown									3	2	0	0
157	Dephospho-CoA kinase domain-containing protein OS=Mus musculus GN=Dcakd PE=2 SV=1	DCAKD_MOUSE	26 kDa		Mus musculus						mitochondrion			3	4	0	0
32	60S ribosomal protein L13a OS=Mus musculus GN=Rpl13a PE=2 SV=1	E9Q5A0_MOUSE (+1)	48 kDa		Mus musculus									0	3	2	2
9	40S ribosomal protein S6 OS=Mus musculus GN=Rps6 PE=1 SV=1	RS6_MOUSE	29 kDa		Mus musculus			cytosolic small ribosomal subunit				nucleolus		0	4	2	3
504	Ubiquitin carboxyl-terminal hydrolase OS=Mus musculus GN=Usp9x PE=2 SV=1	Q4FE56_MOUSE (+1)	290 kDa		Mus musculus									3	4	3	0
528	Voltage-dependent anion-selective channel protein 3 OS=Mus musculus GN=Vdac3 PE=4 SV=1	J3QMG3_MOUSE (+1)	31 kDa		Mus musculus						mitochondrial inner membrane			3	4	2	0
129	Cationic amino acid transporter 3 OS=Mus musculus GN=Slc7a3 PE=2 SV=1	CTR3_MOUSE	67 kDa		Mus musculus								plasma membrane	0	2	4	0
359	Phosphatidate cytidylyltransferase OS=Mus musculus GN=Cds2 PE=2 SV=1	A2AMQ5_MOUSE (+1)	49 kDa		Mus musculus				endoplasmic reticulum					2	0	2	0
425	Receptor-type tyrosine-protein phosphatase F OS=Mus musculus GN=Ptprf PE=1 SV=1	PTPRF_MOUSE	211 kDa	TRUE	Mus musculus									0	2	4	0
530	Wolframin OS=Mus musculus GN=Wfs1 PE=2 SV=1	Q3UN10_MOUSE (+1)	92 kDa		Mus musculus				endoplasmic reticulum					3	5	0	0
183	Estradiol 17-beta-dehydrogenase 11 OS=Mus musculus GN=Hsd17b11 PE=2 SV=1	sp|Q9EQ06|DHB11_MOUSE	33 kDa		Mus musculus									2	3	0	0
82	Alkyldihydroxyacetonephosphate synthase, peroxisomal OS=Mus musculus GN=Agps PE=2 SV=1	A2AL50_MOUSE (+1)	74 kDa		Mus musculus						mitochondrion	nucleolus		2	4	0	0
132	Citrate synthase, mitochondrial OS=Mus musculus GN=Cs PE=1 SV=1	CISY_MOUSE	52 kDa		Mus musculus						mitochondrion			3	2	0	2
53	ADP-ribosylation factor-like protein 8B OS=Mus musculus GN=Arl8b PE=2 SV=1	ARL8B_MOUSE	22 kDa		Mus musculus		spindle midzone			lysosome				3	4	2	0
441	Serine/threonine-protein kinase 11-interacting protein OS=Mus musculus GN=Stk11ip PE=1 SV=1	S11IP_MOUSE	118 kDa		Mus musculus					lysosomal membrane				3	3	2	0
131	Ceramide synthase 5 (Fragment) OS=Mus musculus GN=Cers5 PE=4 SV=1	H3BJQ0_MOUSE (+2)	16 kDa		Mus musculus				endoplasmic reticulum					2	3	2	0

308	Lysophosphatidylcholine acyltransferase 1 OS=Mus musculus GN=Lpcat1 PE=1 SV=1	sp|Q3TFD2|PCAT1_MOUSE	60 kDa		Mus musculus	Golgi apparatus			endoplasmic reticulum					2	3	2	0
455	Solute carrier family 2, facilitated glucose transporter member 1 OS=Mus musculus GN=Slc2a1 PE=1 SV=4	GTR1_MOUSE	54 kDa		Mus musculus		cortical actin cytoskeleton	cytosol				female pronucleus	plasma membrane	0	3	4	0
317	Mannose-P-dolichol utilization defect 1 protein OS=Mus musculus GN=Mpdu1 PE=2 SV=1	MPU1_MOUSE (+1)	26 kDa		Mus musculus									3	3	0	0
71	ATP-citrate synthase OS=Mus musculus GN=Acly PE=1 SV=1	ACLY_MOUSE (+1)	120 kDa		Mus musculus						mitochondrion			0	2	6	0
52	A-kinase anchor protein SPHKAP OS=Mus musculus GN=Sphkap PE=2 SV=1	E9PUC4_MOUSE (+4)	182 kDa		Mus musculus						mitochondrion			4	4	0	0
177	Endoplasmic reticulum resident protein 29 OS=Mus musculus GN=Erp29 PE=1 SV=2	ERP29_MOUSE	29 kDa		Mus musculus				endoplasmic reticulum					4	5	0	0
471	Syntaxin-12 OS=Mus musculus GN=Stx12 PE=1 SV=1	STX12_MOUSE	31 kDa		Mus musculus	Golgi apparatus		BLOC-1 complex						2	3	2	2
485	Thioredoxin-related transmembrane protein 4 OS=Mus musculus GN=Tmx4 PE=2 SV=1	A2ARI0_MOUSE (+1)	21 kDa		Mus musculus				endoplasmic reticulum					2	3	2	0
351	Palmitoyltransferase ZDHHC5 OS=Mus musculus GN=Zdhhc5 PE=1 SV=1	sp|Q8VDZ4|ZDHC5_MOUSE	78 kDa		Mus musculus								plasma membrane	0	0	4	2
212	Golgi-specific brefeldin A-resistance factor 1 OS=Mus musculus GN=Gbf1 PE=1 SV=1	Q6DFZ1_MOUSE	207 kDa		Mus musculus	trans-Golgi network					mitochondrion			3	2	3	0
404	Proton myo-inositol cotransporter OS=Mus musculus GN=Slc2a13 PE=2 SV=2	MYCT_MOUSE	69 kDa		Mus musculus									2	2	3	0
50	60S ribosomal protein L36a OS=Mus musculus GN=Rpl36a PE=2 SV=2	RL36A_MOUSE	12 kDa		Mus musculus									2	2	2	0
498	Tumor protein p53-inducible protein 11 (Fragment) OS=Mus musculus GN=Trp53i11 PE=2 SV=1	A2AGS6_MOUSE (+1)	10 kDa		Mus musculus									3	3	2	0
228	Heterogeneous nuclear ribonucleoprotein U OS=Mus musculus GN=Hnrnpu PE=4 SV=1	G3XA10_MOUSE (+1)	87 kDa		Mus musculus							nucleus		2	3	3	0
342	Neutral amino acid transporter A OS=Mus musculus GN=Slc1a4 PE=1 SV=1	SATT_MOUSE	56 kDa		Mus musculus		intermediate filament							0	2	2	0
486	Tight junction protein ZO-1 OS=Mus musculus GN=Tjp1 PE=2 SV=1	B9EHJ3_MOUSE (+1)	189 kDa		Mus musculus							nucleus	plasma membrane	0	2	5	0
444	Serine/threonine-protein kinase mTOR OS=Mus musculus GN=Mtor PE=1 SV=2	sp|Q9JLN9|MTOR_MOUSE	289 kDa		Mus musculus	Golgi apparatus		cytosol	endoplasmic reticulum	lysosome	mitochondrial outer membrane	PML body		3	0	5	0
43	60S ribosomal protein L27 OS=Mus musculus GN=Rpl27 PE=2 SV=2	RL27_MOUSE	16 kDa		Mus musculus									2	3	2	0
304	Long-chain fatty acid transport protein 4 OS=Mus musculus GN=Slc27a4 PE=1 SV=1	S27A4_MOUSE	72 kDa		Mus musculus				endoplasmic reticulum membrane				brush border membrane	2	3	3	0
527	Vesicular integral-membrane protein VIP36 OS=Mus musculus GN=Lman2 PE=2 SV=2	LMAN2_MOUSE	40 kDa		Mus musculus	Golgi apparatus							integral to plasma membrane	2	6	0	0
327	Mitogen-activated protein kinase kinase kinase kinase 4 OS=Mus musculus GN=Map4k4 PE=4 SV=2	E9PVG7_MOUSE (+3)	147 kDa		Mus musculus									0	2	5	0
186	Eukaryotic translation initiation factor 3 subunit B OS=Mus musculus GN=Eif3b PE=1 SV=1	EIF3B_MOUSE	91 kDa		Mus musculus									3	2	3	0
206	Glucosylceramidase OS=Mus musculus GN=Gba PE=1 SV=1	GLCM_MOUSE	58 kDa		Mus musculus					lysosomal lumen				2	3	2	0

333	Myristoylated alanine-rich C-kinase substrate OS=Mus musculus GN=Marcks PE=1 SV=2	MARCS_MOUSE	30 kDa		Mus musculus		centrosome					germinal vesicle		0	2	2	0
450	Sodium-coupled neutral amino acid transporter 1 OS=Mus musculus GN=Slc38a1 PE=1 SV=1	sp|Q8K2P7|S38A1_MOUSE	54 kDa		Mus musculus								plasma membrane	0	3	3	0
187	Eukaryotic translation initiation factor 3 subunit C OS=Mus musculus GN=Eif3c PE=1 SV=1	EIF3C_MOUSE	106 kDa		Mus musculus									2	5	3	0
189	Exportin-2 OS=Mus musculus GN=Cse1l PE=2 SV=1	XPO2_MOUSE	110 kDa		Mus musculus							nucleus		2	2	0	0
153	Dedicator of cytokinesis protein 6 OS=Mus musculus GN=Dock6 PE=4 SV=1	E9QPN7_MOUSE (+1)	237 kDa	TRUE	Mus musculus									2	2	0	0
439	Septin-9 OS=Mus musculus GN=Sept9 PE=2 SV=1	A2A6U3_MOUSE (+2)	64 kDa		Mus musculus									0	0	2	4
319	Matrin-3 OS=Mus musculus GN=Matr3 PE=1 SV=1	MATR3_MOUSE	95 kDa		Mus musculus							nucleus		2	0	4	0
466	Succinyl-CoA:3-ketoacid coenzyme A transferase 1, mitochondrial OS=Mus musculus GN=Oxct1 PE=1 SV=1	SCOT1_MOUSE	56 kDa		Mus musculus						mitochondrion			2	3	0	0
344	Nicalin OS=Mus musculus GN=Ncln PE=2 SV=1	D3YU17_MOUSE (+1)	63 kDa		Mus musculus									2	6	0	0
192	F-actin-capping protein subunit alpha-2 OS=Mus musculus GN=Capza2 PE=1 SV=3	CAZA2_MOUSE	33 kDa		Mus musculus		cortical cytoskeleton							0	2	0	2
13	40S ribosomal protein S13 OS=Mus musculus GN=Rps13 PE=1 SV=2	RS13_MOUSE	17 kDa		Mus musculus			cytosolic small ribosomal subunit				nucleolus		4	3	0	0
490	Transient receptor potential cation channel subfamily V member 2 OS=Mus musculus GN=Trpv2 PE=1 SV=2	TRPV2_MOUSE	86 kDa		Mus musculus								growth cone membrane	0	3	2	0
396	Protein YIPF5 OS=Mus musculus GN=Yipf5 PE=2 SV=1	YIPF5_MOUSE	28 kDa		Mus musculus	ER to Golgi transport vesicle								2	2	0	0
16	40S ribosomal protein S20 OS=Mus musculus GN=Rps20 PE=1 SV=1	RS20_MOUSE	13 kDa		Mus musculus			cytosolic small ribosomal subunit						0	3	3	0
109	CAAX prenyl protease 1 homolog OS=Mus musculus GN=Zmpste24 PE=1 SV=2	FACE1_MOUSE	55 kDa		Mus musculus				endoplasmic reticulum			nucleus		0	5	3	0
19	40S ribosomal protein SA OS=Mus musculus GN=Rpsa PE=1 SV=4	RSSA_MOUSE	33 kDa		Mus musculus			cytosolic small ribosomal subunit				nucleus	plasma membrane	0	0	3	3
246	Isoform 2 of 60S ribosomal protein L22-like 1 OS=Mus musculus GN=Rpl22l1	sp|Q9D7S7-2|RL22L_MOUSE (+1)	14 kDa		unknown									2	2	2	0
158	Derlin-1 OS=Mus musculus GN=Derl1 PE=1 SV=1	DERL1_MOUSE	29 kDa		Mus musculus				endoplasmic reticulum					2	0	2	0
502	Tyrosine-protein phosphatase non-receptor type 1 OS=Mus musculus GN=Ptpn1 PE=1 SV=2	PTN1_MOUSE	50 kDa		Mus musculus			cytosol	endoplasmic reticulum				plasma membrane	2	5	2	0
170	E3 ubiquitin-protein ligase NEDD4 OS=Mus musculus GN=Nedd4 PE=1 SV=3	NEDD4_MOUSE	103 kDa	TRUE	Mus musculus	Golgi apparatus		cytosol				nucleus	plasma membrane	0	2	2	0
222	H(+)/Cl(-) exchange transporter 7 OS=Mus musculus GN=Clcn7 PE=1 SV=1	CLCN7_MOUSE	89 kDa		Mus musculus					lysosomal membrane				2	0	2	0
516	Vacuolar protein sorting 16 (Yeast) OS=Mus musculus GN=Vps16 PE=4 SV=1	G3X8X7_MOUSE (+1)	95 kDa		Mus musculus		actin filament			lysosomal membrane				0	3	3	0
173	Elongation factor 1-alpha 2 OS=Mus musculus GN=Eef1a2 PE=1 SV=1	EF1A2_MOUSE	50 kDa	TRUE	Mus musculus									2	0	3	0

389	Protein Kidins220 OS=Mus musculus GN=Kidins220 PE=2 SV=1	E9Q9B7_MOUSE	199 kDa		Mus musculus									0	3	3	0
376	Procollagen galactosyltransferase 1 OS=Mus musculus GN=Colgalt1 PE=1 SV=2	GT251_MOUSE	71 kDa		Mus musculus									3	6	0	0
160	Dihydrolipoyl dehydrogenase, mitochondrial OS=Mus musculus GN=Dld PE=1 SV=2	DLDH_MOUSE	54 kDa		Mus musculus						mitochondrion	nucleus		3	6	0	0
208	Glycerol-3-phosphate dehydrogenase, mitochondrial OS=Mus musculus GN=Gpd2 PE=2 SV=1	A2AQR0_MOUSE (+1)	83 kDa		Mus musculus						mitochondrial inner membrane			3	2	0	0
49	60S ribosomal protein L36 OS=Mus musculus GN=Rpl36 PE=3 SV=1	Q6ZWZ4_MOUSE	12 kDa		Mus musculus									0	2	0	2
210	Glypican-1 OS=Mus musculus GN=Gpc1 PE=1 SV=1	GPC1_MOUSE	61 kDa		Mus musculus	Golgi lumen							plasma membrane	0	0	2	2
94	Anoctamin-6 OS=Mus musculus GN=Ano6 PE=1 SV=1	sp|Q6P9J9|ANO6_MOUSE	106 kDa		Mus musculus								plasma membrane	0	0	5	2
467	Sulfated glycoprotein 1 OS=Mus musculus GN=Psap PE=2 SV=1	E9PZ00_MOUSE (+4)	61 kDa		Mus musculus					lysosome	mitochondrion			2	3	0	0
372	Probable ATP-dependent RNA helicase DDX5 OS=Mus musculus GN=Ddx5 PE=1 SV=2	DDX5_MOUSE (+1)	69 kDa		Mus musculus							nucleus		0	2	3	2
312	MCG9889 OS=Mus musculus GN=Gm10709 PE=4 SV=1	D3Z1N9_MOUSE (+3)	18 kDa		Mus musculus									2	0	2	0
362	Phosphoglycerate mutase 1 OS=Mus musculus GN=Pgam1 PE=1 SV=3	PGAM1_MOUSE	29 kDa		Mus musculus									0	0	2	2
47	60S ribosomal protein L31 OS=Mus musculus GN=Rpl31 PE=2 SV=1	RL31_MOUSE	14 kDa		Mus musculus			cytosolic large ribosomal subunit						3	0	2	0
426	Reticulocalbin-1 OS=Mus musculus GN=Rcn1 PE=1 SV=1	RCN1_MOUSE	38 kDa		Mus musculus				endoplasmic reticulum					2	2	0	0
145	Cytochrome b-c1 complex subunit 1, mitochondrial OS=Mus musculus GN=Uqcrc1 PE=1 SV=2	QCR1_MOUSE	53 kDa		Mus musculus						mitochondrion			3	4	0	0
383	Protein Abcc4 OS=Mus musculus GN=Abcc4 PE=2 SV=1	E9Q236_MOUSE	149 kDa		Mus musculus								basolateral plasma membrane	0	2	4	0
147	Cytochrome c oxidase subunit 2 OS=Mus musculus GN=Mtco2 PE=1 SV=1	COX2_MOUSE	26 kDa		Mus musculus						mitochondrial inner membrane			2	2	0	0
241	Isocitrate dehydrogenase [NADP], mitochondrial OS=Mus musculus GN=Idh2 PE=1 SV=3	IDHP_MOUSE	51 kDa		Mus musculus						mitochondrial inner membrane			2	7	0	0
336	NADH-ubiquinone oxidoreductase 75 kDa subunit, mitochondrial OS=Mus musculus GN=Ndufs1 PE=1 SV=2	NDUS1_MOUSE	80 kDa		Mus musculus						mitochondrion			3	2	0	0
57	AP-1 complex subunit mu-1 OS=Mus musculus GN=Ap1m1 PE=1 SV=3	AP1M1_MOUSE	49 kDa		Mus musculus	trans-Golgi network								2	0	2	0
227	Heterogeneous nuclear ribonucleoprotein Q OS=Mus musculus GN=Syncrip PE=2 SV=1	G3V018_MOUSE (+1)	66 kDa		Mus musculus									2	0	2	0
159	Desmoplakin OS=Mus musculus GN=Dsp PE=2 SV=1	DESP_MOUSE	333 kDa		Mus musculus		intermediate filament				mitochondrion	nucleus	cell-cell junction	2	0	3	2
250	Isoform 2 of Caskin-1 OS=Mus musculus GN=Caskin1	sp|Q6P9K8-2|CSKI1_MOUSE (+1)	143 kDa	TRUE	unknown									0	2	3	2
360	Phosphatidylinositide phosphatase SAC1 OS=Mus musculus GN=Sacm1l PE=2 SV=1	SAC1_MOUSE	67 kDa		Mus musculus	Golgi apparatus			endoplasmic reticulum membrane				alpha-amino-3-hydroxy-5-methyl-4-isoxazolepropionic acid	2	4	2	0

													selective glutamate receptor complex				
278	Isoform A of Fragile X mental retardation syndrome-related protein 1 OS=Mus musculus GN=Fxr1	sp|Q61584-2|FXR1_MOUSE (+3)	61 kDa	TRUE	unknown									0	2	2	0
221	Guanine nucleotide-binding protein subunit alpha-13 OS=Mus musculus GN=Gna13 PE=1 SV=1	GNA13_MOUSE	44 kDa	TRUE	Mus musculus							nucleus	plasma membrane	0	2	0	2
409	Ragulator complex protein LAMTOR3 OS=Mus musculus GN=Lamtor3 PE=1 SV=1	LTOR3_MOUSE	14 kDa		Mus musculus									2	2	2	0
112	CDP-diacylglycerol--inositol 3-phosphatidyltransferase OS=Mus musculus GN=Cdipt PE=1 SV=1	CDIPT_MOUSE	24 kDa		Mus musculus	Golgi apparatus			endoplasmic reticulum				plasma membrane	2	2	2	0
401	Protein dopey-2 OS=Mus musculus GN=Dopey2 PE=2 SV=3	sp|Q3UHQ6|DOP2_MOUSE	257 kDa		Mus musculus									3	2	3	0
12	40S ribosomal protein S11 OS=Mus musculus GN=Rps11 PE=2 SV=3	RS11_MOUSE	18 kDa		Mus musculus			cytosolic small ribosomal subunit						0	3	2	0
483	Thioredoxin-dependent peroxide reductase, mitochondrial OS=Mus musculus GN=Prdx3 PE=1 SV=1	PRDX3_MOUSE	28 kDa		Mus musculus			IkappaB kinase complex			mitochondrion			3	3	0	0
106	Beta-mannosidase OS=Mus musculus GN=Manba PE=2 SV=1	MANBA_MOUSE	101 kDa		Mus musculus					lysosome				0	2	2	0
364	Phospholipase D3 OS=Mus musculus GN=Pld3 PE=2 SV=1	PLD3_MOUSE	54 kDa		Mus musculus				endoplasmic reticulum membrane					2	0	2	0
111	CDGSH iron-sulfur domain-containing protein 2 OS=Mus musculus GN=Cisd2 PE=1 SV=1	CISD2_MOUSE (+1)	15 kDa		Mus musculus				endoplasmic reticulum membrane		mitochondrial outer membrane			2	3	0	0
533	cAMP-dependent protein kinase type II-alpha regulatory subunit OS=Mus musculus GN=Prkar2a PE=1 SV=2	KAP2_MOUSE (+2)	45 kDa		Mus musculus								plasma membrane	0	2	3	0
15	40S ribosomal protein S16 OS=Mus musculus GN=Rps16 PE=2 SV=4	RS16_MOUSE	16 kDa		Mus musculus			cytosolic small ribosomal subunit						2	3	0	0
303	Lipopolysaccharide-responsive and beige-like anchor protein OS=Mus musculus GN=Lrba PE=2 SV=1	E9Q3Y4_MOUSE (+2)	317 kDa		Mus musculus									3	0	3	0
42	60S ribosomal protein L26 (Fragment) OS=Mus musculus GN=Rpl26 PE=2 SV=1	B1ARA3_MOUSE (+1)	12 kDa		Mus musculus									2	2	2	0
371	Presenilin 2, isoform CRA_a OS=Mus musculus GN=Psen2 PE=2 SV=1	Q3U4P5_MOUSE (+1)	50 kDa		Mus musculus	Golgi membrane	centrosome	cytosol	endoplasmic reticulum membrane	lysosomal membrane	mitochondrial inner membrane	nucleus	apical plasma membrane	2	2	0	0
368	Poly (ADP-ribose) polymerase family, member 1 OS=Mus musculus GN=Parp1 PE=2 SV=1	Q921K2_MOUSE	113 kDa		Mus musculus							nucleus		2	2	0	0
366	Plexin-B1 OS=Mus musculus GN=Plxnb1 PE=1 SV=2	PLXB1_MOUSE	231 kDa		Mus musculus								integral to plasma membrane	2	0	2	0
66	ATP synthase subunit delta, mitochondrial OS=Mus musculus GN=Atp5d PE=1 SV=1	ATPD_MOUSE	18 kDa		Mus musculus						mitochondrial inner membrane			2	2	0	0
89	Aminoacyl tRNA synthase complex-interacting multifunctional protein 2 OS=Mus musculus GN=Aimp2 PE=2 SV=1	Q8R3V2_MOUSE	31 kDa		Mus musculus							nucleus		2	2	0	0
101	B-cell receptor-associated protein 31 OS=Mus musculus GN=Bcap31 PE=1 SV=4	BAP31_MOUSE	28 kDa		Mus musculus	Golgi membrane			endoplasmic reticulum				integral to plasma membrane	2	2	0	0

Table S2: Normalized GnRH-dependent Changes in PAM Fraction Protein Abundance

Taxonomy	Identified Proteins (401/833)	Gene Name	Accession Number	Molecular Weight	Fold Change (Log? Fold Change)	Mann Whitney Test (P-Value)
Mus musculus	Annexin A2 OS=Mus musculus GN=Anxa2 PE=1 SV=2	Anxa2	ANXA2_MOUSE	39 kDa	-4.23	0.0012
Mus musculus	Desmoplakin OS=Mus musculus GN=Dsp PE=2 SV=1	Dsp	DESP_MOUSE	333 kDa	-3.77	0.0066
Mus musculus	Kinesin heavy chain isoform 5C OS=Mus musculus GN=Kif5c PE=1 SV=3	Kif5c	KIF5C_MOUSE	109 kDa	-1.9	0.32
Mus musculus	CDP-diacylglycerol--inositol 3-phosphatidyltransferase OS=Mus musculus GN=Cdipt PE=1 SV=1	Cdipt	CDIPT_MOUSE	24 kDa	-1.87	0.021
Mus musculus	Junction plakoglobin OS=Mus musculus GN=Jup PE=1 SV=3	Jup	PLAK_MOUSE	82 kDa	-1.6	< 0.0001
Mus musculus	Beta-glucuronidase OS=Mus musculus GN=Gusb PE=2 SV=2	Gusb	BGLR_MOUSE	74 kDa	-1.17	0.034
Mus musculus	Phosphatidylinositide phosphatase SAC1 OS=Mus musculus GN=Sacm1l PE=2 SV=1	Sacm1l	SAC1_MOUSE	67 kDa	-1.11	0.25
Mus musculus	Transcriptional activator protein Pur-beta OS=Mus musculus GN=Purb PE=1 SV=3	Purb	PURB_MOUSE	34 kDa	-1.06	0.57
unknown	Isoform 2 of E3 UFM1-protein ligase 1 OS=Mus musculus GN=Ufl1	Ufl1	sp|Q8CCJ3-1| UFL1_MOUSE (+1)	80 kDa	-1.02	0.95
Mus musculus	Ubiquitin carboxyl-terminal hydrolase OS=Mus musculus GN=Usp9x PE=2 SV=1	Usp9x	Q4FE56_MOUSE (+1)	290 kDa	-0.85	0.53
Mus musculus	Heterogeneous nuclear ribonucleoprotein U OS=Mus musculus GN=Hnrnpu PE=4 SV=1	Hnrnpu	G3XA10_MOUSE (+1)	87 kDa	-0.83	0.61
Mus musculus	Proton myo-inositol cotransporter OS=Mus musculus GN=Slc2a13 PE=2 SV=2	Slc2a13	MYCT_MOUSE	69 kDa	-0.78	0.48
unknown	Isoform 2 of Caskin-1 OS=Mus musculus GN=Caskin1	Caskin1	sp|Q6P9K8-2| CSKI1_MOUSE (+1)	143 kDa	-0.76	0.87
Mus musculus	60S ribosomal protein L26 (Fragment) OS=Mus musculus GN=Rpl26 PE=2 SV=1	Rpl26	B1ARA3_MOUSE (+1)	12 kDa	-0.75	0.11
Mus musculus	60S ribosomal protein L23a OS=Mus musculus GN=Rpl23a PE=1 SV=1	Rpl23a	RL23A_MOUSE	18 kDa	-0.68	0.22
Mus musculus	Phosphatidylinositol 4-kinase type 2-alpha OS=Mus musculus GN=Pi4k2a PE=1 SV=1	Pi4k2a	P4K2A_MOUSE	54 kDa	-0.68	0.00024
Mus musculus	T-complex protein 1 subunit beta OS=Mus musculus GN=Cct2 PE=1 SV=4	Cct2	TCPB_MOUSE	57 kDa	-0.67	0.054
Mus musculus	Valine--tRNA ligase OS=Mus musculus GN=Vars PE=2 SV=1	Vars	SYVC_MOUSE	140 kDa	-0.66	0.085
Mus musculus	Thioredoxin-related transmembrane protein 4 OS=Mus musculus GN=Tmx4 PE=2 SV=1	Tmx4	A2ARI0_MOUSE (+1)	21 kDa	-0.6	0.85
Mus musculus	14-3-3 protein zeta/delta OS=Mus musculus GN=Ywhaz PE=1 SV=1	Ywhaz	1433Z_MOUSE	28 kDa	-0.59	0.45
Mus musculus	Solute carrier family 12 member 4 OS=Mus musculus GN=Slc12a4 PE=4 SV=2	Slc12a4	F8WIJ0_MOUSE (+1)	121 kDa	-0.58	0.069
Mus musculus	Eukaryotic translation initiation factor 3 subunit A OS=Mus musculus GN=Eif3a PE=1 SV=5	Eif3a	EIF3A_MOUSE	162 kDa	-0.55	0.00057
unknown	Isoform 2 of Inositol 1,4,5-trisphosphate receptor type 1 OS=Mus musculus GN=Itpr1	Itpr1	sp|P11881-2| ITPR1_MOUSE (+7)	311 kDa	-0.55	< 0.0001
unknown	Protein Gm10320 OS=Mus musculus GN=Gm10320 PE=4 SV=1	Gm10320	E9PW43_MOUSE (+1)	12 kDa	-0.54	0.0039
Mus musculus	60S ribosomal protein L7a OS=Mus musculus GN=Rpl7a PE=2 SV=2	Rpl7a	RL7A_MOUSE	30 kDa	-0.53	0.0049
Mus musculus	Peptidyl-tRNA hydrolase 2, mitochondrial OS=Mus musculus GN=Ptrh2 PE=2 SV=1	Ptrh2	PTH2_MOUSE	20 kDa	-0.53	0.13

Mus musculus	40S ribosomal protein S4, X isoform OS=Mus musculus GN=Rps4x PE=2 SV=2	Rps4x	RS4X_MOUSE	30 kDa	-0.52	0.18
Mus musculus	Ceramide synthase 5 (Fragment) OS=Mus musculus GN=Cers5 PE=4 SV=1	Cers5	H3BJQ0_MOUSE (+2)	16 kDa	-0.49	0.0039
Mus musculus	Very low-density lipoprotein receptor OS=Mus musculus GN=Vldlr PE=2 SV=1	Vldlr	F8WGI9_MOUSE (+2)	89 kDa	-0.49	0.00097
Mus musculus	Vesicle-associated membrane protein 3 OS=Mus musculus GN=Vamp3 PE=1 SV=1	Vamp3	VAMP3_MOUSE	11 kDa	-0.47	0.44
Mus musculus	40S ribosomal protein S6 OS=Mus musculus GN=Rps6 PE=1 SV=1	Rps6	RS6_MOUSE	29 kDa	-0.46	0.4
Mus musculus	Beta-hexosaminidase subunit alpha OS=Mus musculus GN=Hexa PE=2 SV=2	Hexa	HEXA_MOUSE	61 kDa	-0.46	0.37
Mus musculus	Leucyl-cystinyl aminopeptidase OS=Mus musculus GN=Lnpep PE=1 SV=1	Lnpep	LCAP_MOUSE	117 kDa	-0.46	0.2
Mus musculus	Nischarin OS=Mus musculus GN=Nisch PE=1 SV=2	Nisch	sp|Q80TM9| NISCH_MOUSE	175 kDa	-0.46	0.024
Mus musculus	Serine/threonine-protein kinase MRCK beta OS=Mus musculus GN=Cdc42bpb PE=1 SV=2	Cdc42bpb	MRCKB_MOUSE	195 kDa	-0.46	0.06
Mus musculus	40S ribosomal protein S8 OS=Mus musculus GN=Rps8 PE=1 SV=2	Rps8	RS8_MOUSE	24 kDa	-0.44	< 0.0001
Mus musculus	Interleukin-6 receptor subunit beta OS=Mus musculus GN=Il6st PE=1 SV=2	Il6st	IL6RB_MOUSE	102 kDa	-0.44	0.0066
Mus musculus	Peroxisomal multifunctional enzyme type 2 OS=Mus musculus GN=Hsd17b4 PE=1 SV=3	Hsd17b4	DHB4_MOUSE	79 kDa	-0.43	0.14
Mus musculus	60S ribosomal protein L12 OS=Mus musculus GN=Rpl12 PE=1 SV=2	Rpl12	RL12_MOUSE	18 kDa	-0.41	0.081
Mus musculus	Uncharacterized protein OS=Mus musculus GN=Gm10260 PE=3 SV=2	Gm10260	F6YVP7_MOUSE (+1)	18 kDa	-0.41	0.02
Mus musculus	Citrate synthase, mitochondrial OS=Mus musculus GN=Cs PE=1 SV=1	Cs	CISY_MOUSE	52 kDa	-0.4	0.4
Mus musculus	AP-2 complex subunit mu OS=Mus musculus GN=Ap2m1 PE=1 SV=1	Ap2m1	AP2M1_MOUSE (+1)	50 kDa	-0.39	0.9
Mus musculus	Clathrin coat assembly protein AP180 OS=Mus musculus GN=Snap91 PE=4 SV=2	Snap91	E9Q9A3_MOUSE (+6)	86 kDa	-0.39	0.11
Mus musculus	Dolichyl-diphosphooligosaccharide--protein glycosyltransferase subunit STT3A OS=Mus musculus GN=Stt3a PE=1 SV=1	Stt3a	STT3A_MOUSE	81 kDa	-0.39	0.018
unknown	Isoform LAMP-2B of Lysosome-associated membrane glycoprotein 2 OS=Mus musculus GN=Lamp2	Lamp2	sp|P17047-2| LAMP2_MOUSE (+2)	46 kDa	-0.39	0.72
Mus musculus	Neutral amino acid transporter ASCT2 OS=Mus musculus GN=Slc1a5 PE=2 SV=1	Slc1a5	Q9ESU7_MOUSE	58 kDa	-0.38	0.78
Mus musculus	Vesicle-fusing ATPase OS=Mus musculus GN=Nsf PE=1 SV=2	Nsf	NSF_MOUSE	83 kDa	-0.38	0.0076
unknown	Isoform Smooth muscle of Myosin light polypeptide 6 OS=Mus musculus GN=Myl6	Myl6	sp|Q60605-2| MYL6_MOUSE (+1)	17 kDa	-0.37	0.4
Mus musculus	40S ribosomal protein S3 OS=Mus musculus GN=Rps3 PE=1 SV=1	Rps3	RS3_MOUSE	27 kDa	-0.36	0.081
Mus musculus	60S ribosomal protein L14 OS=Mus musculus GN=Rpl14 PE=2 SV=3	Rpl14	RL14_MOUSE	24 kDa	-0.36	0.41
Mus musculus	Ras-related protein Rab-35 OS=Mus musculus GN=Rab35 PE=1 SV=1	Rab35	RAB35_MOUSE	23 kDa	-0.36	0.083
Mus musculus	Nucleolin OS=Mus musculus GN=Ncl PE=1 SV=2	Ncl	NUCL_MOUSE	77 kDa	-0.35	0.34
Mus musculus	Protein Pi4ka OS=Mus musculus GN=Pi4ka PE=4 SV=1	Pi4ka	E9Q3L2_MOUSE	231 kDa	-0.35	0.22
Mus musculus	AP-2 complex subunit alpha-2 OS=Mus musculus GN=Ap2a2 PE=1 SV=2	Ap2a2	AP2A2_MOUSE	104 kDa	-0.34	0.019
Mus musculus	Importin subunit beta-1 OS=Mus musculus GN=Kpnb1 PE=1 SV=2	Kpnb1	IMB1_MOUSE	97 kDa	-0.33	0.041

Mus musculus	Polyadenylate-binding protein 1 OS=Mus musculus GN=Pabpc1 PE=1 SV=2	Pabpc1	PABP1_MOUSE	71 kDa	-0.33	0.019
Mus musculus	Sodium- and chloride-dependent taurine transporter OS=Mus musculus GN=Slc6a6 PE=1 SV=2	Slc6a6	SC6A6_MOUSE	70 kDa	-0.33	0.33
Mus musculus	60S ribosomal protein L8 OS=Mus musculus GN=Rpl8 PE=2 SV=2	Rpl8	RL8_MOUSE	28 kDa	-0.32	0.00056
Mus musculus	Leucine-rich repeat-containing protein 59 OS=Mus musculus GN=Lrrc59 PE=2 SV=1	Lrrc59	LRC59_MOUSE	35 kDa	-0.32	< 0.0001
Mus musculus	Vacuolar protein sorting-associated protein 35 OS=Mus musculus GN=Vps35 PE=1 SV=1	Vps35	VPS35_MOUSE	92 kDa	-0.32	0.74
Mus musculus	Flotillin 2, isoform CRA_a OS=Mus musculus GN=Flot2 PE=4 SV=1	Flot2	Q5SS83_MOUSE (+3)	47 kDa	-0.31	0.32
unknown	KxDL motif-containing protein 1 (Fragment) OS=Mus musculus GN=Kxd1 PE=2 SV=1	Kxd1	E9Q4P0_MOUSE (+9)	22 kDa	-0.31	0.0028
Mus musculus	Ras GTPase-activating-like protein IQGAP1 OS=Mus musculus GN=Iqgap1 PE=1 SV=2	Iqgap1	IQGA1_MOUSE	189 kDa	-0.31	0.017
Mus musculus	60S ribosomal protein L28 OS=Mus musculus GN=Rpl28 PE=1 SV=2	Rpl28	RL28_MOUSE	16 kDa	-0.3	0.0015
Mus musculus	Calcium-binding mitochondrial carrier protein Aralar1 OS=Mus musculus GN=Slc25a12 PE=1 SV=1	Slc25a12	CMC1_MOUSE	75 kDa	-0.3	0.15
Mus musculus	Calreticulin OS=Mus musculus GN=Calr PE=1 SV=1	Calr	CALR_MOUSE	48 kDa	-0.3	< 0.0001
Mus musculus	NAC-alpha domain-containing protein 1 OS=Mus musculus GN=Nacad PE=1 SV=1	Nacad	NACAD_MOUSE	157 kDa	-0.3	0.00057
Mus musculus	Protein Gcn1l1 OS=Mus musculus GN=Gcn1l1 PE=2 SV=1	Gcn1l1	E9PVA8_MOUSE	293 kDa	-0.3	< 0.0001
Mus musculus	Ragulator complex protein LAMTOR3 OS=Mus musculus GN=Lamtor3 PE=1 SV=1	Lamtor3	LTOR3_MOUSE	14 kDa	-0.3	0.0062
Mus musculus	ATP synthase subunit alpha, mitochondrial OS=Mus musculus GN=Atp5a1 PE=1 SV=1	Atp5a1	ATPA_MOUSE	60 kDa	-0.29	0.0083
Mus musculus	V-type proton ATPase 116 kDa subunit a isoform 1 OS=Mus musculus GN=Atp6v0a1 PE=4 SV=1	Atp6v0a1	K3W4T3_MOUSE (+2)	96 kDa	-0.28	0.0022
Mus musculus	Dedicator of cytokinesis protein 7 OS=Mus musculus GN=Dock7 PE=2 SV=1	Dock7	A2A9M5_MOUSE (+3)	241 kDa	-0.27	0.43
Mus musculus	Eukaryotic translation initiation factor 3 subunit B OS=Mus musculus GN=Eif3b PE=1 SV=1	Eif3b	EIF3B_MOUSE	91 kDa	-0.27	0.3
Mus musculus	Lysosome membrane protein 2 OS=Mus musculus GN=Scarb2 PE=1 SV=3	Scarb2	SCRB2_MOUSE	54 kDa	-0.27	< 0.0001
Mus musculus	Phospholipase C beta 4 OS=Mus musculus GN=Plcb4 PE=2 SV=1	Plcb4	Q91UZ1_MOUSE	135 kDa	-0.27	0.29
Mus musculus	Coatomer subunit beta' OS=Mus musculus GN=Copb2 PE=2 SV=2	Copb2	COPB2_MOUSE	102 kDa	-0.26	0.52
Mus musculus	Dolichyl-diphosphooligosaccharide--protein glycosyltransferase subunit 1 OS=Mus musculus GN=Rpn1 PE=2 SV=1	Rpn1	RPN1_MOUSE	69 kDa	-0.26	0.0015
unknown	Isoform 3 of Sec1 family domain-containing protein 1 OS=Mus musculus GN=Scfd1	Scfd1	sp|Q8BRF7-3| SCFD1_MOUSE (+1)	67 kDa	-0.26	0.29
Mus musculus	Nck-associated protein 1 OS=Mus musculus GN=Nckap1 PE=2 SV=1	Nckap1	A2AS98_MOUSE (+1)	130 kDa	-0.26	0.059
Mus musculus	Lysosomal alpha-glucosidase OS=Mus musculus GN=Gaa PE=1 SV=2	Gaa	LYAG_MOUSE	106 kDa	-0.25	< 0.0001
unknown	Isoform 2 of UPF0577 protein KIAA1324 OS=Mus musculus GN=Kiaa1324	Kiaa1324	sp|A2AFS3-2| K1324_MOUSE (+2)	100 kDa	-0.24	0.32
Mus musculus	Long-chain-fatty-acid--CoA ligase 3 OS=Mus musculus GN=Acsl3 PE=2 SV=2	Acsl3	ACSL3_MOUSE	80 kDa	-0.24	0.023

Mus musculus	Staphylococcal nuclease domain-containing protein 1 OS=Mus musculus GN=Snd1 PE=1 SV=1	Snd1	SND1_MOUSE	102 kDa	-0.24	0.0061
Mus musculus	Reticulon-1 OS=Mus musculus GN=Rtn1 PE=1 SV=1	Rtn1	RTN1_MOUSE	84 kDa	-0.23	0.21
Mus musculus	Vesicle-associated membrane protein-associated protein A OS=Mus musculus GN=Vapa PE=1 SV=2	Vapa	VAPA_MOUSE	28 kDa	-0.23	0.00093
Mus musculus	60S ribosomal protein L27a OS=Mus musculus GN=Rpl27a PE=2 SV=5	Rpl27a	RL27A_MOUSE	17 kDa	-0.22	0.00013
Mus musculus	Large neutral amino acids transporter small subunit 1 OS=Mus musculus GN=Slc7a5 PE=1 SV=2	Slc7a5	LAT1_MOUSE	56 kDa	-0.22	0.14
Mus musculus	40S ribosomal protein S23 OS=Mus musculus GN=Rps23 PE=2 SV=3	Rps23	RS23_MOUSE	16 kDa	-0.21	0.52
Mus musculus	Protein disulfide-isomerase A4 OS=Mus musculus GN=Pdia4 PE=1 SV=3	Pdia4	PDIA4_MOUSE	72 kDa	-0.21	< 0.0001
Mus musculus	Ras-related protein Rab-11B OS=Mus musculus GN=Rab11b PE=1 SV=3	Rab11b	RB11B_MOUSE	24 kDa	-0.21	0.12
Mus musculus	60S ribosomal protein L27 OS=Mus musculus GN=Rpl27 PE=2 SV=2	Rpl27	RL27_MOUSE	16 kDa	-0.2	0.004
Mus musculus	Leucine--tRNA ligase, cytoplasmic OS=Mus musculus GN=Lars PE=2 SV=2	Lars	SYLC_MOUSE	134 kDa	-0.2	0.7
Mus musculus	Radixin OS=Mus musculus GN=Rdx PE=1 SV=3	Rdx	RADI_MOUSE	69 kDa	-0.2	0.14
Mus musculus	60S ribosomal protein L34 OS=Mus musculus GN=Rpl34 PE=3 SV=2	Rpl34	RL34_MOUSE	13 kDa	-0.19	0.00021
Mus musculus	Cytoskeleton-associated protein 5 OS=Mus musculus GN=Ckap5 PE=4 SV=1	Ckap5	K3W4R5_MOUSE (+2)	226 kDa	-0.19	0.86
Mus musculus	Fructose-bisphosphate aldolase OS=Mus musculus GN=Aldoa PE=2 SV=1	Aldoa	A6ZI44_MOUSE (+1)	45 kDa	-0.19	0.015
Mus musculus	Moesin OS=Mus musculus GN=Msn PE=1 SV=3	Msn	MOES_MOUSE	68 kDa	-0.19	0.073
Mus musculus	60S ribosomal protein L17 OS=Mus musculus GN=Rpl17 PE=2 SV=1	Rpl17	Q6ZWZ7_MOUSE (+1)	21 kDa	-0.18	0.0016
Mus musculus	Protein Kif13b OS=Mus musculus GN=Kif13b PE=2 SV=1	Kif13b	E9Q4K7_MOUSE	205 kDa	-0.18	0.0017
Mus musculus	Ubiquitin-like modifier-activating enzyme 1 OS=Mus musculus GN=Uba1 PE=1 SV=1	Uba1	UBA1_MOUSE	118 kDa	-0.18	0.55
Mus musculus	Cartilage acidic protein 1 OS=Mus musculus GN=Crtac1 PE=2 SV=1	Crtac1	CRAC1_MOUSE	70 kDa	-0.17	< 0.0001
Mus musculus	CLIP-associating protein 1 OS=Mus musculus GN=Clasp1 PE=4 SV=1	Clasp1	J3QP81_MOUSE (+7)	161 kDa	-0.17	0.31
Mus musculus	NADH-cytochrome b5 reductase 3 OS=Mus musculus GN=Cyb5r3 PE=2 SV=1	Cyb5r3	F2Z456_MOUSE (+2)	35 kDa	-0.17	0.00032
Mus musculus	Ras-related protein Rab-7a OS=Mus musculus GN=Rab7a PE=1 SV=2	Rab7a	RAB7A_MOUSE	23 kDa	-0.17	0.52
Mus musculus	40S ribosomal protein S27 OS=Mus musculus GN=Rps27 PE=1 SV=3	Rps27	RS27_MOUSE (+1)	9 kDa	-0.16	0.0017
Mus musculus	60S ribosomal protein L7 OS=Mus musculus GN=Rpl7 PE=2 SV=2	Rpl7	RL7_MOUSE	31 kDa	-0.16	< 0.0001
Mus musculus	Nodal modulator 1 OS=Mus musculus GN=Nomo1 PE=1 SV=1	Nomo1	NOMO1_MOUSE	133 kDa	-0.16	0.03
Mus musculus	Ras-related protein Rab-8A OS=Mus musculus GN=Rab8a PE=1 SV=2	Rab8a	RAB8A_MOUSE	24 kDa	-0.16	0.22
Mus musculus	Solute carrier family 12 member 9 OS=Mus musculus GN=Slc12a9 PE=1 SV=2	Slc12a9	S12A9_MOUSE	96 kDa	-0.16	0.064
Mus musculus	60S ribosomal protein L30 OS=Mus musculus GN=Rpl30 PE=2 SV=2	Rpl30	RL30_MOUSE	13 kDa	-0.15	0.0023
Mus musculus	Peroxidasin homolog OS=Mus musculus GN=Pxdn PE=2 SV=2	Pxdn	PXDN_MOUSE	165 kDa	-0.15	0.53
Mus musculus	Protein transport protein Sec61 subunit alpha isoform 1 OS=Mus musculus GN=Sec61a1 PE=2 SV=2	Sec61a1	S61A1_MOUSE	52 kDa	-0.15	0.00056
Mus musculus	Transferrin receptor protein 1 OS=Mus musculus GN=Tfrc PE=1 SV=1	Tfrc	TFR1_MOUSE	86 kDa	-0.15	< 0.0001

Mus musculus	60S ribosomal protein L22 OS=Mus musculus GN=Rpl22 PE=2 SV=2	Rpl22	RL22_MOUSE	15 kDa	-0.14	0.085
Mus musculus	Eukaryotic translation initiation factor 3 subunit C OS=Mus musculus GN=Eif3c PE=1 SV=1	Eif3c	EIF3C_MOUSE	106 kDa	-0.14	0.027
Mus musculus	Translocation protein SEC63 homolog OS=Mus musculus GN=Sec63 PE=1 SV=4	Sec63	SEC63_MOUSE	88 kDa	-0.14	0.15
Mus musculus	Endoplasmin OS=Mus musculus GN=Hsp90b1 PE=1 SV=2	Hsp90b1	ENPL_MOUSE	92 kDa	-0.13	< 0.0001
Mus musculus	Unconventional myosin-VI OS=Mus musculus GN=Myo6 PE=2 SV=1	Myo6	E9PVU0_MOUSE (+1)	146 kDa	-0.13	0.16
Mus musculus	ER membrane protein complex subunit 1 OS=Mus musculus GN=Emc1 PE=1 SV=1	Emc1	sp|Q8C7X2| EMC1_MOUSE	112 kDa	-0.12	0.00032
Mus musculus	MCG13402, isoform CRA_a OS=Mus musculus GN=Ptbp1 PE=2 SV=1	Ptbp1	Q8BGJ5_MOUSE (+1)	57 kDa	-0.12	0.034
Mus musculus	Ras-related protein Rab-10 OS=Mus musculus GN=Rab10 PE=1 SV=1	Rab10	RAB10_MOUSE	23 kDa	-0.12	0.85
Mus musculus	Cytoskeleton-associated protein 4 OS=Mus musculus GN=Ckap4 PE=2 SV=2	Ckap4	CKAP4_MOUSE	64 kDa	-0.11	0.89
Mus musculus	Hypoxia up-regulated protein 1 OS=Mus musculus GN=Hyou1 PE=1 SV=1	Hyou1	HYOU1_MOUSE	111 kDa	-0.11	< 0.0001
unknown	Isoform PLEC-1D of Plectin OS=Mus musculus GN=Plec	Plec	sp|Q9QXS1-10| PLEC_MOUSE (+15)	514 kDa	-0.11	0.92
Mus musculus	Prolow-density lipoprotein receptor-related protein 1 OS=Mus musculus GN=Lrp1 PE=1 SV=1	Lrp1	LRP1_MOUSE	505 kDa	-0.11	0.049
Mus musculus	Very-long-chain enoyl-CoA reductase OS=Mus musculus GN=Tecr PE=1 SV=1	Tecr	TECR_MOUSE	36 kDa	-0.11	0.0005
Mus musculus	V-type proton ATPase subunit d 1 OS=Mus musculus GN=Atp6v0d1 PE=1 SV=2	Atp6v0d1	VA0D1_MOUSE	40 kDa	-0.11	0.001
Mus musculus	60S ribosomal protein L13 OS=Mus musculus GN=Rpl13 PE=2 SV=3	Rpl13	RL13_MOUSE	24 kDa	-0.1	0.6
Mus musculus	60S ribosomal protein L9 OS=Mus musculus GN=Rpl9 PE=2 SV=2	Rpl9	RL9_MOUSE (+1)	22 kDa	-0.1	0.038
unknown	Isoform E2 of Drebrin OS=Mus musculus GN=Dbn1	Dbn1	sp|Q9QXS6-3| DREB_MOUSE (+1)	72 kDa	-0.1	0.018
Mus musculus	Malate dehydrogenase, mitochondrial OS=Mus musculus GN=Mdh2 PE=1 SV=3	Mdh2	MDHM_MOUSE	36 kDa	-0.1	0.44
Mus musculus	Myo1b protein OS=Mus musculus GN=Myo1b PE=2 SV=1	Myo1b	Q7TQD7_MOUSE (+1)	132 kDa	-0.1	0.017
Mus musculus	Protein 4.1 OS=Mus musculus GN=Epb4.1 PE=2 SV=1	Epb4.1	A2A841_MOUSE (+1)	97 kDa	-0.1	0.89
Mus musculus	Secretory carrier-associated membrane protein 1 OS=Mus musculus GN=Scamp1 PE=1 SV=1	Scamp1	SCAM1_MOUSE	38 kDa	-0.1	0.037
Mus musculus	Catenin beta-1 OS=Mus musculus GN=Ctnnb1 PE=1 SV=1	Ctnnb1	CTNB1_MOUSE	85 kDa	-0.09	0.011
Mus musculus	Cleft lip and palate transmembrane protein 1 homolog OS=Mus musculus GN=Clptm1 PE=1 SV=1	Clptm1	CLPT1_MOUSE	75 kDa	-0.09	0.13
unknown	Isoform 2 of CD97 antigen OS=Mus musculus GN=Cd97	Cd97	sp|Q9Z0M6-2| CD97_MOUSE (+3)	80 kDa	-0.09	0.25
Mus musculus	Melanoma inhibitory activity protein 3 OS=Mus musculus GN=Mia3 PE=1 SV=2	Mia3	sp|Q8BI84|MIA3_MOUSE	214 kDa	-0.09	0.0019
Mus musculus	Tumor protein p53-inducible protein 11 (Fragment) OS=Mus musculus GN=Trp53i11 PE=2 SV=1	Trp53i11	A2AGS6_MOUSE (+1)	10 kDa	-0.09	0.26
Mus musculus	Tyrosine-protein kinase OS=Mus musculus GN=Jak1 PE=3 SV=1	Jak1	B1ASP2_MOUSE (+1)	133 kDa	-0.09	0.21
Mus musculus	40S ribosomal protein S2 OS=Mus musculus GN=Rps2 PE=1 SV=3	Rps2	RS2_MOUSE	31 kDa	-0.08	0.15
Mus musculus	60S ribosomal protein L18a OS=Mus musculus GN=Rpl18a PE=1 SV=1	Rpl18a	RL18A_MOUSE	21 kDa	-0.08	0.14
Mus musculus	60S ribosomal protein L23 OS=Mus musculus GN=Rpl23 PE=1 SV=1	Rpl23	RL23_MOUSE	15 kDa	-0.08	0.1

Mus musculus	60S ribosomal protein L6 OS=Mus musculus GN=Rpl6 PE=1 SV=3	Rpl6	RL6_MOUSE	34 kDa	-0.08	0.012
Mus musculus	ADP-ribosylation factor-like protein 8B OS=Mus musculus GN=Arl8b PE=2 SV=1	Arl8b	ARL8B_MOUSE	22 kDa	-0.08	0.3
Mus musculus	ATP-dependent RNA helicase DDX3X OS=Mus musculus GN=Ddx3x PE=1 SV=3	Ddx3x	DDX3X_MOUSE	73 kDa	-0.08	< 0.0001
Mus musculus	Isoleucine--tRNA ligase, cytoplasmic OS=Mus musculus GN=Iars PE=2 SV=2	Iars	SYIC_MOUSE	144 kDa	-0.08	0.67
Mus musculus	Plexin-B2 OS=Mus musculus GN=Plxnb2 PE=1 SV=1	Plxnb2	PLXB2_MOUSE	206 kDa	-0.08	0.099
Mus musculus	Steryl-sulfatase OS=Mus musculus GN=Sts PE=2 SV=1	Sts	STS_MOUSE	67 kDa	-0.08	0.25
Mus musculus	ATP synthase subunit beta, mitochondrial OS=Mus musculus GN=Atp5b PE=1 SV=2	Atp5b	ATPB_MOUSE	56 kDa	-0.07	0.0068
Mus musculus	IgE-binding protein OS=Mus musculus GN=Iap PE=2 SV=1	Iap	IGEB_MOUSE	63 kDa	-0.07	0.66
Mus musculus	Long-chain fatty acid transport protein 4 OS=Mus musculus GN=Slc27a4 PE=1 SV=1	Slc27a4	S27A4_MOUSE	72 kDa	-0.07	0.39
Mus musculus	Peptidyl-prolyl cis-trans isomerase B OS=Mus musculus GN=Ppib PE=2 SV=2	Ppib	PPIB_MOUSE	24 kDa	-0.07	0.042
Mus musculus	Reticulon-4 OS=Mus musculus GN=Rtn4 PE=1 SV=2	Rtn4	sp|Q99P72| RTN4_MOUSE	127 kDa	-0.07	< 0.0001
Mus musculus	Ribosomal protein L19 OS=Mus musculus GN=Rpl19 PE=2 SV=1	Rpl19	A2A547_MOUSE (+1)	23 kDa	-0.07	0.12
Mus musculus	Serine/threonine-protein kinase 11-interacting protein OS=Mus musculus GN=Stk11ip PE=1 SV=1	Stk11ip	S11IP_MOUSE	118 kDa	-0.07	0.53
Mus musculus	60S ribosomal protein L18 OS=Mus musculus GN=Rpl18 PE=2 SV=3	Rpl18	RL18_MOUSE	22 kDa	-0.06	0.048
Mus musculus	60S ribosomal protein L4 OS=Mus musculus GN=Rpl4 PE=1 SV=3	Rpl4	RL4_MOUSE	47 kDa	-0.06	0.21
Mus musculus	ADP/ATP translocase 2 OS=Mus musculus GN=Slc25a5 PE=1 SV=3	Slc25a5	ADT2_MOUSE	33 kDa	-0.06	0.49
Mus musculus	Heterogeneous nuclear ribonucleoprotein K OS=Mus musculus GN=Hnrnpk PE=2 SV=1	Hnrnpk	B2M1R6_MOUSE (+3)	49 kDa	-0.06	0.13
unknown	Isoform 2 of Glucosidase 2 subunit beta OS=Mus musculus GN=Prkcsh	Prkcsh	sp|O08795-2| GLU2B_MOUSE (+1)	60 kDa	-0.06	0.19
Mus musculus	Lipase maturation factor 2 OS=Mus musculus GN=Lmf2 PE=2 SV=1	Lmf2	LMF2_MOUSE	80 kDa	-0.06	0.19
Mus musculus	Syntaxin-12 OS=Mus musculus GN=Stx12 PE=1 SV=1	Stx12	STX12_MOUSE	31 kDa	-0.06	0.52
Mus musculus	60S ribosomal protein L21 OS=Mus musculus GN=Rpl21 PE=2 SV=1	Rpl21	Q9CQM8_MOUSE (+1)	19 kDa	-0.05	0.72
Mus musculus	AP-1 complex subunit beta-1 OS=Mus musculus GN=Ap1b1 PE=1 SV=2	Ap1b1	AP1B1_MOUSE (+2)	104 kDa	-0.05	0.35
Mus musculus	Elongation factor 1-alpha 1 OS=Mus musculus GN=Eef1a1 PE=1 SV=3	Eef1a1	EF1A1_MOUSE	50 kDa	-0.05	0.018
Mus musculus	Erbb2ip protein OS=Mus musculus GN=Erbb2ip PE=2 SV=1	Erbb2ip	B7ZNX6_MOUSE (+4)	158 kDa	-0.05	0.28
Mus musculus	Glucosylceramidase OS=Mus musculus GN=Gba PE=1 SV=1	Gba	GLCM_MOUSE	58 kDa	-0.05	0.46
unknown	Isoform 2 of Acetyl-CoA carboxylase 1 OS=Mus musculus GN=Acaca	Acaca	sp|Q5SWU9-2| ACACA_MOUSE (+1)	270 kDa	-0.05	0.033
unknown	Isoform B of FK506-binding protein 15 OS=Mus musculus GN=Fkbp15	Fkbp15	sp|Q6P9Q6-2| FKB15_MOUSE (+1)	137 kDa	-0.05	0.76
Mus musculus	60S ribosomal protein L13a OS=Mus musculus GN=Rpl13a PE=2 SV=1	Rpl13a	E9Q5A0_MOUSE (+1)	48 kDa	-0.04	0.21
Mus musculus	Carboxypeptidase D OS=Mus musculus GN=Cpd PE=1 SV=2	Cpd	CBPD_MOUSE	152 kDa	-0.04	0.85
Mus musculus	Coatomer subunit gamma-1 OS=Mus musculus GN=Copg1 PE=2 SV=1	Copg1	COPG1_MOUSE	98 kDa	-0.04	0.31
Mus musculus	Golgi-specific brefeldin A-resistance factor 1 OS=Mus musculus GN=Gbf1 PE=1 SV=1	Gbf1	Q6DFZ1_MOUSE	207 kDa	-0.04	0.75
Mus musculus	Minor histocompatibility antigen H13 (Fragment) OS=Mus musculus GN=H13 PE=2 SV=1	H13	A3KGR9_MOUSE (+2)	38 kDa	-0.04	0.078

Mus musculus	Myosin-10 OS=Mus musculus GN=Myh10 PE=1 SV=2	Myh10	MYH10_MOUSE (+2)	229 kDa	-0.04	0.00046
Mus musculus	Ras-related protein Ral-B OS=Mus musculus GN=Ralb PE=2 SV=1	Ralb	RALB_MOUSE	23 kDa	-0.04	0.78
Mus musculus	Sarcoplasmic/endoplasmic reticulum calcium ATPase 2 OS=Mus musculus GN=Atp2a2 PE=3 SV=1	Atp2a2	J3KMM5_MOUSE (+1)	110 kDa	-0.04	0.016
Mus musculus	Tubulin beta-5 chain OS=Mus musculus GN=Tubb5 PE=1 SV=1	Tubb5	TBB5_MOUSE	50 kDa	-0.04	0.16
Mus musculus	60S ribosomal protein L36a OS=Mus musculus GN=Rpl36a PE=2 SV=2	Rpl36a	RL36A_MOUSE	12 kDa	-0.03	0.52
Mus musculus	ATP synthase F(0) complex subunit B1, mitochondrial OS=Mus musculus GN=Atp5f1 PE=1 SV=1	Atp5f1	AT5F1_MOUSE	29 kDa	-0.03	0.85
Mus musculus	Dolichyl-diphosphooligosaccharide--protein glycosyltransferase subunit STT3B OS=Mus musculus GN=Stt3b PE=1 SV=2	Stt3b	STT3B_MOUSE	93 kDa	-0.03	0.12
unknown	Isoform 2 of 40S ribosomal protein S24 OS=Mus musculus GN=Rps24	Rps24	sp|P62849-2| RS24_MOUSE (+2)	15 kDa	-0.03	0.52
Mus musculus	Monocarboxylate transporter 1 OS=Mus musculus GN=Slc16a1 PE=1 SV=1	Slc16a1	MOT1_MOUSE	53 kDa	-0.03	0.53
Mus musculus	Protein disulfide-isomerase A3 OS=Mus musculus GN=Pdia3 PE=1 SV=2	Pdia3	PDIA3_MOUSE	57 kDa	-0.03	< 0.0001
Mus musculus	Alpha-1,3/1,6-mannosyltransferase ALG2 OS=Mus musculus GN=Alg2 PE=2 SV=2	Alg2	ALG2_MOUSE	47 kDa	-0.02	0.56
Mus musculus	Alpha-internexin OS=Mus musculus GN=Ina PE=1 SV=2	Ina	AINX_MOUSE	56 kDa	-0.02	0.012
Mus musculus	Dedicator of cytokinesis protein 11 OS=Mus musculus GN=Dock11 PE=2 SV=1	Dock11	A2AF67_MOUSE	218 kDa	-0.02	0.38
Mus musculus	Integrin beta-1 OS=Mus musculus GN=Itgb1 PE=1 SV=1	Itgb1	ITB1_MOUSE	88 kDa	-0.02	0.41
Mus musculus	Lysophosphatidylcholine acyltransferase 1 OS=Mus musculus GN=Lpcat1 PE=1 SV=1	Lpcat1	sp|Q3TFD2| PCAT1_MOUSE	60 kDa	-0.02	0.48
Mus musculus	Protein Nbas OS=Mus musculus GN=Nbas PE=2 SV=1	Nbas	E9Q411_MOUSE	266 kDa	-0.02	0.67
Mus musculus	Ras-related protein Rab-1B OS=Mus musculus GN=Rab1b PE=1 SV=1	Rab1b	RAB1B_MOUSE	22 kDa	-0.02	0.76
Mus musculus	Surfeit locus protein 4 OS=Mus musculus GN=Surf4 PE=2 SV=1	Surf4	SURF4_MOUSE	30 kDa	-0.02	0.39
Mus musculus	Synaptophysin OS=Mus musculus GN=Syp PE=1 SV=2	Syp	SYPH_MOUSE	34 kDa	-0.02	0.059
Mus musculus	Transforming protein RhoA OS=Mus musculus GN=Rhoa PE=1 SV=1	Rhoa	RHOA_MOUSE	22 kDa	-0.02	0.38
Mus musculus	Bifunctional glutamate/proline--tRNA ligase OS=Mus musculus GN=Eprs PE=1 SV=4	Eprs	SYEP_MOUSE	170 kDa	-0.01	0.1
Mus musculus	cAMP-dependent protein kinase type I-alpha regulatory subunit OS=Mus musculus GN=Prkar1a PE=1 SV=3	Prkar1a	KAP0_MOUSE	43 kDa	-0.01	0.98
Mus musculus	Catenin alpha-1 OS=Mus musculus GN=Ctnna1 PE=1 SV=1	Ctnna1	CTNA1_MOUSE	100 kDa	-0.01	0.14
Mus musculus	Cathepsin D OS=Mus musculus GN=Ctsd PE=1 SV=1	Ctsd	CATD_MOUSE	45 kDa	-0.01	0.95
Mus musculus	Kinectin OS=Mus musculus GN=Ktn1 PE=2 SV=1	Ktn1	F8VQC7_MOUSE (+5)	153 kDa	-0.01	0.55
Mus musculus	Nicastrin OS=Mus musculus GN=Ncstn PE=1 SV=3	Ncstn	NICA_MOUSE	78 kDa	-0.01	0.74
Mus musculus	Protein Atp2b4 OS=Mus musculus GN=Atp2b4 PE=2 SV=1	Atp2b4	E9Q828_MOUSE (+3)	129 kDa	-0.01	0.95
Mus musculus	T-complex protein 1 subunit delta OS=Mus musculus GN=Cct4 PE=2 SV=1	Cct4	G5E839_MOUSE (+1)	55 kDa	-0.01	0.073
Mus musculus	ATP-binding cassette sub-family B member 6, mitochondrial OS=Mus musculus GN=Abcb6 PE=1 SV=1	Abcb6	ABCB6_MOUSE	94 kDa	0	0.0074
Mus musculus	Catenin delta-1 OS=Mus musculus GN=Ctnnd1 PE=2 SV=1	Ctnnd1	E9Q8Z6_MOUSE (+3)	107 kDa	0	0.98

Mus musculus	DNA fragmentation factor subunit beta OS=Mus musculus GN=Cad PE=2 SV=1	Cad	E9QAI5_MOUSE (+1)	236 kDa	0	0.54
Mus musculus	Heat shock protein HSP 90-alpha OS=Mus musculus GN=Hsp90aa1 PE=1 SV=4	Hsp90aa1	HS90A_MOUSE	85 kDa	0	0.82
Mus musculus	Mannosyl-oligosaccharide glucosidase OS=Mus musculus GN=Mogs PE=2 SV=1	Mogs	MOGS_MOUSE	92 kDa	0	0.49
Mus musculus	NADPH--cytochrome P450 reductase OS=Mus musculus GN=Por PE=1 SV=2	Por	NCPR_MOUSE	77 kDa	0	0.9
Mus musculus	1-acyl-sn-glycerol-3-phosphate acyltransferase delta OS=Mus musculus GN=Agpat4 PE=2 SV=1	Agpat4	PLCD_MOUSE	44 kDa	0.01	0.5
Mus musculus	78 kDa glucose-regulated protein OS=Mus musculus GN=Hspa5 PE=1 SV=3	Hspa5	GRP78_MOUSE	72 kDa	0.01	< 0.0001
Mus musculus	Endothelin-converting enzyme-like 1 OS=Mus musculus GN=Ecel1 PE=2 SV=2	Ecel1	ECEL1_MOUSE	88 kDa	0.01	0.17
Mus musculus	GPI transamidase component PIG-S OS=Mus musculus GN=Pigs PE=1 SV=3	Pigs	PIGS_MOUSE	62 kDa	0.01	0.73
Mus musculus	Guanine nucleotide-binding protein G(k) subunit alpha OS=Mus musculus GN=Gnai3 PE=1 SV=3	Gnai3	GNAI3_MOUSE	41 kDa	0.01	0.29
unknown	Isoform 2 of Integrin alpha-3 OS=Mus musculus GN=Itga3	Itga3	sp|Q62470-2| ITA3_MOUSE (+1)	119 kDa	0.01	0.091
Mus musculus	Protein sidekick-1 OS=Mus musculus GN=Sdk1 PE=2 SV=1	Sdk1	sp|Q3UH53| SDK1_MOUSE	240 kDa	0.01	0.87
Mus musculus	Sodium/potassium-transporting ATPase subunit beta-1 OS=Mus musculus GN=Atp1b1 PE=1 SV=1	Atp1b1	AT1B1_MOUSE	35 kDa	0.01	0.21
Mus musculus	Talin-1 OS=Mus musculus GN=Tln1 PE=1 SV=2	Tln1	TLN1_MOUSE	270 kDa	0.01	< 0.0001
Mus musculus	60S ribosomal protein L24 OS=Mus musculus GN=Rpl24 PE=2 SV=2	Rpl24	RL24_MOUSE	18 kDa	0.02	0.39
Mus musculus	60S ribosomal protein L5 OS=Mus musculus GN=Rpl5 PE=1 SV=3	Rpl5	RL5_MOUSE	34 kDa	0.02	0.96
Mus musculus	7-dehydrocholesterol reductase OS=Mus musculus GN=Dhcr7 PE=2 SV=1	Dhcr7	DHCR7_MOUSE	54 kDa	0.02	0.5
Mus musculus	Brefeldin A-inhibited guanine nucleotide-exchange protein 3 OS=Mus musculus GN=Arfgef3 PE=1 SV=1	Arfgef3	BIG3_MOUSE	240 kDa	0.02	< 0.0001
Mus musculus	Calcium/calmodulin-dependent protein kinase type II subunit beta OS=Mus musculus GN=Camk2b PE=1 SV=2	Camk2b	KCC2B_MOUSE (+8)	60 kDa	0.02	0.25
Mus musculus	Flotillin-1 OS=Mus musculus GN=Flot1 PE=1 SV=1	Flot1	FLOT1_MOUSE	48 kDa	0.02	0.26
Mus musculus	Guanine nucleotide-binding protein subunit alpha-11 OS=Mus musculus GN=Gna11 PE=1 SV=1	Gna11	GNA11_MOUSE	42 kDa	0.02	0.13
Mus musculus	Histone H2A type 1-F OS=Mus musculus GN=Hist1h2af PE=1 SV=3	Hist1h2af	H2A1F_MOUSE (+6)	14 kDa	0.02	0.73
unknown	Isoform 2 of Synaptotagmin-like protein 4 OS=Mus musculus GN=Sytl4	Sytl4	sp|Q9R0Q1-2| SYTL4_MOUSE (+2)	57 kDa	0.02	0.68
Mus musculus	Long-chain-fatty-acid--CoA ligase 4 OS=Mus musculus GN=Acsl4 PE=2 SV=2	Acsl4	sp|Q9QUJ7| ACSL4_MOUSE	79 kDa	0.02	0.75
Mus musculus	Atlastin-2 OS=Mus musculus GN=Atl2 PE=1 SV=1	Atl2	sp|Q6PA06| ATLA2_MOUSE	66 kDa	0.03	0.52
Mus musculus	Guanine nucleotide-binding protein G(s) subunit alpha isoforms XLas OS=Mus musculus GN=Gnas PE=2 SV=1	Gnas	sp|Q6R0H7| GNAS1_MOUSE	122 kDa	0.03	0.042
Mus musculus	Histone H3.2 OS=Mus musculus GN=Hist1h3b PE=1 SV=2	Hist1h3b	H32_MOUSE	15 kDa	0.03	0.62
Mus musculus	Phosphate carrier protein, mitochondrial OS=Mus musculus GN=Slc25a3 PE=1 SV=1	Slc25a3	MPCP_MOUSE	40 kDa	0.03	0.15

Mus musculus	Probable cation-transporting ATPase 13A1 OS=Mus musculus GN=Atp13a1 PE=1 SV=2	Atp13a1	AT131_MOUSE	132 kDa	0.03	0.16
Mus musculus	Serine/threonine-protein kinase MRCK alpha OS=Mus musculus GN=Cdc42bpa PE=2 SV=1	Cdc42bpa	D3YYN8_MOUSE (+2)	193 kDa	0.03	0.023
Mus musculus	Dolichyl-diphosphooligosaccharide--protein glycosyltransferase subunit 2 OS=Mus musculus GN=Rpn2 PE=2 SV=1	Rpn2	RPN2_MOUSE	69 kDa	0.04	< 0.0001
unknown	Isoform 2 of Regulator of nonsense transcripts 1 OS=Mus musculus GN=Upf1	Upf1	sp|Q9EPU0-2| RENT1_MOUSE (+1)	123 kDa	0.04	0.46
Mus musculus	Protein disulfide-isomerase A6 OS=Mus musculus GN=Pdia6 PE=1 SV=3	Pdia6	PDIA6_MOUSE	48 kDa	0.04	0.0026
Mus musculus	Uncharacterized protein OS=Mus musculus GN=Gm10036 PE=3 SV=1	Gm10036	E9PYL9_MOUSE (+2)	20 kDa	0.04	1
Mus musculus	Carboxypeptidase E OS=Mus musculus GN=Cpe PE=1 SV=2	Cpe	CBPE_MOUSE	53 kDa	0.05	0.051
Mus musculus	Cullin-associated NEDD8-dissociated protein 1 OS=Mus musculus GN=Cand1 PE=2 SV=2	Cand1	CAND1_MOUSE	136 kDa	0.05	0.53
unknown	Isoform 2 of Neutral alpha-glucosidase AB OS=Mus musculus GN=Ganab	Ganab	sp|Q8BHN3-2| GANAB_MOUSE (+1)	109 kDa	0.05	< 0.0001
unknown	Isoform 2 of Poly(rC)-binding protein 2 OS=Mus musculus GN=Pcbp2	Pcbp2	sp|Q61990-2| PCBP2_MOUSE (+2)	35 kDa	0.05	0.16
Mus musculus	MCG115602 OS=Mus musculus GN=Dnajc13 PE=4 SV=1	Dnajc13	G3X922_MOUSE (+1)	254 kDa	0.05	0.00014
Mus musculus	Ribosome-binding protein 1 OS=Mus musculus GN=Rrbp1 PE=2 SV=1	Rrbp1	A2AVJ7_MOUSE (+1)	158 kDa	0.05	0.00032
Mus musculus	Angiotensin-converting enzyme OS=Mus musculus GN=Ace PE=1 SV=3	Ace	sp|P09470|ACE_MOUSE	151 kDa	0.06	0.083
Mus musculus	Dystonin OS=Mus musculus GN=Dst PE=4 SV=1	Dst	S4R1P5_MOUSE	871 kDa	0.06	0.94
Mus musculus	Extended synaptotagmin-1 OS=Mus musculus GN=Esyt1 PE=2 SV=2	Esyt1	sp|Q3U7R1| ESYT1_MOUSE	122 kDa	0.06	0.0035
unknown	Isoform 3 of Peripheral plasma membrane protein CASK OS=Mus musculus GN=Cask	Cask	sp|O70589-3| CSKP_MOUSE (+4)	102 kDa	0.06	0.027
Mus musculus	Serine/threonine-protein phosphatase 2A 65 kDa regulatory subunit A alpha isoform OS=Mus musculus GN=Ppp2r1a PE=1 SV=3	Ppp2r1a	2AAA_MOUSE	65 kDa	0.06	0.56
Mus musculus	Vesicle transport protein GOT1B OS=Mus musculus GN=Golt1b PE=2 SV=1	Golt1b	GOT1B_MOUSE	15 kDa	0.06	0.48
Mus musculus	Probable ATP-dependent RNA helicase DDX5 OS=Mus musculus GN=Ddx5 PE=1 SV=2	Ddx5	DDX5_MOUSE (+1)	69 kDa	0.07	0.34
Mus musculus	Probable phospholipid-transporting ATPase IIA OS=Mus musculus GN=Atp9a PE=2 SV=1	Atp9a	A2AQC3_MOUSE (+3)	124 kDa	0.07	0.9
Mus musculus	Protein disulfide-isomerase OS=Mus musculus GN=P4hb PE=1 SV=2	P4hb	PDIA1_MOUSE	57 kDa	0.07	< 0.0001
Mus musculus	ATP-binding cassette sub-family A member 7 OS=Mus musculus GN=Abca7 PE=2 SV=1	Abca7	E9Q6G4_MOUSE	238 kDa	0.08	0.012
Mus musculus	Clathrin heavy chain 1 OS=Mus musculus GN=Cltc PE=1 SV=3	Cltc	CLH1_MOUSE (+1)	192 kDa	0.08	0.071
Mus musculus	High affinity cationic amino acid transporter 1 OS=Mus musculus GN=Slc7a1 PE=2 SV=1	Slc7a1	CTR1_MOUSE	67 kDa	0.08	0.06
unknown	Isoform 2 of UPF0577 protein KIAA1324-like homolog OS=Mus musculus		sp|Q3UZV7-2| K132L_MOUSE (+1)	112 kDa	0.08	0.2
unknown	Isoform 4 of Fatty acyl-CoA reductase 1 OS=Mus musculus GN=Far1	Far1	sp|Q922J9-4| FACR1_MOUSE (+1)	60 kDa	0.08	0.85
Mus musculus	Lanosterol synthase OS=Mus musculus GN=Lss PE=2 SV=2	Lss	ERG7_MOUSE	83 kDa	0.08	0.26
Mus musculus	PRA1 family protein 3 OS=Mus musculus GN=Arl6ip5 PE=1 SV=2	Arl6ip5	PRAF3_MOUSE	22 kDa	0.08	0.48
Mus musculus	Ras-related protein Rab-2A OS=Mus musculus GN=Rab2a PE=1 SV=1	Rab2a	RAB2A_MOUSE	24 kDa	0.08	0.0016

Mus musculus	Sodium/potassium-transporting ATPase subunit alpha-1 OS=Mus musculus GN=Atp1a1 PE=1 SV=1	Atp1a1	AT1A1_MOUSE	113 kDa	0.08	< 0.0001
Mus musculus	Erlin-2 OS=Mus musculus GN=Erlin2 PE=1 SV=1	Erlin2	ERLN2_MOUSE	38 kDa	0.09	0.61
Mus musculus	Guanine nucleotide-binding protein G(i) subunit alpha-2 OS=Mus musculus GN=Gnai2 PE=1 SV=5	Gnai2	GNAI2_MOUSE	40 kDa	0.09	0.00024
Mus musculus	Transitional endoplasmic reticulum ATPase OS=Mus musculus GN=Vcp PE=1 SV=4	Vcp	TERA_MOUSE	89 kDa	0.09	< 0.0001
Mus musculus	Tubulin alpha-1B chain OS=Mus musculus GN=Tuba1b PE=1 SV=2	Tuba1b	TBA1B_MOUSE	50 kDa	0.09	0.51
Mus musculus	Calnexin OS=Mus musculus GN=Canx PE=1 SV=1	Canx	CALX_MOUSE	67 kDa	0.1	0.0082
Mus musculus	Elongation factor 1-gamma OS=Mus musculus GN=Eef1g PE=1 SV=3	Eef1g	EF1G_MOUSE	50 kDa	0.1	0.29
Mus musculus	Guanine nucleotide-binding protein G(I)/G(S)/G(T) subunit beta-1 OS=Mus musculus GN=Gnb1 PE=1 SV=3	Gnb1	GBB1_MOUSE	37 kDa	0.1	0.017
Mus musculus	Sortilin-related receptor OS=Mus musculus GN=Sorl1 PE=1 SV=3	Sorl1	SORL_MOUSE	247 kDa	0.1	0.04
Mus musculus	sp|G5E829|AT2B1_MOUSE		sp|G5E829| AT2B1_MOUSE	?	0.1	< 0.0001
Mus musculus	Tyrosine-protein phosphatase non-receptor type 1 OS=Mus musculus GN=Ptpn1 PE=1 SV=2	Ptpn1	PTN1_MOUSE	50 kDa	0.1	0.88
Mus musculus	Histone H4 OS=Mus musculus GN=Hist1h4a PE=1 SV=2	Hist1h4a	H4_MOUSE	11 kDa	0.11	0.013
unknown	sp|P70704-2|AT8A1_MOUSE		sp|P70704-2| AT8A1_MOUSE	?	0.11	0.042
Mus musculus	Tubulin alpha-1A chain OS=Mus musculus GN=Tuba1a PE=1 SV=1	Tuba1a	TBA1A_MOUSE	50 kDa	0.11	< 0.0001
Mus musculus	Unconventional myosin-Va OS=Mus musculus GN=Myo5a PE=2 SV=1	Myo5a	D3YZ62_MOUSE (+2)	212 kDa	0.11	0.015
Mus musculus	Alpha-adducin OS=Mus musculus GN=Add1 PE=2 SV=1	Add1	F8WGR0_MOUSE (+3)	73 kDa	0.12	0.016
Mus musculus	Cell division control protein 42 homolog OS=Mus musculus GN=Cdc42 PE=1 SV=2	Cdc42	sp|P60766| CDC42_MOUSE	21 kDa	0.12	0.048
Mus musculus	Dolichyl-diphosphooligosaccharide--protein glycosyltransferase 48 kDa subunit OS=Mus musculus GN=Ddost PE=1 SV=2	Ddost	OST48_MOUSE	49 kDa	0.12	0.6
Mus musculus	Ezrin OS=Mus musculus GN=Ezr PE=1 SV=3	Ezr	EZRI_MOUSE	69 kDa	0.12	0.00067
Mus musculus	Myosin-9 OS=Mus musculus GN=Myh9 PE=1 SV=4	Myh9	MYH9_MOUSE	226 kDa	0.12	0.00097
Mus musculus	T-complex protein 1 subunit eta OS=Mus musculus GN=Cct7 PE=1 SV=1	Cct7	TCPH_MOUSE	60 kDa	0.12	0.62
Mus musculus	T-complex protein 1 subunit zeta OS=Mus musculus GN=Cct6a PE=1 SV=3	Cct6a	TCPZ_MOUSE	58 kDa	0.12	0.018
Mus musculus	Cation-independent mannose-6-phosphate receptor OS=Mus musculus GN=Igf2r PE=1 SV=1	Igf2r	MPRI_MOUSE	274 kDa	0.13	0.37
unknown	Isoform Alpha-6X1A of Integrin alpha-6 OS=Mus musculus GN=Itga6	Itga6	sp|Q61739-2| ITA6_MOUSE	120 kDa	0.13	0.0028
Mus musculus	40S ribosomal protein S9 OS=Mus musculus GN=Rps9 PE=2 SV=3	Rps9	RS9_MOUSE	23 kDa	0.14	0.0039
Mus musculus	Cytoplasmic FMR1-interacting protein 2 OS=Mus musculus GN=Cyfip2 PE=1 SV=2	Cyfip2	CYFP2_MOUSE	146 kDa	0.14	< 0.0001
Mus musculus	Protein Slc8a2 OS=Mus musculus GN=Slc8a2 PE=2 SV=1	Slc8a2	Q8K596_MOUSE	101 kDa	0.14	0.049
Mus musculus	Copper-transporting ATPase 2 OS=Mus musculus GN=Atp7b PE=1 SV=2	Atp7b	ATP7B_MOUSE	157 kDa	0.15	0.024
Mus musculus	Cytoplasmic dynein 1 heavy chain 1 OS=Mus musculus GN=Dync1h1 PE=1 SV=2	Dync1h1	DYHC1_MOUSE	532 kDa	0.15	< 0.0001
Mus musculus	Elongation factor 2 OS=Mus musculus GN=Eef2 PE=1 SV=2	Eef2	EF2_MOUSE	95 kDa	0.15	0.031

Mus musculus	Spectrin beta chain, non-erythrocytic 1 OS=Mus musculus GN=Sptbn1 PE=1 SV=2	Sptbn1	sp|Q62261| SPTB2_MOUSE	274 kDa	0.15	< 0.0001
Mus musculus	4F2 cell-surface antigen heavy chain OS=Mus musculus GN=Slc3a2 PE=1 SV=1	Slc3a2	4F2_MOUSE (+1)	58 kDa	0.16	< 0.0001
Mus musculus	Fatty acid desaturase 1 OS=Mus musculus GN=Fads1 PE=2 SV=1	Fads1	FADS1_MOUSE	52 kDa	0.16	0.57
Mus musculus	Microtubule-associated protein 1B OS=Mus musculus GN=Map1b PE=1 SV=2	Map1b	MAP1B_MOUSE	270 kDa	0.16	< 0.0001
Mus musculus	Spectrin alpha chain, non-erythrocytic 1 OS=Mus musculus GN=Sptan1 PE=2 SV=1	Sptan1	A3KGU7_MOUSE	285 kDa	0.16	0.13
Mus musculus	CD81 antigen OS=Mus musculus GN=Cd81 PE=1 SV=2	Cd81	CD81_MOUSE	26 kDa	0.17	0.048
Mus musculus	Isoform 2 of AP-2 complex subunit beta OS=Mus musculus GN=Ap2b1	Ap2b1	sp|Q9DBG3-2| AP2B1_MOUSE (+1)	106 kDa	0.17	0.042
unknown	Isoform 2 of Teneurin-4 OS=Mus musculus GN=Tenm4	Tenm4	sp|Q3UHK6-2| TEN4_MOUSE (+3)	313 kDa	0.17	0.00038
Mus musculus	Pyruvate kinase PKM OS=Mus musculus GN=Pkm PE=1 SV=4	Pkm	sp|P52480| KPYM_MOUSE	58 kDa	0.17	0.021
Mus musculus	Ribosomal protein L15 OS=Mus musculus GN=Gm10020 PE=3 SV=1	Gm10020	E9QAZ2_MOUSE (+1)	24 kDa	0.17	0.13
Mus musculus	Sodium/potassium-transporting ATPase subunit alpha-3 OS=Mus musculus GN=Atp1a3 PE=1 SV=1	Atp1a3	AT1A3_MOUSE (+1)	112 kDa	0.17	< 0.0001
Mus musculus	Synaptic vesicle glycoprotein 2A OS=Mus musculus GN=Sv2a PE=1 SV=1	Sv2a	SV2A_MOUSE	83 kDa	0.17	0.63
unknown	tr|A0A0A6YX40|A0A0A6YX40_MOUSE		tr|A0A0A6YX40| A0A0A6YX40_MOUSE	?	0.17	< 0.0001
Mus musculus	40S ribosomal protein S15a OS=Mus musculus GN=Rps15a PE=2 SV=2	Rps15a	RS15A_MOUSE	15 kDa	0.18	0.083
Mus musculus	Alpha-centractin OS=Mus musculus GN=Actr1a PE=2 SV=1	Actr1a	ACTZ_MOUSE	43 kDa	0.19	0.021
Mus musculus	Guanine nucleotide-binding protein G(I)/G(S)/G(T) subunit beta-2 OS=Mus musculus GN=Gnb2 PE=2 SV=1	Gnb2	E9QKR0_MOUSE (+1)	41 kDa	0.19	< 0.0001
Mus musculus	Neural cell adhesion molecule 1 OS=Mus musculus GN=Ncam1 PE=1 SV=3	Ncam1	sp|P13595| NCAM1_MOUSE	119 kDa	0.19	< 0.0001
Mus musculus	UDP-glucose:glycoprotein glucosyltransferase 1 OS=Mus musculus GN=Uggt1 PE=1 SV=4	Uggt1	UGGG1_MOUSE	176 kDa	0.19	0.2
Mus musculus	Actin, cytoplasmic 1 OS=Mus musculus GN=Actb PE=1 SV=1	Actb	ACTB_MOUSE (+1)	42 kDa	0.2	< 0.0001
Mus musculus	Cathepsin B OS=Mus musculus GN=Ctsb PE=1 SV=2	Ctsb	CATB_MOUSE	37 kDa	0.2	0.68
Mus musculus	Cofilin-1 OS=Mus musculus GN=Cfl1 PE=1 SV=3	Cfl1	COF1_MOUSE (+1)	19 kDa	0.2	< 0.0001
unknown	Isoform 2 of Protein scribble homolog OS=Mus musculus GN=Scrib	Scrib	sp|Q80U72-2| SCRIB_MOUSE (+2)	177 kDa	0.2	0.029
unknown	Isoform 2 of Rab GDP dissociation inhibitor beta OS=Mus musculus GN=Gdi2	Gdi2	sp|Q61598-2| GDIB_MOUSE (+1)	47 kDa	0.2	0.0016
Mus musculus	Solute carrier family 12 member 2 OS=Mus musculus GN=Slc12a2 PE=4 SV=1	Slc12a2	E9QM38_MOUSE	131 kDa	0.2	0.67
Mus musculus	Vesicle-trafficking protein SEC22b OS=Mus musculus GN=Sec22b PE=1 SV=3	Sec22b	SC22B_MOUSE	25 kDa	0.2	0.25
Mus musculus	Contactin-1 OS=Mus musculus GN=Cntn1 PE=1 SV=1	Cntn1	CNTN1_MOUSE	113 kDa	0.21	0.003
Mus musculus	Acid sphingomyelinase-like phosphodiesterase 3b OS=Mus musculus GN=Smpdl3b PE=1 SV=1	Smpdl3b	ASM3B_MOUSE	52 kDa	0.22	0.00049
Mus musculus	FERM, RhoGEF and pleckstrin domain-containing protein 1 OS=Mus musculus GN=Farp1 PE=1 SV=1	Farp1	FARP1_MOUSE	119 kDa	0.22	0.0012
unknown	Isoform 1 of Neurofibromin OS=Mus musculus GN=Nf1	Nf1	sp|Q04690-2| NF1_MOUSE (+1)	317 kDa	0.22	0.00093
Mus musculus	Alpha-actinin-4 OS=Mus musculus GN=Actn4 PE=1 SV=1	Actn4	ACTN4_MOUSE	105 kDa	0.23	0.00035

Mus musculus	Coronin-1C OS=Mus musculus GN=Coro1c PE=1 SV=2	Coro1c	COR1C_MOUSE	53 kDa	0.23	0.75
Mus musculus	Voltage-dependent calcium channel subunit alpha-2/delta-1 OS=Mus musculus GN=Cacna2d1 PE=4 SV=2	Cacna2d1	E9Q1X8_MOUSE (+5)	123 kDa	0.23	0.00062
Mus musculus	60S ribosomal protein L10 (Fragment) OS=Mus musculus GN=Rpl10 PE=4 SV=1	Rpl10	I7HLV2_MOUSE (+1)	23 kDa	0.24	0.013
Mus musculus	Neural cell adhesion molecule 2 OS=Mus musculus GN=Ncam2 PE=1 SV=1	Ncam2	sp|O35136| NCAM2_MOUSE	93 kDa	0.24	< 0.0001
Mus musculus	Niemann-Pick C1 protein OS=Mus musculus GN=Npc1 PE=1 SV=2	Npc1	NPC1_MOUSE	143 kDa	0.25	0.27
Mus musculus	Peptidyl-prolyl cis-trans isomerase A OS=Mus musculus GN=Ppia PE=1 SV=2	Ppia	PPIA_MOUSE	18 kDa	0.25	0.00017
Mus musculus	Peroxiredoxin-4 OS=Mus musculus GN=Prdx4 PE=1 SV=1	Prdx4	PRDX4_MOUSE	31 kDa	0.25	0.82
Mus musculus	Ras-related protein Rab-14 OS=Mus musculus GN=Rab14 PE=1 SV=3	Rab14	RAB14_MOUSE	24 kDa	0.25	0.48
Mus musculus	T-complex protein 1 subunit gamma OS=Mus musculus GN=Cct3 PE=2 SV=1	Cct3	E9Q133_MOUSE (+1)	57 kDa	0.25	0.17
Mus musculus	Adenylyl cyclase-associated protein 1 OS=Mus musculus GN=Cap1 PE=1 SV=4	Cap1	CAP1_MOUSE	52 kDa	0.27	0.0039
Mus musculus	Ras-related protein Rab-1A OS=Mus musculus GN=Rab1A PE=1 SV=3	Rab1A	RAB1A_MOUSE	23 kDa	0.27	0.56
Mus musculus	G protein-regulated inducer of neurite outgrowth 1 OS=Mus musculus GN=Gprin1 PE=1 SV=2	Gprin1	GRIN1_MOUSE	95 kDa	0.28	0.014
Mus musculus	Glyceraldehyde-3-phosphate dehydrogenase OS=Mus musculus GN=Gapdh PE=1 SV=2	Gapdh	G3P_MOUSE (+1)	36 kDa	0.28	0.0013
unknown	Isoform Alpha-2 of Guanine nucleotide-binding protein G(o) subunit alpha OS=Mus musculus GN=Gnao1	Gnao1	sp|P18872-2| GNAO_MOUSE	40 kDa	0.28	< 0.0001
Mus musculus	Afadin OS=Mus musculus GN=Mllt4 PE=4 SV=2	Mllt4	E9Q852_MOUSE (+3)	205 kDa	0.29	< 0.0001
Mus musculus	Glycerophosphoinositol inositolphosphodiesterase GDPD2 OS=Mus musculus GN=Gdpd2 PE=1 SV=1	Gdpd2	GDPD2_MOUSE	61 kDa	0.29	0.046
Mus musculus	Methionine--tRNA ligase, cytoplasmic OS=Mus musculus GN=Mars PE=2 SV=1	Mars	E9QB02_MOUSE (+1)	102 kDa	0.29	0.41
Mus musculus	Microtubule-actin cross-linking factor 1 (Fragment) OS=Mus musculus GN=Macf1 PE=2 SV=1	Macf1	F7ACR9_MOUSE	608 kDa	0.29	0.024
Mus musculus	Very-long-chain (3R)-3-hydroxyacyl-[acyl-carrier protein] dehydratase 3 OS=Mus musculus GN=ptplad1 PE=1 SV=2	ptplad1	HACD3_MOUSE	43 kDa	0.29	0.029
Mus musculus	Endoplasmic reticulum metallopeptidase 1 OS=Mus musculus GN=Ermp1 PE=1 SV=2	Ermp1	sp|Q3UVK0| ERMP1_MOUSE	100 kDa	0.3	0.48
Mus musculus	Heat shock protein HSP 90-beta OS=Mus musculus GN=Hsp90ab1 PE=1 SV=3	Hsp90ab1	HS90B_MOUSE	83 kDa	0.3	0.11
unknown	Isoform 2 of Microtubule-associated protein 4 OS=Mus musculus GN=Map4	Map4	sp|P27546-2| MAP4_MOUSE (+3)	117 kDa	0.3	0.019
unknown	Isoform Alpha of MAGUK p55 subfamily member 6 OS=Mus musculus GN=Mpp6	Mpp6	sp|Q9JLB0-2| MPP6_MOUSE	61 kDa	0.3	0.013
Mus musculus	DnaJ homolog subfamily C member 10 OS=Mus musculus GN=Dnajc10 PE=1 SV=2	Dnajc10	DJC10_MOUSE	91 kDa	0.31	0.095
Mus musculus	Protein Utrn OS=Mus musculus GN=Utrn PE=2 SV=1	Utrn	E9Q6R7_MOUSE	393 kDa	0.31	< 0.0001
Mus musculus	Syntaxin-binding protein 1 OS=Mus musculus GN=Stxbp1 PE=1 SV=2	Stxbp1	sp|O08599| STXB1_MOUSE	68 kDa	0.31	< 0.0001
Mus musculus	60S ribosomal protein L3 OS=Mus musculus GN=Rpl3 PE=2 SV=3	Rpl3	RL3_MOUSE	46 kDa	0.32	0.13
Mus musculus	Filamin-B OS=Mus musculus GN=Flnb PE=1 SV=3	Flnb	FLNB_MOUSE	278 kDa	0.32	< 0.0001

Mus musculus	Probable ATP-dependent RNA helicase DDX6 OS=Mus musculus GN=Ddx6 PE=1 SV=1	Ddx6	DDX6_MOUSE	54 kDa	0.32	0.95
Mus musculus	Signal sequence receptor, delta OS=Mus musculus GN=Ssr4 PE=2 SV=1	Ssr4	Q9D8L3_MOUSE (+1)	19 kDa	0.32	0.92
Mus musculus	V-type proton ATPase catalytic subunit A OS=Mus musculus GN=Atp6v1a PE=1 SV=2	Atp6v1a	sp|P50516|VATA_MOUSE	68 kDa	0.32	< 0.0001
unknown	Isoform 2 of Catenin alpha-2 OS=Mus musculus GN=Ctnna2	Ctnna2	sp|Q61301-2| CTNA2_MOUSE (+1)	100 kDa	0.33	0.99
unknown	Isoform 2 of Unconventional myosin-Ic OS=Mus musculus GN=Myo1c	Myo1c	sp|Q9WTI7-2| MYO1C_MOUSE (+2)	118 kDa	0.35	0.018
Mus musculus	Lanosterol 14-alpha demethylase OS=Mus musculus GN=Cyp51a1 PE=2 SV=1	Cyp51a1	CP51A_MOUSE	57 kDa	0.35	0.55
Mus musculus	Ras-related protein Rap-1A OS=Mus musculus GN=Rap1a PE=2 SV=1	Rap1a	RAP1A_MOUSE	21 kDa	0.35	0.097
Mus musculus	Heat shock cognate 71 kDa protein OS=Mus musculus GN=Hspa8 PE=1 SV=1	Hspa8	HSP7C_MOUSE	71 kDa	0.36	< 0.0001
Mus musculus	Coatomer subunit alpha OS=Mus musculus GN=Copa PE=1 SV=2	Copa	COPA_MOUSE (+1)	138 kDa	0.37	0.63
Mus musculus	Filamin, alpha OS=Mus musculus GN=Flna PE=4 SV=1	Flna	B7FAU9_MOUSE (+1)	280 kDa	0.37	< 0.0001
Mus musculus	V-type proton ATPase subunit B, brain isoform OS=Mus musculus GN=Atp6v1b2 PE=1 SV=1	Atp6v1b2	VATB2_MOUSE	57 kDa	0.38	< 0.0001
Mus musculus	T-complex protein 1 subunit alpha OS=Mus musculus GN=Tcp1 PE=1 SV=3	Tcp1	sp|P11983| TCPA_MOUSE	60 kDa	0.4	0.65
Mus musculus	3-ketoacyl-CoA thiolase A, peroxisomal OS=Mus musculus GN=Acaa1a PE=2 SV=1	Acaa1a	THIKA_MOUSE	44 kDa	0.41	0.71
Mus musculus	Membrane-associated progesterone receptor component 2 OS=Mus musculus GN=Pgrmc2 PE=1 SV=2	Pgrmc2	PGRC2_MOUSE	23 kDa	0.41	0.07
Mus musculus	Fatty acid desaturase 2 OS=Mus musculus GN=Fads2 PE=2 SV=1	Fads2	FADS2_MOUSE	52 kDa	0.42	0.34
Mus musculus	Uncharacterized protein OS=Mus musculus GN=Gm8730 PE=2 SV=1	Gm8730	E9Q070_MOUSE	34 kDa	0.42	0.17
Mus musculus	Band 4.1-like protein 2 OS=Mus musculus GN=Epb41l2 PE=1 SV=2	Epb41l2	E41L2_MOUSE	110 kDa	0.43	0.0027
Mus musculus	Beta-hexosaminidase subunit beta OS=Mus musculus GN=Hexb PE=2 SV=2	Hexb	HEXB_MOUSE	61 kDa	0.43	0.89
Mus musculus	Fatty acid synthase OS=Mus musculus GN=Fasn PE=1 SV=2	Fasn	FAS_MOUSE	272 kDa	0.44	< 0.0001
Mus musculus	Procollagen-lysine,2-oxoglutarate 5-dioxygenase 3 OS=Mus musculus GN=Plod3 PE=1 SV=1	Plod3	PLOD3_MOUSE	85 kDa	0.44	0.53
Mus musculus	Atrial natriuretic peptide receptor 2 OS=Mus musculus GN=Npr2 PE=2 SV=2	Npr2	sp|Q6VVW5| ANPRB_MOUSE	117 kDa	0.45	< 0.0001
Mus musculus	Guanine nucleotide-binding protein G(q) subunit alpha OS=Mus musculus GN=Gnaq PE=1 SV=4	Gnaq	GNAQ_MOUSE	42 kDa	0.46	0.011
unknown	Isoform 2 of 60S ribosomal protein L22-like 1 OS=Mus musculus GN=Rpl22l1	Rpl22l1	sp|Q9D7S7-2| RL22L_MOUSE (+1)	14 kDa	0.46	0.56
Mus musculus	RAS-related C3 botulinum substrate 1, isoform CRA_a OS=Mus musculus GN=Rac1 PE=2 SV=1	Rac1	Q3TLP8_MOUSE (+1)	23 kDa	0.49	0.029
Mus musculus	Ras-related protein Rab-18 OS=Mus musculus GN=Rab18 PE=2 SV=2	Rab18	RAB18_MOUSE	23 kDa	0.52	0.41
Mus musculus	Thioredoxin-related transmembrane protein 1 OS=Mus musculus GN=Tmx1 PE=1 SV=1	Tmx1	TMX1_MOUSE	31 kDa	0.52	0.1
Mus musculus	T-complex protein 1 subunit epsilon OS=Mus musculus GN=Cct5 PE=1 SV=1	Cct5	TCPE_MOUSE	60 kDa	0.54	0.07
Mus musculus	Ras-related protein Rab-5C OS=Mus musculus GN=Rab5c PE=1 SV=2	Rab5c	RAB5C_MOUSE	23 kDa	0.55	0.059
Mus musculus	Serine/threonine-protein phosphatase PP1-alpha catalytic subunit OS=Mus musculus GN=Ppp1ca PE=1 SV=1	Ppp1ca	PP1A_MOUSE	38 kDa	0.55	0.047

unknown	Isoform Short of Tripeptidyl-peptidase 2 OS=Mus musculus GN=Tpp2	Tpp2	sp|Q64514-2| TPP2_MOUSE	138 kDa	0.57	< 0.0001
Mus musculus	Tyrosine-protein kinase receptor OS=Mus musculus GN=Igf1r PE=2 SV=1	Igf1r	E9QNX9_MOUSE (+1)	155 kDa	0.6	0.021
unknown	Isoform 2 of Seizure 6-like protein 2 OS=Mus musculus GN=Sez6l2	Sez6l2	sp|Q4V9Z5-2| SE6L2_MOUSE (+1)	99 kDa	0.63	0.92
Mus musculus	Alpha-enolase OS=Mus musculus GN=Eno1 PE=1 SV=3	Eno1	ENOA_MOUSE	47 kDa	0.65	0.00029
Mus musculus	Plasma membrane calcium-transporting ATPase 2 OS=Mus musculus GN=Atp2b2 PE=2 SV=1	Atp2b2	F8WHB1_MOUSE	137 kDa	0.66	< 0.0001
Mus musculus	Eukaryotic initiation factor 4A-I OS=Mus musculus GN=Eif4a1 PE=1 SV=1	Eif4a1	IF4A1_MOUSE	46 kDa	0.68	0.85
Mus musculus	Voltage-dependent anion-selective channel protein 3 OS=Mus musculus GN=Vdac3 PE=4 SV=1	Vdac3	J3QMG3_MOUSE (+1)	31 kDa	0.69	0.1
Mus musculus	Inactive tyrosine-protein kinase 7 OS=Mus musculus GN=Ptk7 PE=1 SV=1	Ptk7	PTK7_MOUSE	118 kDa	0.7	0.035
Mus musculus	ADP/ATP translocase 1 OS=Mus musculus GN=Slc25a4 PE=1 SV=4	Slc25a4	ADT1_MOUSE	33 kDa	0.71	0.97
Mus musculus	Malectin OS=Mus musculus GN=Mlec PE=2 SV=2	Mlec	MLEC_MOUSE	32 kDa	0.72	0.17
Mus musculus	T-complex protein 1 subunit theta OS=Mus musculus GN=Cct8 PE=2 SV=1	Cct8	H3BL49_MOUSE (+1)	53 kDa	0.74	0.11
Mus musculus	Sterol-4-alpha-carboxylate 3-dehydrogenase, decarboxylating OS=Mus musculus GN=Nsdhl PE=2 SV=1	Nsdhl	NSDHL_MOUSE	41 kDa	0.8	0.21
Mus musculus	L-lactate dehydrogenase OS=Mus musculus GN=Ldha PE=3 SV=1	Ldha	G5E8N5_MOUSE (+1)	40 kDa	0.81	0.0063
Mus musculus	V-type proton ATPase subunit H OS=Mus musculus GN=Atp6v1h PE=1 SV=1	Atp6v1h	VATH_MOUSE (+1)	56 kDa	0.88	0.0071
Mus musculus	Sodium/potassium-transporting ATPase subunit beta-3 OS=Mus musculus GN=Atp1b3 PE=1 SV=1	Atp1b3	AT1B3_MOUSE	32 kDa	0.93	0.047
Mus musculus	Histone H2B type 1-B OS=Mus musculus GN=Hist1h2bb PE=1 SV=3	Hist1h2bb	H2B1B_MOUSE (+9)	14 kDa	0.95	0.071
Mus musculus	Protein Gm9493 OS=Mus musculus GN=Gm9493 PE=4 SV=1	Gm9493	F6SVV1_MOUSE (+1)	22 kDa	0.95	0.034
Mus musculus	Protein dopey-2 OS=Mus musculus GN=Dopey2 PE=2 SV=3	Dopey2	sp|Q3UHQ6| DOP2_MOUSE	257 kDa	0.97	0.25
Mus musculus	Isoform 2B of GTPase KRas OS=Mus musculus GN=Kras	Kras	sp|P32883-2| RASK_MOUSE	21 kDa	0.98	0.076
Mus musculus	Long-chain-fatty-acid--CoA ligase 1 OS=Mus musculus GN=Acsl1 PE=1 SV=2	Acsl1	ACSL1_MOUSE (+1)	78 kDa	1.03	0.53
Mus musculus	Caprin-1 OS=Mus musculus GN=Caprin1 PE=1 SV=2	Caprin1	CAPR1_MOUSE	78 kDa	1.29	0.07
Mus musculus	Procollagen-lysine,2-oxoglutarate 5-dioxygenase 2 OS=Mus musculus GN=Plod2 PE=2 SV=1	Plod2	E9Q718_MOUSE (+1)	87 kDa	1.37	0.42
Mus musculus	Lysosome-associated membrane glycoprotein 1 OS=Mus musculus GN=Lamp1 PE=1 SV=2	Lamp1	LAMP1_MOUSE	44 kDa	2.01	0.4